Contribution du Vehicle-to-Grid (V2G) à la gestion énergétique d'un parc de Véhicules Électriques sur le réseau de distribution

Siyamak Sarabi

ParisTech
INSTITUT DES SCIENCES ET TECHNOLOGIES
PARIS INSTITUTE OF TECHNOLOGY

ARTS ET MÉTIERS ParisTech

2016 - ENAM - 0050

École doctorale n° 432 : Sciences des Métiers de l'ingénieur

Doctorat ParisTech

THÈSE

pour obtenir le grade de docteur délivré par

École Nationale Supérieure d'Arts et Métiers

Spécialité "Génie électrique"

présentée et soutenue publiquement par

Siyamak SARABI

le 29 Novembre 2016

Contribution of Vehicle-to-Grid (V2G) to the energy management of Plug-in Electric Vehicles' fleet on the distribution network

"Contribution du Vehicle-to-Grid (V2G) à la gestion énergétique d'un parc de Véhicules Électriques sur le réseau de distribution"

Directeur de thèse : **Benoit ROBYNS**
Co-encadrant de thèse : **Arnaud DAVIGNY - Vincent COURTECUISSE**

Jury

M. Bernard MULTON,	Professeur, Ecole Normale Supérieure de Rennes, SATIE	Président
M. Alfred RUFER,	Professeur, Ecole Polytechnique Fédérale de Lausanne	Rapporteur
M. Seddik BACHA,	Professeur, Université Grenoble Alpes, G2Elab	Rapporteur
M. Benoît ROBYNS,	Professeur, L2EP-HEI	Examinateur
M. Arnaud DAVIGNY,	Enseignant – Chercheur, L2EP-HEI	Examinateur
M. Vincent COURTECUISSE,	Directeur Travaux Réseaux Postes Sources, SEOLIS	Examinateur
M. Guillaume GAZAIGNES,	Responsable Innovation & Recherche Energie, SNCF	Invité
M. Martin REGNER,	Ingénieur Systèmes Electriques Intelligents, ADEME	Invité

Arts et Métiers ParisTech - Campus de Lille
EA 2697 - L2EP - Laboratoire d'Electrotechnique et d'Electronique de Puissance, F-59000 Lille, France

THÉSE

To the meaning of love, my wife:

Reyhaneh

And To the source of love, my parents and sister:

Maryam, Siavash and Sima

Acknowlegment

This PhD thesis is financially supported by ADEME (French Environment and Energy management Agency), SNCF (French national Railway Network), GEREDIS Deux-Sèvres (Deux-Sèvres Department Distribution System Operator (DSO)) and SEOLIS (Energy supplier of department Deux-Sèvres) and the PhD works has been done in Ecole des Hautes études d'ingénieur (HEI) of L2EP (Lille Laboratory of Electrical Engineering and Power Electronics), from October 2013 to October 2016. I would like to appreciate all of the mentioned companies and organizations.

I express my special thanks to my director of thesis, Professor Benoit Robyns, *Directeur de la Recherche* of Ecole des Hautes études d'ingénieur and my co-supervisors, Dr. Arnaud Davigny, *Enseignant – Chercheur* at HEI, Dr. Vincent Courtecuisse, *Directeur Travaux Réseaux Postes Sources* at SEOLIS and Dr. Yann Riffonneau, *Chargé d'études électricité* at AREP for all of their supports and technical advices during 3 years of my thesis work. I also appreciate M. Martin Regner, the supervisor from ADEME, for his helps and supports during my thesis.

I would like to express my gratitude to all the jury members for accepting to be as the members of jury for my PhD defense session.

I would like to express my appreciation to Professor Bernard Multon from Ecole normale supérieure de Rennes (Laboratoire SATIE) for his presence as the president of the jury.

I would like to acknowledge Professor Alfred Rufer from Ecole Polytechnique Fédérale de Lausanne and Professor Seddik Bacha from Université Grenoble Alpes (Laboratoire G2ELAB) for accepting to be the examiners of the thesis.

I would like to also appreciate Mrs. Marie-Pierre Houry, *Head of Grid Development Studies Department* at RTE France for her valuable remarks and review of the manuscript.

I will never forget the support and advices of the industrial partners of the project in SNCF, Dr. Bogdan Vulturescu, M. Frédéric Chauvet and M. Guillaume Gazaignes and in GEREDIS Deux-Sèvres and SEOLIS, M. Mehdi GHERIBI, M. Rémy Viaud, M. Aurelien MORAND and M. Leo Coutard.

I would like to appreciate Dr. Antoine Henneton, *Directeur Adjoint de la Recherche* of HEI for his supports and Dr. Patrick Debay, *Responsable du département EEA (Energie, Electricité et Automatique)* for providing me the opportunity of being as teaching assistant in academic year 2015-2016 in HEI.

I will never forget all my friends and colleagues during these three years of my PhD thesis for their supports and positive energy and efforts to keep the office always warm and friendly:

"Dr. Jonathan Lesel, Dr. Petronella Pankovits, Dr. Anouar Bouallaga, Fabien Mollet, Dr. Mouloud Guemri, Dr. Faycal Bensmaine Dr. Sid Ali Amamra, Dr. Hayriye Gidik, Dr. Stojanka Petrusic, Dr. Lounes Koufi, Dr. Mohammed Amine Kenai and all future doctors, Haibo Zhang, Ehsan Enferad, Géraldine Ventoruzzo, Jad Nassar, and Volahasina Rasendramalala."

And at the end I should say that without the supports of my parents and sister this long way was never to be ended. During these years I was so fortune to be with my love, Reyhaneh, for her lovely supports and patient. Without all of them it was not possible at all.

Contents

List of figures

List of Tables

List of Acronyms

ADEME Agence De l'Environnement et de la Maîtrise de l'Energie. 3

AEI Annual Energy Invoice. 65

AIEM Annual Energy Invoice Minimization. 64

ANFIS Adaptive Neuro-Fuzzy Inference System. 81

AVPM Available Vehicle-to-Grid Power Modeling. 83

BEV Battery Electric Vehicle. 25

BFC Bidding Flexibility Calculation. 83

BLP Binary Linear Programming. 65

BM Balancing Mechanism. 45

BMS Battery Management System. 16

CON Consumption without Plug-in Electric Vehicle. 189

CRE Commission de Régulation de l'Energie. 7

DESS Distributed Energy Storage Systems. 26

DG Distributed Generation. 29

DLP Daily Load Profile. 18

DOD Depth Of Discharge. 182

DSO Distribution System Operator. 7

ECM Energy Cost Minimization. 45

EDF Electricité de France. 7

EMI Electromagnetic Interference. 16

EMS Energy Management System. 128

ENEDIS Major French Distribution System Operator. 8

ENTSO-E European Network of Transmission System Operators for Electricity. 27

ETCM Energy Transmission Cost Minimization. 45

EV Electric Vehicle. 2

EVN Electric Vehicle Non-supervised. 189

EVS Electric Vehicle Supervised. 189

EVSE Electric Vehicle Supply Equipment. 15

FISSA Fuzzy Inference System Service Assessment. 83

FPE Fundamental Parameters Estimation. 83

G2V Grid-to-Vehicle. 12

GEV Generalized Extreme Value. 51

GRD Gestionaire des Réseaux de Distribution. 7

GRT Gestionaire du Réseau de Transport. 7

HEV Hybrid Electric Vehicle. 13

HTA Haute Tension A. 26

HTB Haute Tension B. 7

HV High Voltage. 7

ICE Internal Combustion Engine. 12

L2EP Laboratory of Electrical Engineering and Power Electronics of Lille. 3

LMO Lithium Manganese Oxide. 183

LV Low Voltage. 7

MMSV Multivariate Modeling of Stochastic Variables. 83

MV Medium Voltage. 7

NOME Nouvelle Organisation du Marché de l'Électricité. 10

PAR Peak-to-Average Ratio. 189

PAUM Probabilistic Availability Uncertainty Modeling. 83

PDF Probability Distribution Function. 51

PEV Plug-in Electric Vehicle. 13

PFC Power Factor Correction. 16

PHEV Plug-in Hybrid Electric Vehicle. 13

PPC Procured Power Capacity. 128

RES Renewable Energy Sources. 2

RLP Reference Load Profile. 66

RTE Réseau de Transport d'Electricité. 7

RTS Regulatory Tariff Sales. 186

SEI Solid Electrolyte Interphase. 182

SMT Spot Market Tariff. 186

SOC State of Charge. 16

SPE Subscribed Power Exceeding. 28

TGV Train à Grande Vitesse. 46

THD Total Harmonic Distortion. 15

TSO Transmission System Operator. 7

TURPE Tarifs d'Utilisation des Réseaux Publics d'Electricité. 55

V2B Vehicle-to-Building. 20

V2G Vehicle-to-Grid. 2

V2H Vehicle-to-Home. 18

V2S Vehicle-to-Station. 20

V2V Vehicle-to-Vehicle. 19

ZEV Zero Emission Vehicle. 13

Publications

Peer reviewed International Journals

1. Potential of Vehicle-to-Grid Ancillary Services Considering the Uncertainties in Plug-in Electric Vehicle Availability and Service/Localization Limitations in Distribution Grids, S. Sarabi, A. Davigny, V. Courtecuisse, Y. Riffonneau, B. Robyns, Applied Energy, Elsevier, Vol. 171, pp. 523-540, June 2016.
2. Supervision of Plug-in Electric Vehicles Connected to the Electric Distribution Grids, S. Sarabi, L. Kefsi, A. Merdassi, B. Robyns, International Journal of Electrical Energy, Vol. 1, No. 4, pp. 256-263, December 2013.

International Conferences with Proceedings

3. Distribution Grid Planning Enhancement Using Profiling Estimation Technic, S. Sarabi, A. Davigny, V. Courtecuisse, L. Coutard, B. Robyns, CIRED Workshop 2016, Helsinki, 06/2016
4. V2G Electric Vehicle Charging Scheduling for Railway Station Parking Lots Based on Binary Linear Programming, S. Sarabi, A. Davigny, Y. Riffonneau, B. Robyns, IEEE International Energy Conference (ENERGYCON 2016), Leuven, 04/2016.
5. Contribution and impacts of grid integrated electric vehicles to the distribution networks and railway station parking lots, S. Sarabi, A. Davigny, Y. Riffonneau, V. Courtecuisse, B. Robyns, 23^{rd} International Conference and Exhibition on Electricity Distribution (CIRED15), Lyon, 07/2016.
6. Traffic-based Modeling of Electric Vehicle Charging Load and its Impact on the Distribution Network and Railway Station Parking Lots, S. Sarabi, A. Davigny, Y. Riffonneau, V. Courtecuisse, B. Robyns, 3^{rd} International Symposium on Environment-Friendly Energies and Applications (EFEA 2014), Paris, 11/2014.
7. The Feasibility of the Ancillary Services for Vehicle-to-Grid Technology, S. Sarabi, A. Bouallaga, A. Davigny, B. Robyns, V. Courtecuisse, Y. Riffonneau, M. Régnier, 11^{th} IEEE International Conference on the European Energy Market (EEM2014), Krakow, 05/2014.
8. Electric Vehicle Charging Strategy based on a Dynamic Programming Algorithm, S. Sarabi, L. Kefsi, IEEE International Conference on Intelligent Energy and Power System (IEPS), Kiev, 07/2014.

Invited Conferences

9. The Feasibility of the Ancillary Services for Vehicle-to-Grid Technology, S. Sarabi, A. Bouallaga, A. Davigny, B. Robyns, V. Courtecuisse, Y. Riffonneau, M. Régnier, 2^{nd} Edition International Conference, "Electromobility: Challenging Issues", Paris, 12/2014.

Certificate for Excellent paper, *in* 6^{th}*International Conference on Computer and Electrical Engineering, Paris, 10/2013.*
Title: "Supervision of Plug-in Electric Vehicles Connected to the Electric Distribution Grids"

General introduction

Context

The challenges concerning the energy resources limitation, the provision of available fossil fuel sources and environmental issues linked to the greenhouse gases increment enforce human beings to investigate the sustainable solutions. Renewable Energy Sources (RES) such as wind, solar, geothermal, hydropower, biomass and biofuels are the leading sustainable solutions. Concerning the environmental challenges and CO_2 emissions the transportation sector is the major producer after the energy producers (e.g. power generation plants and industries).

In addition, the transition from conventional internal combustion engine to electric machine for vehicle's propulsion system, in the concept of transportation electrification is accelerating recently. Environmental concerns, by considering more green energy, generated from renewable resources and fossil fuel source limitations lead to more electrification of transport sector. Supporting the electricity demand of such growing fleet should be covered by more RES to prevent extra dependency to the fossil fuels. In the future smart, grid the interaction between RES and electric vehicles becomes more and more vital. Concurrently, the impact of increased electric vehicles fleet on the electrical grid should be identified.

In France, a perspective view estimates 2 millions Electric Vehicle (EV) up to 2020 and 23% RES production of total energy productions [Louati 13]. Based on an average normal distribution, the energy which is needed to support those EVs fleet is around 21 GWh per day [Sarabi 13]. Comparing to registered statistics from 2011, (i.e. 52 MWh energy need for EVs and 13% RES productions) EVs' energy need increase much faster than RES productions. Moreover, technological possibilities to achieve mostly EVs support by RES productions considering their location and availability limitations could not be guaranteed in near future. Based on these facts, the necessity to identify the large number of EVs impact on electrical grid will be increased.

It is important to consider that without any energy management system, the increasing electricity energy demand could cause negative effects on the grid, especially at distribution grid level. Charging coordination and time of charge management based on different electricity tariff is introduced as an alternative. At higher level to cope with upcoming issues and taking advantage from increased demand, the ability of delivering power from vehicle to the grid is introduced. This technology for the first time has been coined Vehicle-to-Grid (V2G) by AC propulsion Inc. [Emadi 05]. This ability opened new research horizons to take advantage of EVs increment on the grid. One of these horizons can be assessed as V2G grid ancillary services support. In response to the question of "Can customers contribute to the ancillary services?" P. Sandrin [Sandrin 96] says that the customers can act as a generator and also interruptible load, where these contributions should be rewarded for their participation to the grid services.

In this thesis, the contribution of vehicle-to-grid technology into the electrical grid ancillary service support is studied. The main objective is to provide a real-time supervision system which is able to control the charging demand of a considerable amount of electric vehicle, let us say fleet of electric vehicles, which are connected simultaneously to the distribution grid. These vehicles are considered as V2G-enabled vehicles which have ability of delivering power to the distribution grid.

Industrial Partners

This thesis benefits from Laboratory of Electrical Engineering and Power Electronics of Lille (L2EP) experiences in the field of electrical networks and their interactions with multi source and multi storage generation systems, their energy supervision strategies. On the other hand, the experiences obtained from electric vehicle grid integration project, which is called *VERDI* (Véhicule Électrique et Energies Renouvelable dans un Réseaux de Distribution Intelligent), will be taken into account in this project, where the main features of current project compared to *VERDI* is increasing the degree of freedom and ability of delivering power to the grid from a fleet of EV. In addition, extension of case study for integration of electric vehicles in railway station energy hub is investigated.

The industrial partnership of the *SNCF*, the French national railway station, *Séolis*, energy supplier Company and *GEREDIS Deux-Sèvres*, distribution system Operator Company at Deux-Sèvres, increases the technical support and interests of the project. The concept of smart grid for future electrical networks conveying the interaction between EVs inside the railway station parking with the grid, and power market participation of EV fleet, for the aim of ancillary services support for energy purchase price optimization from the energy supplier point of view, and energy transmission cost optimization from the distribution operator point of view.

In addition the concept of environmental issues concerning the impact of future electrical grid on the environment, increases the motivation for interaction of renewable energy sources and green transportation concepts (zero emission vehicles) where this project is coming an appropriate point for Agence De l'Environnement et de la Maîtrise de l'Energie (ADEME) to cover half finance of the project.

Problem and objective

In this project the objective is to firstly, identify the impacts and limitations of electric vehicles on the electrical distribution grid where the possibility of grid ancillary services support by electric vehicle fleet is also addressed. Secondly, thanks to the concept of V2G, which provide bidirectional power flow between vehicles and grid, a supervision system capable to coordinate the charging and/or discharging interval of the electric vehicle fleet will be designed. The present thesis is the results of the three years studies on the subject which is represented in 5 main chapters.

In chapter 1, a bibliographical study on the electrical grid, electric vehicles and Vehicle-to-Grid technology is presented. In this context, different technologies for electric vehicles, their charging infrastructures and communication protocols are discussed. The possible criteria of research in this domain also are discussed.

In chapter 2, the impacts and contribution of V2G-enabled electric vehicles are discussed, where these studies are concentrated on two particular case studies, a regional distribution grid and a railway station serving plug-in electric vehicles charging infrastructure in its parking.

In third chapter, V2G ancillary services and the PEV potential for participation in different services are studied, where the vehicles availability and grid localization limitation are modeled as uncertainties.

In chapter 4, the main contribution of thesis about real-time energy management system for V2G-enabled PEV fleet is presented. Different parts containing, forecasting algorithms, off-line optimization algorithms and real-time supervision system are presented precisely. The impact of V2G technology on battery degradation is also discussed and modeled in this chapter.

In fifth chapter, a co-simulation approach has been used in order to validate the supervision system at the distribution grid level and identify the technical impacts of supervision system on the voltage drop and losses in the distribution grid.

References

[Emadi 05] Ali Emadi. Handbook of automotive power electronics and motor drives. CRC press, 2005. 3

[Louati 13] Sami Louati, Didier Reynaud, Hélène Thiénard & Arnaud Bouissou. *Chiffres clés des energies renouvelables, edition 2013*, June 2013. 3

[Sandrin 96] Patrick Sandrin. *System-services: several questions, in an integrated utility perspective [ancillary services].* In Pricing of Ancillary Services: an International Perspective (Digest No: 1996/164), IEE Colloquium on, page 7–1. IET, 1996. 3

[Sarabi 13] Siyamak Sarabi, Laid Kefsi, Asma Merdassi & Benoit Robyns. *Supervision of Plug-in Electric Vehicles Connected to the Electric Distribution Grids.* International Journal of Electrical Energy, vol. 1, no. 4, pages 256–263, 2013. 3

Chapter 1

Introduction to electrical networks and grid integration of electric vehicles

“ The important criterion of your impact is: has what you have done generated a following? With fuzzy sets, I can definitely say, ’Yes’. ”

Lotfi A. Zadeh

Contents

1.1 Electrical networks

One of the cleanest way of energy transfer is the electrical form of transformation. In actual electrical grid structure, the power plants, mainly constructed in countryside and far away from the cities, transfer the energy of different sources such as coal, gas, fossil fuels, nuclear, wind, solar and hydro to the electricity and the transmission lines transfer the clean and safe electricity to the cities and consumers sites. The nominal rate of output voltage of the power plants are in the range of 20 to 30 kV with extremely high current which provide for instance the nominal range of output power of 400, 600 to 1000 MW for combined cycle and 900, 1300 and 1500 MW for each nuclear tower in nuclear power plants. This high range of current in the output in term of losses inside the transmission and distribution grid bring the interest of using step-up transformers as a substation unit at the output of the power plants. Hence, the nominal output power of such substations is in range of 400 kV. The electricity transmitted to the cities using the transmission grid, will be distributed to the consumers in cities using the distribution grids. In France, the management of French public electricity networks assigned by article 2 of the Law of 10 February 2000 to two types of actors:

- The Transmission System Operator (TSO) (Gestionaire du Réseau de Transport (GRT)) that operates the high and very high voltage grid and so-called Réseau de Transport d'Electricité (RTE) operates at voltages of 63 kV, 90 kV, 150 kV, 225 kV and 400 kV.
- Distribution System Operator (DSO) (Gestionaire des Réseaux de Distribution (GRD)) who operates medium and low voltage networks.

Managers of transmission and distribution networks employ monopolies regulated by the Energy Regulatory Commission (Commission de Régulation de l'Energie (CRE)).

1.1.1 French public transmission grid

In France the public transmission of electricity consists of a grid called "large transport and interconnection", on the one hand, and a network called "Repartition", on the other. Their total length is about 100,000 km. The large transportation network and interconnection, operating at 400 and 225 kV (called "High Voltage (HV) networks"), can carry large amounts of power over long distances. Its lines form what they can be called "electricity highways". They serve the interconnections with the networks of foreign countries, nuclear power plants and some large hydro and thermal production facilities, and distribution networks. The distribution grid transports electricity regionally. It is operated with other voltage levels Haute Tension B (HTB) (225, 90 and 63 kV). Its lines are used to transmit electricity to industrial consumers and to distribution grid. They also collect energy from the intermediate-sized production facilities. The public transmission of electricity is the property of RTE Transport, a subsidiary of Electricité de France (EDF) in 100%, and is operated by itself.

1.1.2 French public distribution grid

Public distribution grid routes electrical energy not only among individuals but also among small industries. They also collect the energy produced by most wind farms, photovoltaic production facilities and the majority of co-generation plants. They are composed of networks operating at 20 kV and 15 kV, called "Medium Voltage (MV) networks", and networks operating at 400 V and 230 V AC single phase, called "Low Voltage (LV) networks". Their total length is over 1.3 million kilometers in France. The interface between the public transmission network and public distribution networks consists of about 2,200 transformer stations HV / MV called

"substations" ("Poste source" in French). The interface between the MV and LV networks is made by the said transformer stations "distribution substation" ("Poste de distribution" in French). There are more than 700,000.

The public distribution networks are owned by municipalities. These may delegate all or part of their competence the licensing authority for inter-departmental or unions. If they do not provide themselves governed through these, licensing authorities have entrusted the management of their distribution network to Major French Distribution System Operator (ENEDIS), a subsidiary of EDF in 100% (95% for networks distribution of the continental metropolitan territory), or local distribution companies (LDCs) through concession contracts. In Corsica and in the departments and communities overseas, EDF Island Energy Systems (IES) is the manager of public distribution systems. Boards and ELD number are about 160. Four of them have over 100,000 customers. They are named GEREDIS (Deux-Sèvres), Strasbourg Electricity Networks (ESR - Bas-Rhin), DTH and URM (Metz).

1.1.3 Electricity production in France

Electricity production in France is dominated by nuclear power (77% of total production in 2012). This is while renewable energies and fossil fuels are accounted for 15% and 8%, respectively. The largest share of nuclear power in the world is dedicated to France with the biggest net exports of electricity.

According to the International Energy Agency (IEA), France electricity production of 559 TWh in 2012, slightly down from 570 and 567 TWh produced in 2008 and 2004, respectively. France is the world's 8th largest producer of electricity. In 2012, the top ten countries produced 7,290 TWh, or 66.7% of global electricity production of 22,668 TWh. These countries were China (22%), followed by the United States (18.8%), India (5.0%), Russia (4.7%), Japan (4.5%), Canada (2.8%), Germany (2.7%), France (2.5%), Brazil(2.4%), and South Korea (2.3%). The rest of the world produced 32.3% [IEA 15].

France is also the world's second largest producer of nuclear electricity, behind the United States and ahead of Russia and Korea. In terms of nuclear share on the total domestic electricity generation, France has by far the highest percentage portion of any country in the world. While during last decade, renewable energy production (mainly solar and wind) are replacing the share of nuclear. As shown in the Figure 1.1, the share of nuclear energy is decreased while renewable energy sources are developing more and more. This is the new era of energy industry, where classical energy sources are giving the place to the renewable sources.

1.1.4 Electricity consumption in France

Electric energy consumption is the form of energy consumption that uses the electric energy. Consumption of electric energy is measured in watt-hours (Wh). The electricity consumption depends on different factors based on each country features. In France, the electricity consumption is highly sensitive to the climate condition . In 2014, the hottest year on record since the beginning of the 20^{th} century according to Météo France, gross power consumption contracted by 6% versus 2013 and ended the year at 465.3 TWh, the lowest level since 2002 [RTE 15a].

The moderate level of national consumption and the relatively low prices on the French bulk electricity market provided the opportunity for France to assist its European neighbors with electricity exports (Shown in Figure 1.2). Net exports amounted to 65.1 TWh as at the end of 2014, + 18 TWh against 2013 and a record high since 2003. Electricity trades were especially high in 2014 (exports: 92 TWh, imports: 27 TWh) [RTE 15b].

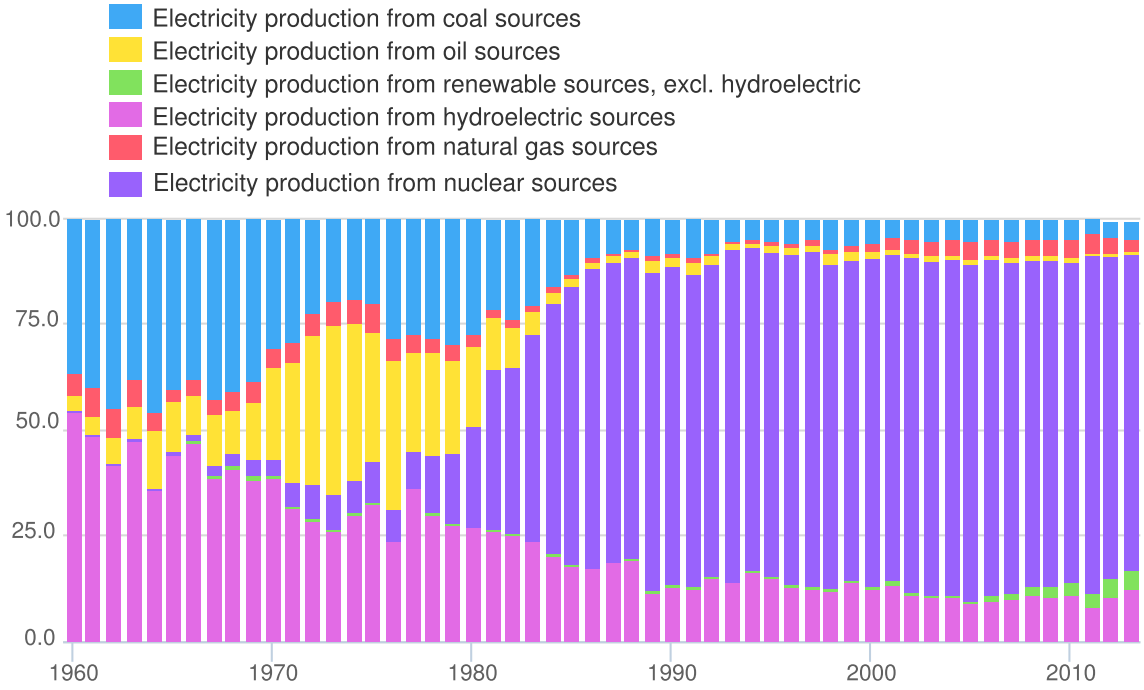

Figure 1.1: This chart shows the indicator called Electricity production by sources with the unit % of total for France between 1960 to 2013 [BLU 15].

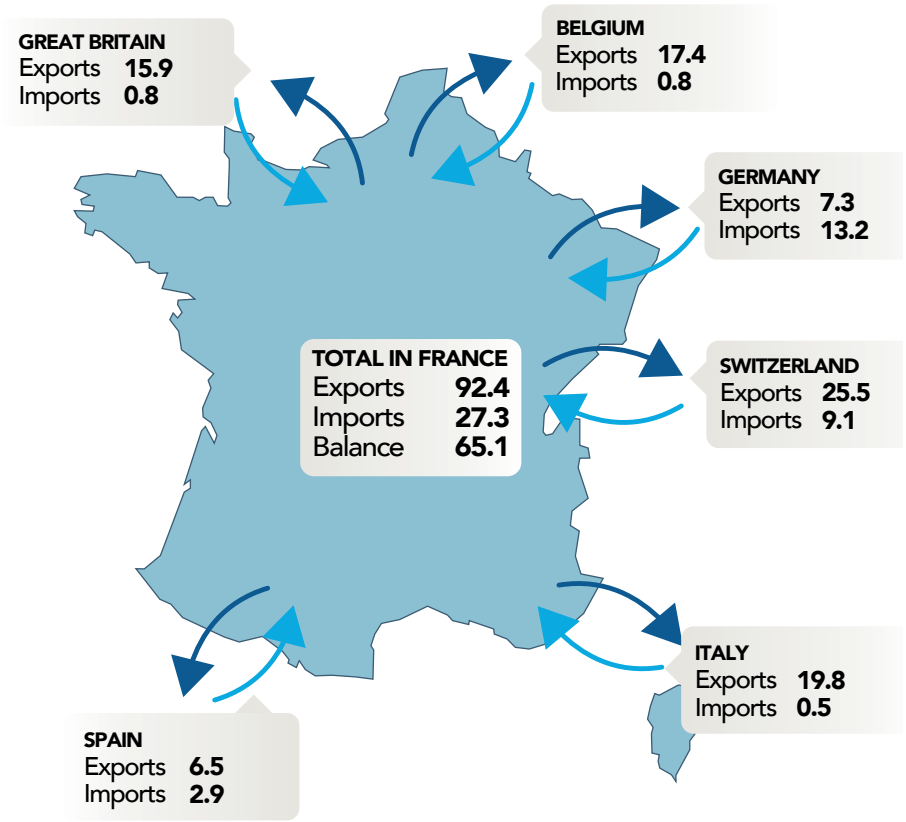

Figure 1.2: Contractual trades in TWh in 2014 [RTE 15b].

1.1.5 Energy market in France

The French energy market is highly concentrated. Electricity is still largely dominated by EDF, the vertically incorporated French utility holder that is still organized by the state. RTE, and the distribution system operator, ENEDIS, are totally owned by EDF. ENEDIS manages about 95% of the electricity distribution network in mainland France. This network belongs to municipalities or groups of municipalities that subcontract to ENEDIS as an operator through a public service delegation. In 2010, the French government approved an energy law (Nouvelle Organisation du Marché de l'Électricité (NOME)) designed to increase competition in the retail electricity market. By this law, EDF has the obligation to make available up to 25% of the nuclear electricity it generates to alternative suppliers on the wholesale market at a regular price, which has set at 42 €/MWh in 2012 [DEL 15].

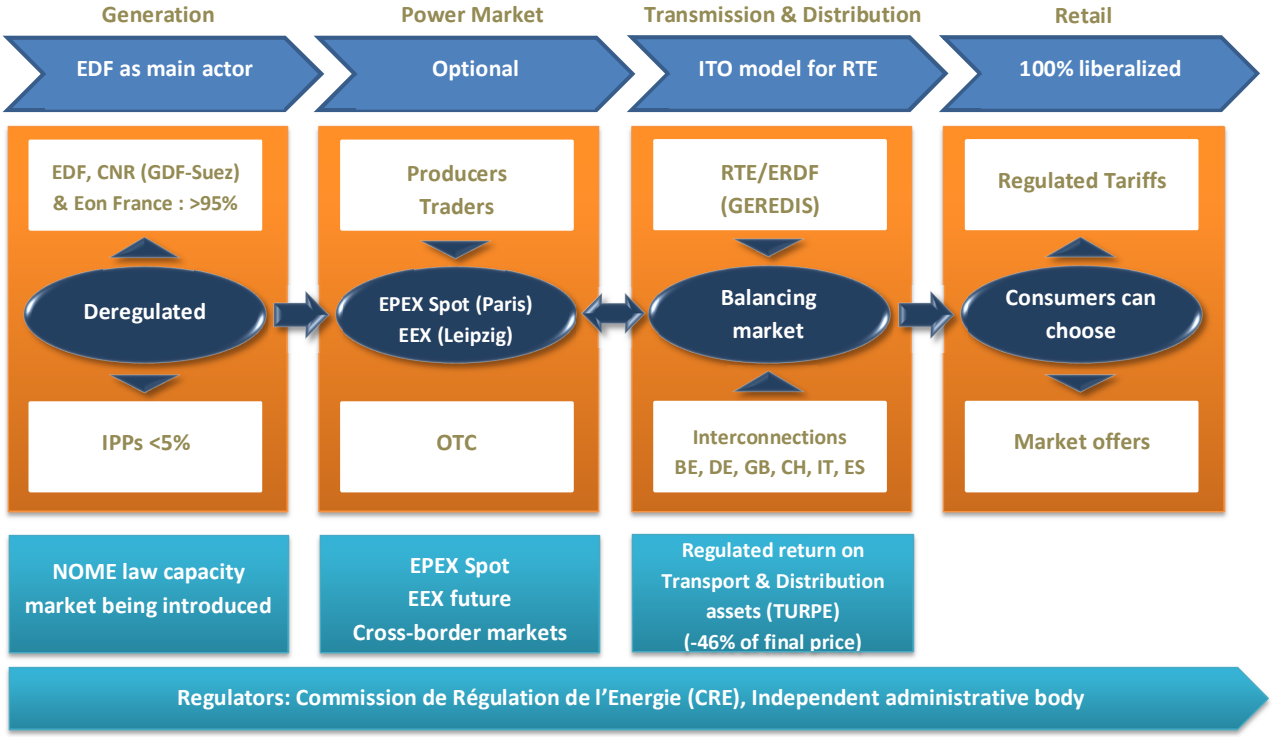

Figure 1.3: Market mechanism [DEL 15].

The different phases and relations in French energy market is represented in Figure 1.3. In the deregulated market, the electricity is owned majorly by EDF, CNR and Eon France upto 95% where the rest is dedicated to the Independent Power Producers (IPP). In the next phase, the producers and traders and deregulated market members participate in European energy markets such as EPEX[1] and EEX[2] in an OTC[3] market way. The TSO and DSO

[1]The European Power Exchange SE (EPEX SPOT SE) is an exchange for power spot trading in Germany, France, Austria, Switzerland and Luxembourg. EPEX SPOT is 100 % owner of APX Group, which operates the power spot markets in Belgium, the Netherland and the United Kingdom.

[2]European Energy Exchange AG, Germany's energy exchange, is the leading energy exchange in Central Europe. It develops, operates and connects secure, liquid and transparent markets for energy and related products. On the EEX spot and derivatives markets, power, natural gas, CO_2 emission allowances, coal and guarantees of origin are traded

[3]An over-the-counter (OTC) market is a decentralized market, without a central physical location, where market participants trade with one another through various communication modes such as the telephone, email and proprietary electronic trading systems. An OTC market and an exchange market are the two basic ways of organizing financial markets. In an OTC market, dealers act as market makers by quoting prices at which they

will participate in balancing market in order to stabilize the grid. This is in connection with all European neighbors. This makes a bidirectional market between European markets and national market. Finally, in next phase the liberalization of the markets aiming to provide regulated tariff energy to the customers will be implemented.

1.1.5.1 NOME law

In December 2010, France approved the law NOME to promote competition in the retail electricity market. In practice, the law allows retailers to buy nuclear production from the incumbent, at a regulated access price. This mechanism works up to a ceiling of 100 TWh, which represents one quarter of the incumbent's production from nuclear plants. Each retailer is assigned a share of that amount proportionally to its portfolio of clients.

In the continue of the following chapter, the integration of electric vehicle in to the electrical networks, electric vehicle types and technologies and Vehicle-to-Grid technology as the main part of the thesis are introduced.

1.2 Integration of electric vehicle into the electrical grid

Nowadays, the concept of smart grid and its definition, application, impacts and contribution to the conventional electrical grid are widely discussed in academic and industrial societies. The problem of traditional energy sources restrictions, their environmental impacts and technical criteria improvement of electrical grids lead to introducing new concept of grids which have bidirectional contribution between production and consumption. In such idea, the presence of renewable energy sources such as solar and wind and electric vehicle (EV) with vehicle-to-grid (V2G) technology become highlighted. These distributed generation sources can be stored in peak hours and reused during off-peak hours. On the contrary, it is important also to take into consideration the unwanted impacts of growing electrified transportation on the electrical grid, due to the coincidence of daily load peak and charging time of EVs [Shafiee 13].

In France, a perspective planning estimates 2 million electric vehicles up to year 2020 [Negre 11]. However, the new scenqrios studied by ENEDIS qnd RTE are estimating much less that that, compared to the actual evolution of electric vehicle market, something between 400,000 to 850,000 EV on 2020. ENEDIS, an electricity distribution network company in France for a fleet of 1 million EV has estimated 2.5TWh annual energy consumption during charging process, which counts 0.5% of total consumption in 2013. While, in term of instantaneous power demand for case of rapid charging with 43 kW charging power, 47% of available power of the national grid can be solicited. This can be reached up to 100% at MV and LV distribution network level [ERDF 14]. To cope with upcoming issues due to this large demand, the implementation of charging infrastructures and supervised intelligent charging/discharging energy management strategies are in hand projects for future. In order to define potentials of electric vehicles to respond to the grid services, the impacts of different scenarios, containing coordinated and uncontrolled charging at different operational modes, should be taken into consideration.

In addition to that, in order to provide contribution of EVs to the electrical network the concept of Vehicle-to-Grid should be studied deeply along with possible ancillary services which are applicable from both grid and EV side. Integration of EVs to the electrical networks needs both technical and financial consideration. The technical points are related to the standards,

will buy and sell a security or currency. A trade can be executed between two participants in an OTC market without others being aware of the price at which the transaction was effected. In general, OTC markets are therefore less transparent than exchanges and are also subject to fewer regulations [INV 15].

protections and safe charging process particularly for EV and EV owner. While from grid point of view, respecting the connection standards containing admissible voltage and current level and power quality respecting. These requirements are thoroughly discussed after an introduction on electric vehicles in the next sections. before that, a possible market contribution of electric vehicle and particularly, EVs with V2G technology are presented thereafter.

A conceptual market model containing different actors from production to consumption level is presented in Figure 1.4. This concept inspired from [Lopes 11, Rious 13] explains different actions between market actors. An aggregator entity responsible for power aggregation of electric vehicle plays the roll of interface between electricity market and single EVs. TSO, DSO and Energy provider are the classical players of the market. In addition, retailer entities in connection with EVs contribution such as parking facilities and battery providers are also considered as possible market players in relation with EVs and aggregators. Sell and Buy offers between different market actors are illustrated in the figure. The novelty of the market is related to the contribution of EVs to the market where the V2G and Grid-to-Vehicle (G2V) are presented. Selling energy and reserve offer to the market by aggregator is showing the contribution of V2G to the market. The G2V is related to the energy need for charging the battery bought by aggregator. This concept certainly can be evaluated in order to provide an accurate market contribution defining the share of each actors.

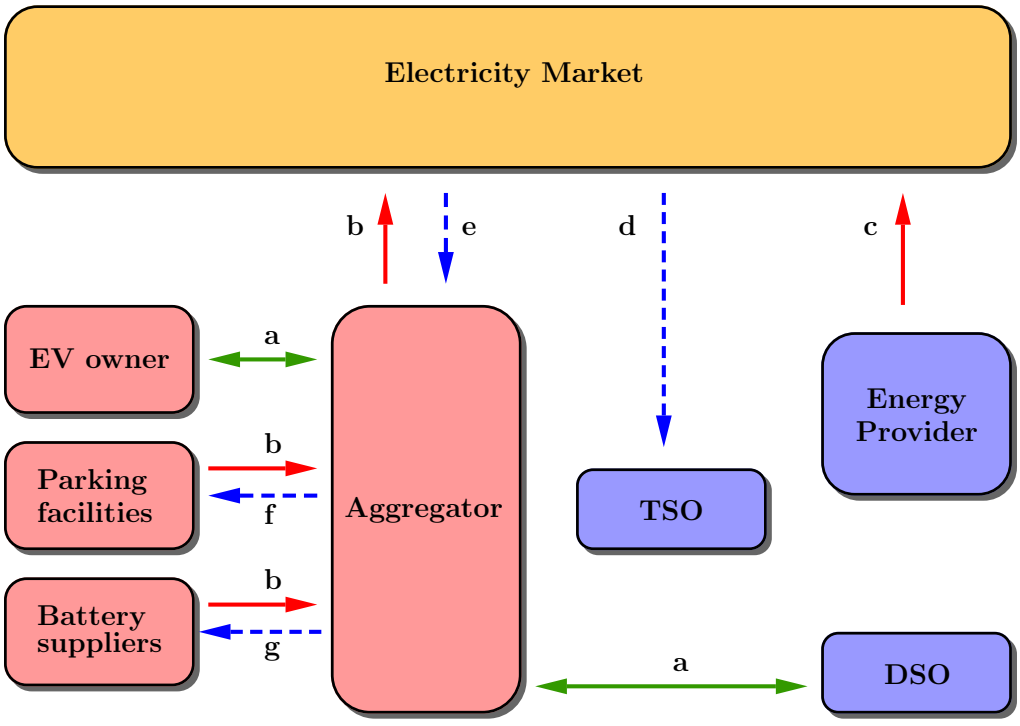

Figure 1.4: EV integration in to the electricity market.

1.2.1 Electric Vehicle (EV)

The main feature of a EV is its propulsion system which is an electric motor instead of Internal Combustion Engine (ICE). This motor is running by power stored in the battery. In the case of plug-in EVs the battery will be charged frequently by plugging in to the grid (120V or 240V) [Emadi 05]. The charging process for Hybrid Electric Vehicle (HEV) will be done by ICE when the vehicle is working on nonelectric mode. EVs because of their no direct emission feature are called as Zero Emission Vehicle (ZEV) and are often, regarding GHG emissions and depending on the electric mix, more environment friendly compared to gasoline or liquefied petroleum gas (LPG) powered vehicles. As there are less mechanical movements maintenance is also minimal. They are also more energy efficient than combustion engines.

In the EVs the electrical energy is stored in a battery or supercapacitor, where in a fuel cell is converted from chemical energy or in a flywheel converted from mechanical energy. This energy will be used to power the electric motor for making the propulsion to the vehicle by turning the wheels. As in this process there is no fuel to burn no local pollution will be produced at the end of the process. Although the main drawback of the EVs is about their autonomy that makes them weak compare to ICE vehicles. In fact by a full-charged battery they could only travel in the average range of 100 km, where the recharging process takes some hours. While the ICE vehicles could be driven much more than that with a tankful and they will be refueled rapidly. However, the technology is trying to find the best solution to improve the disadvantages of EVs compared to ICE. Maybe this point is a key feature to bring another type of vehicle called as Hybrid EV, the electric vehicles with ICE propulsion system in side.

1.2.2 Hybrid electric vehicle (HEV)

The other type of electric vehicles is hybrid electric vehicles. In fact in these cars both electric motor and IC engine are embedded. The IC engine has more efficiency in high speed and load where the EVs are more efficient in low range speed and load. This gives the opportunity to use electric propulsion in the urban area and IC engine mode in the road and out of the cities. There are different types of hybrid vehicles which are depending to the connection of the propulsion systems.

1.2.2.1 Parallel hybrid

In the parallel hybrid vehicles there is a direct connection between hybrid unit and the wheels like the conventional vehicles but an electric motor driving the wheels as well (Fig. 2.12(a)). In this type the vehicle can use the power generated from ICE for highway driving and power generated from electric motor for accelerating. This type of configuration is more powerful compared to series configuration as there are two propulsion systems driving the wheels simultaneously. There are different type of mechanical coupling in the parallel hybrid configuration such as torque, speed and torque and speed coupling.

1.2.2.2 Series hybrid

In the series configuration the thermal engine by using a generator is supplying the battery to feed the electric motor (Fig. 2.12(b)). In this configuration there is no mechanical connection between hybrid unit and the wheels therefore all the power is transferred electrically to an electric motor which drives the wheels. One of the advantages of series compared to parallel is that the IC engine will never work idle which reduces the emissions. This configuration leads to no need to a transmission system for some type of series configuration [Emadi 05], [Ehsani 09],

[Skvarenina 01]. This drive train may need a battery charger to charge the batteries by a wall plug-in from the power network. In this case, the vehicle will be able to be connected to the electrical grid where these types of EV and HEVs are called as Plug-in Electric Vehicle (PEV) and Plug-in Hybrid Electric Vehicle (PHEV), respectively,

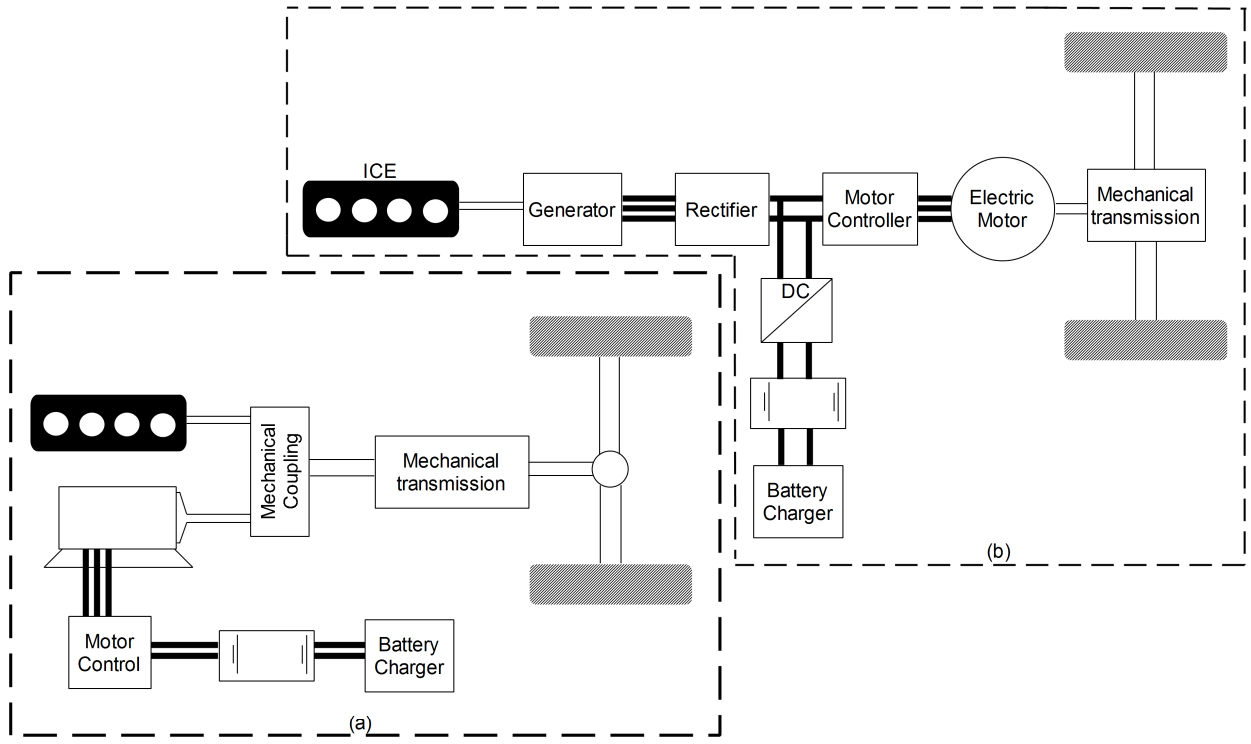

Figure 1.5: Configuration of (a) a parallel hybrid and (b) a series hybrid electric drive train

1.2.3 Plug-in Electric/Hybrid Vehicles (PEV/PHEV)

Plug-in electric vehicles are those motor vehicles which can be connected to an electrical source to charge their energy storage unit (battery, supercapacitor) [Sandalow 09]. This feature makes them more flexible compared to hybrid vehicles with no outside recharging ability. These configurations are based on IEC 62196 which is an international standard for set of electrical connectors and charging modes for electric vehicles maintained by International Electrotechnical Commission. In France, currently three types of charging infrastructure are delivering charging services to the electric vehicles (Table.1.1)[IEC 03].

The ability of connection between plug-in EVs and electrical grids brings new challenges for both electric vehicles and the grids. The increasing number of electric vehicles asking to charge their battery through their plug-in connections causes some negative effects on the electrical grids. Moreover, bidirectional power flow between the vehicles and grids opens new technological domains containing advantages and drawbacks. As in this thesis the concentration is on this recent discussed technology an introduction to the concepts of vehicle-to-Grid would be proper. Before that, a review on EV charging systems and standards are brought.

1.2.4 Electric vehicle charging system

Recently, large amount of researchers are concerning the charger models. However, most of the actual chargers of EVs and PHEVs in the market are devices with nonlinear behavior generating

Table 1.1: Different charging mode for PEV/PHEV

Charging mode	Power	Connector socket
Normal Charging	3.7kW single phase (230V - 16A)	IEC 62196 Type 3
Accelerated Charging	23kW three phase (400V - 32A)	IEC 62196 Type 3
Fast Charging	43kW three phase (400V - 64A)	Cable attached to the station
Fast Charging	50kW DC Mixed AC and DC	Cable attached to the station

harmonics of current. The power quality of the EV chargers are the important factor where it is expected to have major electrified transportation. These are concerning voltage profile, harmonic and fundamental losses and current Total Harmonic Distortion (THD) and current imbalance. In addition, for V2G technology, there is no bidirectional charger available in the market. Hence the main challenge for the V2G technology remains at the level of modelling for bidirectional power flow between the grid and the battery. The other important factor is considering the time consumed for charging process. This depends on total energy amount stored in the battery and the power rate of the charger. Based on the topology of the charger the possibility of reactive power control is another aspect of the chargers that should be taken into accounts. Here in this thesis at first a brief introduction on actual technology of charging for the electric vehicles is presented. Afterwards, the proposed topologies for bidirectional charging system are presented which are compatible for V2G technology. These topologies are gathered from the recent researches from all around the world.

1.2.4.1 Level 1 charging

Level 1 charging is the use of a standard AC 230 Volt household outlet (in Europe). Electric vehicles come with on-board charging electronics, as well as cords and equipment that allow the driver to plug their car into an outlet in their garage, carport or driveway. This is the cheapest and most convenient home-based charging method, but it is also the slowest. Charging times vary greatly from vehicle to vehicle, but generally take around 5-10 twenty hours for a fully depleted battery to be at full capacity. However, since the average French drives less than 30 km per day and many electric vehicles have battery capacities of 100 km or more, most drivers find that their daily commutes barely deplete battery charge and only require Level 1 charging overnight. For example, if the driver of a Renault ZOE – which has about a 210 km range – drives 30 km daily, the battery will only be depleted 15% each day. Since Level 1 charging will recover about 35 km of range per hour, the Renault ZOE will be back to full charge after 2 hours.

1.2.4.2 Level 2 charging

Level 2 chargers uses a 230 V single phase AC outlet or 400 V three phase AC outlet, and is therefore a bit faster than Level 1 charging. Drivers Level 2 charge their vehicles through charging stations often located in public places, such as at the commercial centers, restaurant, city park, or even workplaces. Level 2 charging is sometimes referred to as "opportunity charging" because drivers usually use this type of charging whenever they have the chance, for example, when they are at work or on-the-go in public. Some people choose to purchase a Level 2 home charging station, also called Electric Vehicle Supply Equipment (EVSE), which cost about 1,500

€ - 2,000 €. Most drivers would not need the extra equipment if their daily commutes are short and they are able to adequately Level 1 charge their vehicles overnight. Level 2 charging speeds are variable and depend upon the maximum power rating of the charging station as well as the maximum power rating of the vehicle's on-board charging electronics. Generally speaking, Level 2 charging takes around 3-5 hours for a full charge.

1.2.4.3 Level 3 charging

Level 3 charging is the fastest and most powerful type of charging available. Also called DC charging, it bypasses EV on-board chargers to charge the battery directly. As a result, DC charging can provide a vehicle with a full charge in minutes instead of hours. The Blink DC Fast Charger boasts a full charge in less than 30 minutes. DC charging stations are used for EVs as well as large vehicles like electric buses, and are found in public and commercial areas, airports, and transportation corridors [ELE 12].

1.2.4.4 Electric vehicle Supply Equipment (EVSE)

EVSE is a protocol to help keep the driver and electric vehicle safe while charging. Using two-way communication between the charger and vehicle, the correct charging current is set based on the maximum current the charger can provide as well as the maximum current the car can receive. As part of the protocol, a safety lock-out exists, preventing current from flowing when the charger is not connected to the vehicle. It ensures that if a cable is not correctly inserted, power will not flow through it. EVSE can also detect hardware faults, disconnecting the power and preventing battery damage, electrical shorts or worse still, fire [GRE 13]. From the physical point of view, the conductors, including the ungrounded, grounded, and equipment grounding conductors, the electric vehicle connectors, attachment plugs, and all other fittings, devices, power outlets or apparatuses installed specifically for the purpose of delivering energy from the premises wiring to the electric vehicle, are included in the EVSE system [Rawson 99]. The EVSE based on type of charging station has different components.

1.2.4.5 EVSE for On-board charging

For level 1 and 2 charging, there is a dedicated (on-board) charger inside the vehicle. Therefore, the EVSE for these levels, contains only the protection unit in order to ensure a safe charging system both for driver and the vehicle as well. Figure 1.6 show an EVSE along with on-board charger system. The output of EVSE is a protected AC voltage appropriate for level 1 and 2 charging systems of EV's on-board chargers. On-board charger contains an Electromagnetic Interference (EMI) filter, a rectifier along with Power Factor Correction (PFC) unit and a DC/DC converter in order to provide suitable DC voltage for charging the battery. Battery Management System (BMS) unit is also responsible of controlling the charging status based on State of Charge (SOC) of the battery by controlling the current and voltage of the battery.

1.2.4.6 EVSE for Off-board charging

Fast charging systems, particularly DC fast charging systems has an off-board charging system embedded in EVSE station. The input to the car is directly a DC current and is usually based on standard SAE J1772. In this case EMI filter, rectifier and DC/DC converter are embedded in EVSE. Figure 1.7 shows an example of DC fast charging stations for charging Nissan cars manufactured by DBT-CEV®.

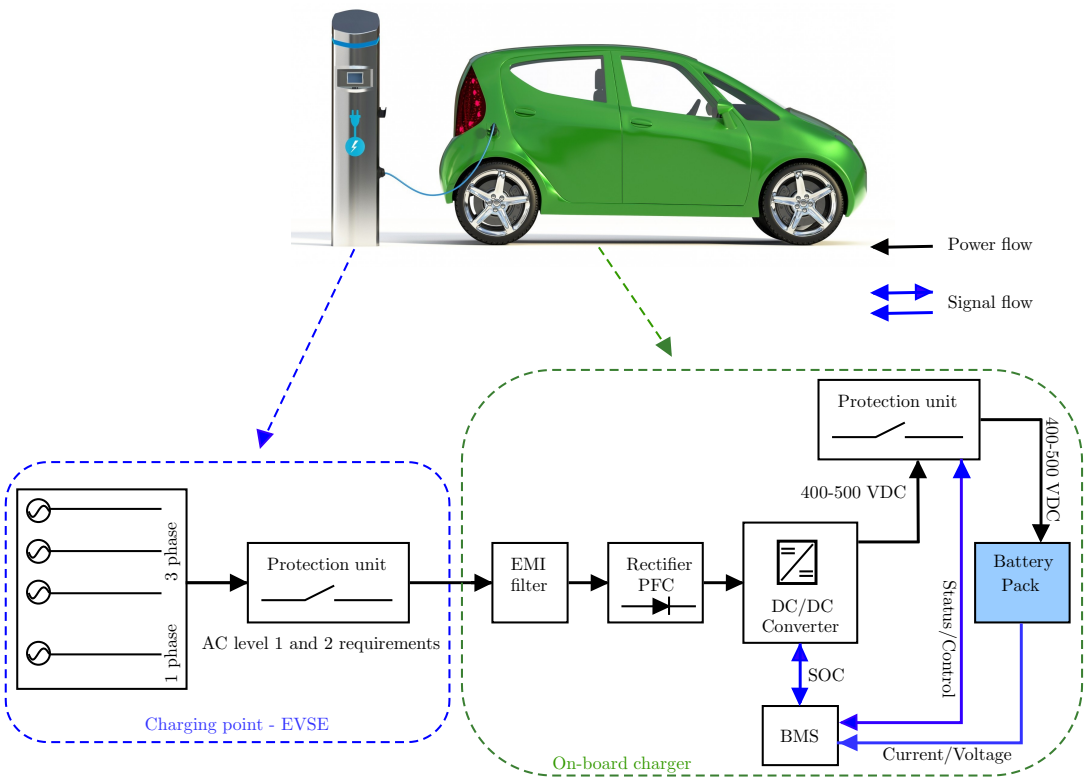

Figure 1.6: Charging configuration and EVSE for AC level 1 and 2 [Mwasilu 14, MDE 15].

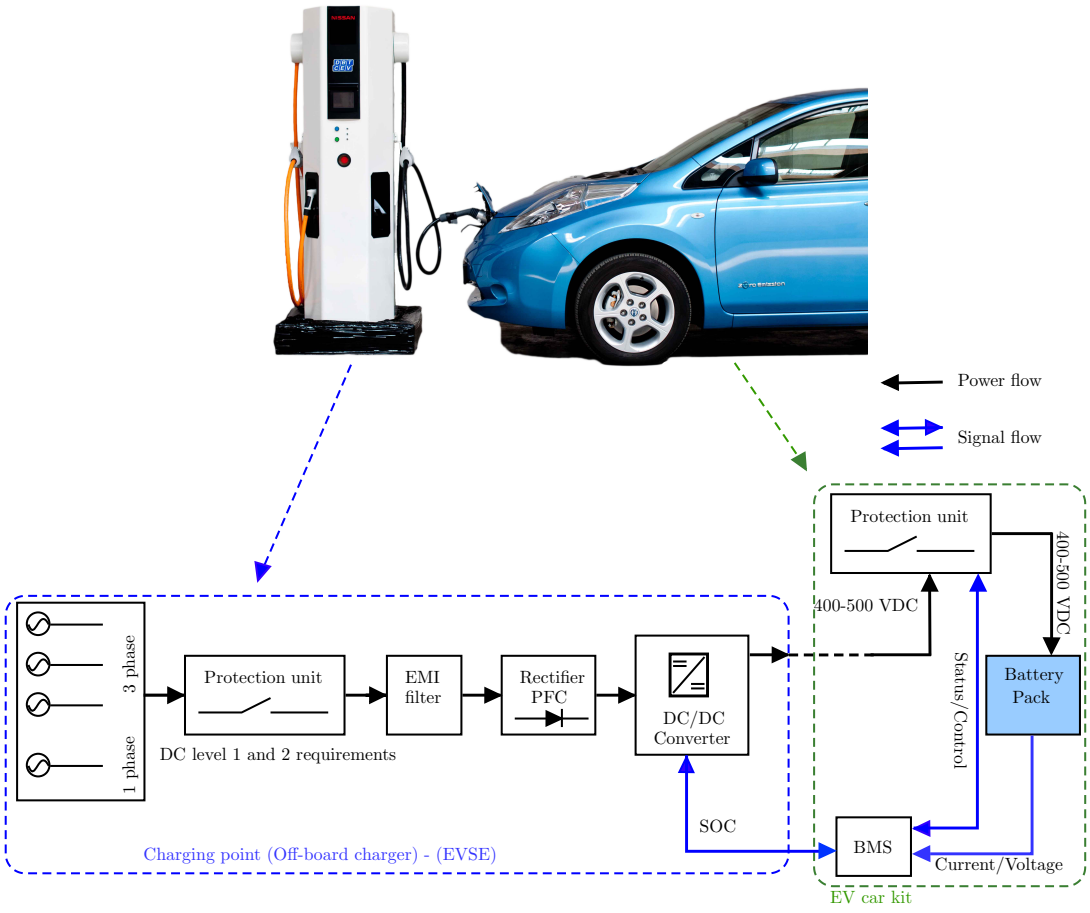

Figure 1.7: Charging configuration and EVSE for DC level 1 and 2 fast charging [Mwasilu 14, DBTCEV 15].

1.3 Vehicle-to-Grid (V2G) technology

1.3.1 Definition

The ability of delivering power from vehicle to the grid, for the first time has been coined "Vehicle-to-grid" (V2G) by AC propulsion Inc. [Emadi 05]. This ability opened new research horizons to take advantage of EVs increment on the grid. In fact in this technology, the plug-in electric or hybrid electric vehicle communicates with electrical grid to sell energy and capacity by managing its charging rate which is achievable by accelerating or decelerating the charging rate or delivering power to the grid.

By this way the vehicles can propose services to the electrical grid, such as providing peak power, regulation and spinning reserves. The studies show that the electric vehicles are not used over than 90 % of the daily time. The usual daily trips in France [CGD 10], Germany [CMS 11] or New York city [White 11] is a mean value between 30 and 50 km. Let consider an EV with 24 kWh battery capacity and 150 km autonomy. Therefore, for a case of normal charging (3 kW) a single EV needs 1 and half hour to 4 hour average charging time. This makes it fully charged and uselessly plugged, in most of the plugged-in time. For this reason, the EVs fleets have high potential for grid service support in these periods. This point could not be taken into account without consideration of EV owner priority and technical limitations concerning to the extra battery degradation due to V2G service concentration.

1.3.2 Types (V2H-V2V-V2B-V2S)

1.3.2.1 Vehicle-to-Home

Vehicle-to-Home (V2H) is a system that allows the driver to supply the home with the energy stored in the battery of the electric vehicle. The EV will be charged during the low demand interval (mostly during night) and will supply back the home when electricity is expensive or in case of any power outage. The system helps alleviate consumption of power in peak periods when demand is highest. Further, it can also be leveraged as backup power supply for emergencies. The challenges under development are related to protection units and standards of providing power control systems. Both on-board and off-board charge are considered for V2H application which guarantees the bidirectional power flow between the home and the vehicle. Figure 1.8 shows a concept of V2H. Some main features of V2H are listed as follow [Liu 13]:

- V2H involves a single EV in a single house.
- V2H has a very simple configuration, hence it is easy to accomplish in reality.
- V2H is able to smooth the household Daily Load Profile (DLP)) with active power exchange.
- V2H is able to provide the reactive power to the home grid or even to the community grid.
- The reactive power support can be implemented without involving, or independent of, the GEV battery, because each charger can solely offer its capacitor for the grid operation.
- V2H can further interact with V2V and V2G operations.
- V2H has a very high efficiency during the operation.
- V2H is easy to be installed without largely changing the existing home grid.
- V2H can improve the effectiveness of home renewable energies by using GEV storage.
- Smart home becomes more attractive with the V2H operation.

- V2H can greatly improve the development of the smart grid.

Figure 1.8: Vehicle-to-Home concept from Nissan motor corporation.

1.3.2.2 Vehicle-to-Vehicle

When a number of vehicles are parked at the same parking or connected to the same grid, can exchange power in order to keep balance of demand and supply. By using this operation power reserve can be kept within the community of the vehicles. This can greatly reduce power loss and trading loss between the local community and also the power grid. The Vehicle-to-Vehicle (V2V) can be performed in existing grid. A framework of DC common grid for V2V concept is illustrated in Figure 1.9 where it shows different vehicles connected to the same DC grid. Using this framework, losses casued by electrical energy conversion in the charger will be decreased. V2V framework has distinct features [Liu 13, Wang 14]:

- Generally, V2V involves multiple EVs.
- V2V uses smart homes and parking lots for power exchange.
- V2H is incorporated into the V2V system. V2H mainly focuses on a domestic house with only one EV interaction, whereas V2V aims to interact with a group of EVs and coordinate them with the power grid. This kind of dividing the frameworks of V2H and V2V can improve the EV coordination with the power grid based on the number of EVs available.
- The EV aggregator is employed for coordinated control of the V2V and grid operation.
- Power exchanges among EVs, and then is requested if necessary from the power grid.
- The framework of V2V is comparatively less simple and less flexible.
- V2V has uncomplicated infrastructure requirements and small transmission losses.
- V2V can be further cooperated with small-scale renewable energies for the community grid operation.
- V2V can further improve the development of the smart grid.

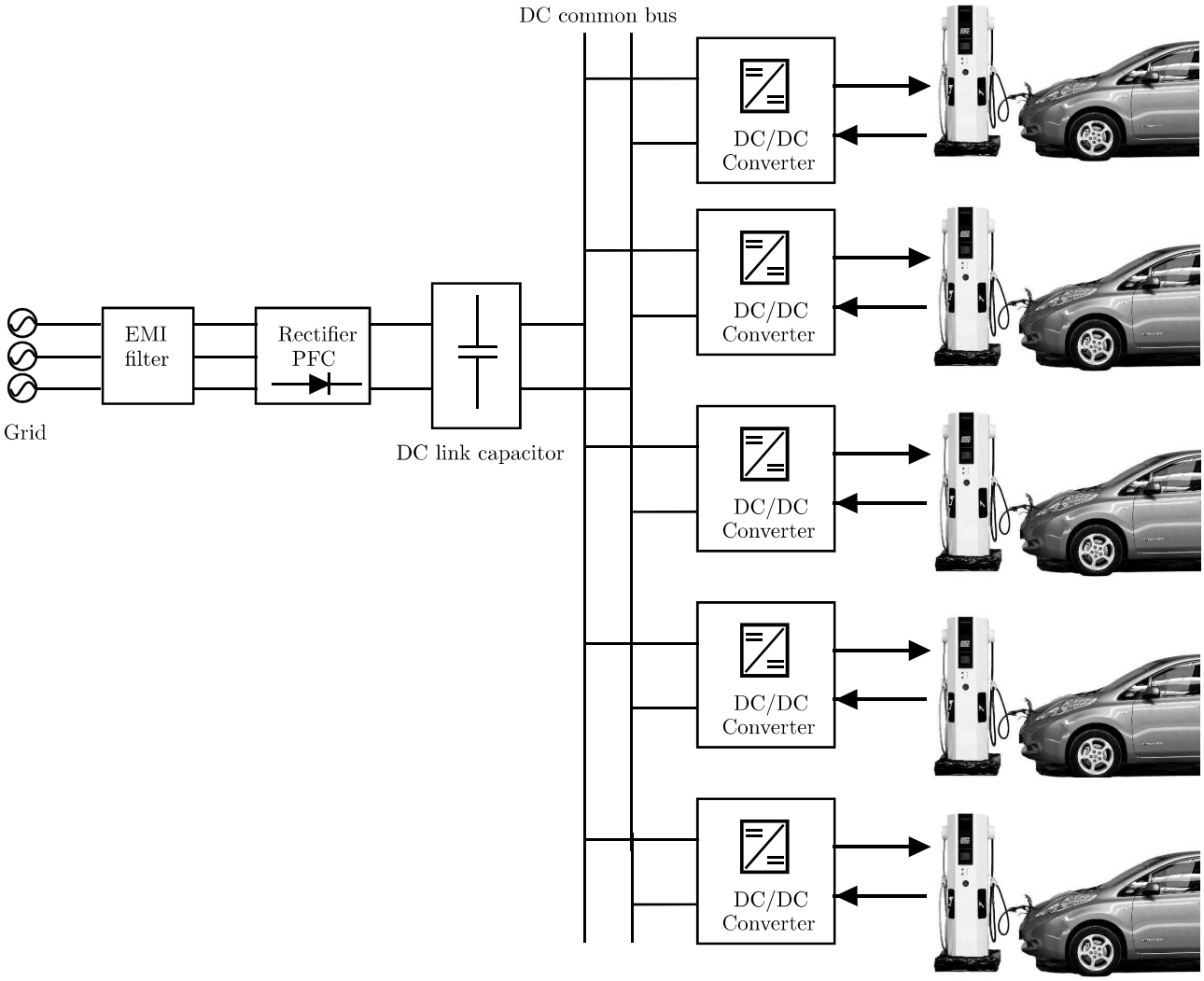

Figure 1.9: Vehicle-to-Vehicle concept by using common DC grid [Yong 15].

1.3.2.3 Vehicle-to-Building

The Vehicle-to-Building (V2B) technology can be considered as combination of V2H and V2V where numerous vehicles are connecting to the same grid inside a parking of a building. This building can be a residential or commercial one. The vehicles in this concept can supply the grid consumption during the peak hours and to be charged at off-peak hours. A more enhanced version considering another sources of energy (renewable energy) connected to the grid of the building can generate a microgrid concept. Figure 1.10 shows a project in Japan where 6 Nissan LEAFs supply an office building to test the V2B technology [NLV].

1.3.2.4 Vehicle-to-Station

The proposed concept of current thesis, is the ability of EVs to supply a railway station internal consumption. This is why the Vehicle-to-Station (V2S) acronym is chosen for this concept. In this concept, it is supposed to have numerous EVs plugged-in inside the railway station parking. These are the vehicles coming in the morning to the station until the afternoon. The availability period of these vehicles are during the day, so they can be used to feed the station. There are challenges related to the availability of the vehicles and the willingness of the owners, where each issue has been sufficiently analyzed in this thesis. Figure 1.11 shows an illustration of this

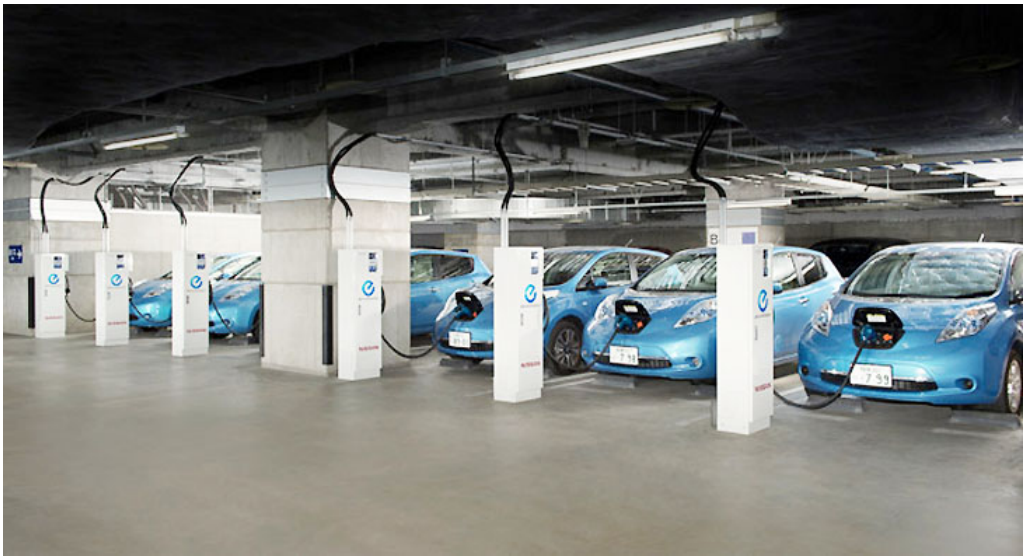

Figure 1.10: Vehicle-to-Building project. 6 Nissan LEAFs feeding an office building in Japan.

concept.

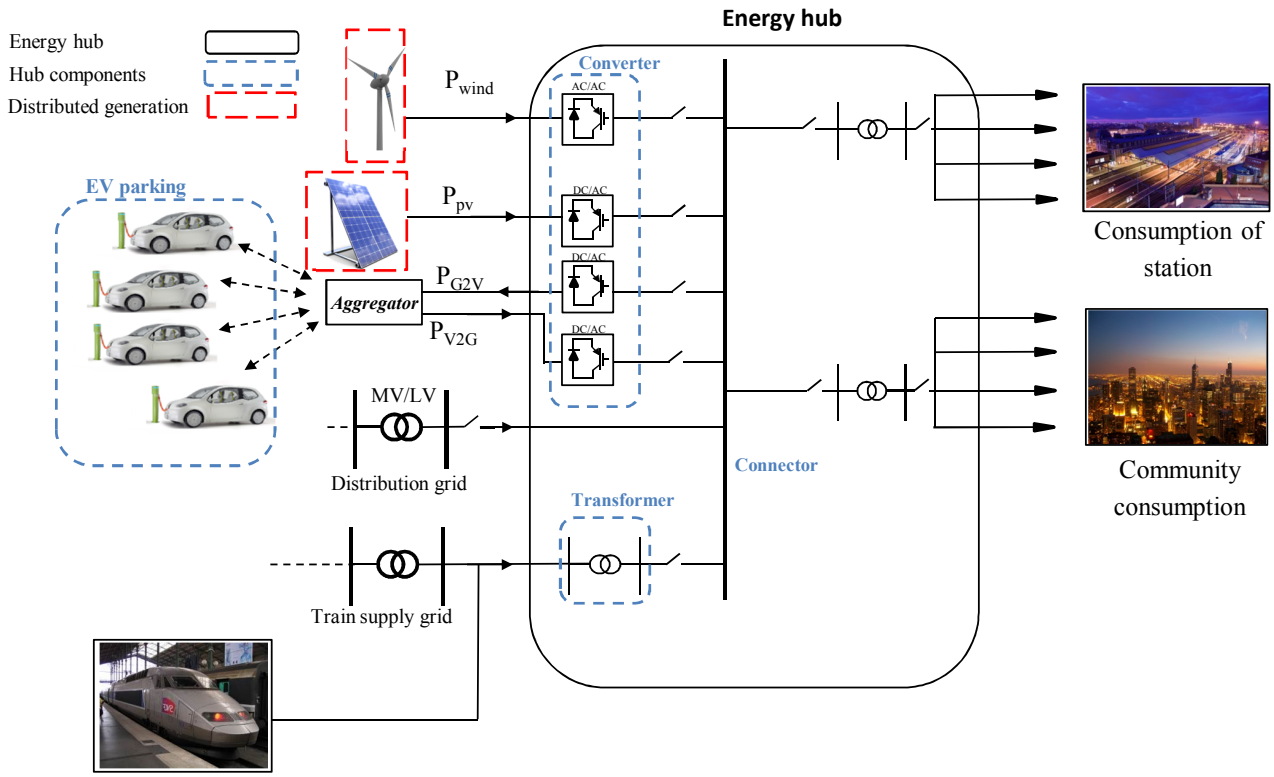

Figure 1.11: Energy hub at railway station, V2S concept proposed in this thesis.

1.3.3 V2G Aggregator

For the purpose of grid support, e.g. frequency regulation, power system operators can communicate with PEVs or PHEVs through a dedicated communication link. Rather than the power utilities having to communicate with each PEV individually, an aggregator can be formed that would act and communicate as a commercial retailer between the power utilities and the mul-

tiple PEVs for selling and buying powers. In addition, as each PHEV has a very small capacity from a grid perspective, it is necessary to implement an aggregating control system, managing a large number of vehicles. Based on the real time grid situations, the aggregators will make real time decisions of charging or discharging of PEVs [Datta 14]. In the context of smart grid, further aggregators can be added for better coordination and reliability. V2G based aggregator system is shown in Figure 1.12. The key elements in an indirect V2G system architecture are aggregators. They act as an interface between the grid and a group of PEV and PHEV. [Quinn 10] shows that presence of an aggregation entity increase the reliability and meeting the minimum contractible power requirements of the V2G ancillary service compared to direct deterministic architecture.

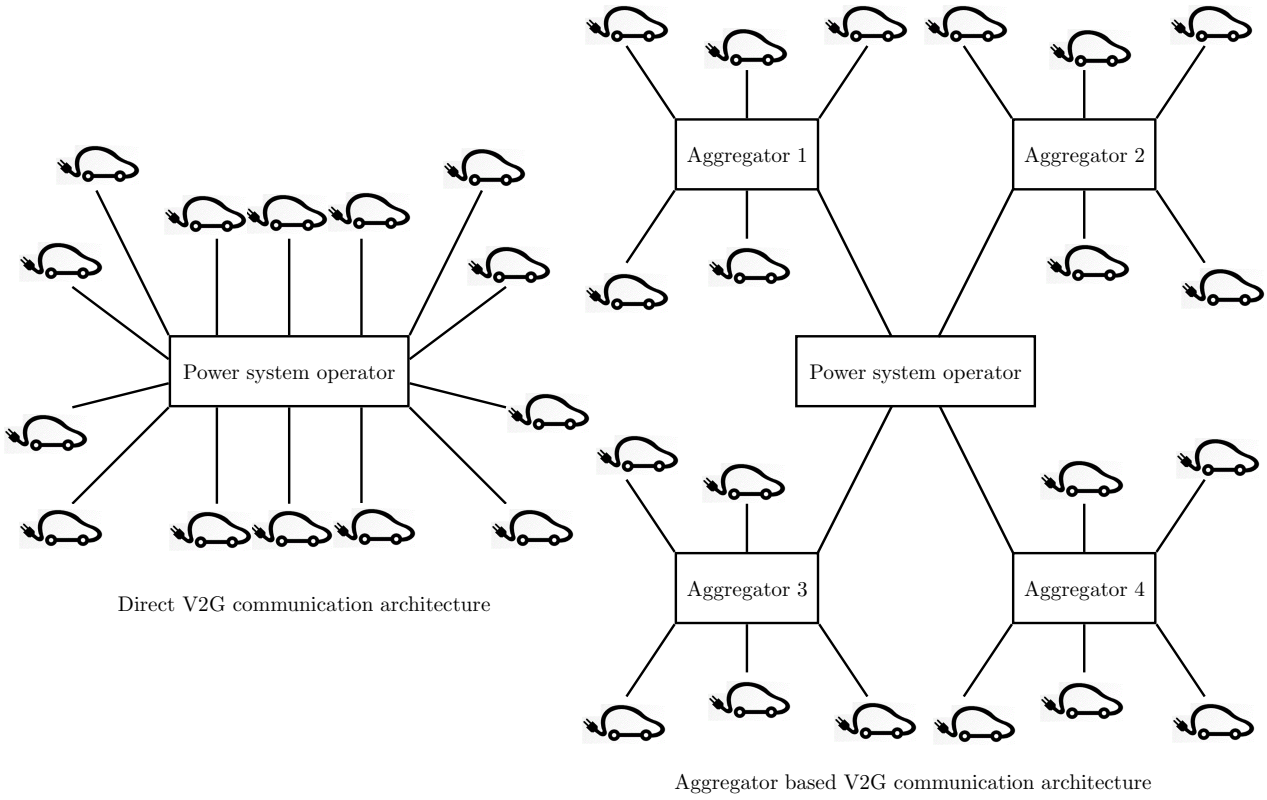

Figure 1.12: Two possible communication architecture for V2G technology ancillary services.

1.3.4 Aggregator strategies

Different strategies for V2G aggregator are proposing everyday by reserchers all around the world [Sandels 10, Khalid 13, Xu 14, Momber 15]. The aim of each aggregator depends on the objective of each type. Optimal aggregator strategies are proposing to reduce the cost functions, related to energy cost for grid utilities or even charging price for the PEV and PHEV owners. These strategies are also considering different ancillary services markets such as regulation, peak power and cost minimization. The structure of an aggregator for a regulation service is depicted in Figure 1.13 [Wang 13]. This shows the flow of necessary information between PEV fleet, the aggregator and power system operator. The aggregator based on the recieved information will make decision for PEV charging/discharging command. These decisions are also based on price of electricity and regulation reference announced by the grid operator. In this model, there is only one aggregation entity managing all the PEVs. In another structure a distrbuted

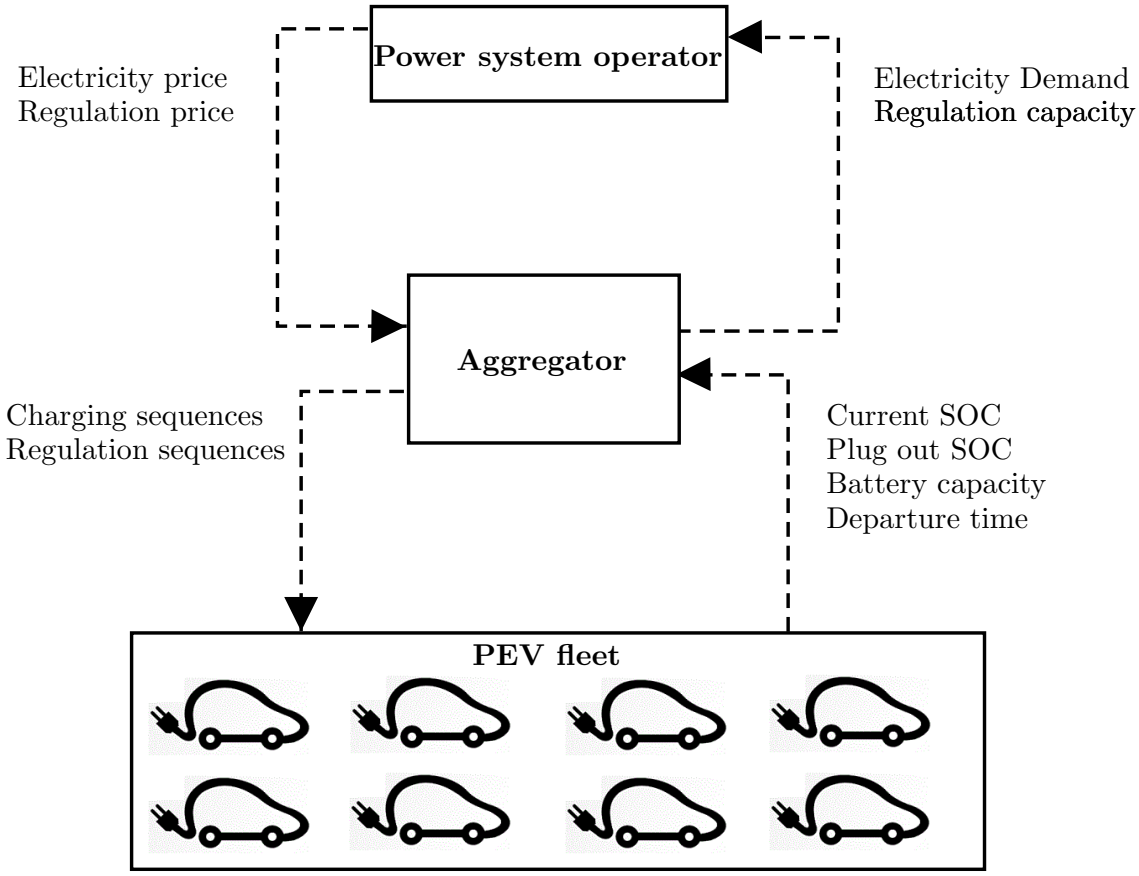

Figure 1.13: Aggregator strategy for regulation service, aggregator acting as an interface between PEV fleet and grid operator.

structure is proposed by [Xu 14] (Figure 1.14). Multiple aggregators at distribution grid level communicate with DSO in order to manage their under control PEV fleet. By aggregating the charging load demand within each independent aggregator before the centralized coordination at the DSO, the computational burden is effectively alleviated, and the reduced volume of data exchanged between the DSO and aggregators enables less investments on communication infrastructure. The detailed customer charging requirement privacies could also be properly protected. In addition, in cases of communication lost between the DSO and aggregator or DSO failure, each aggregator could still easily operate individually to respond the available service. Another strategy for V2G aggegator is proposed by [Sandels 10]. In this strategy, depicted in Figure 1.16, the PEV and PHEVs are devided into different group based on their available SOC and each group provide different service in order to respond to regulation service. Regulation signals are mainly two types; regulation up when the production is less than consumption and regulation down when production is more than consumption. The PEVs can do different act in order to respond the different regulation signals (Figure 1.15).

1.3.5 V2G communication

The vehicle manufacturers and charging station manufacturers have provided consumers options for charging preferences, while there are no existing communications between consumers and the utilities to manage the charging demand. There is also wide variation between manufacturers in their approach to support vehicle charging. There are in-vehicle networks, charging station networks, utility networks each using either cellular, Wi-Fi, ZigBee or other proprietary

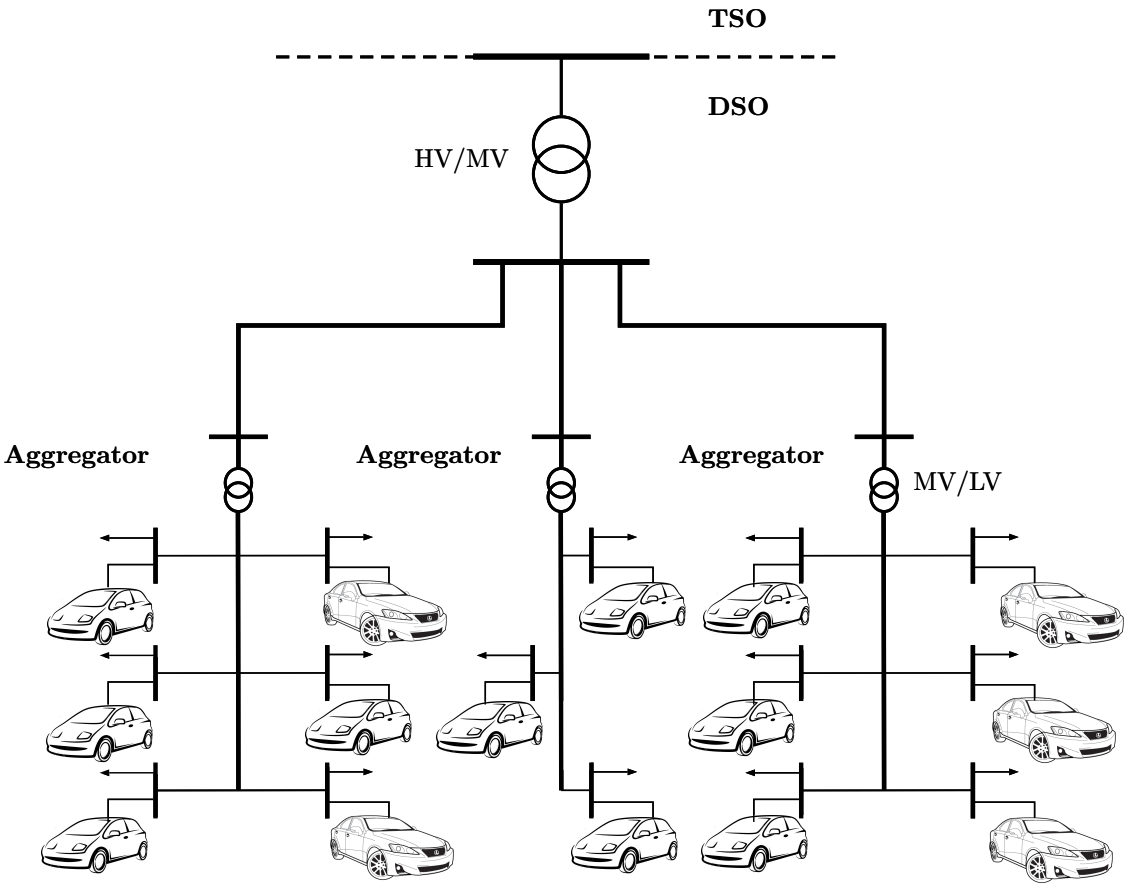

Figure 1.14: Distributed aggregation strategy at distribution grid level, DSO as grid operator and each MV/LV substation as an aggregator entity.

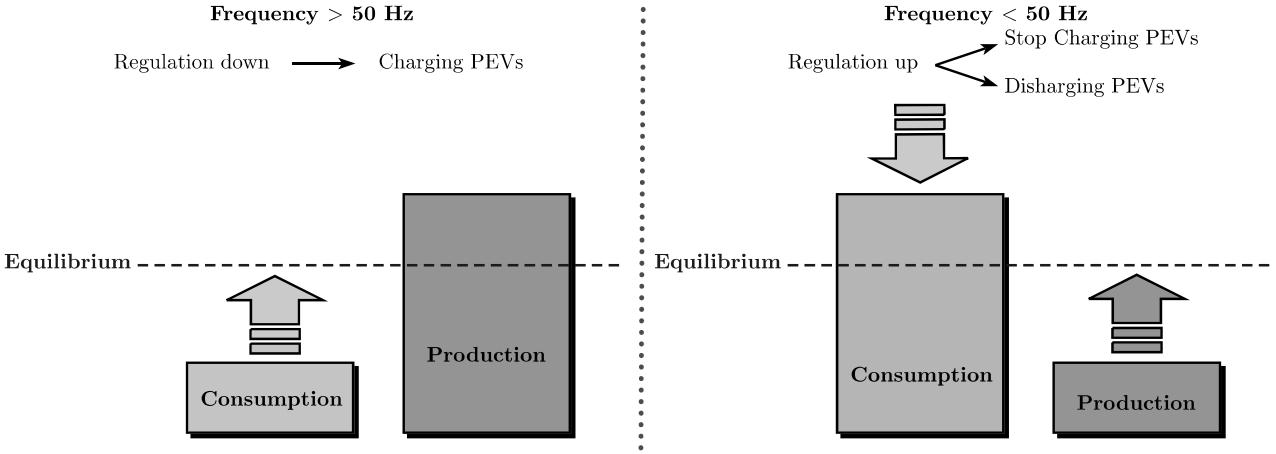

Figure 1.15: Different functionality of aggregator decision based on regulation signals.

communication technology with no standards currently available for interoperability. SAE, the International Standards Organization / International Electrotechnical Commission (ISO/IEC), ANSI, National Institute of Standards and Technology (NIST) and several industrial organizations are working towards the development of interoperability standards. Pacific Northwest National Laboratory (PNNL) has participated in the development and testing of these standards in an effort to accelerate the adoption and development of communication modules [Gowri 11].

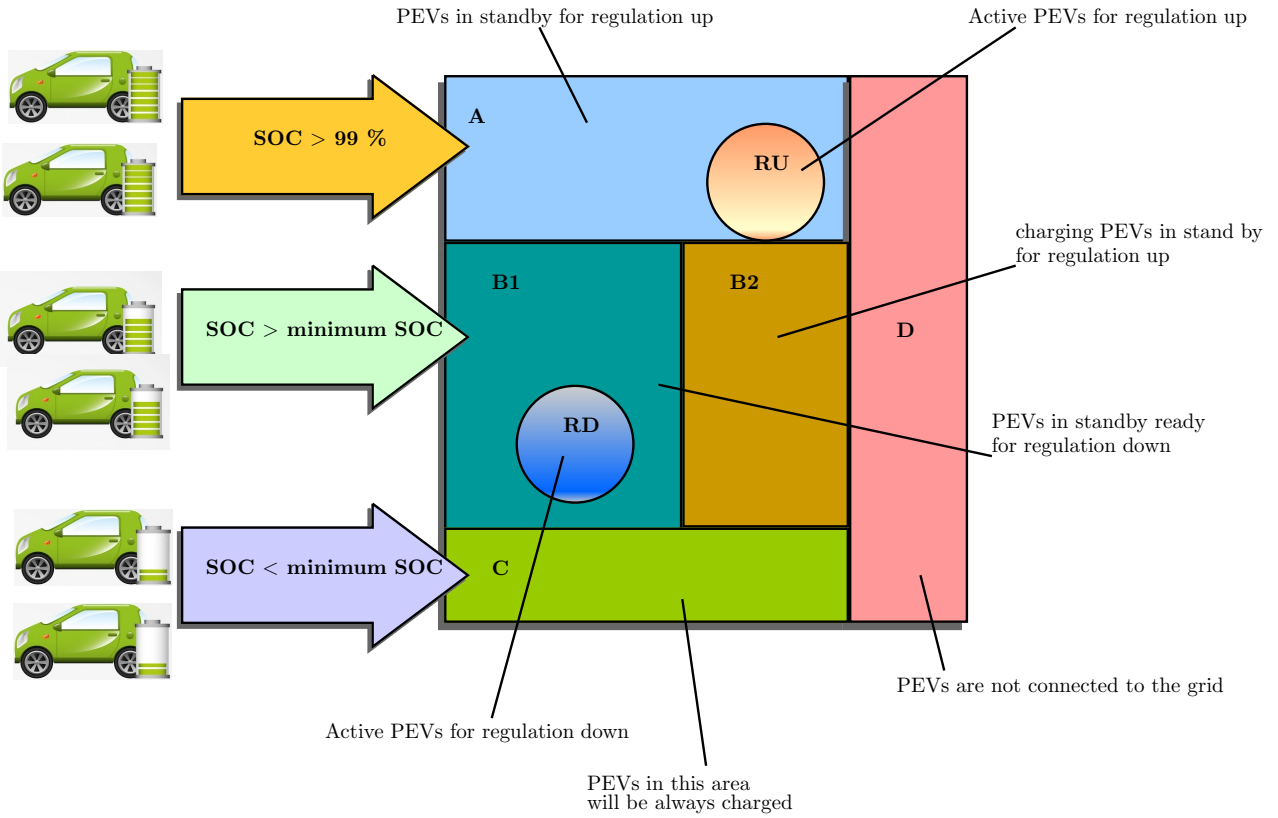

Figure 1.16: Groupping process strategy for aggregator of regulation service.

1.3.5.1 ISO/IEC 15118: Vehicle to grid communication interface

ISO 15118 specifies the communication between Electric Vehicles (EV), including Battery Electric Vehicles and Plug-In Hybrid Electric Vehicles, and the Electric Vehicle Supply Equipment (EVSE). As the communication parts of this generic equipment are the Electric Vehicle Communication Controller (EVCC) and the Supply Equipment Communication Controller (SECC), ISO 15118 describes the communication between these components [IEC 13]. IEC 15118 contains eight parts where three parts of it is already developed:

- Part 1 (2013): General information and use-case definition
- Part 2 (2014): Network and application protocol requirements ISO 15118-2:2014 specifies the communication between Battery Electric Vehicle (BEV) or plug-in hybrid electric vehicles (PHEV) and the Electric Vehicle Supply Equipment. The application layer message set defined in ISO 15118-2:2014 is designed to support the energy transfer from an EVSE to an EV [IEC 14].
- Part 3 (2015): Physical and data link layer requirements ISO 15118-3:2015 specifies the requirements of the physical and data link layer for a high-level communication, directly between BEV or PHEV, termed as EV (electric vehicle) [ISO-1], based on a wired communication technology and the fixed electrical charging installation [Electric Vehicle Supply Equipment (EVSE)] used in addition to the basic signalling, as defined in IEC-1 [IEC 15].

1.3.5.2 Open Charge Point Protocol (OCCP)

OCCP is a communication protocol between charging stations and a central management system. Currently, most of public charging stations are using the protocol version 1.5. In new

version 2.0, uses Hyper Text Transfer protocol (HTTP) for data transferring [Wellisch 15]. Its aim was to create an open application protocol which allows EV charging stations and central management systems from different vendors to communicate with each other. It is in use by a large number of vendors of EV charging stations and central management systems all over the world. Figure 1.17 shows a basic schematic of V2G and smart charging communication protocols.

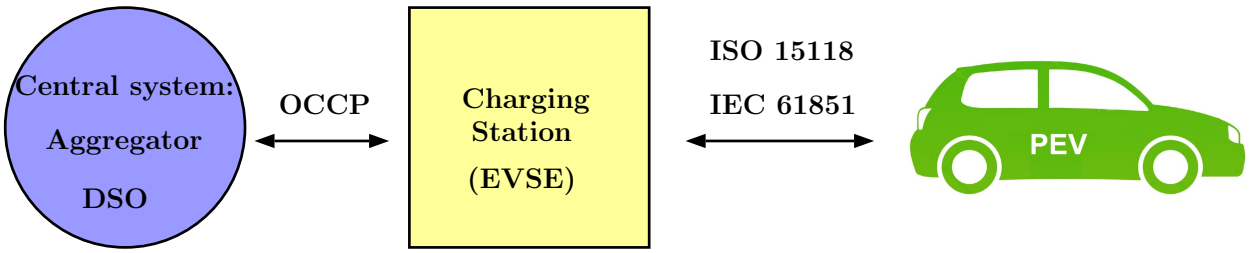

Figure 1.17: Smart charging communication protocol containing V2G communication.

1.3.6 Actual constraints of V2G implementation

Based on the actual progress of the technologies and current standards of the ancillary services, the implementation of V2G ancillary services is not possible. In other word, there are some constraints that limit the participation of actual electric vehicles into the V2G ancillary services. These constraints are composed of two parts; first the technological limitation of bi-directional power flow for the actual electric vehicles and secondly, the requirements of ancillary services at the distribution grid level. These two limitations are explained afterwards.

The actual electric vehicle's battery chargers are only designed for unidirectional power flow which permits only the charging actions for EV batteries. While for V2G action, a bidirectional converter needs to be designed and implemented in vehicles for n-board charging systems or at charging stations for off-board charging modes.

Based on the actual French grid code, the contribution of any controllable load connected to the distribution grid into the frequency regulation service is restricted. This is due the standards that limit the connection of MV feeders (départ Haute Tension A (HTA)) in the lack of balanced frequency. In the case of frequency drop the MV feeders will be disconnected by the disjuncture connected to the head of each feeder. Therefore, the actual grid code need to be modified in order to make possible the contribution of V2G-enabled EVs into the grid ancillary services.

In the continue of the following chapter, the possible ancillary services that can be provided by EVs are introduced. These services are the possible contribution of EVs in the frame of V2G technology.

1.4 V2G Ancillary Services

For the sake of maintaining grid reliability and balance of production and consumption, the existence of ancillary services are necessary. These services support the reliable transmission of power from producers to the customers [Yilmaz 13]. In this section analyses about the competitive V2G ancillary services, by inspiration from Distributed Energy Storage Systems (DESS) ancillary services for distribution MV and LV grid provided in [Delille 09], will be conducted. Therefore, the competitive services, considering the DESS services requirement (Table 1.2), will be assessed.

Table 1.2: DESS Ancillary service requirement

Ancillary Services	DESS services requirement			
	Minimum required power	Required interval	Benefitted stake-holder	Appropriate V2G scenario
AS1	1 MW	30 sec - 15 min	TSO	S7-S8
AS2	2-3 MW	30 sec - ALAR*	TSO	S7-S8
AS3	10 MW	30 min - 6h	TSO	Several S8
AS4	500 kW (MV) 100 KW (LV)	2 -10h	TSO - DSO - Costumer	S3-S4
AS5	100 kvar	ALAR	DSO	S3-S4
AS6	100 kW - 2 MW	20min -1h30	Distributed generators	S3 to S8

*As Long As Required

1.4.1 Regulation

Regulation consists of the processes which lead to balance the production and consumption in the whole electricity grid to achieve fine-tune of frequency of the grid. In France the RTE, which is part of the European Network of Transmission System Operators for Electricity (ENTSO-E), is acting as a TSO, responsible for regulation services. This service consists of primary, secondary and tertiary control. an example of power plant outage leading the activation of the services are illustrated in the Figure 1.18.

1.4.1.0.1 Primary control (AS1) Primary control is acting automatically within 15 to 30 seconds to stabilize the frequency at a reference value of 50 Hz. However, the dynamic time response should be more faster something around 1 to 10 seconds. This regulation is common (i.e. similar to PJM[4] frequency response) for all the ENTSO-E members with a 3000 MW capacity [Petit 13]. All generating units with a capacity higher than 40 MW have to contribute to primary control. This represent 600 MW for the French system.

In France, the primary reserve receives a fixed capacity payment, i.e. 8 €/MW within 30 minutes [Petit 13]. The ability of an aggregated EV fleet providing primary control has been assessed in [Petit 13] where the results showed contribution to funding energy cost and battery investment cost reduction. For this service, the requirements is met by minimum V2G power of 2.7 and 2.4 MW (atleast 5000 EVs fleet), respectively. controlling these amount of EVs needs aggregation strategies at TSO level.

1.4.1.0.2 Secondary control (AS2) The secondary reserve will be activated automatically after primary within 100 to 200 seconds. All producers in France with more than 120 MW capacities are required to allocate a portion to the secondary reserve to provide total capacity

[4]PJM Interconnection LLC (PJM) is a regional transmission organization (RTO) in the United States. It is part of the Eastern Interconnection grid operating an electric transmission system serving all or parts of Delaware, Illinois, Indiana, Kentucky, Maryland, Michigan, New Jersey, North Carolina, Ohio, Pennsylvania, Tennessee, Virginia, West Virginia, and the District of Columbia.

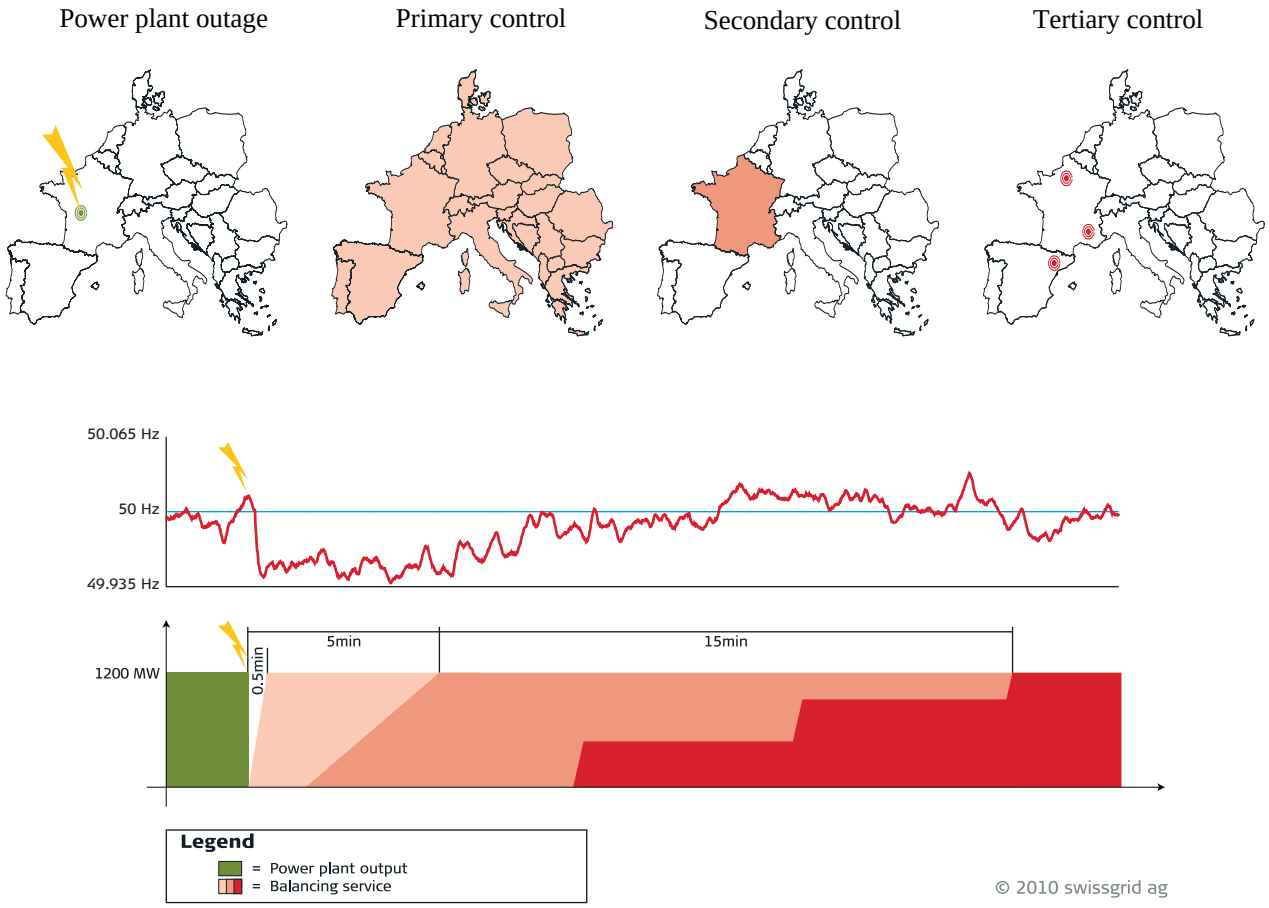

Figure 1.18: Example of a power plant outage in France with three level of regulation [Beck 10].

between 500 to 1000 MW for secondary reserve. Secondary reserve makes possible the restoring for primary control, where tertiary makes it for secondary. Secondary reserve is paid for capacity, the same as primary, and for energy delivered, (i.e. 9.3 €/MWh [Petit 13]). For the EV owners secondary reserve is more interesting since they will be paid for both energy and capacity.

1.4.1.0.3 Tertiary control (Balancing mechanism)(AS3) The French producers and customers, subject to the availability of 10 MW, are encouraged to participate in adjustment mechanism (balancing mechanism). This bid will be additional to the contracted reserves. Balancing mechanism is a part of tertiary control of the regulation services which is called as 30 minutes complementary tertiary reserve [Rebours 05]. In this service, Controlling the EV fleet is much more difficult as the bidding capacity is quite larger. Although, the interests for capacity payment increase the EV owners participation.

1.4.2 Peak power shaving (AS4)

For the DESS application, peak shaving and valley filling is when a storage unit is used to shift the load from peak to off-peak hours. Thanks to a supervision system, by controlling the charging periods of EVs fleet and shifting as often as possible the charging time to the off-peak hours, the number of Subscribed Power Exceeding (SPE) will be reduced. Therefore, the interests are:

- The investment for grid infrastructure reinforcement will be postponed (e.g. investment

reduction up to 35% for distribution networks [P. Fernandez 11]).

- The energy transmission cost minimization; In France, distribution system operator (DSO) pays to TSO for its energy transmission cost which highly depends on SPE and extracted energy.
- As a point of view of an energy supplier, for the sake of energy purchase price optimization, the customers should be encouraged to participate in peak shaving service by consuming more during low-cost periods and less during high-cost hours. This could be an opportunity for V2G enabled EVs to contribute to the grid ancillary services.
- The customers (e.g. EV owner) by participating in this service can minimize the energetic part of their invoice (i.e. maintain at the level it was before purchasing an EV) as well as gain from V2G services. This participation in case of predictable peaks and short period can be profitable (e.g. up to 100 €/kW [Delille 09]).

For this service, 540 kW power for MV level can be considered. A supervision system, in DSO level, can properly manage a fleet of 500 to 1000 EVs to participate in peak shaving service.

1.4.3 Reactive power compensation (AS5)

As a part of power quality services, thanks to the power electronics converters, the reactive power correction can be tackled by V2G by controlling the angle between voltage and current without any major effect on the charging process. This can be achieved in both charging and discharging periods. For this service 500 EVs fleet can be sufficient.

1.4.4 Renewable energy support (AS6)

The variable behavior of renewable energy sources (e.g. wind and solar) reduces their contribution to the grid service as there is no high reliability to their availability. Thanks to the storage systems, their contribution to the ancillary services, such as primary control will be increased. In this case the Distributed Generation (DG) producers are able to provide reliable control power to the grid. V2G fleet can act as a DESS to support the storage need of the DG centers by coordination of its charging time with the production of DG center. The only thing that may reduce the interests for EV owners is the stochastic behavior of such sources, when the proposed charging periods may not be necessarily at the availability periods of the EVs.

1.4.5 Base load (AS7)

Base load power is provided continuously by large generation unit which has low cost per kWh. V2G has been analyzed for this service [Kempton 05a], [Kempton 05b] showing that there is no competitive price as the EVs have limited storage capacity, high energy cost per kWh and less charging access at transmission level.

1.5 Conclusion

Integration of electric vehicle to the electrical networks along with literature review on electrical networks in France and V2G technology were introduced in this chapter. The integration of EVs has two main aspects, which should be accurately studied: market contribution and technical contribution. This integration from many points can have negative impacts, if there is no

coordination and central control system. These impacts are mainly discussed in second chapter of the thesis and some possible solutions are examined, where their benefits are also investigated. In addition, thanks to the technologies, such as Vehicle-to-Grid and its different types (V2H-V2V-V2B-V2S), the contribution of EVs can have numerous possibilities that should be carefully studied; The contribution from technical point of view but also financial point for both grid and EV owners. The exact and clear benefits for the EV owners and grid is a difficult task to respond, where in this thesis the aim is to clarify the possibilities to provide possible technical and financial services incorporated with benefits for both side. The concentration will be more on services for DSO and parking facilities in railway stations.

1.6 Résumé

Dans ce chapitre, un état de l'art sur les réseaux électriques, les véhicules électriques et la technologie Vehicle-to-Grid a été mené. Dans le contexte des réseaux électriques, les différents types de réseau ont été présentés avec une vision globale sur les marchés d'énergies et les services systèmes potentiels pour les véhicules électriques. Ensuite, une étude sur les différentes technologies de propulsion des véhicules électriques a été faite. Les normes actuelles de recharges des VE dans le monde et en France ont été présentées. A la fin de ce chapitre, la technologie V2G a été introduite avec l'ensemble des types et les structures des agrégateurs et les normes de télécommunication. En dernier, les services système potentiels pour la technologie V2G ont été présentés.

1.6.1 Réseaux électriques

Pour être acheminée depuis les centres de production vers les consommateurs, l'électricité emprunte :

- le réseau public de transport d'électricité, destiné à transporter des quantités importantes d'énergie sur de longues distances ;
- le réseau public de distribution, destiné à acheminer l'électricité en moins grande quantité et sur de courtes distances.

Le réseau de transport a vocation à acheminer des quantités importantes d'électricité sur de grandes distances, entre les régions et vers les pays voisins. RTE est le gestionnaire du réseau public de transport d'électricité français. Ce réseau est constitué de toutes les lignes exploitées à une tension supérieure à 50 kV sur le territoire métropolitain continental.

Le réseau achemine l'électricité entre les producteurs d'électricité et les consommateurs industriels directement raccordés au réseau ou les distributeurs d'électricité. L'énergie électrique produite est portée à un niveau de tension de 400 kV, ce qui permet de la transporter sur de longues distances en minimisant les pertes. La tension est ensuite abaissée en 225 kV, puis 90 ou 63 kV pour l'alimentation régionale et locale en électricité.

La France s'est fixée l'objectif de porter à 32% en 2030 la part des énergies renouvelables dans la consommation finale d'énergie. L'insertion des énergies renouvelables dans les réseaux de transport et de distribution est donc un enjeu majeur de la transition énergétique.

Les réseaux de distribution acheminent l'électricité sur de plus courtes distances, pour une alimentation de la consommation locale, mais aussi le raccordement de certains producteurs d'électricité de petite et moyenne puissance. Ils sont constitués d'ouvrages de moyenne tension (entre 1 000 V et 50 kV) et d'ouvrages de basse tension (inférieure à 1 000 V).

Dans ce chapitre les services systèmes potentiels au niveau des réseaux de distribution et du transport ont été présentés.

RTE dispose de réserves de puissance mobilisables pour contribuer à maintenir l'équilibre entre la production et la consommation d'électricité : notamment les services système (réserves primaire et secondaire) et le mécanisme d'ajustement (réserve tertiaire), auxquels participent la plupart des grandes installations de production, et, de plus en plus, certaines installations de consommation.

Les réserves primaire et secondaire sont activées automatiquement avec un délai qui va de quelques secondes à quelques minutes. L'activation de la réserve tertiaire se fait manuellement par appel aux producteurs et aux consommateurs connectés au réseau pour qu'ils modifient très rapidement leur programme de fonctionnement prévu.

1.6.2 Intégration des véhicules électriques sur les réseaux électriques

Actuellement, le concept de réseau intelligent (smart grid) et ses définitions, les applications, les impacts et la contribution au réseau électrique classique sont largement discutés dans les sociétés académiques et industrielles. Le problème des limitations des ressources d'énergie fossile, leurs impacts environnementaux conduisent à l'introduction de nouveau concept de réseau qui inclue la contribution bidirectionnelle entre la production et la consommation. Dans cette idée, la présence des sources d'énergie renouvelables telles que le solaire photovoltaïque, l'éolien et les véhicules électriques (VE) avec la technologie vehicle-to-grid (V2G) est mise en avant. Ces sources de productions décentralisées peuvent être stockées pendant les heures de pointe et réutilisées pendant les heures creuses. Au contraire, il est également important de prendre en considération les impacts indésirables de la croissance du transport électrifiée sur le réseau électrique, en raison de la coïncidence du pic de la charge quotidienne (consommation classique) et les charges des véhicules électriques.

Dans ce chapitre, les normes actuelles de recharge des VEs en France sont présentées ainsi que leurs impacts sur les réseaux de distribution ont été étudiés. Ensuite, la technologie V2G a été introduite. Cette technologie, pourrait offrir une solution aux opérateurs d'énergie et une rémunération aux propriétaires de voitures électriques. En fonction du type de dimension de réseau électrique auquel le véhicule est connecté, plusieurs types de cette technologie sont possibles. Par exemple, l'énergie stockée dans les batteries pourrait suppléer directement aux exigences électriques de l'habitation durant les pointes de consommation ou une panne du réseau électrique, auquel cas on parle du concept Vehicle-to-Home (V2H) [Dargahi U. 14].

Ensuite, une étude sur les stratégies de gestion du V2G a été effectuée. Dans ce contexte un organisme d'agrégation a été introduit. L'agrégateur se situe entre les producteurs d'électricité et les consommateurs. D'un côté, il garantit aux premiers une capacité virtuelle d'allégement de la demande électrique lors des pics de consommation et de l'autre il propose des services de gestion de l'énergie aux consommateurs, leur permettant une réduction des factures d'énergie électrique. Les différentes technologies de télécommunications, les normes et les architectures sont aussi présentées. La norme de communication pour la technologie V2G a été introduite sous le nom d'ISO 15118. Cette norme précise la communication entre le véhicule, la batterie et les équipements d'alimentation (EVSE). Cette norme contient 8 parties à laquelle 3 parties sont actuellement développées.

1.6.3 Les contraintes actuelles pour l'intégration du V2G

Par rapport à l'état d'avancement des technologies et des normes actuelles de services système, la mise en œuvre de services système du V2G n'est pas une tache simple à faire. En d'autres mots, il existe certaines contraintes qui limitent la participation des véhicules électriques actuels dans les services système du V2G.

Ces contraintes sont composées de deux parties; premièrement, les limites technologiques de flux de puissance bidirectionnels pour les véhicules électriques actuels et deuxièmement, les exigences de services système aux niveaux des réseaux de distribution. Ces deux limites sont expliquées par la suite.

Les chargeurs de batterie du véhicule électrique sont uniquement conçus pour le rechargement qui n'autorise que les actions de charge pour les batteries des VEs. Alors que pour l'action V2G, un convertisseur bidirectionnel doit être conçu et mis en œuvre dans les véhicules pour les systèmes de recharge à bord ou dans les bornes de recharge pour les systèmes de recharges hors-bord.

En France, avec le grid code actuel, la contribution de toute les charges contrôlables connectées aux réseaux de distribution pour le réglage de fréquence est restreinte. Cela est dû plan

de sureté qui impose un délestage fréquence métrique des départs HTA dans le cas d'une forte chute de fréquence. Dans le cas de la baisse de fréquence, le départ concerné sera déconnecté par le disjoncteur connecté à la tête de chaque départ. Par conséquent, le grid code actuel nécessite d'être modifié afin de rendre possible la contribution du V2G dans les services système.

1.6.4 Les services système pour le V2G

Dans la dernière section de ce chapitre, un état de l'art sur les services système possibles pour la technologie V2G est présenté. De plus, une étude a été réalisée au troisième chapitre de ce mémoire qui est dédié aux services système possibles pour le V2G en tenant compte des incertitudes et des contraintes aux niveaux de la disponibilité des véhicules électriques.

Dans ce chapitre en considérant les flottes des VEs comme une unité d'stockage d'énergie, les services possibles pour l'unité de stockages sont étudiés pour les véhicules électriques.

1.6.4.1 Réglage primaire de la fréquence

La constitution de la réserve primaire est assurée par l'ensemble des producteurs européens interconnectés aux réseaux de transport de la plaque continentale européenne synchrone. Pour dimensionner cette réserve, on considère qu'elle doit pouvoir répondre à la perte simultanée des deux plus gros groupes de production présents sur cette plaque, soit une puissance de 3000 MW.

En France, la réserve primaire reçoit un paiement de capacité fixe, c'est-à-dire 8 €/MW dans les 30 minutes. La capacité d'une flotte de VE, fournissant le réserve primaire a été évaluée en [Petit 13] où les résultats ont montré la contribution au financement du coût de l'énergie et à la réduction des coûts d'investissement de la batterie. Pour ce service, les exigences sont remplies par la puissance minimum du V2G de 2,7 et 2,4 MW (au moins 5000 VEs). Le contrôle de ces nombres de VEs a besoin de stratégies proposées par un agrégateur au niveau de GRT.

1.6.4.2 Réglage secondaire de la fréquence

Tous les producteurs de la zone France possédant des groupes de production de plus de 120 MW ont l'obligation d'affecter une partie de leur puissance à la réserve secondaire. Cette dernière est comprise entre 500 MW et 1000 MW, selon la plage horaire et la période de l'année. Le réserve secondaire est payée pour la capacité, la même prime que celle de la réserve primaire, et de l'énergie livrée, (c'est-à-dire 9.3 €/MWh). Pour les propriétaires de VEs la réserve secondaire est plus intéressante car elles sont versées pour l'énergie et la capacité.

1.6.4.3 Réglage tertiaire de la fréquence ou mécanisme d'ajustement

Tous les producteurs et consommateurs français, ainsi que certains acteurs étrangers peuvent, à condition de disposer de 10 MW, participer au mécanisme d'ajustement. Dans ce service, la gestion de la flotte des VEs est beaucoup plus difficile car la capacité d'appel d'offres est assez grande. Bien que les intérêts pour le paiement de capacité augmenteront la participation des propriétaires des VEs dans ce service.

1.6.4.4 Lissage des points

L'écrêtement des pointes est lorsqu'une unité de stockage est utilisée pour décaler la charge de pic en dehors des heures de pointe. Grâce au système de supervision, en contrôlant les périodes de rechargement des VEs et décaler le temps de charge aux heures creuses, le dépassement de puissance souscrite sera réduit.

Pour ce service, 540 kW de puissance pour le niveau HTA peut être considérée. Un système de supervision d'un GRD peut gérer une flotte de 500 à 1000 VEs, afin de participer au service d'écrêtement de pointe (lissage des pointes).

1.6.5 Conclusion

L'intégration des véhicules électriques dans les réseaux électriques avec une étude bibliographique sur les réseaux électriques en France et la technologie de V2G ont été présentées dans ce chapitre. L'intégration des VEs a deux aspects principaux qui devraient être étudiés avec précision; La contribution du marché et la contribution technique. Cette intégration en de nombreux points, peut avoir des impacts négatifs s'il n'y a pas de coordination et un système de contrôle centralisé. Ces impacts sont principalement discutés en deuxième chapitre de la thèse et de quelques solutions possibles sont examinées, où leurs prestations sont également étudiés. En outre, grâce aux technologies, tels que V2G et ses différents types (V2H-V2V-V2B-V2S), la contribution des VEs peut avoir de nombreuses possibilités qui devraient être étudiées attentivement; La contribution du point de vue technique mais aussi financier pour les propriétaires des VEs et le réseau. Les avantages exacts et clairs pour les VEs et le réseau est un tâche difficile à traiter, où dans cette thèse l'objectif est de clarifier les possibilités d'offrir des services techniques et financières possibles accompagnement des avantages pour les deux côtés.

1.7 References

[Beck 10] Martin Beck & Marc Scherer. *Overview of ancillary services.* https://www.swissgrid.ch/dam/swissgrid/experts/ancillary_services/Dokumente/D100412_AS-concept_V1R0_en.pdf, 2010. vi, 29

[BLU 15] BLU. *Electricity production by sources in France.* www.bluenomics.com, 2015. vi, 10

[CGD 10] CGD. *La mobilité des Français: panorama issu de l'enquête nationale transports et déplacements 2008.* http://www.developpement-durable.gouv.fr/IMG/pdf/Rev3.pdf, Dec. 2010. 19

[CMS 11] CMS. *Continental Mobility Study.* http://www.contionline.com/generator/www/com/en/continental/csr/themes/downloads/download/umfrage_mobilitaetsstudie_en.pdf, 2011. 19

[Dargahi U. 14] Ardavan Dargahi U. *Gestion des flux multi-énergie pour les systèmes V2H.* PhD thesis, Grenoble, 2014. 33

[Datta 14] M. Datta. *Fuzzy logic based frequency control by V2G aggregators.* In Power Electronics for Distributed Generation Systems (PEDG), 2014 IEEE 5th International Symposium on, pages 1–8, June 2014. 23

[DBTCEV 15] DBTCEV. *DBTCEV, DBT charging electric vehicle.* www.dbtcev.fr/en/, 2015. vi, 18

[DEL 15] DEL. *Deloitte, Europeen energy market reform country profile: France.* www2.deloitte.com, 2015. vi, 11

[Delille 09] Gauthier Delille, Bruno Francois, Gilles Malarange & Jean-Luc Fraisse. *Energy storage systems in distribution grids: new assets to upgrade distribution networks abilities.* In Proc. 20th International Conference and Exhibition on Electricity Distribution (CIRED2009), 2009. 27, 30

[Ehsani 09] Mehrdad Ehsani, Yimin Gao & Ali Emadi. Modern electric, hybrid electric, and fuel cell vehicles: fundamentals, theory, and design. CRC press, 2009. 14

[ELE 12] ELE. *Electric car pledge, Electric Vehicle Charger Types.* www.electriccarpledge.com, 2012. 17

[Emadi 05] Ali Emadi. Handbook of automotive power electronics and motor drives. CRC press, 2005. 14, 19

[ERDF 14] ERDF. *ERDF, Prepare Electric vehicle develoment.* www.erdf.fr/ERDF_Preparer_developpement_vehicules_electriques, 2014. 12

[Gowri 11] Krishnan Gowri, Robert G Pratt, Frank K Tuffner & Michael CW Kintner-Meyer. Vehicle to grid communication standards development, testing and validation: status report. Pacific Northwest National Laboratory, 2011. 25

[GRE 13] GRE. *Green car report, Electric vehicle Supply Equipment.* www.greencarreports.com, 2013. 17

[IEA 15] IEA. *International Energy Agency, Key world energy statistics.* www.iea.org/publications/freepublications, 2015. 9

[IEC 03] IEC. Iec 62196-1 plugs, socket-outlets, vehicle couplers and vehicule inlets – conductive charging of electric vehicles–part 1: Charging of electric vehicles up to 250 a a.c. and 400 a d.c. IEC, 2003. 15

[IEC 13] IEC. *Road vehicles - Vehicle to grid communication interface - Part 1: General information and use-case definition.* www.iso.org/iso/catalogue_detail.htm?csnumber=55365, 2013. 26

[IEC 14] IEC. *Road vehicles - Vehicle to grid communication interface - Part 2: Network and application protocol requirements.* www.iso.org/iso/catalogue_detail.htm?csnumber=55366, 2014. 26

[IEC 15] IEC. *Road vehicles - Vehicle to grid communication interface - Part 3: Physical and data link layer requirements.* www.iso.org/iso/catalogue_detail.htm?csnumber=55367, 2015. 26

[INV 15] INV. *Investopedia, Over-The-Counter market.* www.investopedia.com, 2015. 12

[Kempton 05a] Willett Kempton & Jasna Tomić. *Vehicle-to-grid power fundamentals: Calculating capacity and net revenue.* Journal of Power Sources, vol. 144, no. 1, pages 268–279, June 2005. 30

[Kempton 05b] Willett Kempton & Jasna Tomić. *Vehicle-to-grid power implementation: From stabilizing the grid to supporting large-scale renewable energy.* Journal of Power Sources, vol. 144, no. 1, pages 280–294, June 2005. 30

[Khalid 13] M.W. Khalid, A.T. Al-Awami & E. Sortomme. *Stochastic-programming-based bidding strategy for V2G services.* In Innovative Smart Grid Technologies Europe (ISGT EUROPE), 2013 4th IEEE/PES, pages 1–5, Oct 2013. 23

[Liu 13] Chunhua Liu, K.T. Chau, Diyun Wu & Shuang Gao. *Opportunities and Challenges of Vehicle-to-Home, Vehicle-to-Vehicle, and Vehicle-to-Grid Technologies.* Proceedings of the IEEE, vol. 101, no. 11, pages 2409–2427, Nov 2013. 19, 20

[Lopes 11] João A Peças Lopes, Filipe Joel Soares & Pedro M Rocha Almeida. *Integration of electric vehicles in the electric power system.* Proceedings of the IEEE, vol. 99, no. 1, pages 168–183, 2011. 13

[MDE 15] MDE. *Modern Energy, Electric vehicle charger.* www.modernenergy.co.nz, 2015. vi, 18

[Momber 15] I. Momber, A. Siddiqui, T. Gomez San Roman & L. Soder. *Risk Averse Scheduling by a PEV Aggregator Under Uncertainty.* Power Systems, IEEE Transactions on, vol. 30, no. 2, pages 882–891, March 2015. 23

[Mwasilu 14] Francis Mwasilu, Jackson John Justo, Eun-Kyung Kim, Ton Duc Do & Jin-Woo Jung. *Electric vehicles and smart grid interaction: A review on vehicle to grid and renewable energy sources integration.* Renewable and Sustainable Energy Reviews, vol. 34, pages 501 – 516, 2014. vi, 18

[Negre 11] L. Negre. *Green Book on charging infrastructure of electric vehicle,French Ministry of Ecology, sustainable development and energy.* www.developpement-durable.gouv.fr, 2011. 12

[NLV] NLV. 21

[P. Fernandez 11] Luis P. Fernandez, Tomás Gomez San Roman, Rafael Cossent, Carlos Mateo Domingo & Pablo Frias. *Assessment of the Impact of Plug-in Electric Vehicles on Distribution Networks.* IEEE Transactions on Power Systems, vol. 26, no. 1, pages 206–213, February 2011. 30

[Petit 13] Marc Petit & Yannick Perez. *Vehicle-to-grid in France: What revenues for participation in frequency control?* In European Energy Market (EEM), 2013 10th International Conference on the, page 1–7. IEEE, May 2013. 28, 29, 34

[Quinn 10] Casey Quinn, Daniel Zimmerle & Thomas H. Bradley. *The effect of communication architecture on the availability, reliability, and economics of plug-in hybrid electric vehicle-to-grid ancillary services.* Journal of Power Sources, vol. 195, no. 5, pages 1500 – 1509, 2010. 23

[Rawson 99] Mark Rawson & Sue Kateley. *Electric vehicle charging equipment design and health and safety codes*. Rapport technique, SAE Technical Paper, 1999. 17

[Rebours 05] Yann Rebours & Daniel Kirschen. *A Survey of Definitions and Specifications of Reserve Services*. Tech. rep., Univ. Manchester, 2005. 29

[Rious 13] Vincent Rious. *Intégration économique de véhicules rechargeables dans un système électrique*. www.microeconomix.fr, 2013. 13

[RTE 15a] RTE. *RTE, 2014 Annual electricity report*. www.rte-france.com, 2015. 9

[RTE 15b] RTE. *RTE, France Electricity Report for 2014*. www.rte-france.com, 2015. vi, 9, 10

[Sandalow 09] David B Sandalow. Plug-in electric vehicles: what role for washington? Brookings Institution Press, 2009. 15

[Sandels 10] C. Sandels, U. Franke, N. Ingvar, L. Nordstrom & R. Hamren. *Vehicle to Grid - Monte Carlo simulations for optimal Aggregator strategies*. In Power System Technology (POWERCON), 2010 International Conference on, pages 1–8, Oct 2010. 23, 24

[Shafiee 13] Soroush Shafiee, Mahmud Fotuhi-Firuzabad & Mohammad Rastegar. *Investigating the impacts of plug-in hybrid electric vehicles on power distribution systems*. Smart Grid, IEEE Transactions on, vol. 4, no. 3, pages 1351–1360, 2013. 12

[Skvarenina 01] Timothy L Skvarenina. The power electronics handbook. CRC press, 2001. 15

[Wang 13] Ran Wang, Yifan Li, Ping Wang & D. Niyato. *Design of a V2G aggregator to optimize PHEV charging and frequency regulation control*. In Smart Grid Communications (SmartGridComm), 2013 IEEE International Conference on, pages 127–132, Oct 2013. 23

[Wang 14] Miao Wang, M. Ismail, Ran Zhang, Xuemin Shen, E. Serpedin & K. Qaraqe. *A semi-distributed V2V fast charging strategy based on price control*. In Global Communications Conference (GLOBECOM), 2014 IEEE, pages 4550–4555, Dec 2014. 20

[Wellisch 15] D. Wellisch, J. Lenz, A. Faschingbauer, R. Pöschl & S. Kunze. *Vehicle-to-Grid AC Charging Station: An Approach for Smart Charging Development*. IFAC-PapersOnLine, vol. 48, no. 4, pages 55 – 60, 2015. 13th IFAC and IEEE Conference on Programmable Devices and Embedded SystemsPDES 2015. 27

[White 11] Corey D White & K Max Zhang. *Using vehicle-to-grid technology for frequency regulation and peak-load reduction*. Journal of Power Sources, vol. 196, no. 8, pages 3972–3980, 2011. 19

[Xu 14] Zhiwei Xu, Zechun Hu, Yonghua Song, Wei Zhao & Yongwang Zhang. *Coordination of {PEVs} charging across multiple aggregators*. Applied Energy, vol. 136, pages 582 – 589, 2014. 23, 24

[Yilmaz 13] Murat Yilmaz & Philip T. Krein. *Review of the Impact of Vehicle-to-Grid Technologies on Distribution Systems and Utility Interfaces*. IEEE Transactions on Power Electronics, vol. 28, no. 12, pages 5673–5689, December 2013. 27

[Yong 15] Jia Ying Yong, Vigna K. Ramachandaramurthy, Kang Miao Tan & N. Mithulananthan. *Bi-directional electric vehicle fast charging station with novel reactive power compensation for voltage regulation*. International Journal of Electrical Power and Energy Systems, vol. 64, pages 300 – 310, 2015. vi, 21

Chapter 2

Impacts and contribution of electric vehicles and V2G on distribution grid

" Nothing ever develops on its own, isolated from the past. There's always a foundation for our knowledge that others have laid and that we build upon. "

Ali Javan

Contents

2.1 Introduction

In this chapter, firstly a state of the art of different impacts of increased number of EVs on the electrical grid will be reviewed. Afterwards, the modeling of EV fleet charging profile based on probability distribution functions will be conducted. Example of two different case studies, one for a regional distribution network and other one the typical railway station parking lots and the impacts of EV charging profile on each case will be assessed.

2.2 Impact of EVs on grid: a review

The presence of plug-in electric vehicles is becoming more common as a low or even zero emission mode of transportation which will be dramatically increased in near future especially at distribution network level. Future smart grid provides the opportunities to bring not only the energy storage options as a positive outcome but also address negative power quality effects presented by highly nonlinear charging systems for PEV and PHEVs [Masoum 10]. The other specific challenges to the grid consist of voltage deviation, power losses in charging periods, transformer and feeder overloads [Clement-Nyns 10]. Generally the main impacts of uncontrolled charging of EVs contain as follow [Raghavan 12];

- Distribution transformer losses increment
- Increment of thermal loading on distribution transformer which lead to reducing the transformer life
- Voltage deviation and voltage unbalance increment
- Harmonic distortion increment due to nonlinear loads
- Peak power augmentation which leads to extra investment on distribution system reinforcement

A background of major impacts of uncoordinated electric vehicles charging is presented thereafter.

2.2.1 Transformer losses and loss of life

Transformers are among the most costly network equipment in the medium and low voltage distribution networks. Therefore, transformer aging influenced by more losses and hotspot temperature is a key factor when evaluating the impacts of EV charging and decide whether or not to employ charging coordination [Hilshey 13, Turker 12a]. Transformer aging is highly depends on health state of Internal solid insulation material. This will be impacted by internal transformer temperature and particularly hottest point temperature so-called hotspot temperature.

A time series model of transformer aging method is discussed in [Roe 09] and claim that EV uncontrolled charging could decrease transformer life by 93%. Another study [Shao 09] concludes that even 10% penetration of EV charging could induce additional transformer overloading beyond predicted overloading. Moreover, the investigation results in [Grahn 11] indicates that arbitrary charging of the electric vehicles could lead to increased peak power, effecting the transformer loss of life negatively, when exponential aging behavior occur (Fig. 2.1).

In figure below, two peaks power induced by EVs charging (around $T = 600min$ and $T = 1000min$) are effecting the hotspot temperature and transformer loss of life. These results

underline the impact of uncoordinated charging of the electric vehicle on the major distribution network devices where should be prevented by proposing supervision systems with charging coordination purposes.

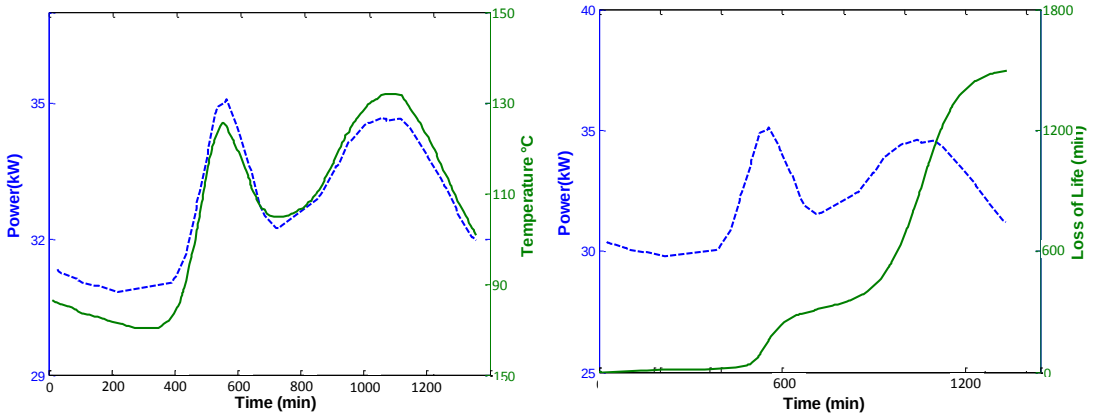

Figure 2.1: Impact of EV charging on hotspot temperature and loss of life of the distribution transformer [Grahn 11].

2.2.2 Voltage deviation

The root mean square (rms) voltage in power system frequency (50 Hz) is usually used to assess voltage status. EN50160[1] allows voltage deviation of ±10% of nominal voltage [Gray 14]. The charging of electric vehicles is also influencing the voltage of the grid node where the vehicle is connected and charging [Geth 12]. This deviation should be prevented in case of high penetration of electric vehicles. An illustrative example of different charging penetration of electric vehicles on IEEE 13 node test feeder is depicted in Fig. 2.2.

2.2.3 Harmonic distortion due to EV charging

Harmonic for a wave is the frequency component of the wave which is integer multiple of the fundamental wave's frequency. For instance for case of 50Hz fundamental frequency the harmonics contain 100Hz, 150Hz, 200Hz, ...etc. EV interface devices (e.g. chargers and filters) use the power electronics convertors where they are highly non-linear load devices due to their switching cell functionalities. Therefore, the current drawn by convertors from the grid includes harmonics (i.e. in switching cells frequency of PWM controllers and filtering) (Fig. 2.3). Despite the claim of EV manufacturers that they limit the negative effect of power quality problems, current and voltage distortion can be occurred due to malfunctioning of interface devices [Putrus 09].

Also based on a harmonic power flow analysis for integrated EVs in the grid in [Zhang 13], due to the existence of power electronic elements a large quantity of harmonics are generated by EVs charging process. The power quality problem deduced by this fact is serious if there is no harmonic elimination or decreasing system. Passive filter banks placement and optimal dispatch of LTC and shunt capacitors are introduced as some solution for power quality improvement of the grid in presence of nonlinear loads [Masoum 10].

[1]EN 50160 gives the main voltage parameters and their permissible deviation ranges at the customer's point of common coupling in public low voltage (LV) and medium voltage (MV) electricity distribution systems, under normal operating conditions.

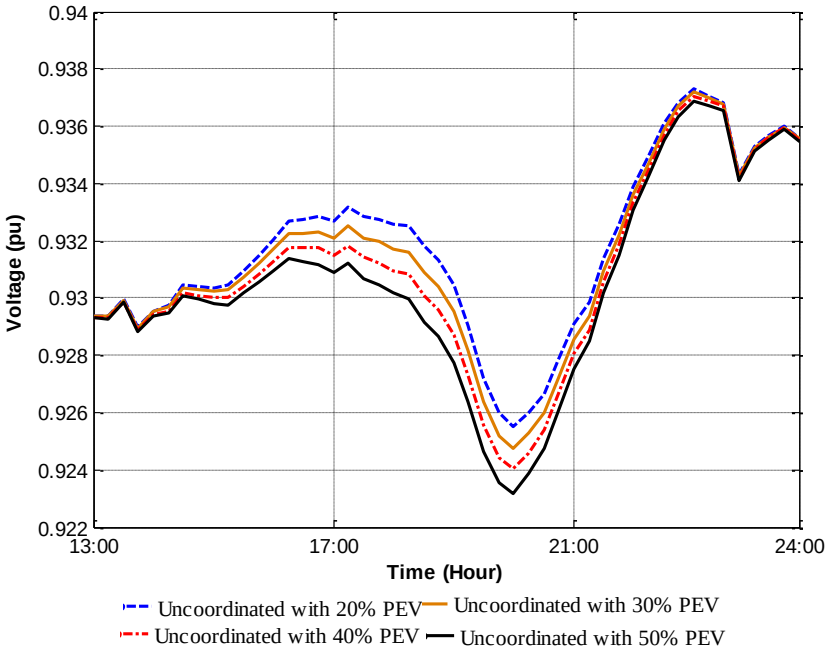

Figure 2.2: Voltage drop due to high penetration of electric vehicle charging for IEEE 13 node test feeder [Sarabi 13]

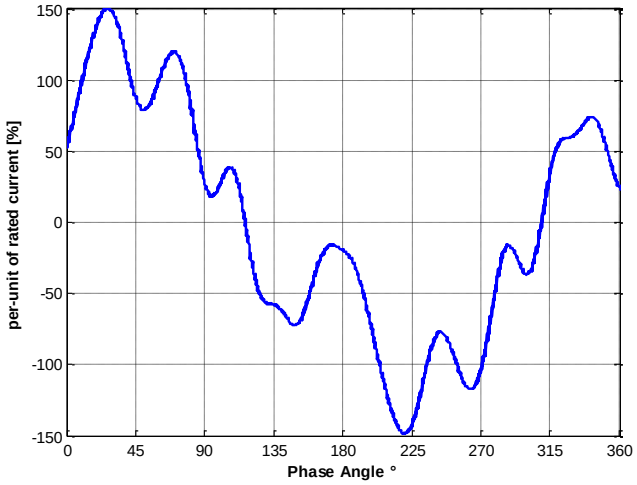

Figure 2.3: An example of waveform of injected current for a EV charger in charging period [Masoum 10].

2.2.4 Peak Power Increment

Depending on daily load profile of the electrical network, EV charging profile could impose peak power augmentation. Considering the arrival time of the vehicles' fleet, if a network with daily afternoon and night peak power is affected by EV charging, the extra increment of instantaneous power demand will be happened. This is the case for winter DLP in France where the penetration of 2 million electric vehicles up to to 2020 will impose near to 4GW peak power demand depicted in Fig. 2.4. However, the proposition of supervision for managing the charging time of the EVs and considering bidirectional power flow (V2G) mode control has been studied in [Sarabi 13] where the valley filling of the DLP instead of peak increment has been proposed as a solution.

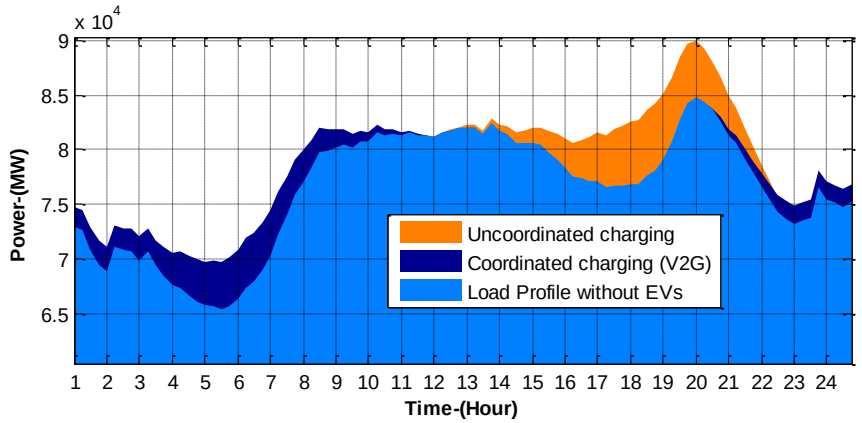

Figure 2.4: The effect of peak power increment due to EV charging profile in France on a typical winter day [Sarabi 13].

2.2.5 Conclusion

The main impacts of electric vehicle charging demand on the electrical grid have been discussed. Each impact could be considered as one assessment criteria for analyzing the strategies, controller designs and supervision systems of EV fleet charging/discharging coordination. Based on the objective functions for each controller system, one, two or many of such technical impacts can be taken into account to prevent, reduce or optimize their performance criteria. In the next section after modeling of EV charging profile the impacts of EV penetration will be assessed more from the economic point of view.

2.3 Introduction of case studies

In this thesis, the contribution and impact of electric vehicles and V2G technology are studied for two different case studies. The energy management strategies for possible ancillary services are also assessed for these cases. The first case is the regional distribution grid of Deux-Sèvres department which contains 14 HV/MV substations at the border of Transmission network and distribution network. For some services the whole grid containing renewable energy production (wind farm and solar distributed generation) are considered. While, for some other services the focus is on one single HV/MV substation.

In the second step a concept of railway station containing electric vehicle charging stations is studied and possible services with energy management strategies are proposed and their applicability are analyzed using economic and technical indicators. In the continue these two case studies are introduced.

2.3.1 Regional distribution grid (Department of Deux-Sèvres)

GEREDIS Deux-Sèvres is the distribution system operator of Deux-Sèvres department's distribution grid. It serves more than 150,000 subscription points. The key characteristics of this entity is depicted in Fig. 2.5. Based on the electric vehicle evolution scenarios in France, Deux-Sèvres department will accommodate a considerable number of EVs within next years. Therefore, the strategic planning needs to be active in term of future grid planning and energy management of the future smart grid actors. In this thesis based on the proposition of project supervisors and engineers of GEREDIS, three important anillary services are analyzed from EV charging coordination and V2G technology. Energy Transmission Cost Minimization (ETCM), Energy Cost Minimization (ECM) and Balancing Mechanism (BM) are studied in this project.

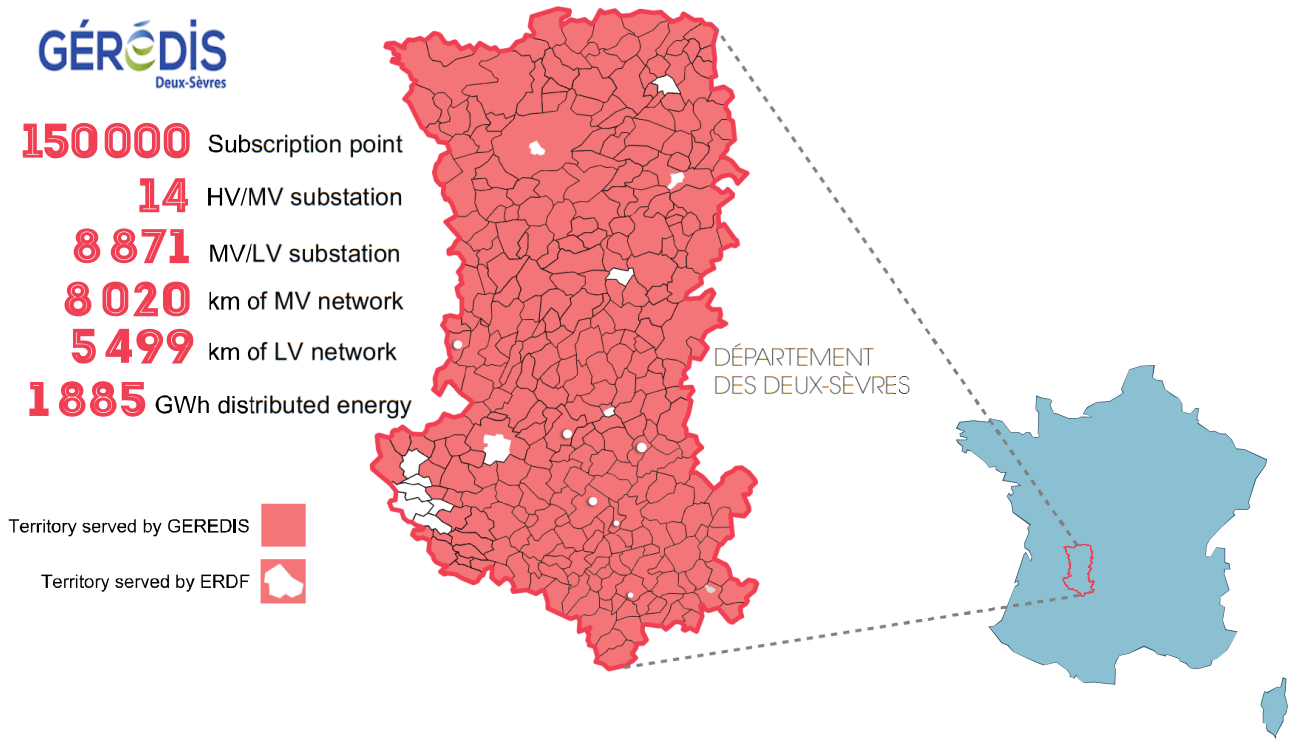

Figure 2.5: GEREDIS territory and grid key values

2.3.2 Railway station parking lot

SNCF, is France's national railway company and accomplishes the rail circulation in France. SNCF operates the country's national rail services, including the Train à Grande Vitesse (TGV) (high-speed train). Its functions include operation of railway services for passengers and freight, maintenance and signaling of rail infrastructure.

In this thesis a concept is proposed in order to study the flexibility of SNCF railway stations to be as a part of future smart grid actors. For this reason the integration of electric vehicles and V2G technology contribution on the railway stations parking lots are studied in this thesis. Three categories of railway stations in France are existed which are considered as case study. These categories are brought in Table 2.1.

Table 2.1: Different categories of SNCF railways stations and case studies subscription informations.

Category	A	B	C
No. trips/year	$>= 250,000$	$100,000 - 250,000$	$<= 100,000$
Subscribed power (kW)	200 - 400	400	100
Subscription contract	Green Tariff	Green Tariff	Yellow Tariff

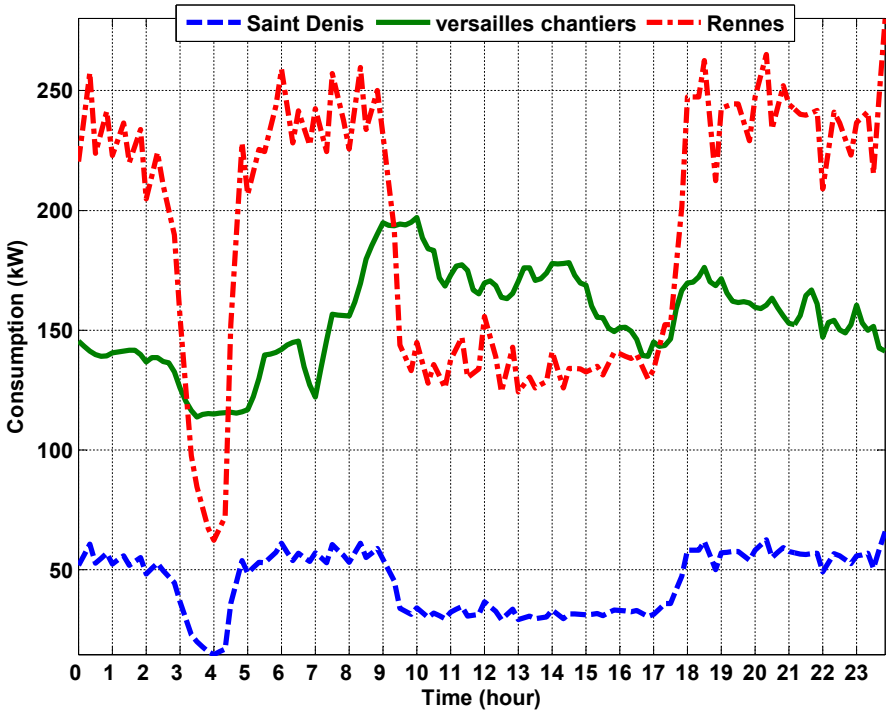

Figure 2.6: Typical daily load profile of three railway stations under study.

2.4 Electric vehicle's uncontrolled charging modeling

In order to be able to understand the problematic of EVs charging from the grid point of view, and even proposing the solutions for reduction of the negative impacts, charging demand behavior of the EVs fleet should be studied precisely. As today the fleets of electric vehicles are not available in huge quantity, therefore, the modeling of load profile of them is not an easy task. In this thesis, possible modeling approaches for EV charging profiling modeling are proposed and discussed in detail. These modeling approaches are mainly based on probabilistic

methods by using the traffic flow information. Different fleets of vehicles are analyzed but more specifically, vehicles doing daily home-work commuting are the main concentration of this study. For Deux-Sèvres department, the vehicles' charging profile for two charging scenarios, one at home and the other at office, are assessed. Moreover, for railway station parking lots, the vehicles which are parked during the day are studied. It supposed that these vehicles belongs the peoples who doing daily trips with TGV and trains. In this chapter the EV charging profile from probabilistic view and traffic based view are modeled.

2.4.1 Probabilistic modeling

Electric vehicle charging demand are modeled through different methodologies. Reference [Han 11] calculates achievable power capacity by binomial distribution of clustered PEVs with similar plug-in probability and power capacity. Reference [Fluhr 10] uses the survey data to identify the location of PEVs during the day using a stochastic modeling framework to estimate available stored energy into the PEV battery. In [Soares 11] Monte Carlo simulation is used in order to estimate the probability of transition between different states, e.g. parked or movement for different parking location for evaluation of PEVs charging impact on the grid. A non-homogeneous semi-Markov process is used in [Rolink 13] for PEV availability and identifying the charging load, while in [Gonzalez Vaya 14] a continuous time non-Markov chain is chosen as the mobility patterns do not fulfill the Markov property (memorylessness). Reference [Agarwal 14] uses the trip chains for mobility modeling of PEV fleet in order to estimate the aggregated power capacity of available PEVs and concluded that the home and office car parks have maximum availability among other place parkings. Among all of these researches backgrounds and our case study mobility survey, we concluded that the PEVs are parked in home and office parkings mostly a day and their service providing potential at these time intervals is relatively higher than other places, such as parking lots of shopping centers or the streets, which are highly stochastic and periodically short.

In this thesis, the daily home-work commuting are modeled based on probabilistic approach for stochastic variables, such as , arrival time, departure time and driving distance.

For the DSO, managing the load is a major issue specially when there is local RES production at their network. The presence of EV load is also important as their simultaneous charging load can cause major problem for the grid. In this study the focus is on a distribution substation in the range of 90/20-15 kV with 3 transformers 36 MVA. The diagram is depicted in Fig. 2.7. This grid has also distributed wind productions, which motivates to use its production locally. With rate of EV production in France, it is supposed for this grid to serve near 1300 EVs for the year 2020. The uncontrolled charging profile of this fleet will be analysed where all the EVs have been considered as Normal charging mode arrived around 8:00 at office parking and ask for charging instantaneously. Their departure time is also around 17:00.

2.4.1.1 Probabilistic algorithm

In this research, the focus is on the French electric vehicle market and the EV production between the years 2010 to 2015. The proposed algorithm with inspiration from [19] generates a fleet of EVs based on information (e.g., battery capacity, daily driving distance and commuting times). This algorithm consists of 5 steps explained precisely thereafter.

1. **EV type and capacity:** In the first step, the algorithm chooses the type of each EV in the fleet based on the market contribution portion available in [20]. The selection is random but with the probability of market contribution for each type. By choosing the

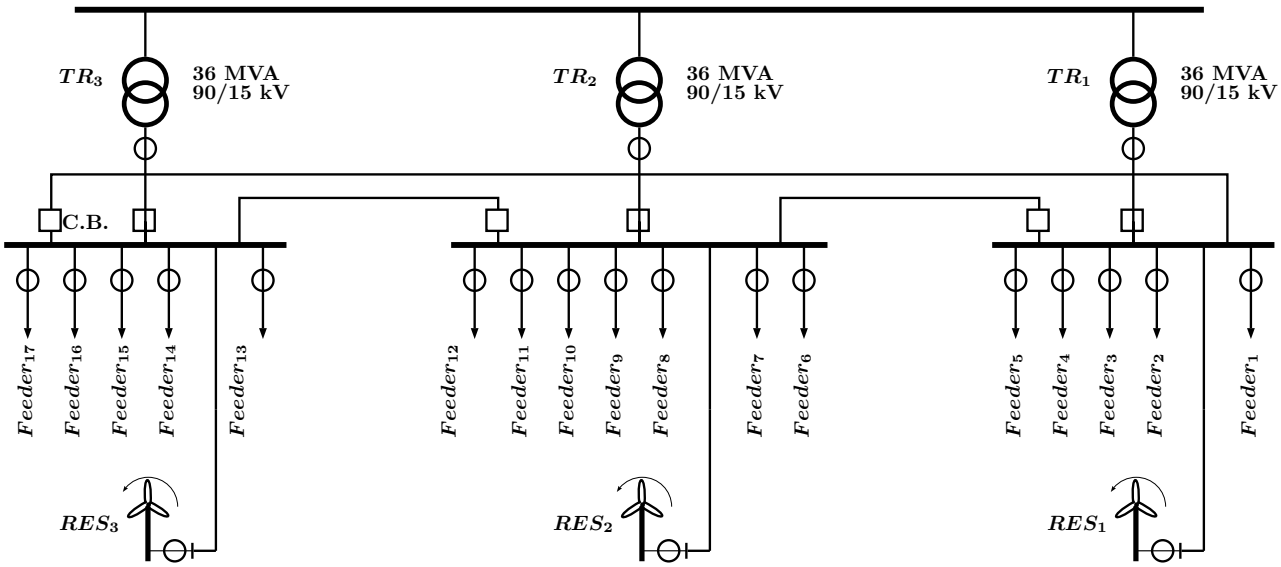

Figure 2.7: Diagram of HV/MV substation under study in Deux-Sèvres department.

EV type the other characteristics such as, battery capacity, battery type and NEDC[2] autonomy will be provided.

2. **Driving distance (D_d):** The information related to the daily driving distance has been considered based on 30 km average daily home/work distance in France [21]. The algorithm based on uniform distribution dedicates randomly driving distance, since the battery was fully charged, D_d [10 km, 50km], to the every single vehicles.

3. **Commuting times:** Based on the traffic habits of Deux-Sèvres department in France, the departure time from home to office in the morning is around 8h00 and the return time is around 17h00. To generate the set of arrival and departure time for the vehicles,the parameters are considered as in Table 2.2.

Table 2.2: Parameters for normal distribution of arrival and departure time to home/office.

Distribution	Home departure	Home arrival	Office arrival	office departure
$\mu(hh:mm)$	07:45	17:15	08:15	16:45
$\sigma(hh:mm)$	00:30	00:30	00:30	00:30

4. **Arrival SOC:** The assumption in this study is that the all EVs are used by commuting purpose and every EV will be charged and discharged once in a day, where the V2G application is also included. The available SOC at the moment of arrival (SOCarrival), by assuming linearly drop with the distance of travel, can be calculated as in (2.1):

$$SOC^i_{arrival} = \left(1 - \frac{D^i_d}{A^i}\right) \times 100\% \tag{2.1}$$

[2]New European Driving Cycle

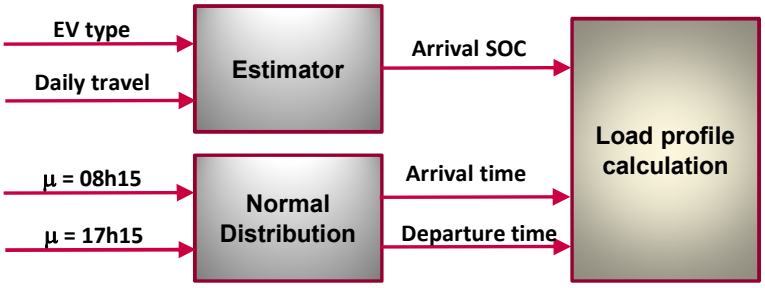

Figure 2.8: Probabilistic algorithm for load profile calculation of electric vehicles.

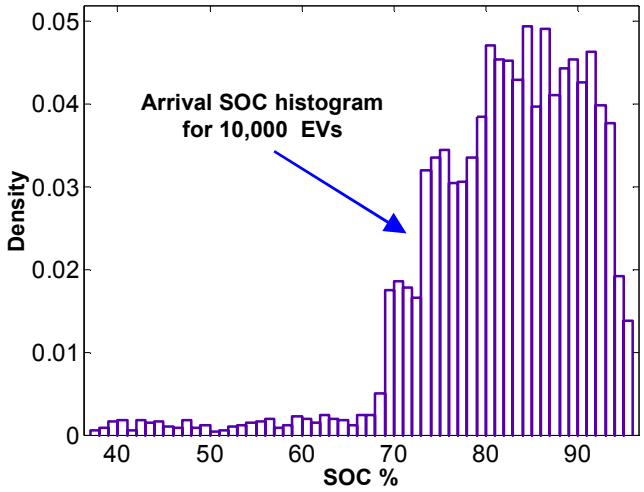

Figure 2.9: Arrival SOC histogram for 10,000 EVs, output of the algorithm.

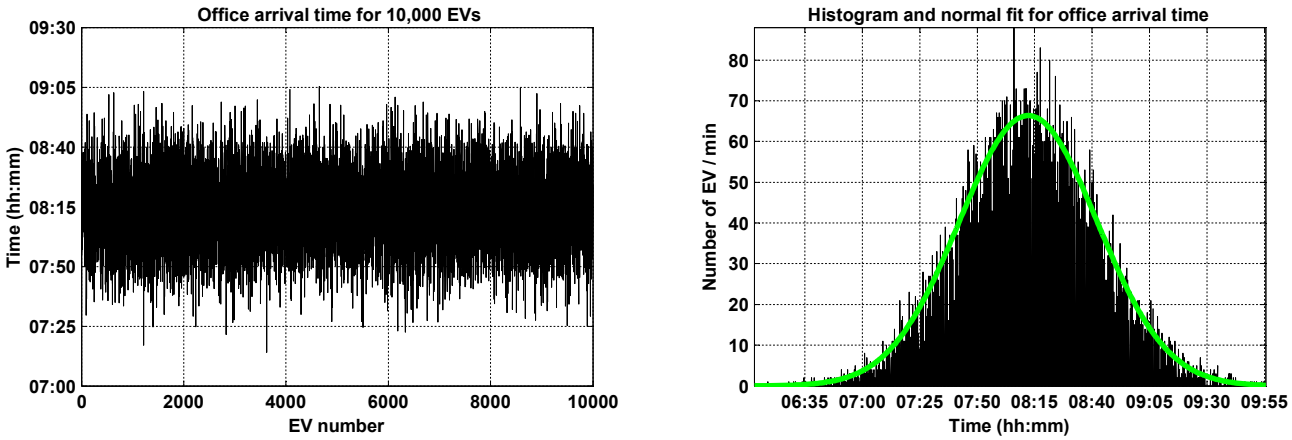

Figure 2.10: Output of algorithm for office arrival fleet.

2.4.2 Traffic based modeling

To study the impact of increased number of EVs on the electrical grid, a specific driving pattern, hypothesis or an exact periodical time interval has often been chosen. Problem of such modeling methods is that there is no dynamic between real traffic behavior of the roads and chosen pattern. In this study, we have considered the daily traffic behavior of the transportation fleet (Fig. 2.12) as an inspiring pattern to estimate the arrival and departure time of the vehicles used for working and daily short trip motives [SYT 13]. For this reason, the real-time traffic load data have been considered as pattern. Thanks to that, it would be possible to identify the differences between working days, and weekends. This will be valuable for annual impact

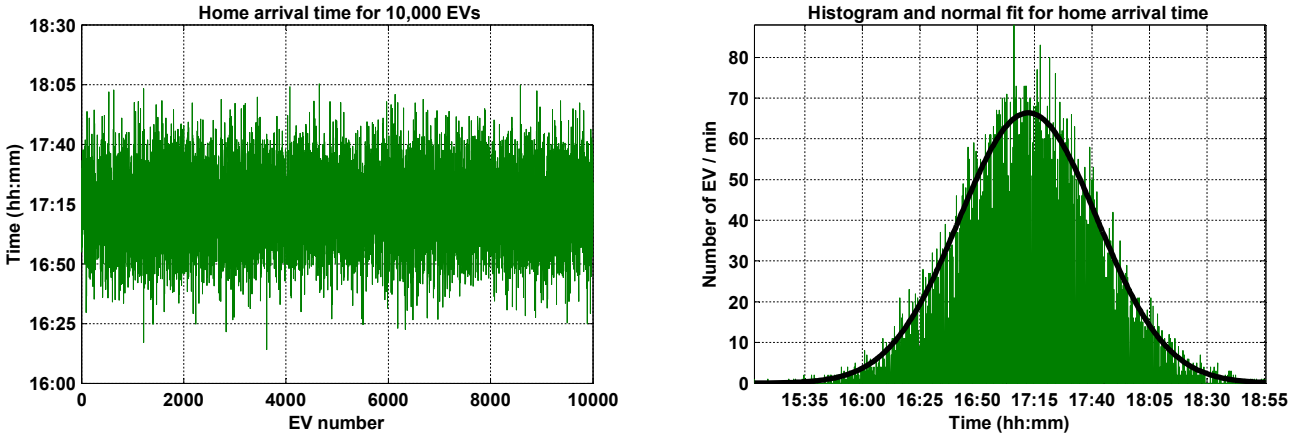

Figure 2.11: Output of algorithm for home arrival fleet.

analysis of the EVs. In this case, we have concentrated on annual average value of traffic data available for one complete week (Monday to Sunday) (Fig. 2.13). After that, for each single day the best-fitted probability distribution functions to data is identified, where the proper parameters for each distribution is calculated through a linear optimization problem.

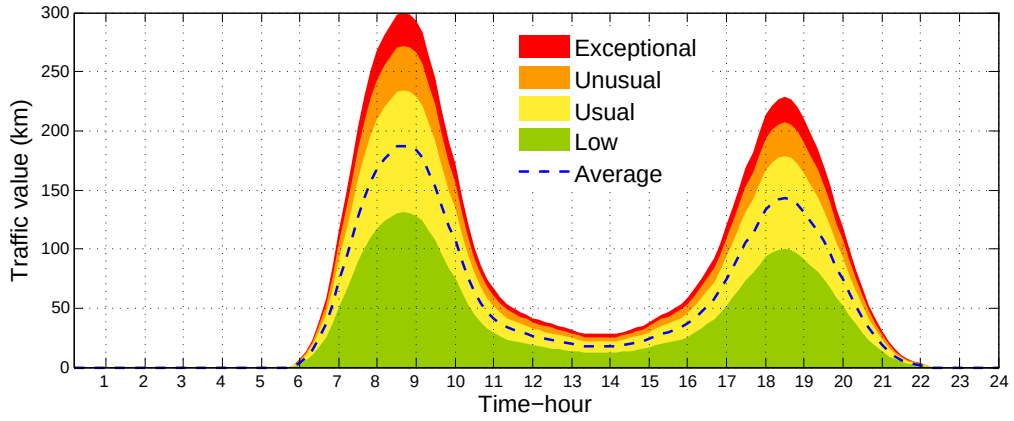

Figure 2.12: An example of daily traffic evolution on Monday in Paris (dashed line is the annual average for Monday)

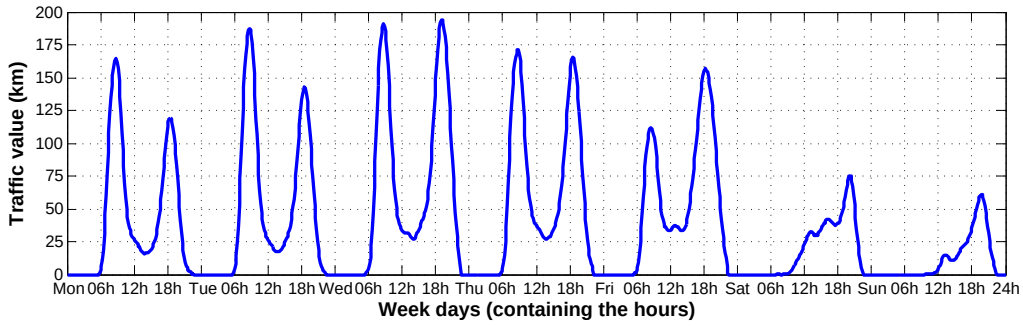

Figure 2.13: Weekly Annual Average variation of traffic load in Île-de-France

2.4.2.1 Working Days Modeling

The aim of this part is to find the best-fitted representative Probability Distribution Function (PDF) for working days of the week. From the obtained distribution function, the departure time of the vehicles could be estimated. However as the arriving time to the charging stations are addressed, a proper delay is considered (e.g. 1 hour). Looking at the working day traffic information, there are two major peaks one around 8:00 AM and another at 18:00. The first peak could be estimated as departure time from home to work and the second one from work to home. Since there is a nonsymmetrical shape around the peaks, normal distribution could not be chosen while a PDF with shape parameter could be more adaptable. Gamma distribution as a two-parameter family of continuous probability functions and Generalized Extreme Value (GEV) distribution as a three-parameter PDF are adaptable for the peaks fitting estimation. Gamma distribution is used for modeling the first peak at morning where GEV with a fixed negative shape parameter ($\xi = -1/2$) is used to model the second peak at evening. Therefore, the other parameters should be estimated in order to generate the best-fitted PDF to the peaks. Equation (2.2) represents the shape-scale parameterization PDF of gamma distribution with gamma function ($\Gamma(k)$). Equation (2.3) represents the GEV PDF with negative shape parameter ($\xi = -1/2$).

$$f(t;k;\theta) = \frac{t^{k-1}e^{-x/\theta}}{\theta^k \Gamma(k)} \tag{2.2}$$

$$g(t;\mu,\sigma,\xi) = \frac{1}{\sigma} r(t)^{\xi+1} e^{-r(t)} \tag{2.3}$$

$$r(t) = \begin{cases} (1+(\frac{t-\mu}{\sigma})\xi)^{-1/\xi} & , \text{ if } \xi \neq 0 \\ e^{-(t-\mu)/\sigma} & , \text{ if } \xi = 0 \end{cases} \tag{2.4}$$

In order to estimate the optimum parameters (k, θ, μ, σ) for the best-fitted PDF to the real traffic data, $y(t)$, the estimation errors, $e_1(k,\theta)$ and $e_2(\mu,\sigma)$ should be minimized.

$$f_{norm}(t;k;\theta) = \frac{f(t;k;\theta) - minf(t;k;\theta)}{maxf(t;k;\theta) - minf(t;k;\theta)} \tag{2.5}$$

$$y_{norm}(t) = \frac{y(t) - min(y(t))}{max(y(t)) - min(y(t))} \tag{2.6}$$

$$e_1(k,\theta) = \min_{k,\theta} \sum_{t=0}^{24} |y_{norm}(t) - f_{norm}(t;k;\theta)| \tag{2.7}$$

$$s.t.\ \ 0 < t < 24,\ (time\ step = 10min)$$
$$2 < k < 12 \in \mathbb{R},$$
$$0 < \theta < 4 \in \mathbb{R},$$

$$g_{norm}(t;\mu,\sigma,\xi) = \frac{g(t;\mu,\sigma,\xi) - min(g(t;\mu,\sigma,\xi))}{max(g(t;\mu,\sigma,\xi)) - min(g(t;\mu,\sigma,\xi))} \tag{2.8}$$

$$e_2(\mu,\sigma) = \min_{\mu,\sigma} \sum_{t=0}^{24} |y_{norm}(t) - g_{norm}(t;\mu,\sigma,\xi)| \tag{2.9}$$

$$s.t.\ \ 0 < \mu < 10 \in \mathbb{R},$$
$$0 < \sigma < 2 \in \mathbb{R},$$

The best-fitted PDF for two peaks from gamma and GEV distribution with optimized parameters ($\mu = 6, \sigma = 0.9, k = 5.25, \theta = 4$) are depicted in Fig. 2.14. This process has been

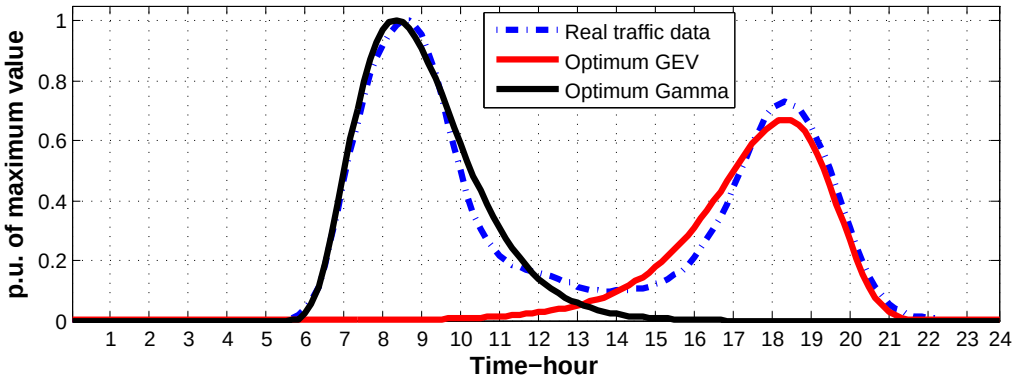

Figure 2.14: Normalized Optimum gamma and GEV PDF fitted to traffic data for working days (e.g. Monday)

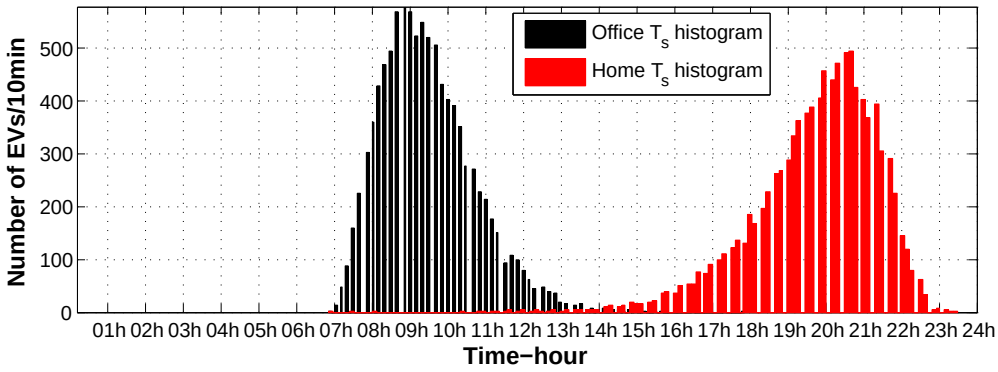

Figure 2.15: Stationing time histogram for working days (e.g. Monday)

repeated for 5 days of the working days to obtain the optimum parameters for each single day of the week. After that, the stationing time T_s of the vehicles (i.e. arrival at office parking's in the morning and arrival at home parking in the evening) will be generated from optimum gamma and GEV distribution (Fig. 2.15).

2.4.2.2 Weekend Modeling

In order to model the weekend days (Saturday and Sunday), as there is no major departure from home to work during the morning, there is no peak in traffic data around 8:00 AM. However, arriving at home could make a peak with less amplitude (i.e. compared to working days) around 20:00 PM. An optimum GEV distribution is needed to cover the proper distribution of stationing time for weekend (Fig. 2.16 and 2.17).

2.4.2.3 Charging profile

Based on the probabilistic algorithm proposed in [Sarabi 14], the required amount of energy for each EV battery to be full-charged at its departure time will be calculated (2.11). Each vehicle by choosing its arbitrary charging mode will be charged for T_c interval starting from its stationing time T_s. Required paremeters are defined in Table 2.3.

$$SOC^i_{arrival} = \left(1 - \frac{D^i_d}{A^i}\right) \times 100\% \tag{2.10}$$

$$E^i_{G2V} = (1 - SOC^i_{arrival}) \times E^i_{EV} \times \mu_c \tag{2.11}$$

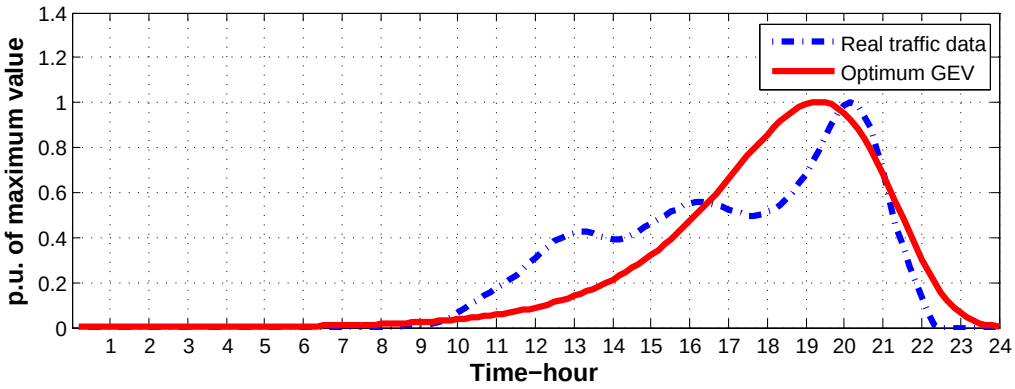

Figure 2.16: Normalized Optimum GEV PDF fitted to traffic data for weekend (e.g. Saturday)

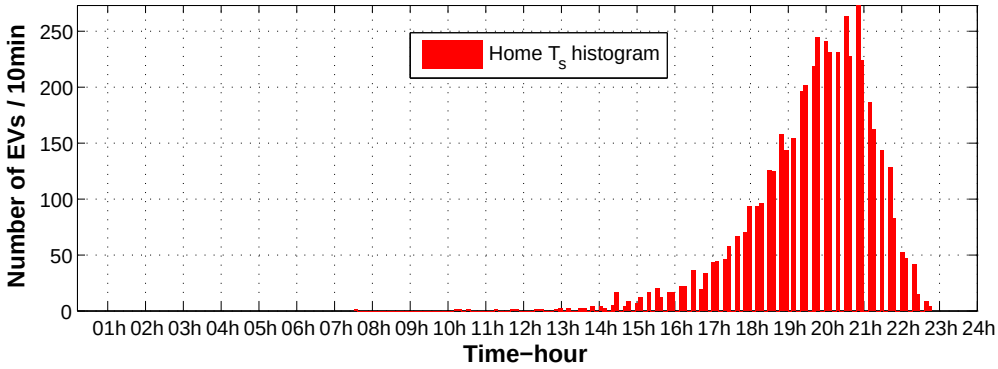

Figure 2.17: Stationing time histogram for weekend (e.g. Saturday)

Table 2.3: Charging profile parameters' definition

Parameter	Definition and value
A	EV's autonomy in the range of $80 < A < 250km$.
D_d	Daily Driving distance in the range of $10 < D_d < 50km$.
E_{EV}	battery capacity in the range of $8 < E_{EV} < 30kWh$.
μ_c	Charging efficiency $\mu_c = 0.97$ for 3kW charging rate [Turker 12b].
C_r	Charging rate, $NC = 3kW, RC = 43\ and\ 23kW$.

$$T_c^i = \frac{E_{G2V}^i}{C_r^i} \tag{2.12}$$

$$CP_i(t) = \begin{cases} C_r^i & , T_s^i < t < T_s^i + T_c^i \\ 0 & , \text{ elsewhere} \end{cases} \tag{2.13}$$

$$P_{fleet}(t) = \sum_{i=1}^{n} CP_i(t), \quad 0 < t < 24 \tag{2.14}$$

In (2.10), the State of charge (SOC) of the i^{th} EV at its arrival time to the parking will be calculated based on its driving distance. Afterwards, its required amount of energy, E_{G2V}, will be defined. In (2.13), the charging profile of the EV will be determined, where at the end the total charging profile of the fleet will be addressed in (2.14). The charging profile of the morning and evening are considered separately, therefore the summation of both will give

the final daily load profile of the EVs fleet that should be considered for impact analysis on distribution network (Fig. 2.18).

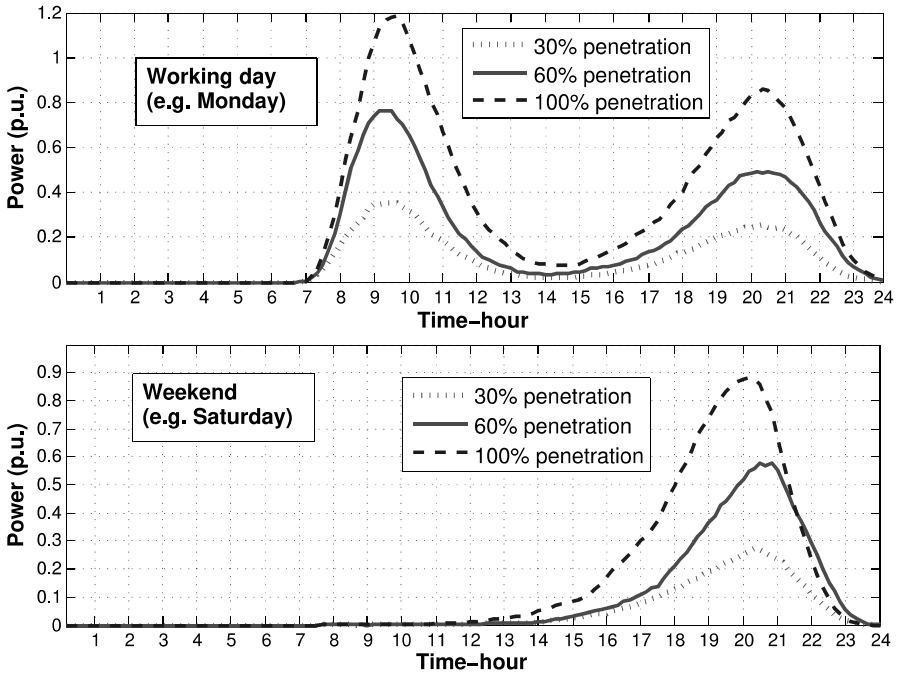

Figure 2.18: Charging profile of 10,000 EV for impact analysis of distribution network

2.5 Impact and contribution of EV/V2G on regional distribution grid

The impact of EV and their contributions using V2G technology are analyzed for energy transmission cost minimization based on the demand of project supervisors. Using probabilistic modeling approach explained in previous section, the load profile of EVs for home and office scenario is modeled. After that, two charging scenarios are considered and the impact of both scenarios is analyzed. The first one is uncontrolled charging scenario which is obtained from the algorithm. The second one is the supervised charging scenario which needs an optimization problem in function of minimizing the energy transmission cost. In fact, the energy transmission cost is considered as objective function of optimization problem and by using an optimization technic the charging demand associated to energy transmission cost minimization are calculated. In the next step the optimization problem will be defined and the proper method for solving the problem will be presented. Finally, the results of optimization are brought and the discussion will complete the section. This step will identify the impact of EV/V2G coordination contribution into the distribution grids' transmission costs.

2.5.1 Scenarios and assumptions

For this analysis, the energy transmission cost is considered as objective while the constraints are mainly limited to the electric vehicles' availability. Two charging scenarios are considered for the vehicles doing daily commuting between office and home. The first one is charging scenario at office and the second one is the charging scenario at home. The assumption of this study are mainly based on the scenarios and assumption generated by previous works on the

same case studies [Bouallaga 15] in order to be able to compare the obtained results to show the advantages of V2G technologies compared to simple charging coordination strategies. In fact, the inputs for this part of study are generated using the probabilistic algorithm explained completely in section 2.4.1.1. The following values are considered as the assumption of the study:

PEV fleet number for 2030	2700
Office departure time	17:00
Home departure time	06:00
Subscribed power	54980 kW

2.5.2 Optimization problem

The distribution grid system operators have to pay the transmission system operators (TSO) a yearly bill related to energy transmission which is called energy transmission cost (ETC). This invoice has several different components, where two of them are more interesting in term of energy management objective [Bouallaga 13]. These components are energy absorption (EA) and subscribed power exceeding (SPE) with a fix part. In order to minimize ETC Invoice, the electric vehicle fleet can have interesting contribution through following means of actions:

- Charging during the low cost energy price.
- Charging during the surplus of RES production.
- Discharging during the high cost energy price.
- Discharging during the surplus of consumption compared to RES in high cost intervals.

ETC is calculated based on tariffs defined by TSO which is called Tarifs d'Utilisation des Réseaux Publics d'Electricité (TURPE) [TURPE 15]. To have it minimized, the problematic defined in form of equation (2.15) is considered with constraints of EVs availability, battery SOC limitation, RES intermittency, energy tariff and subscribed power limit. This optimization problem is solved using interior point method for its nonlinear objective function. EA represents Energy Absorbed the part of the bill related to consumed energy. SPE represents Subscribed Power Exceeding. In the following equation, ΔP shows the subscribed power exceeding and E_i represents the energy consumed in the i^{th} hourly tariffs. In this example five different hourly tariffs are considered: Peak hours (HP), winter peak hours (HPH), winter off-peak hours (HCH), summer peak hours (HPE) and summer off-peak hours (HCE). The objective for our optimization is to minimize the energy transmission cost which is obtaining from equation 2.15 with subscribed power exceeding components calculated by equation 2.16.

$$EA = a_2 P_{subscribed} + \sum_{i=1}^{n} d_i E(t)_i + \sum_{12months} SPE(t) \tag{2.15}$$

$$SPE(t) = \sum_{i=1}^{n} (\alpha . \sqrt{\sum (\Delta P(t)^2)}) \tag{2.16}$$

For the calculation of ΔP the equation 2.17 is used.

$$\Delta P(t) = P_{PS}(t) - P_{subscribed}(t) \tag{2.17}$$

where $P_{PS}(t)$ is the injected or absorbed power in the level of HV/MV substation. The core of the optimization poblem is in this variable when the sum of all consumption and productions are

considered. In fact the electric vehicles' charging demand is contributing in the energy transmission cost minimization by applying the impacts on the $P_{PS}(t)$ parameter. This parameter is obtained by equation 2.18.

$$P_{PS}(t) = P_{con}(t) \pm P_{EV}(t) - P_{wind}(t) - P_{PV}(t) \tag{2.18}$$

Where, $P_{con}(t)$ is the consumption of classical consumers of the grid, $P_{EV}(t)$ is the power demand from the electric vehicle fleet, which could be positive when the vehicles are charged and negative when discharged and is equivalent of $P_{fleet}(t)$ in equation 2.14, $P_{wind}(t)$ is the wind active power production and $P_{PV}(t)$ is the photovoltaic active power production.

Nonlinear programming solvers needs the optimization problem in the following form:

$$\begin{gathered} \min_x f(x) \\ s.t. \\ \begin{cases} c(x) \leqslant 0 \\ c_{eq}(x) = 0 \\ A.x \leqslant 0 \\ A_{eq}.x = b_{eq} \\ lb \leqslant x \leqslant ub \end{cases} \end{gathered} \tag{2.19}$$

where x is optimization variable, c is the nonlinear inequality constraint function, c_{eq} is the nonlinear equality constraint function, A is the parameters of non-equality constraint, A_{eq} is the parameters of equality constraints and lb and ub define the lower and upper limit variation of variable x, respectively. Considering the energy transmission cost minimization problem, the equation 2.15 is equivalent of $f(x)$ function as the objective function. The constraints for this optimization problem as discussed previously, are the availability of the EVs and EV batteries SOC limitation. These constraints are representing an area of acceptance for the optimization problem which is presented in Fig. 2.19. Lower bound and upper bound are limiting the actions of charging and discharging which can generate the power of boundary values corresponds to the lower and upper bound lines in the figure. This boundaries are calculated based on maximum achievable power of the fleet and availability of the electric vehicles.

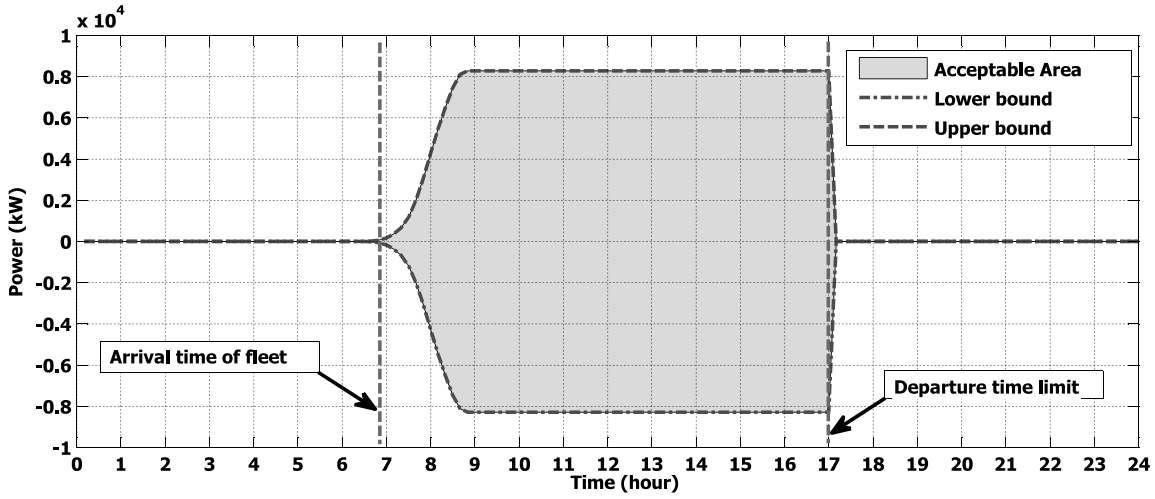

Figure 2.19: Lower bound, upper bound and availability of EVs as the constraints for optimization problem.

As the objective function is nonlinear an algorithm of nonlinear optimization technic for convex problem is welcomed. Inter point method is chosen as solver algorithm for this opti-

mization problem. *fmincon* function in *Matlab*© is used for this optimization problem. The results of the aforementioned problem are brought in next section.

2.5.3 Results

This optimization algorithm is applied for the scenario of charging at office and charging at home as explained in section 2.5.1. Different types of the outputs for both charging scenarios are brought to show the functionality of the optimization algorithm. Fig. 2.21 shows an example of day 39 (winter working day). In this example the V2G functionality is activated in order to reduce the subscribed power exceeding of normal load profile without EV charging (P_{PS}) while the charging demand (G2V energy) are distrbuted optimaly in order to limit the exceeding of subscribed power. In addition the V2G action is occured in the period of high price energy and the charging action is at middle price period which brings benefits of difference between the price for the EV owners and also the DSO.

In Fig. 2.22 an example of optimum load profile in function of energy price is depicted. The V2G energy is occured during high price period and charging demands are concentrated to the middle price periods. The full charging of the vehicles are limited to 17h00 for office scenario and this is the reason that the charging demands are oriented to middle price periods.

In Fig. 2.23 an example of one winter day when there is more production than consumption is presented. It is evident that the charging of electric vehicles are concentrated on these periods in order to consume the local production of renewable energies. As it is shown even if the price is high the EVs are to be charged in order to use the surplus produced energy of the renewable sources.

In Fig. 2.24, an example of charging scenario at home is presented. The optimization algorithm correctly minimized the subscribed power exceeding and by using V2G discharged the energy of the batteries during high price periods in order to benefit from low price period for recharging the batteries.

In Fig. 2.25 one home charging scenario for summer is represented. In this example, during 18 to 20 PM even with the high price of the energy the charging of the EVs are activated in order to use the surplus energy of the renewable energies as it is shown in this figure at part (d). The charging of the EVs are terminated until 6 AM as it is already considered as constraints for EVs charging scenario at home.

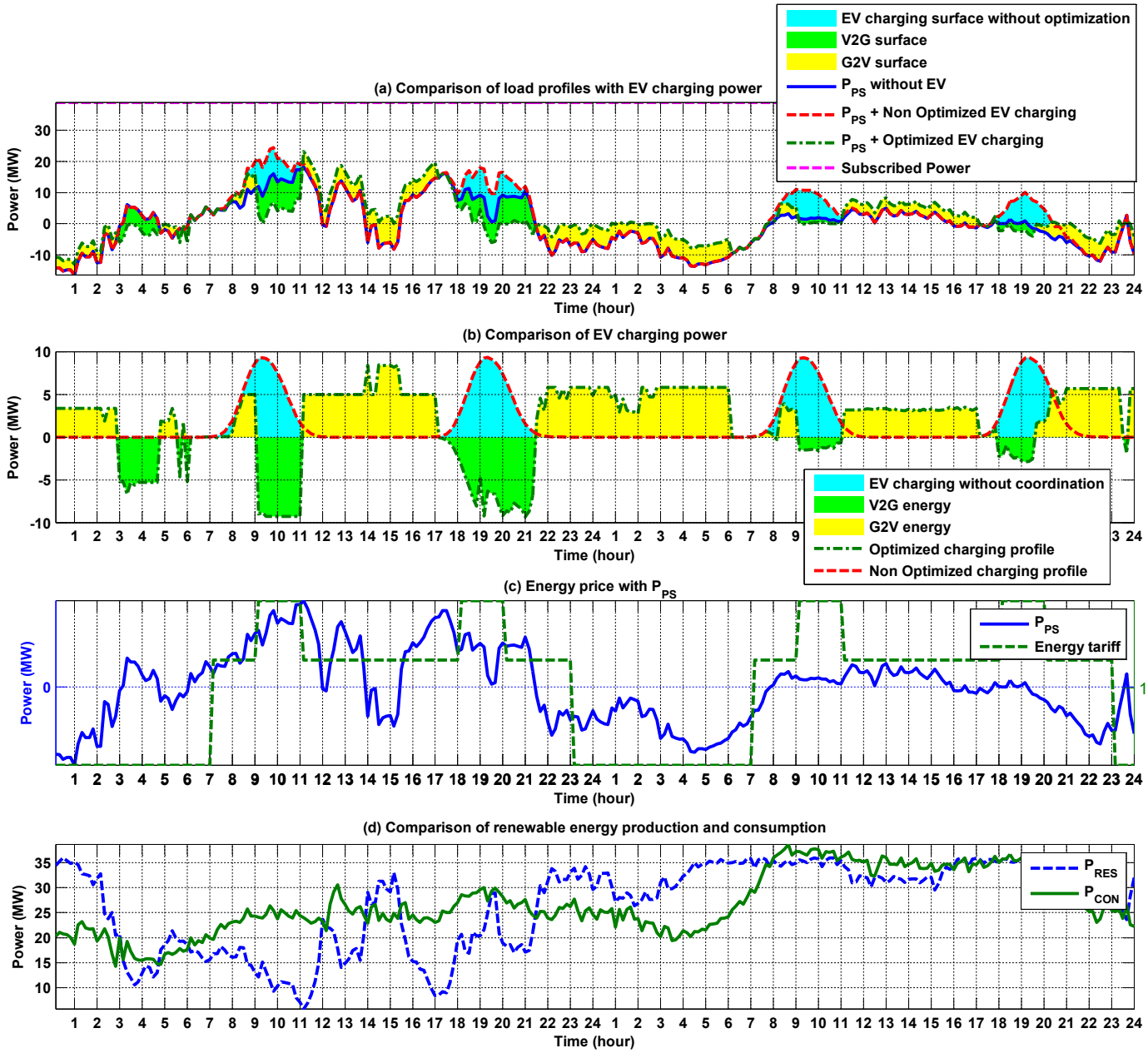

Figure 2.20: Comparing the optimization result for one winter day and home/office charging scenario, case of subscribed power exceeding limitation using V2G.

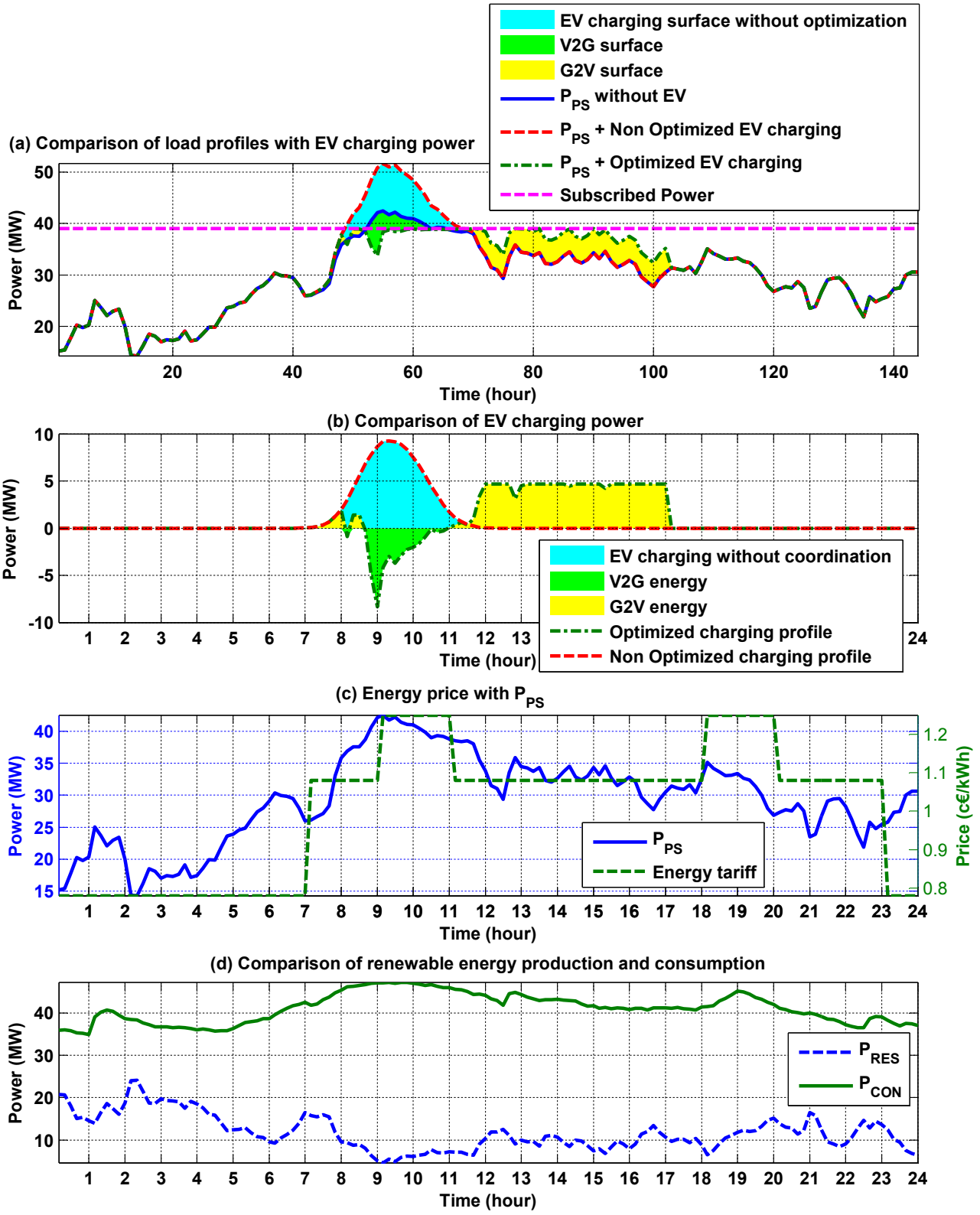

Figure 2.21: Comparing the optimization result for one winter day and office charging scenario, case of subscribed power exceeding limitation using V2G.

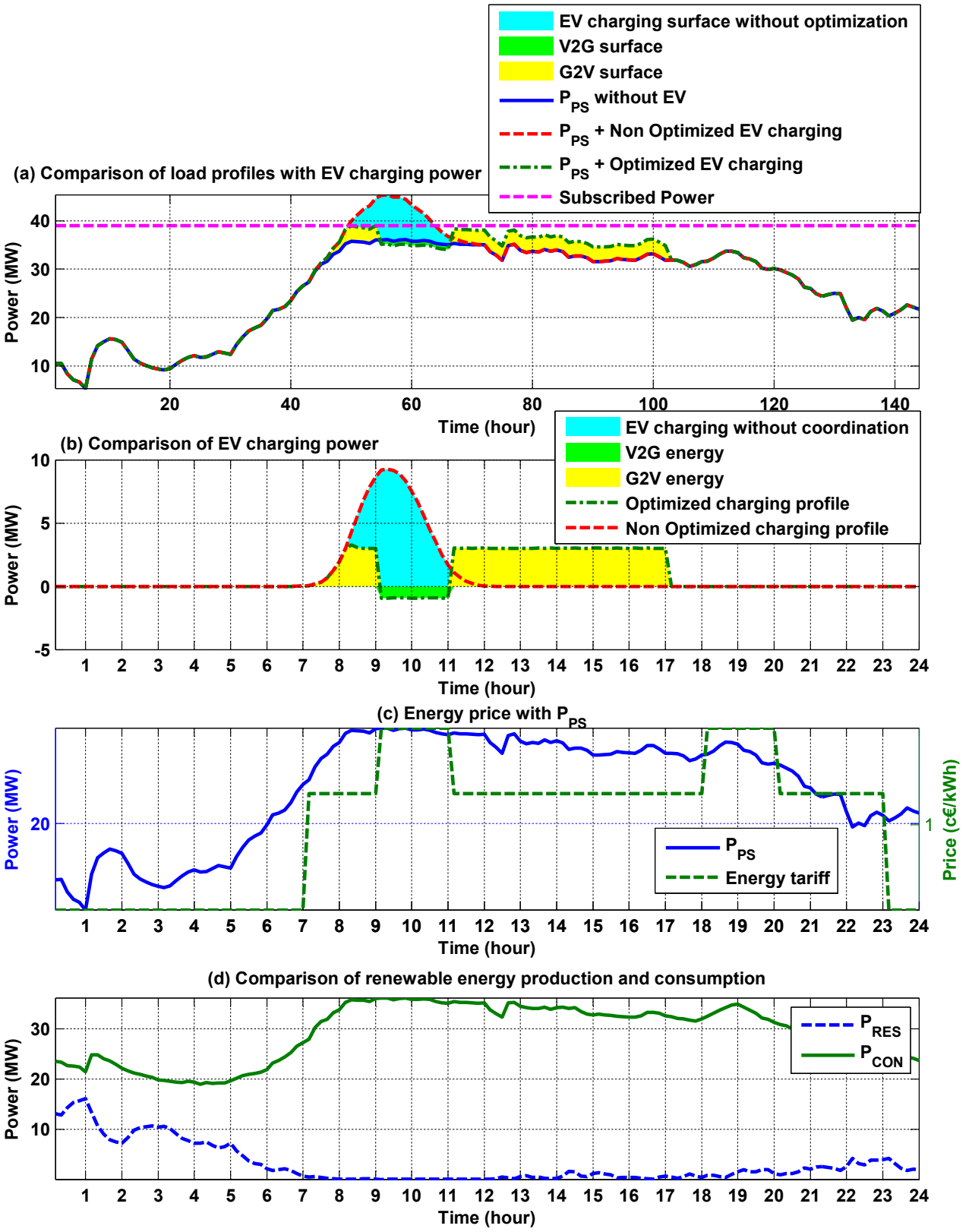

Figure 2.22: Comparing the optimization result for one winter day and office charging scenario, case of energy price orientation using V2G.

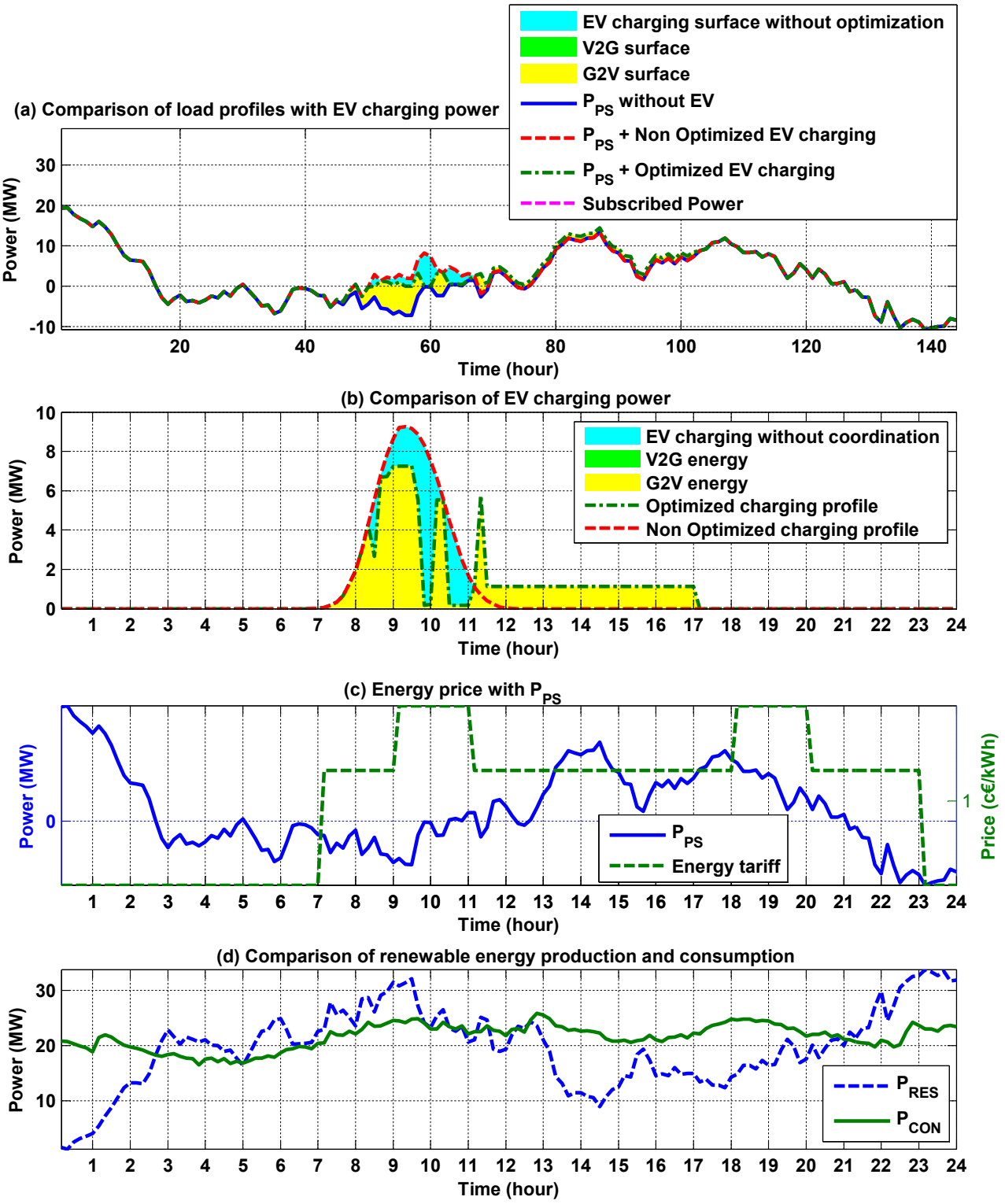

Figure 2.23: Comparing the optimization result for one winter day and office charging scenario, case of local production of renewable energy surplus compared to the consumption.

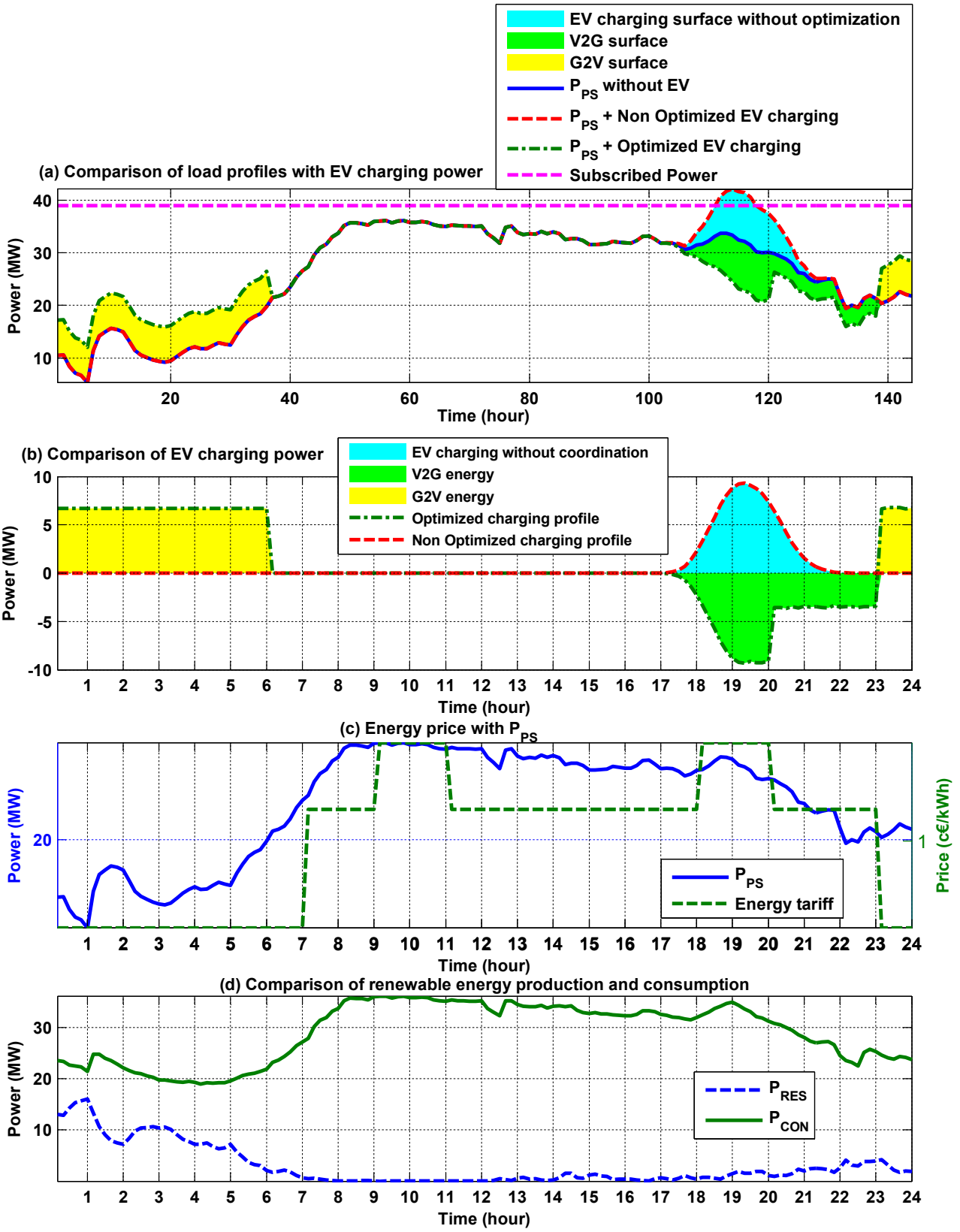

Figure 2.24: Comparing the optimization result for one winter day and home charging scenario, case of subscribed power exceeding limitation and off-peak hours orientation of EV charging using V2G.

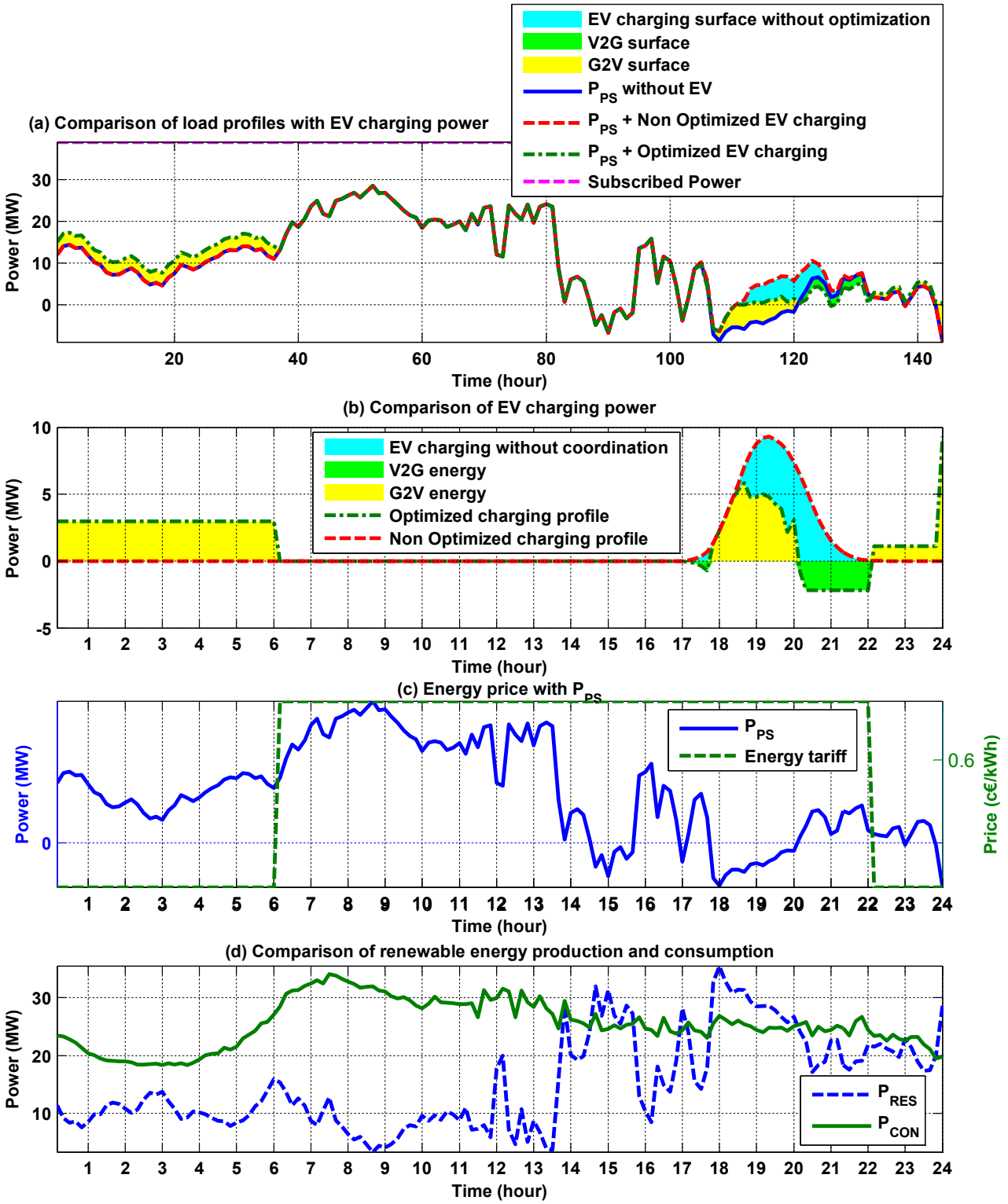

Figure 2.25: Comparing the optimization result for one summer day and home charging scenario, case of local production of renewable energy surplus compared to the consumption.

2.6 Impact and contribution of EV/V2G on railway station parking lots

Railway station for its local consumption should pay to energy supplier companies an annual bill corresponding to its consumption. The presence of EV charging stations may lead the energy consumption of the railway station to fluctuate. Here a charging/discharging management strategy is developed by optimizing the energy bill and controlling the load variation. At first, an optimization problem will find the proper energy distribution to minimize the invoice. Then second optimization problem will determine the charging/discharging time of the EVs to achieve the previously explained objective.

2.6.1 Railway station charging profile modeling and scenarios

The railway stations in France are the subject of smart grid developments with possible energy interactions between the grid and the users. Their connection to the distribution grid is through a MV/LV substation with range of 20-15/0.4 kV. These stations are supposed to act as an energy hub with different components such as local Renewable Energy Sources (RES) and electric vehicle charging stations. To analyse the impact of daily arrived EV to the parking, different scenarios have been considered. In this study the possibility and contribution of coordinated charging/discharging is also taken into account. These scenarios are based on arrival time and departure time of the EVs to the parking. The arrival time of the vehicles are distributed normally between 7:00 to 9:00 whereas the departure time is distributed normally between 16:00 to 20:00. The average availability interval is around 10 hours during which EV can be used for charging coordination. The total number of 10 charging station has been considered as base case. The capacity of the railway station is also evaluated from 1 to 50 charging stations. Charging stations are divided into several types of charging process, different cases have been studied and are described as follow;

Normal Charging (NC)

Normal charging case is the principle charging option for majority of EVs with 3 to 3.7kW charging rate. For an EV with 20 kWh battery capacity, it takes 6 to 8 hours to be fully charged. In this scenario all the vehicles arriving to the parking will choose NC charging mode.

Accelerated Charging (A.C)

Accelerated charging case is the charging mode with three phase circuit and 23 kW charging rate power. For an EV with 20 kWh battery, 1 hour is enough to be fully charged. In this scenario all the EVs are considered as choosing AC charging mode.

Rapid Charging (RC)

Rapid charging is the case for charging station in highways and freeways where the users need to have their battery fully charged very short. Charging rate of 43 kW lead to charging a 20 kWh battery in less than half an hour. This scenario is also considered that all EV in the parking can be charged at this rate.

Mixed Charging (MC)

In this option 40% of the station are RC charging mode, 20% of them are AC charging mode and 40% of the rest are NC charging mode.

2.6.2 Optimization problem

An algorithm based on two layer optimization is discussed here. Annual Energy Invoice Minimization (AIEM) algorithm at first minimizes the subscribed power of the station based on future energy consumption provision. Afterwards, using a convex optimization method the daily

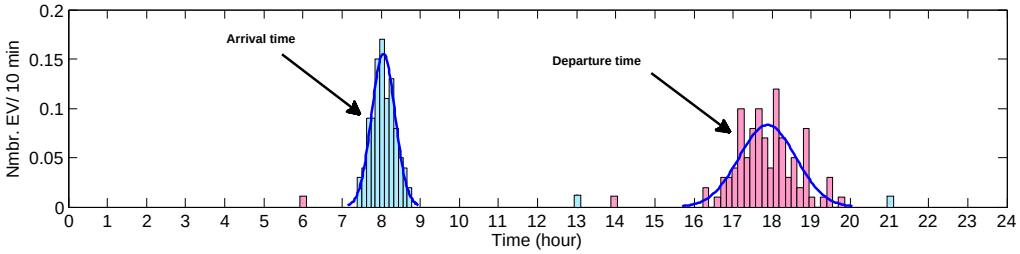

Figure 2.26: Arrival and departure time histogram for railway station charging scenarios.

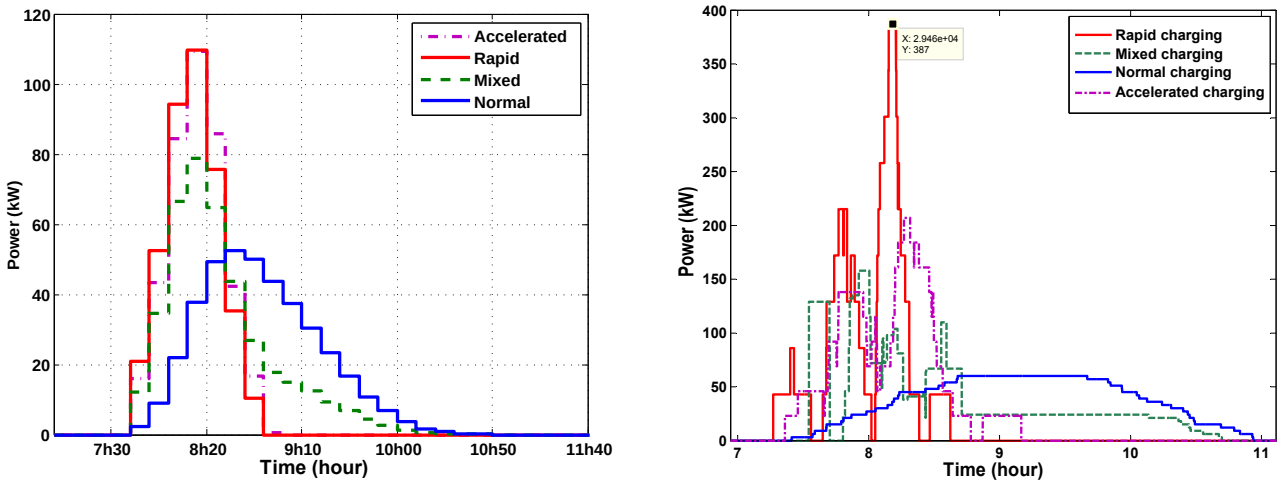

(a) 10 minutes average.

(b) In seconds.

Figure 2.27: Charging profile of 20 EVs for impact analysis of Railway stationing.

load profile of the station will be recalculated for the aim of minimizing the Annual Energy Invoice (AEI). This DLP will be called as reference load profile and will be used as reference for second layer optimization. The second layer uses a Binary Linear Programming (BLP) algorithm in order to reschedule the charging procedure of PEVs in the station. The algorithm will take just zeros and ones as its possible values for the optimization variables which lead to calculation time reduction comparing to the continuous linear programming algorithms. The flowchart of the proposed algorithm is brought in Fig. 2.28, where it shows the flow of data and process simultaneously. The different parts of this algorithm will be explained thoroughly afterwards.

2.6.2.1 Optimizing subscribed power (P_{sub})

The subscribed power is contracted one time per year and should be carefully chosen. Comparing to the annual consumption, choosing high value of subscribed power leads to extra payment on subscription component while, low value causes increment on subscribed power exceeding component. Hence choosing appropriate subscribed power leading to optimum invoice needs to have *a priori* knowledge on amount and manner of consumption. Having a typical annual load profile, optimum subscribed power can be found via a convex optimization problem.
The yearly energy invoice is calculated using following formula [Sarabi 15].

$$Cost = \sum_{j=1}^{5}(d_j E_j) + \sum_{j=1}^{5}(K.T_j\sqrt{\sum(\Delta P_j)^2}) + \alpha.P_{sub} \tag{2.20}$$

$$E_j = \int_{t_j^a}^{t_j^b} LP(t)d(t) \tag{2.21}$$

Where the first component is for consumed energy E_j, with its price d_j, in €/kWh during 5 different periodical tariffs j. The second components is for penalty of subscribed power exceeding with T, the reduction coefficient for each tarif and K the price of subscribed power (P_{sub}) exceeding in €/kW. ΔP is the amplitude of P_{sub} exceeding averaged during 10 minutes intervals. Finally, the third components which is the subscription part with base rate value of α in €/kW/year. LP is representing the load profile of the station where its variation should be controlled in order to minimize the invoice. The optimum subscribed power of the under studying station is obtained using a convex optimization as 69 kW. Note that this subscription is considering the annual consumption without PEVs load demand.

2.6.2.2 Energy invoice optimization

In this part optimizing the invoice using optimized subscribed power and actual load profile is addressed. In fact the load profile leading to minimum invoice will be found. This load profile will be considered as reference for charging/discharging scheduling problem in next section. This part is considered as the first layer of optimization.

$$\min_{RLP(t)} Cost \tag{2.22}$$

Subject to:

$$\int_{t_j^a}^{t_j^b} DLP(t)d(t) = \int_{t_j^a}^{t_j^b} LP(t)d(t) \tag{2.23}$$

Now $RLP(t)$ is the Reference Load Profile (RLP) which can minimize the invoice. This reference is considered in scheduling problem.

2.6.2.3 Mixed integer linear programming (MILP)

Mixed integer programming is an optimization method that combines continuous and discrete variables. MIP can model complex planning and control problems involving both discrete and continuous variables. In this part this method is used for coordination of PEV charging time. In order to decrease the calculation time, considering the number of variables, a modified version of MILP is used which is explained in next section.

2.6.2.4 Binary Linear programming (BILP)

Binary linear programming is a modifed version of MILP when the variables are binary values. It means that the acceptable values for all the variables could be either 0 or 1. In Figure 2.29, it is shown that how choosing BILP instead of MILP can decrease the problem complexity and consequently decrease the calculation time. There is one way to consider three possibilities for three actions, -1, 0 and 1 for discharging, no charging and charging, respectively. In other hand only two possibilities can be chosen. 0 for no charging and 1 for charging/discharging, where the choose between charging and discharging can be done by a reference parameters.

2.6.2.5 Formulation of PEV scheduling problem

Charging scheduling problem of N PEVs are formulated as a vector in time with elements equal to the 10 minutes time step over a day, which is equivalent to a row vector with size 1 by 144. This is called day sample times as k. The question to be answered is how coordinate

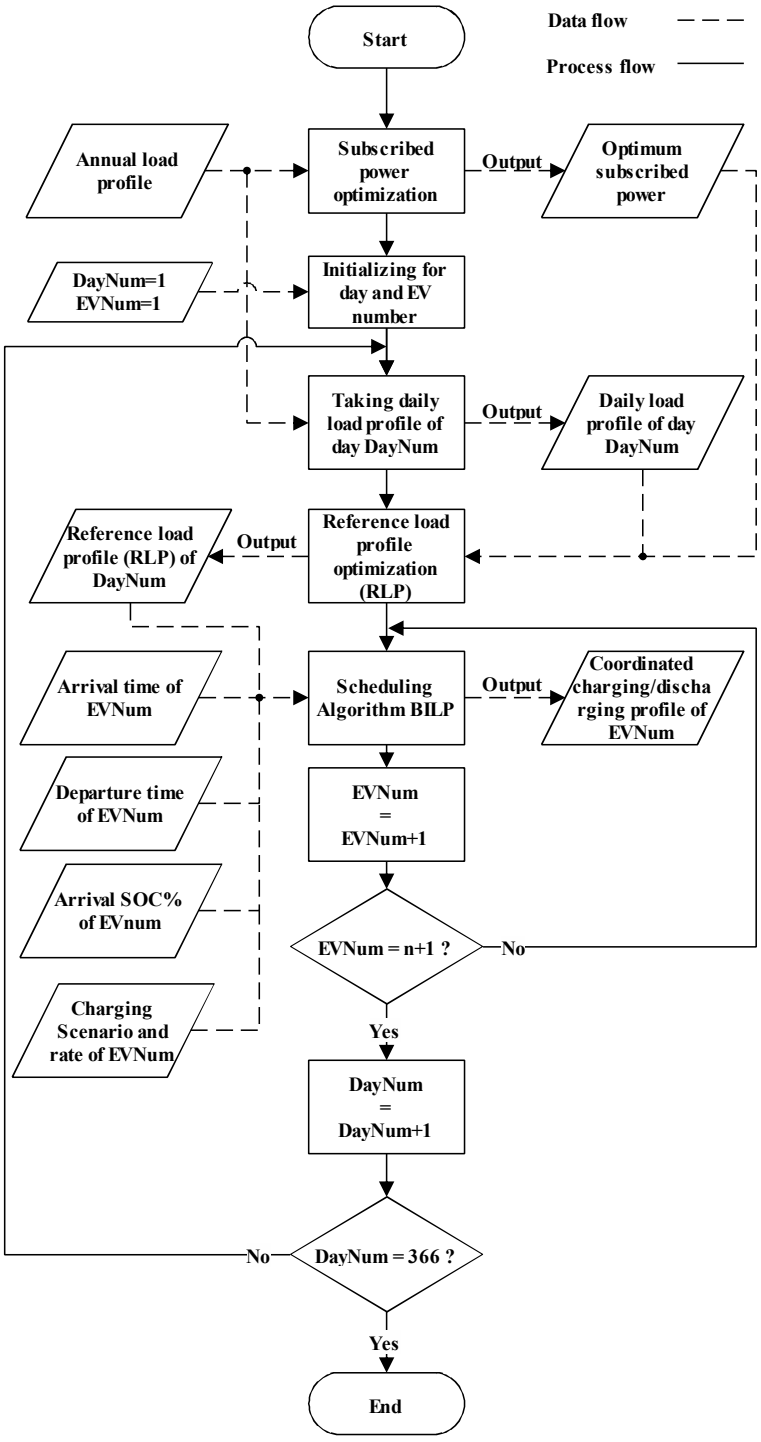

Figure 2.28: Flowchart of AEIM algorithm

the charging, no charging and discharging commands between plug-in time steps to achieve the objective of the coordination. For this reason $EV_{cp}^{i}(t)$ is defined as charging profile of PEVs with sample time coefficients of a_k as BLP variables and charging rate of CR^i. This charging rate is positive for charging and negative for discharging and the value is defined by the charging scenarios.

$$\begin{cases} EV_{cp}^{i}(k) = [a_1, a_2, ..., a_k] \times CR^i \\ i = [1, N] \in \mathbb{N}. \end{cases} \tag{2.24}$$

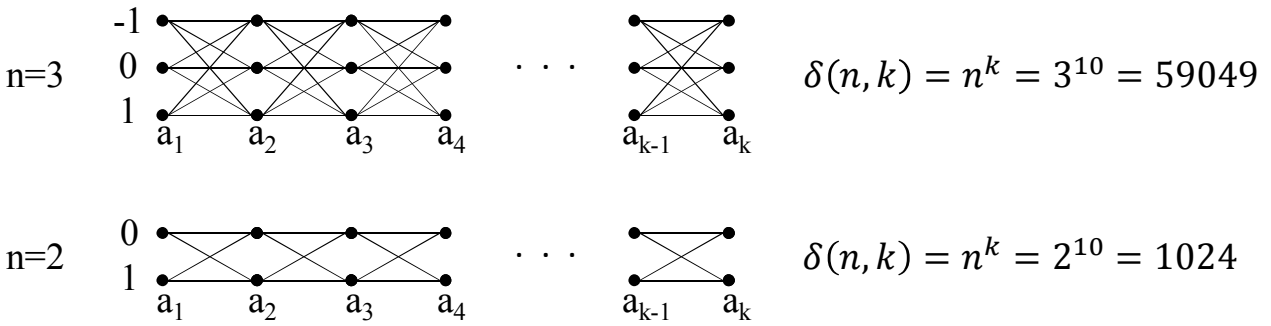

Figure 2.29: Comparison of number of possibilities for case of charging/discharging control with mixed integer variables and binary variables.

In equation (2.25), $Cap^i(k)$ represents the distance between RLP and actual LP. In fact, the purpose is to minimize this distance in order to minimize the energy invoice which is already minimized by RLP.

$$Cap^i(k) = LP(k) - RLP(k) \tag{2.25}$$

$$\gamma^i(k) = -\left|Cap^i(k)\right| \tag{2.26}$$

$$C^i(k) = \left(\gamma^i(k) + CR^i(k)\right) \times a_k \tag{2.27}$$

$$k = [1, 144] \in \mathbb{N} \tag{2.28}$$

$$a_k = [0, 1] \tag{2.29}$$

In order to prevent trivial answer of 0 for binary linear programming minimization problem, the coefficient $\gamma^i(k)$ is defined. Finally for optimization problem, $C^i(k)$ is defined as objective function.

$$\underset{a_1,..,a_k}{\text{Minimize}} \quad \sum_{k=1}^{T} C^i(k) \tag{2.30}$$

Subject to:

$$\sum_{k=1}^{T} A_{eq}(k).a_k = SOC^i_{need} \tag{2.31}$$

$$\sum_{k=1}^{T} A(k).a_k \leq SOC^i_{max} \tag{2.32}$$

$$\sum_{k=1}^{T} -A(k).a_k \leq -SOC^i_{min} \tag{2.33}$$

Constraint (2.31), ensure the energy need of each single PEV during its plug-in interval. Constraints (2.32) and (2.33) guarantee the charging scheduling within possible range of SOC variation. Where SOC^i_{min} is considered as 20% to minimize the battery depth of discharge and SOC^i_{max} is equal to 100%, the constraint for departure of all PEVs.

$$A_{eq} = \frac{Cap^i(k)}{|Cap^i(k)|} \tag{2.34}$$

$$A_{eq} = [-1, 1] \in \mathbb{Z} \tag{2.35}$$

For principle formulation of linear programming the A_{eq} is the coefficient of linear equality constraints where for this problematic, its values are -1 for discharging, 0 for idle mode and 1 for charging mode. Finally, the matrix A for non-equality constraints is defined as follow:

$$A = \begin{bmatrix} 1 & 0 & \cdots & 0 \\ 1 & 1 & \cdots & 0 \\ \vdots & \vdots & \ddots & \vdots \\ 1 & 1 & \cdots & 1 \end{bmatrix} \times \begin{bmatrix} A_{eq}(1) & 0 & \cdots & 0 \\ 0 & A_{eq}(2) & \cdots & 0 \\ \vdots & \vdots & \ddots & \vdots \\ 0 & 0 & \cdots & A_{eq}(k) \end{bmatrix}$$

2.6.2.6 Optimum schedule for i^{th} PEV

After each iteration of the optimization algorithm in order to calculate the charging schedule of i^{th} PEV a factor of SOC progress as $SOC^i_{sign}(k)$ is defined.

$$SOC^i_{sign}(k) = [a_k] \times \begin{bmatrix} A_{eq}(1) & 0 & \cdots & 0 \\ 0 & A_{eq}(2) & \cdots & 0 \\ \vdots & \vdots & \ddots & \vdots \\ 0 & 0 & \cdots & A_{eq}(k) \end{bmatrix}$$

Where the final optimized charging profile of concerned PEV considering its charging rate CR^i, will be as follow:

$$EV^i_{cp}(k) = \left[SOC^i_{sign}(1), \cdots, SOC^i_{sign}(k)\right] \times \left[CR^i\right] \tag{2.36}$$

2.6.2.7 Updated functions for next PEVs

In order to calculate the charging profile of next PEVs (based on their arrival time) the functions $LP(k)$ and $Cap^i(k)$ should be updated considering the optimized charging profile of previous PEVs.

$$LP^{i+1}(k) = LP^i(k) + EV^i_{cp}(k) \tag{2.37}$$

$$Cap^{i+1}(k) = LP^{i+1}(k) - RLP(k) \tag{2.38}$$

2.6.2.8 Constraints for PEV's Energy need

The PEVs which will arrive with low SOC rate have extra constraints that are introduced in form of two algorithms. If the number of admissible charging samples $Nb.^+$, is less than required charging sample time of a PEV (T^i_c), the A_{eq} will be updated until respecting the PEVs charging need constraint. This is considered in form of following algorithm.

$$\begin{cases} Nb.^+ & A_{eq} > 0 \\ Nb.^+ & A_{eq} < 0 \end{cases} \tag{2.39}$$

Algorithm 1 Charging need check in A_{eq} vector

1: **if** $T^i_c > Nb.^+$ **then**
2: Put 1 in vector A_{eq} where
3: $A_{eq} \times Cap^i(k)$ has smallest value.
4: **else**
5: **end if**

In addition, when a PEV arrives with SOC less than minimum SOC of the scheduling algorithm constraint, the constraint (2.32) will be updated by following algorithm in order to enforce the scheduling algorithm to start by charging the concerned PEV instead of discharging its battery.

Algorithm 2 Updating Minimum SOC constraint

if $SOC^i_{arrival} < SOC^i_{min}$ **then**
  $\sum_{k=1}^{T} -A(k).a_k \leq 0$
else
end if

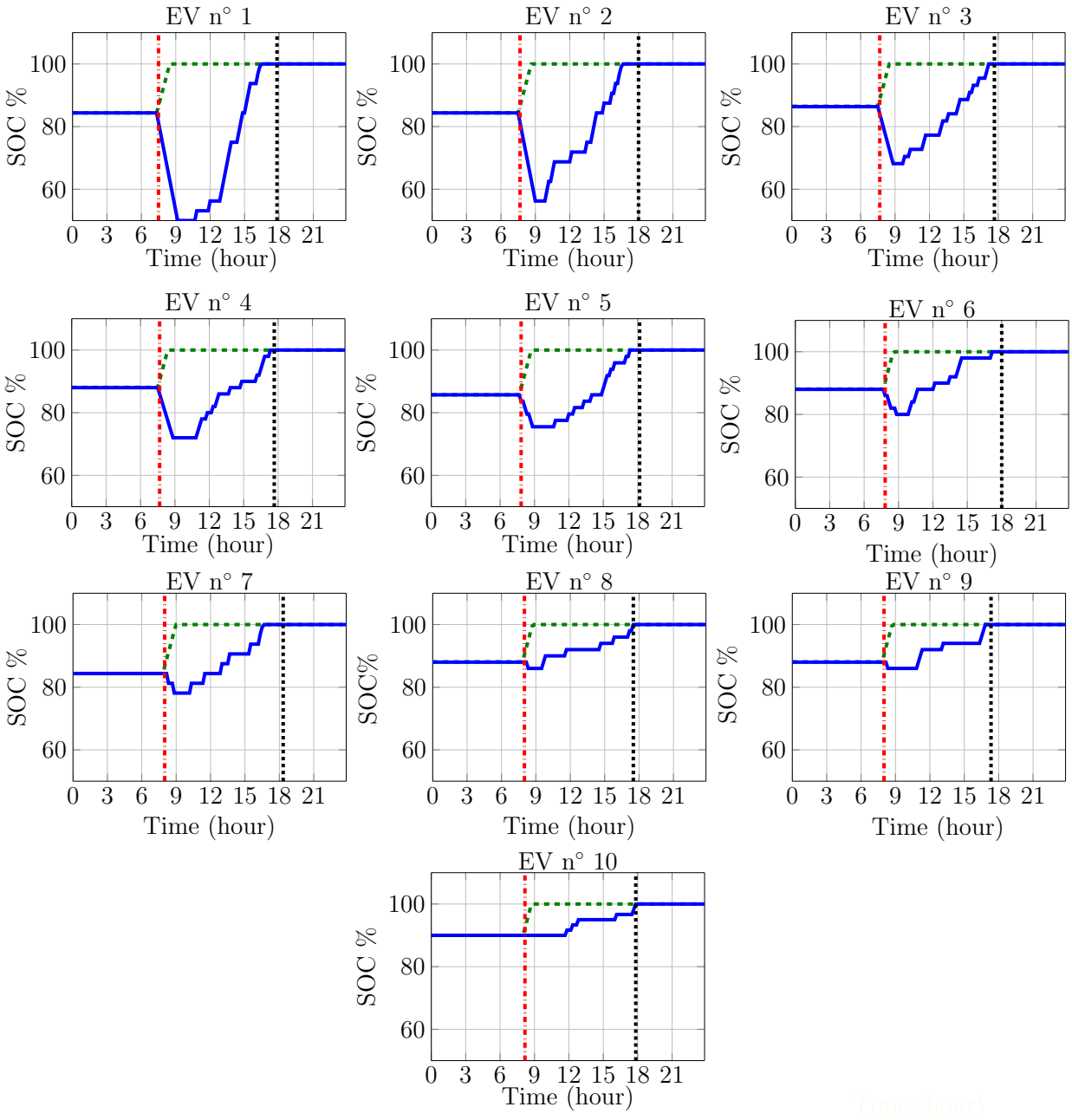

Figure 2.30: SOC evolution comparison for a case of 10 PEVs.

2.6.3 Results

For a case study of 10 PEVs in Scenario 1, the variation of state of charging due to charging by the proposed approach is compared with non-controlled case in Fig. 2.30. The arrival time and departure time of each PEV is indicated to show the respecting of users satisfaction having fully-charged battery at departure time for all PEVs. Due to the peak of consumption during the morning the PEVs arriving sooner have been asked to provide V2G for peak power reduction of the station. For the other PEVs charging coordination is applied in order to minimize the impact of charging on peak to average ratio of the DLP and consequently reducing AEI.

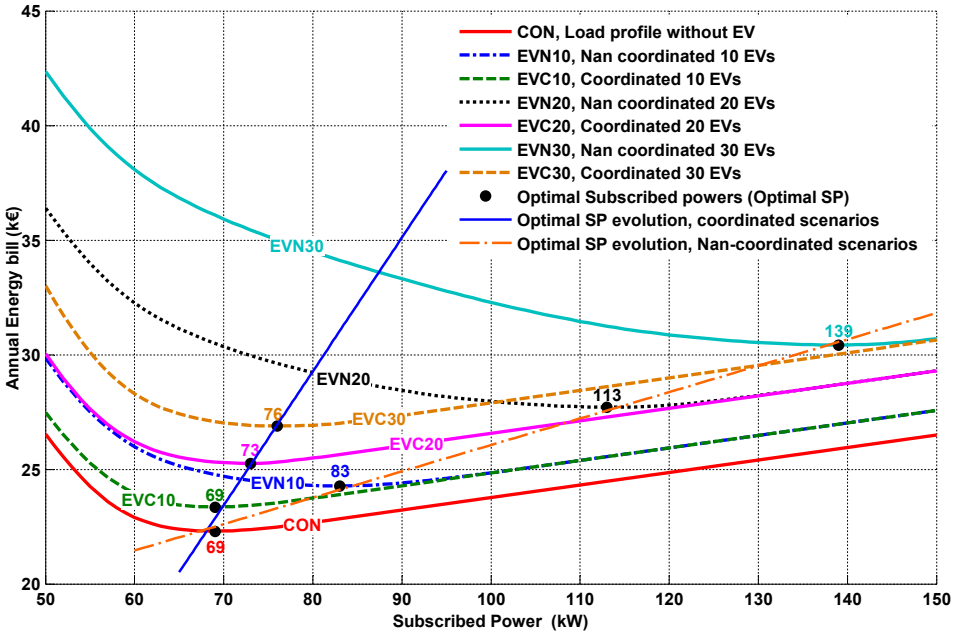

Figure 2.31: Comparison of optimum subscribed power evolution in function of number of vehicles for non-cordinated and coordinated scenarios.

The performance of proposed approach is evaluated using three indicators. Maximum power of yearly load profile is considered as the first indicator in order to represents the effectiveness of the scheduling scheme compare to non-controlled scenarios (Fig. 2.32a). As it is illustrated, the maximum power is linearly increasing by PEV number increment for all non-controlled scenarios. S2 shows a stochastic variation as it has stochastic number of PEVs shared between 3 charging modes. S3 and S4 have reletively the same ΔP_{max} as the 10 minutes averaged power are considered in AEI calculation. However, for most of optimum scenarios the value of ΔP_{max} remained relatively constant and it shows the effective performance of AEIM algorithm for peak-to-average reduction of station's consumption.

$$\Delta P_{max} = P_{max}^{withPEV} - P_{max}^{withoutPEV} \tag{2.40}$$

Optimum subscribed power is the second indicator where the impact of scheduling scheme leads to subscribed power reduction (Fig. 2.32b). A sharp increment is occurred after 5 PEVs for most of non-controlled scenarios, while for optimum scenarios the optimum P_{sub} can remain as 69 or 70 kW up to hosting 20 PEVs (the actual horizon), the subscribed power of actual contract without PEVs.

Finally, the AEI of the station is presented for all the scenarios in Fig. 2.32c. A slight increment of AEI for optimum scenarios is representing the energy part of the AEI, while the considerable differences betwwen non-controlled and optimum scenarios is evident. This

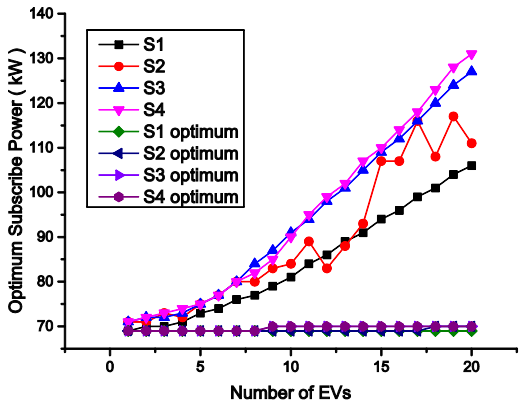

(a) Comparison of optimum P_{sub}.

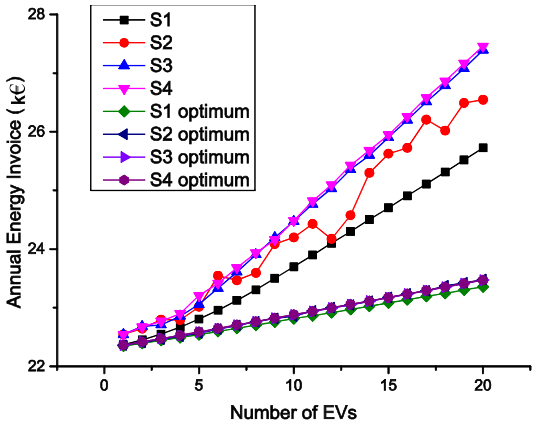

(b) Comparison of AEI for all scenarios.

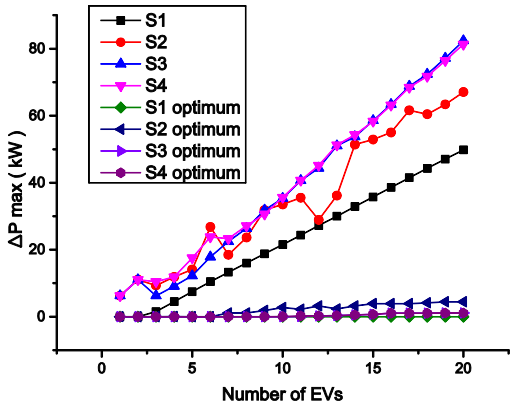

(c) Comparison of maximum power increment.

Figure 2.32: Comparison of different indicator for optimum and non-optimum scenarios

difference is comming from the impact of AEIM on peak power reduction and subscribed power optimization. Comparing the worst case, S4, the contribution of AIEM leads to approximately 20% reduction of AEI for 20 PEVs scenario.

In term of the subscribed power evolution in function of EV increment, three selected scenarios have been chosen to compare the optimum subscribed powers of coordinated and non-coordinated cases. The results for 10, 20 and 30 EVs fleet are depicted in Fig. 2.31 where the slight increment of optimum SP is evident compared to the case of non-coordinated. This is valuable from financial point of view for the stakeholders of the charging infrastructures inside the railway stations.

2.6.4 Conclusion

In this study, contribution of AEIM algorithm to peak power reduction and AEI minimization of a railway station, hosting up to 20 PEVs, were presented. The proposed algorithm is able to minimize the peak power using V2G ability of PEVs parked during the day inside the railway station parking lots. In addition, charging scheduling is applied in order to minimize the annual energy invoice of the station. The minimization of the invoice is conducted using subscribed power minimization, subscribed power exceeding minimization, and PEVs charging during low cost hours. As in this case study the electricity price during the most of the plug-in intervals was constant, the impact of later factor was not evident. However, peak power reduction and

exceeding minimization leads to minimizing up to 20% of AEI of the station. As the future works this algorithm would be updated for real-time applications and share of the same amount of V2G between all PEVs and priority based V2G service participation.

2.7 Résumé

Ce chapitre consiste en une étude des impacts des véhicules électriques sur les réseaux de distribution. Deux cas d'études principaux de la thèse ont été présentés et les études d'analyses des impacts de la demande des charges des véhicules électriques ont été évaluées. Ces impacts ont été évalués au point de vue économique pour les services minimisation des facteurs énergétiques et minimisation du facteur d'acheminement d'électricité.

Le déploiement massif des Véhicules Électriques et des Véhicules Hybrides Rechargeables va augmenter la consommation électrique, notamment dans le secteur résidentiel, les pertes dans les lignes et la chute de tension dans les réseaux de distribution. Cet effet va diminuer aussi la fiabilité et la qualité de la puissance électrique fournie aux consommateurs éventuels. Les deux moyens d'aider au déploiement des VE sont soit renforcer le réseau électrique national et la production d'énergie, soit limiter les impacts négatifs et/ou saisir les opportunités des VE grâce aux technologies V2G et la coordination des charges des véhicules électriques. Ces derniers sont les sujets principaux de cette thèse qui sont développés au cours des prochains chapitres.

Dans cette thèse, la contribution et l'impact des véhicules électriques et de la technologie V2G sont étudiés pour deux cas d'études différents. Les stratégies de gestion énergétique pour les services système possibles sont également évaluées pour ces cas. Le premier cas est un réseau de distribution régional du département des Deux-Sèvres qui contient 14 postes source (HTB/HTA) à la frontière du réseau de transport et du réseau de distribution. Pour certains services, le réseau entier, contenant la production d'énergie renouvelable (éolien et solaire), est considéré. Alors que, pour certains autres services, l'accent est mis sur un seul poste source.

Dans le deuxième cas, un concept de gare, contenant les bornes de recharges des VEs, est étudié et les services possibles avec les stratégies de gestion de l'énergie sont proposés pour les véhicules électriques. Ensuite, leur applicabilité est analysée à l'aide d'indicateurs économiques et techniques.

2.7.1 Modèle probabiliste de la charge des véhicules électriques

Pour pouvoir comprendre la problématique du rechargement des VEs du point de vue de réseau et de proposer des solutions pour la réduction des impacts négatifs, l'imputation du comportement de demande de la flotte EVS devrait être étudiée précisément. Comme aujourd'hui les flottes de véhicules électriques ne sont pas disponibles en quantité suffisante, la modélisation du profil de charge n'est pas une tâche facile. Dans cette thèse, des approches de modélisation possibles pour les VEs comme l'imputation de la modélisation de profilage sont utilisée et discutée. Ces approches de modélisation sont principalement basées sur des méthodes probabilistes en utilisant les informations du flux de trafic.

Les différentes flottes de véhicules sont analysées, mais plus spécifiquement, les véhicules faisant le trajet quotidien "travail-domicile" est le point principal de cette étude. Pour le département des Deux-Sèvres, la courbe de charge des véhicules pour deux scénarios de recharge, un à la maison et l'autre au travail est évaluée. De plus, pour des parkings de gare, les véhicules qui sont garés pendant la journée sont étudiés. Il a supposé que ces véhicules appartiennent à des personnes qui font des voyages quotidiens avec le TGV et des trains régionaux.

Dans ce chapitre, la courbe de charge des véhicules est modélisée au point de vue probabiliste et du flux de trafic.

2.7.2 Impact des véhicules électriques sur les réseaux de distribution

L'impact des VEs et de leurs contributions en utilisant la technologie V2G sont analysés pour la minimisation de coût d'acheminement d'électricité basée sur les conseils des encadrants du projet. En utilisant l'approche probabiliste, expliquée dans la section précédente, les courbes de charge des VEs pour les scénarios de recharges à domicile et à travail ont été modélisées. Après cela, deux scénarios de recharges sont considérés et l'impact des deux scénarios est analysé. Le premier est le scénario de recharge sans supervision, qui est obtenu de l'algorithme. Le deuxième est le scénario de recharge supervisé, qui a besoin d'un problème d'optimisation basé sur une fonction d'objective de minimisation du cout d'acheminement d'électricité.

En effet, le coût d'acheminement d'électricité est considéré comme la fonction objective d'un problème d'optimisation et en utilisant une méthode d'optimisation, la demande de recharge optimisée associée à la minimisation de coût d'acheminement d'électricité est calculée. Dans ce chapitre le problème d'optimisation est défini et la méthode convenable pour résoudre le problème est présentée. Finalement, les résultats d'optimisation sont présentés et la discussion terminera la section. Cette section identifiera la contribution de coordination VE/V2G au service de minimisation du coût d'acheminement d'électricité.

Le résultat de cette partie a été utilisé pour le superviseur temps réel développé dans le quatrième chapitre. Pour un scenario de 2700 véhicules électriques (provision de l'année 2030 de poste source étudié) la potentiel de V2G a été estimé autour de 200 k€ minimisation du facteur d'acheminement d'électricité. Toutefois, cet apport devra être réétudier en prenant en compte les impacts sur les batteries des VE au point de vue économique afin de pouvoir estimer les bénéficies associés à chaque utilisateur de VE.

2.7.3 Impact des véhicules électriques sur la consommation des gares

La gare pour sa consommation locale devrait verser à des fournisseurs d'énergies, une facture annuelle correspond à sa consommation. La présence des bornes de recharge des VEs peut mener à l'augmentation de la consommation d'énergie de la gare. Dans cette section une stratégie de gestion des recharges/décharges des VEs est développée en optimisant la facture d'énergétique en pilotant la variation de la charge. Au début, un problème d'optimisation déterminera la distribution appropriée d'énergie pour minimiser la facture. Puis, le deuxième problème d'optimisation déterminera l'heure de recharge/décharge des VEs afin d'atteindre l'objectif précédemment expliqué.

Afin d'analyser l'impact des VEs quotidiennement arrivés au stationnement dans les gares, différents scénarios ont été considérés. Dans cette étude la possibilité et la contribution de la recharge/décharge coordonnée est également prise en considération. Ces scénarios sont basés sur l'heure d'arrivée et l'heure de départ des VEs au stationnement. Les heures d'arrivée des véhicules sont distribuées sous la forme d'une répartition normale (Gaussien) entre 7h00 et 9h00, tandis que l'heure de départ est distribuée entre le 16h00 et 20h00. L'intervalle moyen de disponibilité est environ 10 heures. Le où les VEs peuvent être employés pour le rechargement supervisé. Le nombre total des stations de la charge a été considéré à 10 comme situation de base. La capacité de la gare est également évaluée de 1 à 50 stations de charge. Des stations de charge sont divisées en plusieurs types de recharge et différents cas ont été étudiés.

Dans cette étude, la contribution de l'algorithme d'optimisation développé pour la réduction de pic de puissance et la minimisation du facteur d'énergétique d'une gare, accueillant jusqu'à 20 VEs, ont été présentées. L'algorithme proposé peut minimiser le pic de puissance en utilisant la capacité de V2G des VEs, garés pendant la journée dans les parkings de la gare. En outre, l'établissement du programme de remplissage est appliqué afin de minimiser la facture annuelle d'énergie de la gare. La minimisation de la facture est possible en utilisant la minimisation de

puissance souscrite, la minimisation de dépassement de puissance souscrite, et la recharge des VEs pendant des heures creuses (prix bas). Comme dans ce cas d'étude, le prix de l'électricité, pendant la plupart des intervalles des disponibilités des VEs, était constant, la contribution du dernier élément n'était pas aussi importante. Cependant, la minimisation de pic de puissance et la minimisation de dépassement mènent à minimiser jusqu'à 20% de la facture annuelle d'énergétique.

2.7.4 Conclusion

Dans ce chapitre une étude des impacts des véhicules électriques sur les réseaux de distribution a été menée. Ces impacts sont étudiés particulièrement pour deux cas d'étude ; le réseau de distribution du département Deux-Sèvres et les trois gares types de SNCF. Pour le cas d'étude du réseau de distribution, les véhicules sont considérés comme une flotte qui font le trajet quotidien "domicile–travail" et pour le cas d'étude des gares, comme une flotte qui font le même trajet mais leur disponibilité est considérée que pendant le temps qu'ils sont garés dans les parkings de la gare. Ces impacts sont étudiés autour des indicateurs économiques comme le coût d'acheminement d'électricité pour le gestionnaire de réseau de distribution et le facture énergétique annuelle de la gare pour SNCF. En deuxième étape, la possibilité de diminuer les impacts négatifs grâce au superviseur ont été étudié. Cette partie a été faite grâce aux méthodologies d'optimisation comme la programmation linéaire. Alors que dans les prochains chapitres, un système de supervision en temps réel sera développé pour ce but.

2.8 References

[Agarwal 14] L. Agarwal, Wang Peng & L. Goel. *Probabilistic estimation of aggregated power capacity of EVs for vehicle-to-grid application.* In 2014 International Conference on Probabilistic Methods Applied to Power Systems (PMAPS), pages 1–6, July 2014. 47

[Bouallaga 13] A. Bouallaga, A. Merdassi, A. Davigny, B. Robyns & V. Courtecuisse. *Minimization of energy transmission cost and CO2 emissions using coordination of electric vehicle and wind power (W2V).* In PowerTech (POWERTECH), 2013 IEEE Grenoble, pages 1–6, June 2013. 55

[Bouallaga 15] Anouar Bouallaga. *Gestion énergétique d'une infrastructure de charge intelligente de véhicules électriques dans un réseau de distribution intégrant des énergies renouvelables.* PhD thesis, Université Lille 1 Sciences et Technologies, 2015. 55

[Clement-Nyns 10] K. Clement-Nyns, E. Haesen & J. Driesen. *The Impact of Charging Plug-In Hybrid Electric Vehicles on a Residential Distribution Grid.* IEEE Transactions on Power Systems, vol. 25, no. 1, pages 371–380, February 2010. 41

[Fluhr 10] J. Fluhr, K.-H. Ahlert & C. Weinhardt. *A Stochastic Model for Simulating the Availability of Electric Vehicles for Services to the Power Grid.* In 2010 43rd Hawaii International Conference on System Sciences (HICSS), pages 1–10, January 2010. 47

[Geth 12] F. Geth, N. Leemput, J. Van Roy, J. Buscher, R. Ponnette & J. Driesen. *Voltage droop charging of electric vehicles in a residential distribution feeder.* In Innovative Smart Grid Technologies (ISGT Europe), 2012 3rd IEEE PES International Conference and Exhibition on, pages 1–8, Oct 2012. 42

[Gonzalez Vaya 14] M. Gonzalez Vaya, G. Andersson & S. Boyd. *Decentralized control of plug-in electric vehicles under driving uncertainty.* In Innovative Smart Grid Technologies Conference Europe (ISGT-Europe), 2014 IEEE PES, pages 1–6, October 2014. 47

[Grahn 11] P. Grahn, J. Rosenlind, P. Hilber, K. Alvehag & L. Soder. *A method for evaluating the impact of electric vehicle charging on transformer hotspot temperature.* In Innovative Smart Grid Technologies (ISGT Europe), 2011 2nd IEEE PES International Conference and Exhibition on, pages 1–8, Dec 2011. vi, 41, 42

[Gray 14] M.K. Gray & W.G. Morsi. *Power Quality Assessment in Distribution Systems Embedded With Plug-In Hybrid and Battery Electric Vehicles.* Power Systems, IEEE Transactions on, vol. PP, no. 99, pages 1–9, 2014. 42

[Han 11] Sekyung Han, Soohee Han & K. Sezaki. *Estimation of Achievable Power Capacity From Plug-in Electric Vehicles for V2G Frequency Regulation: Case Studies for Market Participation.* IEEE Transactions on Smart Grid, vol. 2, no. 4, pages 632–641, December 2011. 47

[Hilshey 13] AD. Hilshey, P.D.H. Hines, P. Rezaei & J.R. Dowds. *Estimating the Impact of Electric Vehicle Smart Charging on Distribution Transformer Aging.* Smart Grid, IEEE Transactions on, vol. 4, no. 2, pages 905–913, June 2013. 41

[Masoum 10] Mohammad AS Masoum, Sara Deilami & Syed Islam. *Mitigation of harmonics in smart grids with high penetration of plug-in electric vehicles.* In

Power and Energy Society General Meeting, 2010 IEEE, page 1–6. IEEE, 2010. vi, 41, 42, 43

[Putrus 09] G.A Putrus, P. Suwanapingkarl, D. Johnston, E.C. Bentley & M. Narayana. *Impact of electric vehicles on power distribution networks*. In Vehicle Power and Propulsion Conference, 2009. VPPC '09. IEEE, pages 827–831, Sept 2009. 42

[Raghavan 12] S.S. Raghavan & A Khaligh. *Impact of plug-in hybrid electric vehicle charging on a distribution network in a Smart Grid environment*. In Innovative Smart Grid Technologies (ISGT), 2012 IEEE PES, pages 1–7, Jan 2012. 41

[Roe 09] C. Roe, E. Farantatos, J. Meisel, AP. Meliopoulos & T. Overbye. *Power System Level Impacts of PHEVs*. In System Sciences, 2009. HICSS '09. 42nd Hawaii International Conference on, pages 1–10, Jan 2009. 41

[Rolink 13] J. Rolink & C. Rehtanz. *Large-Scale Modeling of Grid-Connected Electric Vehicles*. IEEE Transactions on Power Delivery, vol. 28, no. 2, pages 894–902, April 2013. 47

[Sarabi 13] Siyamak Sarabi, Laid Kefsi, Asma Merdassi & Benoit Robyns. *Supervision of Plug-in Electric Vehicles Connected to the Electric Distribution Grids*. International Journal of Electrical Energy, vol. 1, no. 4, pages 256–263, 2013. vi, 43, 44

[Sarabi 14] S. Sarabi, A Bouallaga, A Davigny, B. Robyns, V. Courtecuisse, Y. Riffonneau & M. Regner. *The feasibility of the ancillary services for Vehicle-to-grid technology*. In European Energy Market (EEM), 2014 11th International Conference on the. IEEE, May 2014. 52

[Sarabi 15] S. Sarabi, A. Davigny, Y. Riffonneau, V. Courtecuisse & B. Robyns. *Contribution and Impacts of Grid Integrated Electric Vehicles to the Distribution Networks and Railway Station Parking Lots*. In Electricity Distribution (CIRED 2015), 23rd International Conference and Exhibition on, pages 1–5, June 2015. 65

[Shao 09] Shengnan Shao, M. Pipattanasomporn & S. Rahman. *Challenges of PHEV penetration to the residential distribution network*. In Power Energy Society General Meeting, 2009. PES '09. IEEE, pages 1–8, July 2009. 41

[Soares 11] F.J. Soares, J.A. Peças Lopes, P.M. Rocha Almeida, C.L. Moreira & Luís Seca. *A stochastic model to simulate electric vehicles motion and quantify the energy required from the grid*. In 17th Power Systems Computation Conference, pages 1–7, Stockholm, 2011. 47

[SYT 13] SYT. *Real time traffic state in Île-de-france*. http://www.sytadin.fr/sys/barometre_courbe_cumul.jsp.html, 2013. 49

[Turker 12a] H. Turker, S. Bacha, D. Chatroux & A. Hably. *Low-Voltage Transformer Loss-of-Life Assessments for a High Penetration of Plug-In Hybrid Electric Vehicles (PHEVs)*. IEEE Transactions on Power Delivery, vol. 27, no. 3, pages 1323–1331, July 2012. 41

[Turker 12b] H. Turker, S. Bacha, D. Chatroux & A Hably. *Modelling of system components for Vehicle-to-Grid (V2G) and Vehicle-to-Home (V2H) applications with Plug-in Hybrid Electric Vehicles (PHEVs)*. In Innovative Smart Grid Technologies (ISGT), 2012 IEEE PES, pages 1–8, Jan 2012. 53

[TURPE 15] TURPE. *Tarif d'Utilisation des Réseaux Publics d'Electricité*. http://www.enedis.fr/sites/default/files/enedis_bareme_turpe_16.pdf, 2015. 55

[Zhang 13] Ze Zhang, Hsiao-Dong Chiang & Tao Wang. *Harmonic analysis of power system with wind generations and plug-in electric vehicles*. In Electrical Power Energy Conference (EPEC), 2013 IEEE, pages 1–6, Aug 2013. 42

Chapter 3

V2G Ancillary services for distribution grids: Potential assessments

Contents

3.1 Introduction

V2G enabled PEVs, which have the ability to inject power to the grid, have been presented as grid supporters [Tomić 07] and potential ancillary service (A/S) providers, where eventually make the transportation electrification beneficial for the grids [Kempton 05].
In the literature, the economic [Luo 12], [De Los Rios 12], [Han 12], [Gao 13] and technical [Ehsani 12], [Han 11] feasibilities of PEV fleet as the energy storage and service providers are discussed. They are considered in different services markets such as, regulation, spinning reserve [Pavić 15], peak power support [Jian 15] and power quality [Falahi 13] and more from economic point of view. While, technical analyses are mainly limited to capacity estimation, optimal coordination, aggregator communication architectures and battery degradation impacts [Han 11, Jian 15, Quinn 10, Bishop 13]. The points related to aggregator volume requirements, grid/services localization limitations and PEVs availability uncertainty impacts on bidding capacities are not discussed or less explored. In addition, the aggregator volume in terms of the required number of vehicles for providing each ancillary service is not analyzed up to now.

In term of the energy management systems for plug-in electric vehicles and V2G technologies, different scheduling and management schemes are developed. An adaptive intelligent system using fuzzy logic controller and Adaptive Neuro-Fuzzy Inference System (ANFIS) is developed in [Khayyam 14]. In [Khayyam 13] an intelligent energy management using cloud computing network is proposed. These technics reduce operation of electric vehicle, grid and parking lot as well as the load demand prediction. A large scale fuzzy logic based intelligent control for V2G is also proposed in [Khayyam 12] which provides different services such as, peak power, balancing control, load levelling and voltage regulation. For specific services, different control strategies are developed. For instance, a preventive control strategy for controlling static voltage stability is proposed in [WANG 15, Wang 14] which maintains the static voltage stability of power system under the V2G concept and evaluates the V2G response capability with different charging strategies during a whole day.

The innovative aspects of the presenting work in this chapter compared to the aforementioned researches is considering the uncertainty impact on the V2G capacity, and scalability of the flexible V2G power capacity for different level of distribution grid by considering localization limitation of different services. Hence the service assessment can be applicable up to the low voltage (LV) distribution grid services such as voltage regulation and load levelling at LV grid. Interdependency of stochastic variables such as arrival time, departure time and driving distance are also modelled and their impacts on the contracted power are analyzed.

The novelty of the presenting work is that it has provided a multi-level methodological approach in order to assess the V2G potential, suitable for regional distribution system operators. In this approach, the PEVs' availability uncertainty and localization/limitation are considered as the main factors affecting the potential of V2G for grid ancillary service participation. A probabilistic model is developed in order to estimate the availability uncertainty using only daily trips probability data. The interdependency of the stochastic variables are also modeled using a copula function. This modeling approach, takes into account the impact of uncertainty on the bidding capacities and improve the reliability of the contracted bidding. In addition, in order to be realistic, the distribution of electric vehicles in the distribution grid is estimated using real customers' distribution data to estimate the real potential of PEV fleet for different ancillary services.

A/S providers at the distribution grid level are faced with the localization limitation for each type of service. Such limitations make difficult to achieve the services' requirements for PEV aggregators, as the aggregated number of PEVs at the different level of the grid is not always sufficient. Moreover, the aggregators need to have sufficient information for offering a

reliable bidding capacity, which depend upon the type of services for which they would be the candidate. However, the general requirements are the amount of energy in form of power and time interval. These are predefined by grid actors based on the grid characteristics in different countries[1]. The constraints related to PEVs aggregation such as, available aggregated power and PEVs availability uncertainty should be taken into account in order to be competitive in the markets. These constraints are the main concerns of this chapter, where the effort is to propose an approach for potential assessment of a candidate PEV fleet under an aggregation contract, particularly at the level of distribution grid by considering;

1. Available V2G power of the fleet.
2. Availability uncertainty of the fleet and its impacts on the bidding capacities' reliability.
3. The flexibility of the available power interval under bidding capacity contracts.
4. Distribution grid services/localization limitations.

In this chapter, at first the general approach for ancillary service assessment of V2G enabled PEVs at the distribution grid level is introduced. Afterwards, all necessary input data for the assessment are identified. The methodology is applied on Niort, a city in west of France, considering its mobility statistics and distribution grid topology. The methodologies for available V2G power modeling, availability uncertainty modeling, the flexibility of the bidding capacities' calculation and the service assessment system will be explained thoroughly in the next sections. A general research background is presented to show actual solutions and the main contribution of this thesis for V2G ancillary service assessment.

3.2 Literature review

Different methods have been proposed for capacity estimation of PEV fleet, but none of them consider the localization limitation of the services. Reference [Han 11] calculates achievable power capacity by binomial distribution of clustered PEVs. Reference [Fluhr 10] uses the survey data to identify the location of PEVs during the day. In [Soares 11] Monte Carlo simulation is used to estimate the probability of transition between different states, e.g. parked or movement for different parking location. A non-homogeneous semi-Markov process is used in [Rolink 13] for PEV availability and identifying the charging load, while in [Gonzalez Vaya 14] a continuous time non-Markov chain is chosen as the mobility patterns do not fulfill the Markov property (memorylessness). Reference [Agarwal 14] uses the trip chains for mobility modeling of PEV fleet and concluded that the home and office car parks have maximum availability among other place parkings. Among all of these researches backgrounds and our case study mobility survey, it is concluded that the PEVs are parked in home and office parkings mostly a day and their service providing potential at these time intervals is relatively higher than other places, such as parking lots of shopping centers or the streets, which are highly stochastic and periodically short.

The second limitation is the uncertainties associated with availability of the PEVs for service providing. Reference [Mathieu 13] defines the uncertainty sources as the model based uncertainties and forecasting based uncertainties. The model-based uncertainties come from the aggregated battery model instead of the individual battery model [2]. The second source is

[1] From August 2014, RTE, the French transmission system operator (TSO), announced that industrial consumers henceforth could be reserve service providers with a minimum power of 2 MW [RTEPress 14]. This is also estimated for the distributed energy storage systems at the distribution grid level with a minimum of 1 to 2 MW power [Delille 09].

[2] In modeling large number of PEVs it would be impractical to model all batteries' dynamics in detail.

related to forecasting data such as arrival, departure time, driving behavior and arrival state of charge (SOC) of PEVs. In [Vayá 14], the driving behavior uncertainty is modeled with individual driving behavior with the non-Markov chain process by the states' transition probabilities defined based on mobility survey data. In [Momber 15], a two-state single node Monte Carlo simulation is used to represent the uncertainty in driving behavior by concentrating on stochastic variables with the independent sampling process. While in this chapter, interdependency of stochastic variables are modeled in a multivariate manner using copula function.

The predictable sources of uncertainties are normally following a particular probability distribution. These are known as arrival time, departure time and driving distance distribution. In addition, in the future smart grid, the communication infrastructures will facilitate accessibility and predictability of such information. Therefore, considering highly enough accurate prediction system, the uncertainties associated with prediction errors can be negligible. In the other side, there are some sources of uncertainty, which are not predictable at all, like the unforeseen departure of PEVs during their stationing time (plug-in time). Considering that, a probabilistic approach is proposed for this study, that can provide the probability distribution function (pdf) of availability uncertainty. The advantage with this approach is the ability to quantify the availability uncertainty impact on the bidding capacities by only knowing the daily trips percentage, arrival and departure time probability of the fleet.

3.3 General Approach

The general approach consists of 6 sub-blocks, each doing a particular task for the final objective (Fig. 3.1):

1. Available Vehicle-to-Grid Power Modeling (AVPM)
2. Fundamental Parameters Estimation (FPE)
3. Multivariate Modeling of Stochastic Variables (MMSV)
4. Probabilistic Availability Uncertainty Modeling (PAUM)
5. Bidding Flexibility Calculation (BFC)
6. Fuzzy Inference System Service Assessment (FISSA)

AVPM: In this study, the focus is on PEVs doing daily home-work commuting for ancillary service assessment as they have the most reliable behavior among the other motives trips. For this reason, the available V2G power of the fleet has been modeled for two potential intervals, one in the morning, after PEV arrival to the offices and second one in the evening, when the vehicles come back to the home parkings. The outputs of FPE, MMSV and PAUM blocks will be used in AVPM block in order to calculate the AVP for each potential intervals. The assumption made for home V2G scenario and office V2G scenario are brought in the next sections.

FPE: Fundamental parameters for modeling the available V2G power are calculated in FPE block, which contain arrival SOC, V2G energy, G2V energy and plug-in interval. These parameters which are the indirect parameters will be calculated using the output parameters of MMSV block and averaged PEV characteristic parameters such as, driving efficiency, charging, discharging efficiency, NEDC autonomy and averaged battery capacity of the fleet.

MMSV: The main inputs, defining the available V2G power of the fleets, consist of arrival time, departure time and daily driving distance for each individual vehicle. This information

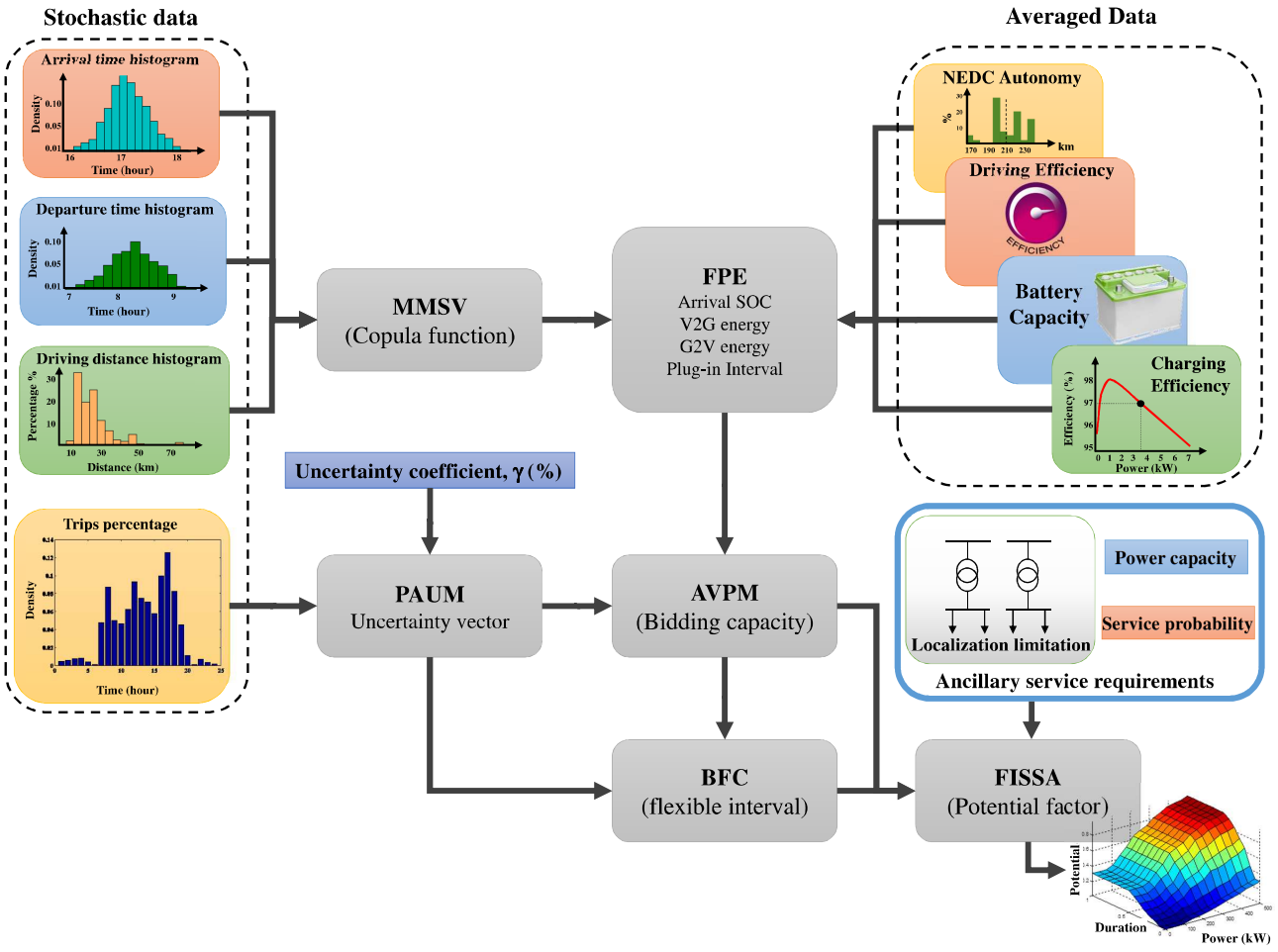

Figure 3.1: General framework of V2G ancillary service assessment approach.

comes from the probability distribution of each variable from mobility survey results of the case study (middle city), while the interdependency of these variables are not always available. In fact, utilizing multivariate modeling approach the correlation between two variables can be identified considering the type of under studying fleet and the vehicle's driving behavior. In this work, correlation between arrival time, departure time and driving distance is explored for PEVs doing daily home-work commuting using copula function. This issue is considered as one of the possible uncertainty on the contracted V2G power.

PAUM: A novel approach is proposed in PAUM block, which uses only the daily trips percentage data in order to associate a probability density function to the availability uncertainty phenomena, by filtering the known components of the Gaussian mixture model of trips percentage. These known components are the arrival and departure trips pdf. It means that the trips which may happen stochastically during the plug-in interval of the parked PEVs are certainly existed on the daily trips percentage data. However, the part of density which is related to their previous trips for home/office arriving/departing should be removed from the global density function fitted to the daily trips percentage.

BFC: After defining the AVP and its potential bidding capacities for both scenarios, the flexibility of each bidding capacity will be calculated in BFC block using a global stochastic optimization method so-called "Free Pattern Search" which is chosen for its robustness and convergence quality for high dimension stochastic problems.

FISSA: Finally, in FISSA block a fuzzy inference system (FIS) is designed for service

assessment of each PEV fleet based on the PEVs population provision of under studying city. This system uses the AVP of each bidding and its flexibility as FIS inputs and will generate a potential factor of 0 to 1 in order to evaluate the fleet potential for each service. The membership functions of the inputs are designed based on the A/S power and time requirements, while the frequency of each service utilization is considered by hourly probability values of each service's activation signal. In addition, a grid service/localization limit factor is considered to evaluate the aggregated number of PEVs at the appropriate location of the grid. At the end, an illustrative indicator is made in order to facilitate the evaluation of fleet/services under PEV provision scenarios.

3.4 Case study and Input data

This study is proposed in order to analyze the potential of PEV fleet for ancillary service providing, particularly for distribution grid level. It is assumed for the current assessment, the minimum statistical information about the under studying place is available, where the approach will be applicable to the future case studies when the communicable data can be available via the smart grid communication infrastructures. This approach is practical for local distribution system operators (DSO) managing the middle cities' distribution grid operations. Niort, a city in west of France, is considered as the case study in this chapter where the statistical data are available for this city from the municipality online data sources and INSEE, the French national institute of statistics and economics studies [ins 10]. Based on the previous scenario of electric vehicle evolution of France conducted by sustainable development ministry, 2 million electric vehicles are supposed to be registered up to 2020 [Sarabi 13] (High Scenario). However, based on the actual evolution rate a new scenario is proposed by ENEDIS, a major French DSO, which has estimated maximum of 800,000 electric vehicles up to 2020 [Sarabi 15] (Low Scenario). The two evolution scenarios up to 2030 are considered in this study as the PEV evolution scenarios illustrated in Fig. 3.2. Having the vehicle fleet statistics of Niort city department and its municipality population, the PEV evolution can be calculated for this city. As proposed by [Salah 15], the cars-per-capita quota is used in order to transfer the unit from population to the car number. The PEV provision scenarios of the year 2020, 2025 and 2030 are considered as the case study (Table. 3.1).

Table 3.1: PEV evolution scenarios for Niort city.

Evolution horizon	**Low Scenario** (PEV numbers)	**High Scenario** (PEV numbers)
2020	851	2127
2025	1808	5849
2030	2659	9572

The input data for this study are divided into two main natures; averaged data and stochastic data. Averaged data are related to the information correspond with the vehicle characteristics, which help to estimate the available and consumed energy of the vehicle's battery. For this study, based on the actual French electric vehicles market, the values are considered as in Table. 3.2. The stochastic variables which are mainly four variables come from statistical survey and databases for Niort city:

1. Arrival time distribution
2. Departure time distribution

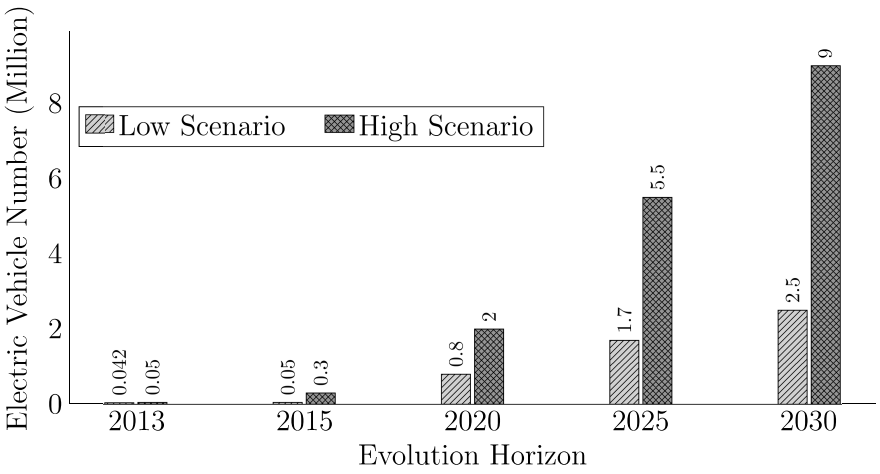

Figure 3.2: Electric vehicles' Evolution Scenarios in France.

3. Daily Driving distance distribution

4. Daily trips percentage

Table 3.2: Averaged PEV characteristics in French market.

Parameter	**Symbol**	**Value**
Battery Capacity	E_{ev}	22 kWh
Charging/Discharging efficiency	η_{cd}	97.5%
Charging/Discharging power	P_{ch}	3.7 kW
NEDC autonomy	A	210 km
Driving efficiency	η_{ev}	97%
Admissible depth of discharge	DoD	80%

The arrival and departure time's distribution of both home and office scenario are following approximately a Gaussian distribution by the parameters presented in the Table. 3.3. The daily driving distance distribution of home scenario takes into account a daily round trip and for office scenario, a single way trip to the office and both are approximated to follow the same distribution (Fig. 3.3).

Daily trips percentage data show the hourly percentage of the trips for a working day done by personal vehicles for the Niort city. This distribution is used in order to model the availability uncertainty of the PEVs (Fig. 3.4). The available number of PEVs for home scenario is correlated with PEV fleet in Niort, while for office scenario as the estimation of the available number of PEVs in the office parking during the day is difficult, their possible number is calculated based on grid capacity of each professional customer contract. In the next section, the AVP modeling approach is explained along with problem formulation and flowchart.

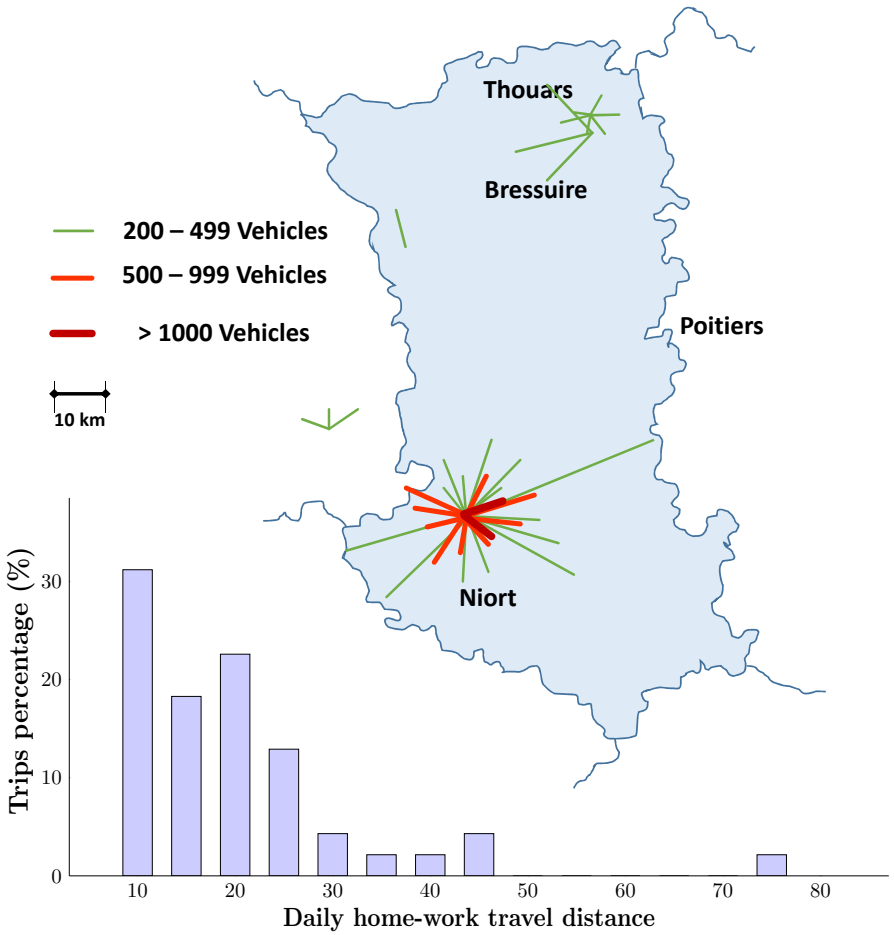

Figure 3.3: Daily driving distance for home-work commuting in Niort [ins 10].

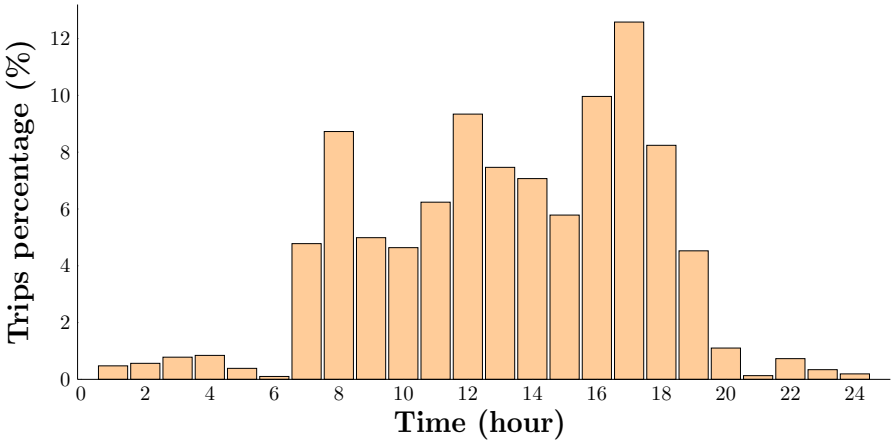

Figure 3.4: Daily trips percentage in Niort city [ins 03].

Table 3.3: Home-work PEV fleet normal distribution function parameters.

Distribution	μ **(hh:mm)**	σ **(minutes)**
Home departure	07:45	30
Home arrival	17:15	30
Office arrival	08:15	30
Office departure	16:45	30
Home-work trips	08:00	30
Work-home trips	17:00	30

3.5 Available V2G power modeling (AVPM)

In this part, Available V2G power (AVP) of PEVs doing home-work daily commuting based on real statistics data are estimated where their possible interdependency is modeled by the copula function. Secondly, three bidding capacities of high-potential intervals are introduced, and further analysis will be concentrated on these three bidding capacities. Different scenarios in terms of aggregator volume (number of PEVs in the fleet) will be studied in which their bidding capacities will be assessed for different ancillary services. In this study, AVP of home-work commuting PEV fleet has been evaluated in two potential intervals. First V2G at work only and second V2G at home only. The main assumptions behind the work are as follows:

- Charging/discharging rate at normal level (16A, 230 V, 3.7 kW).
- The PEV will provide V2G service once in a day and will be full charged once in a day.
- 2 scenarios for V2G service assessment have been considered:
  - V2G at home (the PEV will make a round trip and then provide V2G at home only).
  - V2G at work (the PEV after arrival to the office will provide V2G at work, considering energy need for its return and minimum energy of 20% as constraint to reduce degradation impact of V2G, i.e. 80% Depth of Discharge (DoD)).

For home scenario, PEVs will be fully charged at departure time, while at the office scenario, PEVs have sufficient energy for the return trip plus 20% energy in battery (the charging process will be done at off-peak hours and during the home parking period). These assumptions were made to evaluate the maximum possible potential for aggregated V2G power during each interval. The fact is that, if we consider that PEVs will provide V2G services both at home and office, leading to portioned aggregated V2G power between home and office intervals.

3.5.1 Fundamental parameter estimation (FPE)

AVP modeling flowchart is provided in Fig. 3.5. In order to model the available V2G power, there is some information that should be acquired. Availability of each PEV in the V2G enabled parking, and its stored battery energy at arrival time is the key information in defining the AVP. Availability of PEVs will be identified by their arrival time to home/work parking and departure time from home/work for home/work V2G scenarios. Assuming N PEVs with full-charged battery at home departure moment, the arrival state of charge ($SOC^i_{arrival}$) of the i^{th} PEV battery can be estimated as follows:

$$SOC^i_{arrival} = (1 - \frac{D^i_d}{A^i}) \times 100\% \tag{3.1}$$

This is under the assumption of linear SOC drop with travel distance [Zhou 11]. D^i_d denotes the driving distance of i^{th} PEV from home to work for work scenario and round trip for home scenario. The probability densities of arrival time ($T_{arrival}$), departure time ($T_{departure}$) and driving distance (D_d) have been presented in previous section . In this section, the steps to model AVP are presented. The interdependency of these stochastic variables and their impacts on AVP will be analyzed afterwards. In current calculation, the averaged correlation coefficients are considered, where their calculations will be explained in MMSV block section. After SOC estimation, Available V2G energy should be estimated for each V2G scenario.

$$E^i_{v2g} = (DoD \times E_{ev} - \frac{D^i_d}{\eta_{ev}})\eta_{cd} \tag{3.2}$$

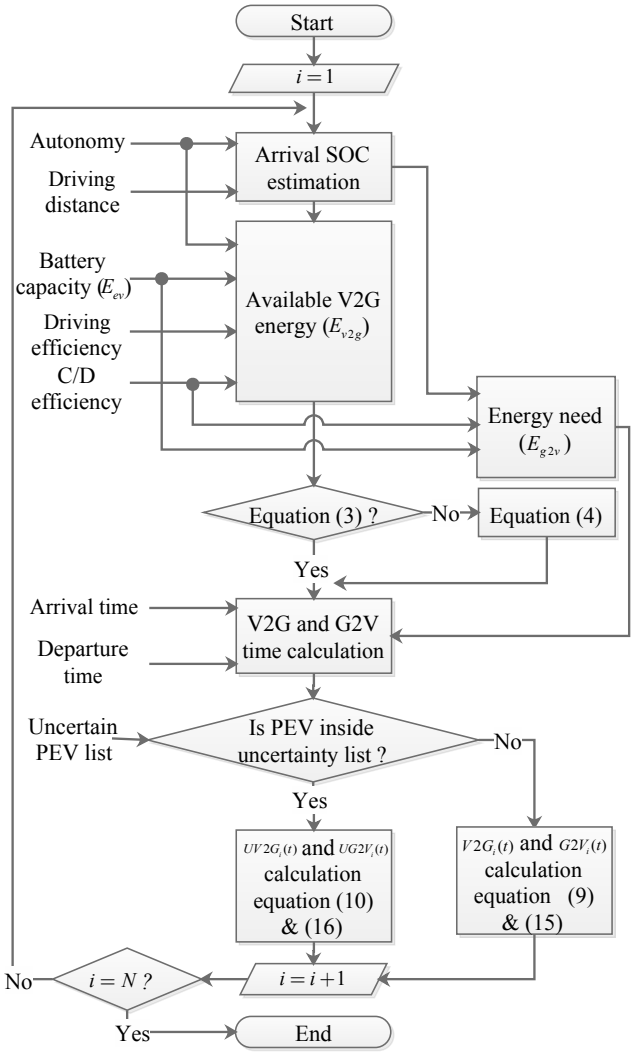

Figure 3.5: The flowchart of AVPM.

For estimated V2G energy following constraint should be satisfied:

$$2E^i_{v2g} + \frac{D^d_i}{\eta_{ev}} \leq T^i_{plug-in} \times P_{ch} \tag{3.3}$$

Where $T_{plug-in}$, is the plug-in interval of the PEV. If (3.3) did not satisfy, the V2G energy should be recalculated as follows:

$$E^i_{v2g} = \frac{(T^i_{plug-in} \times P_{ch})}{2} - E^i_{g2v} \tag{3.4}$$

For office scenario, the consideration is vehicle needs to have the same amount of energy as it has already consumed for arrival to the work, plus 20% SOC to limit DOD at 80%.

$$E^i_{v2g-work} = (DoD \times E_{ev} - \frac{2D^i_{d-work}}{\eta_{ev}})\eta_{cd} \tag{3.5}$$

The duration of V2G and G2V action can be easily calculated by dividing the energy by charging/discharging rate:

$$T^i_{v2g} = \frac{E^i_{v2g}}{P_{ch}} \tag{3.6}$$

$$T^i_{g2v} = \frac{E^i_{g2v}}{P_{ch}} \tag{3.7}$$

After identifying the V2G and G2V energy, the planning should be applied. The charging and discharging planning should be done in a way to have maximum difference and minimum overlap between V2G and G2V power curves. The reason behind this choice is to be able to estimate the maximum achievable V2G power capacity of the fleet. This leads to analyze the potential services with respect to the maximum achievable V2G power of each bidding capacity, which will be presented afterwards. Overlapping of V2G and G2V power or mixed planning, i.e. charging/discharging at the same time horizon, leads to reduce the V2G capacity of the fleet from aggregator capacity point of view. For home V2G planning the plug-in interval ($PI_i(t)$) and V2G interval ($V2G_i(t)$) are defined as follows:

$$PI_i(t) = \begin{cases} 1, & T^i_{arrival} < t < T^i_{departure} \\ 0, & elsewhere \end{cases} \tag{3.8}$$

$$V2G_i(t) = \begin{cases} 1, & T^i_{arrival} < t < T^i_{arrival} + T^i_{v2g} \\ 0, & elsewhere \end{cases} \tag{3.9}$$

It means that, the PEVs are asked to be discharged upon their arrival, to have time to be fully charged up to departure time. In fact, after discharging period the PEV has time to recharge its battery and being full-charged for departure.

We define here the uncertain V2G time vector to complete formulation, where the complete approach to the uncertainty modeling is explained in the next section. Uncertain V2G time vector is:

$$UV2G_i(t) = UA_i(t) \times PI_i(t) \times V2G_i(t) \tag{3.10}$$

Where $UA_i(t)$, is the unavailability vector and the output of PAUM block. We define γ as the uncertainty coefficient, the portion of PEVs fleet, which have uncertain behavior potential.

$$K = \gamma \times N, \forall K \in Q \tag{3.11}$$

$$M = N - K, \forall M \in E \tag{3.12}$$

Where Q is the integer set of uncertain PEVs numbers, and E is the integer set of certain PEVs, where the following low is consistent:

$$E \cup Q = N \tag{3.13}$$

Finally, the V2G power called AVP for home scenario is as follows:

$$P_{v2g}(t) = \sum_{i=1}^{K}(UV2G_i(t) \times P_{ch}) + \sum_{i=1}^{M}(V2G_i(t) \times P_{ch}) \tag{3.14}$$

The G2V interval for calculation of G2V power should be defined as follows:

$$G2V_i(t) = \begin{cases} 1, & T^i_{departure} - (T^i_{g2v} + T^i_{v2g}) < t < T^i_{departure} \\ 0, & elsewhere \end{cases} \tag{3.15}$$

Uncertain G2V time vector is necessary for uncertain PEV and is obtained using:

$$UG2V_i(t) = UA_i(t) \times PI_i(t) \times G2V_i(t) \tag{3.16}$$

Using uncertain G2V vector and G2V vector, the G2V power of the fleet is estimated by using equation (3.17):

Table 3.4: Bidding capacities' characteristics for home and office scenarios.

Scenario	BC1		BC2		BC3	
	pi (h)	Power (kW)	pi (h)	Power (kW)	pi (h)	Power (kW)
Home Scenario	5.5	550	4.2	1750	3	3050
Office Scenario	5.2	550	4	1750	2.9	3050

$$P_{g2v}(t) = \sum_{i=1}^{K}(UG2V_i(t) \times P_{ch}) + \sum_{i=1}^{M}(G2V_i(t) \times P_{ch}) \tag{3.17}$$

The final output of this block for a case of 1000 PEV fleet is depicted in Fig. 3.6 and 3.7. The potential bidding capacities from AVP at home and office are explained afterwards.

3.5.2 Bidding capacities (BC)

In this part, the bidding capacities are introduced. Based on the distribution function of arrival time, we have proposed three indicative intervals, so-called "potential interval (pi)", where there are a considerable cumulated number of PEVs and the V2G capacity of the fleet can be contracted. These three capacities, proportional with the number of available PEVs, are called bidding capacity for service market participation. We define the bidding capacity z, $(1 \leq z \leq 3 \in \mathbb{N})$ and its function, $BC_z(t)$, with its capacity value, Cap_z during its interval from t_1 to t_2.

$$BC_z(t) = \begin{cases} Cap_z, & t_1 < t < t_2 \\ 0, & elsewhere \end{cases} \tag{3.18}$$

The three indicative times have been chosen in order to propose biding start times BS_z for each bid as follows:

$$BS_z = \begin{cases} \mu - \sigma, & z = 1 \\ \mu, & z = 2 \\ \mu + \sigma, & z = 3 \end{cases} \tag{3.19}$$

The potential interval for each bid will be started from bidding start time until the power capacity equals to $BC_z(BS_z)$ as it is shown in the figures for both scenarios. In the Fig. 3.6, the V2G power called AVP, is starting right after the availability of the fleet shown in form of the arrival time histogram. It increases up to its maximum value correspond to the whole fleet available PEVs, which is 3.7 MW active power. Due to the constraints of the PEVs such as, maximum battery DoD and their availability interval, the AVP decreases to zero until around 22:00 PM. The G2V power corresponds to PEVs charging is completely separated from V2G power starting from 2:00 AM ending by the departure of the whole fleet around 9:00 AM. From the modeled AVP, three candidates bidding capacities are extracted with the characteristics represented in Table. 3.4. In Fig. 3.7, the AVP is modeled with same strategy while the constraints are minimum required energy for return trip and minimum battery DoD. These two modeled AVPs will be analyzed for V2G A/S potential assessment in the next sections. Prior to that, the impact of interdependency of stochastic variables and PEVs' availability uncertainty on the proposed bidding of each AVP will be analyzed.

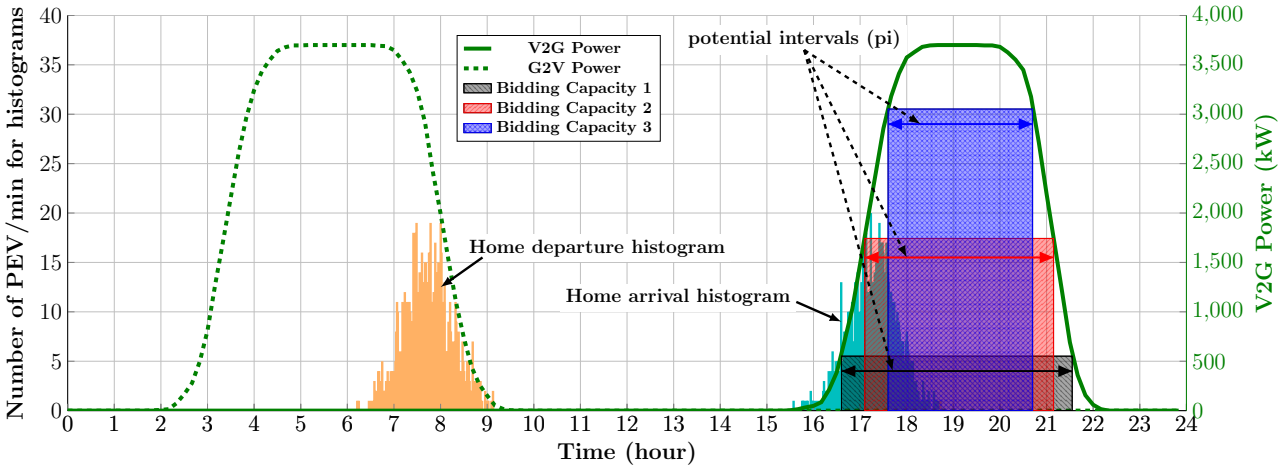

Figure 3.6: The output of AVPM algorithm for home scenario, a fleet of 1000 PEV.

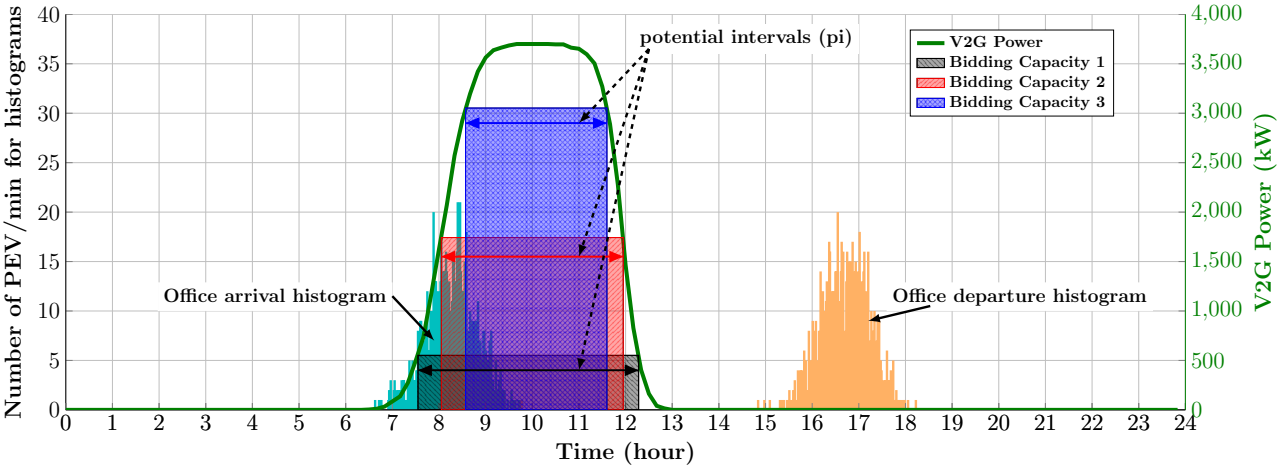

Figure 3.7: The output of AVPM algorithm for office scenario, a fleet of 1000 PEV.

3.6 Multivariate Modeling of stochastic variables

In the probabilistic analysis with stochastic variables, the correlation between the variables should be taken into account even by knowing the marginal distribution of each single variable to avoid inconsistent and unreliable estimation [Haghi 10, Gill 12, Papaefthymiou 09]. For the PEV fleet of daily home-work commuting, dependency of their departure times, arrival times and driving distances should be taken into consideration as they have key roles in modeling AVP and V2G energy capacity. However, the correlation between these stochastic variables can be estimated through statistical data as in [Lojowska 12, Pashajavid 14, Tan 14] but their dependency impact on AVP and V2G energy should also be considered to provide a reliable marginal power capacity for aggregators. The latter is the case of this section. These dependencies can be analyzed with copula function. Copulas are functions that quantify the dependency of stochastic variables knowing the marginal distribution of each variable and construct a correlated multivariate surface between each two univariate stochastic variables. The approach of generating correlated samples using t copula sampling process is used in this chapter where the notion and copula-based sample generation are explained thoroughly in [Pashajavid 14]. t copula is used as it has tailed dependence modeling ability and is more suitable for real data modeling [Tan 14].

3.6.1 The *t copula*

A d-dimensional copula C is a d-dimensional distribution function on $[0,1]^d$ with standard uniform marginal distributions [Demarta 05]. For each random variable x, copula functions are used to correlate univariate marginal cumulative distribution functions (CDF), $F_1(x_1)$, $F_2(x_2), ..., F_d(x_d)$, to their joint CDF, $F(x_1, x_2, \ldots, x_d)$ [Pashajavid 14, Cherubini 04]:

$$C(F_1(x_1), F_2(x_2), ..., F_d(x_d)) = F(x_1, x_2, ..., x_d) \tag{3.20}$$

Conversely, any copula C can be used to join any type of marginal distribution and construct a multivariate distribution function with the same marginal. The unique t copula for any uniform random variable $u = (u_1, u_2, ..., u_d) \in [0,1]^d$ is given by:

$$C^t_{\nu,P}(u) = \int_{-\infty}^{t_\nu^{-1}(u_1)} \int_{-\infty}^{t_\nu^{-1}(u_2)} \cdots \int_{-\infty}^{t_\nu^{-1}(u_d)} \frac{\Gamma(\frac{\nu+d}{2})}{\Gamma(\frac{\nu}{2})\sqrt{(\pi\nu)^d\,|P|}} (1 + \frac{\acute{x}P^{-1}x}{\nu})^{-\frac{\nu+d}{2}} dx \tag{3.21}$$

Where t_ν^{-1} denotes the inverse CDF function of a standard univariate t_ν distribution with degree of freedom ν and symmetric positive definite correlation matrix P with unity diagonal elements.

3.6.2 AVP variation calculation

Generally, using the historical data or datasets gathered from statistical surveys, the correlation between stochastic variables can be easily estimated by fitting the multivariate distribution function to the datasets employing the maximum likelihood estimation (MLE). This approach leads to extraction of correlation matrix elements, which are representative of correlation degree between each two single marginal distribution [Lojowska 12, Pashajavid 14]. However, in this study there is no such available datasets. Instead, an approach is proposed to quantify the impact of stochastic variable's dependencies on AVP. Afterwards, the correlation matrix elements associated with average AVP variation are considered as the case study. In order to analyze the correlation between departure time, arrival time and driving distance for home-work commuting fleet, we assume that the working hours are fixed for whole fleet. In this case the dependency of these variables rationally should be either blue or red transition lines between possible linguistic correlations' states defined in Fig. 3.8. While, the other transitions will not provide reliable samples to take into account for daily home-work driving pattern estimation. It means that, for a PEV departing soon from home and arriving late to home, the driving distance should have been long and vice versa.

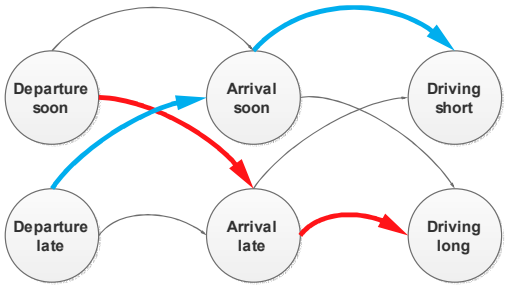

Figure 3.8: Possible correlation states' transitions.

These correlations frame, present a linear direct correlation between driving distance and arrival time and a linear indirect correlation between departure and arrival time. Using a t

copula function, the univariate marginal distribution of departure, arrival and driving distance can be related to their joint distribution as follows:

$$C(F_1(T_{departure}), F_2(T_{arrival}), F_d(D_d)) = F(T_{departure}, T_{arrival}, D_d) \tag{3.22}$$

Considering the possible mentioned transitions, the elements of correlation matrix P will vary as follows:

$$P_{3\times3} = \begin{bmatrix} 1 & \rho_{12} & \rho_{13} \\ \rho_{21} & 1 & \rho_{23} \\ \rho_{31} & \rho_{32} & 1 \end{bmatrix} \tag{3.23}$$

where,

$$\begin{aligned} \rho_{12} = \rho_{21} \in [-1, 0] \\ \rho_{13} = \rho_{31} \in [-1, 0] \\ \rho_{23} = \rho_{32} \in [0, 1] \end{aligned} \tag{3.24}$$

Where ρ_{12} indicates the correlation between departure time and arrival time, ρ_{23} indicates the correlation between arrival time and driving distance and ρ_{13} denotes the correlation between departure time and driving distance. In order to measure the sensitivity of AVP to the different possible correlation an optimization approach is proposed where the variables will be the correlation matrix elements associated with maximum variation of AVP;

$$\min_{\substack{\rho_{12},\rho_{23},\rho_{32} \\ \rho'_{12},\rho'_{23},\rho'_{32}}} \left(\sum \left| P^w_{v2g}(t) - P^v_{v2g}(t) \right|\right)^{-1} \tag{3.25}$$

Subject to:

$$\begin{aligned} \{\rho_{12}, \rho_{13}, \rho'_{12}, \rho'_{13}\} \in [-1, 0] \\ \{\rho_{23}, \rho'_{23}\} \in [0, 1] \\ x^T P x \geq 0 \end{aligned} \tag{3.26}$$

Where w and v are the two extreme cases of AVP affected by possible correlation between variables. The last constraint checks if the correlation matrix is positive definite or not for any possible x. This approach is tested on home V2G scenario as the case study where it is applicable on work V2G scenario as well. The results of optimization are brought in Table. 3.5.

Table 3.5: Results of optimization for effect of correlation coefficients

Parameter	**Optimum value**
ρ_{12}	-0.3960
ρ_{13}	-0.4950
ρ_{23}	0.99
ρ'_{12}	-0.5940
ρ'_{13}	-0.6930
ρ'_{23}	0

Using the obtained results, the AVP of the two extreme cases is calculated where these two cases will never happen (Fig. 3.9). Under considering the realistic case, there is always a correlation between three variables. The average value considered as the case study while in real case, the statistic's data or smart metering communication data can help to estimate the

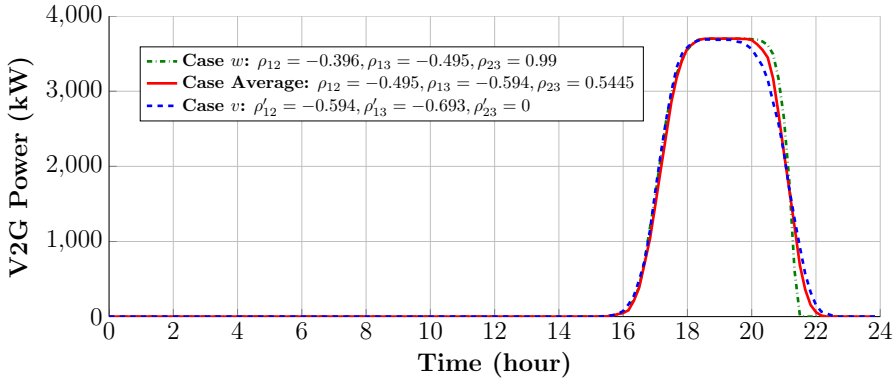

Figure 3.9: Effect of various possible correlation between stochastic variables on the AVP.

best correlation coefficients. The results show that the peak of AVP during its *pi* is the same for all three cases and there is only a negligible variation in power descending period.

In this chapter, the parameters for average variation of AVP are considered as the case study, where the impacts of correlation between variables are illustrated in Fig. 3.10. As it is shown, the marginal distributions for both non-correlated and correlated variables are approximately the same, while the orientation patterns in 2D copula surface between each pair of stochastic variables are different. The orientation differences are justifiable considering the correlation states transitions shown in Fig. 3.8. In other word, the vehicles departing soon in the morning have potential to arrival late as they have had longer driving distance and *vice versa*. This effect is considered in AVP modeling procedure. The other effect, comming from unpredictable availability uncertainties, which is modeled using a probabilistic model, is explained in next section.

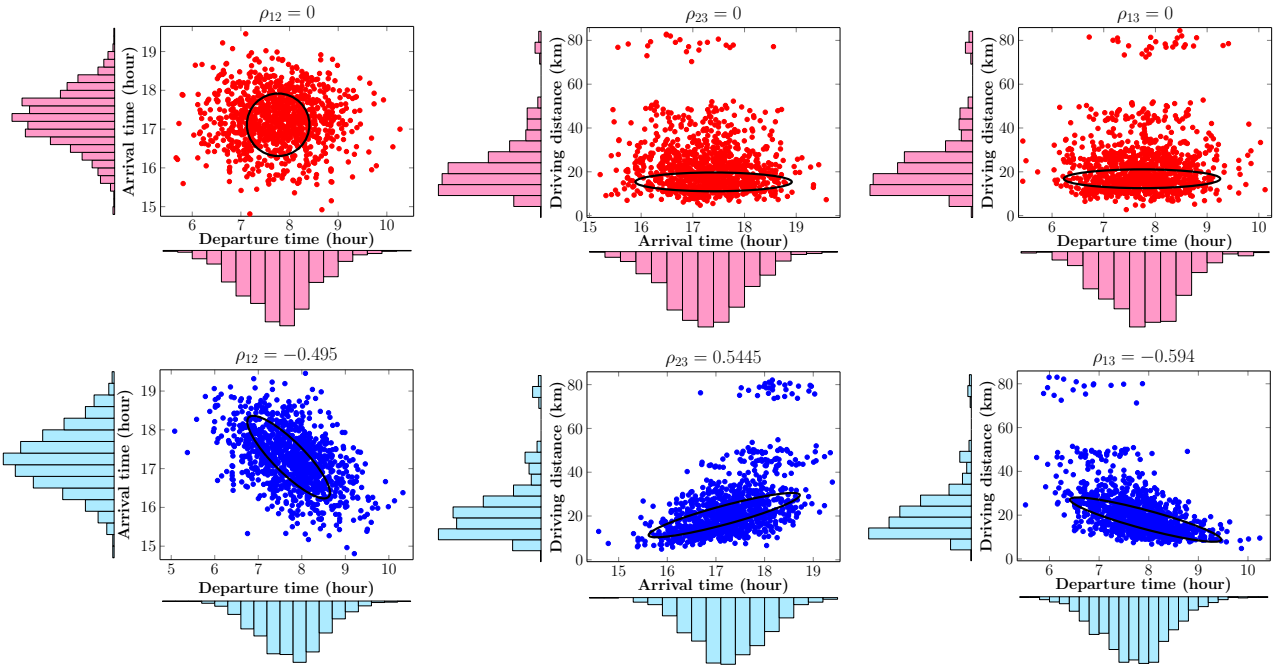

Figure 3.10: Upper subplots: non-correlated stochastic variables, Lower subplots: correlated stochastic variables with averaged coefficients (Considered as the case study for AVP calculation).

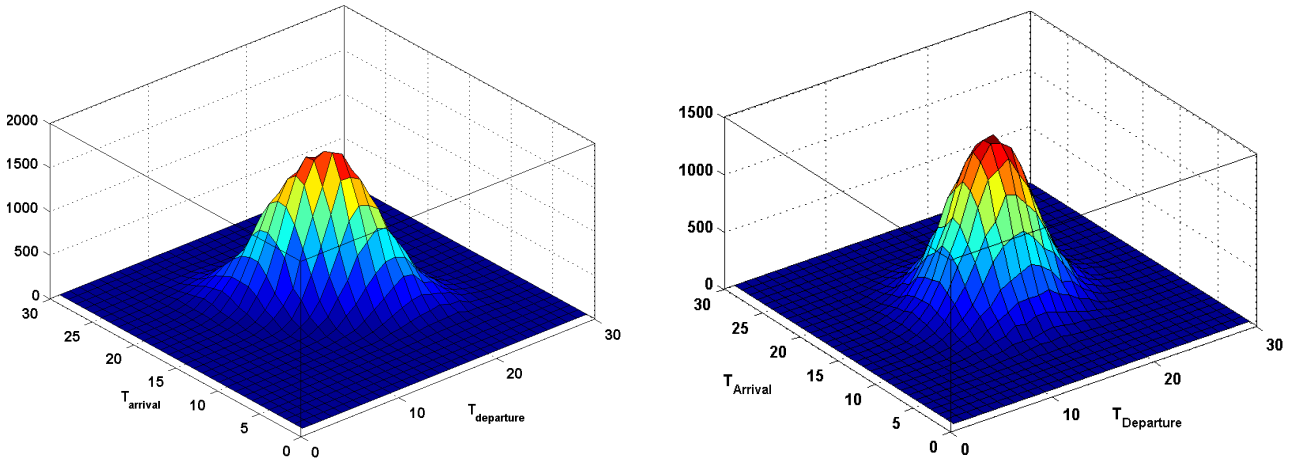

(a) With Correlation.

(b) With no Correlation $\rho_{xx} = 0$.

Figure 3.11: Comparison of correlation surface between arrival and departure time for case of without correlation and with correlation.

3.6.3 Variance-based sensitivity analysis for V2G power

Using Variance based sensitivity analysis the impact of different correlation parameters on V2G power is analyzed. To reduce the computation an average variation function (equation 3.27) is defined while the simulation has been already done by LHS (Latin Hypercube Sampling) (leading to more reliable result compare to MCS with lower iteration number).

$$f(\rho_{12}, \rho_{23}, \rho_{13}) = \frac{1}{N} \sum_{i} \left| P^{w}_{v2g}(\rho_{12}, \rho_{23}, \rho_{13}) - P^{0}_{v2g}(0, 0, 0) \right| \tag{3.27}$$

The variation bounds for the parameters are introduced in the form of equation 3.28:

$$\begin{aligned} \{\rho_{12}, \rho_{13}\} &\in [-1, 0] \\ \{\rho_{23}\} &\in [0, 1] \end{aligned} \tag{3.28}$$

This function is calculated for all possible variation of copula parameters and a sensitivity analysis has been done over the mentioned function. Variance expression decomposed to the terms as number of parameters. In the following equations 3.29 and 3.30, i and j indicates the parameters for sensitivity analysis. here these are correlation coeficients, ρ_{12}, ρ_{23} and ρ_{13}. Sensitivy analysis is considered for all of the possible decomposition between these parameters. The $X_{\sim i}$ notation indicates the set of all variables except X_i.

$$V_i = Var_{Xi}(E_{X\sim i}(Y \mid X_i)) \tag{3.29}$$

$$V_{ij} = Var_{Xij}(E_{X\sim ij}(Y \mid X_{ij})) - V_i - V_j \tag{3.30}$$

The first order and second order sensitivity indices are calculated for this analysis where the results are brought in the Fig 3.12a.

The function 3.27 will measure the averaged variation of AVP compare to non-correlated case with zero correlation parameters. For our case with 3 parameters, sensitivity is measured in term of decomposed sensitivity indices including first order sensitivity indices $S_{\rho 12}$,$S_{\rho 13}$,$S_{\rho 23}$ and second order indices $S_{\rho 12\rho 23}$,$S_{\rho 13\rho 23}$,$S_{\rho 12\rho 23}$ [14]. The results are brought in Fig. 3.12 where it shows the highest sensitivity to $S_{\rho 23}$ index. This index indicates the sensitivity of AVP to the $S_{\rho 23}$ parameter which is the correlation between arrival time and driving distance. It is concluded that the available V2G power is highly sensitive to the correlation between arrival time and driving distance variables while it has no major sensitivity to the two other parameters

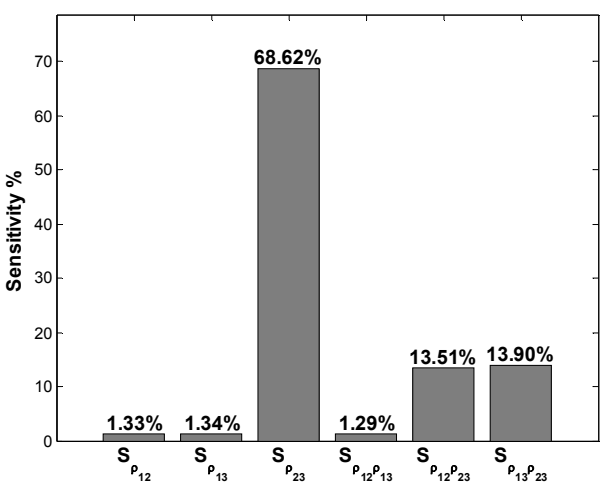

(a) Variance based sensitivity analysis parameters for V2G.

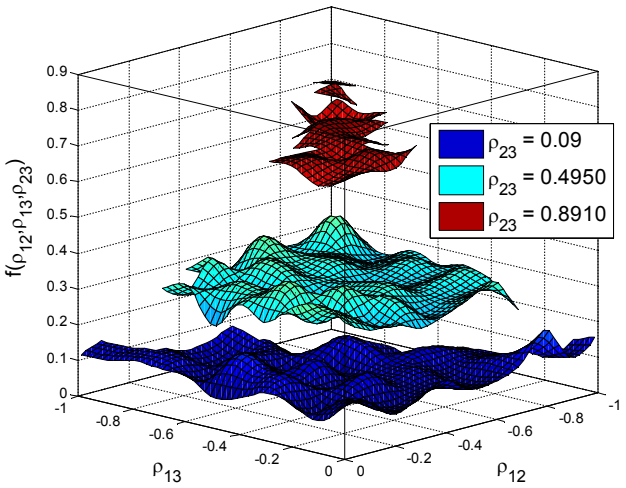

(b) Example Surfaces of function 3.27 showing the effect of the parameter ρ_{23}.

Figure 3.12: Charging profile of 20 EVs for impact analysis of Railway station.

3.7 Probabilistic availability uncertainty modeling (PAUM)

In this study, the idea of modeling the availability uncertainty is to have a quantitative vision over the reliability of V2G bidding capacity. In fact, by this approach the impact of uncertainty on AVP can be analyzed. Availability uncertainty can have different reasons; Later arrival or sooner departure compared to the estimated or declared arrival and departure time, sudden departure in case of an urgent during the plug-in interval or any partial unavailability due to the leisure motives. Whatever the case, the PEV's unavailability from the aggregator point of view will be considered as V2G power unavailability and will impose negative impacts on contracted bidding capacity. Therefore, it is necessary to take into account the availability uncertainty factor prior to the capacity announcement.

The PEVs unavailability during their plug-in interval is highly stochastic and difficult to model. However, its stochastic nature follows a particular probability distribution which can be detected in daily trips percentage data. In this chapter, an approach is proposed to model availability uncertainty knowing only the daily trips percentage and the fact that the trips leading to unavailability are included in trips probability distribution. Two parameters have been considered for each PEV in order to model its unavailability:

1. Departure moment as $T_{depstart}$
2. Unavailability period as DUR_{UN}

In addition, an uncertainty coefficient has been introduced as, $\gamma = [0, 1] \in \mathbb{R}$, the portion of PEVs fleet, which have potential of availability uncertainty. In another word, $\gamma = 1$, means that all of the PEVs inside the fleet will experience at least a short departure during the plug-in time. Monte-Carlo simulation (MCS) is used to generate samples with given trips percentage and prepare inputs for Gaussian mixture model (GMM) with a given number of components. Two major Gaussian components will be considered as trips related to departure from home to work in the morning and departure from work to home in the afternoon. By filtering these two components probability of the other motives' trips leading to availability uncertainty can be detected. In the second step, using a uniform distribution by lower bound as home arrival time and upper bound as V2G interval the sampling process of $T_{depstart}$ will be bounded over V2G interval and conducted by filtered GMM probability distribution. For DUR_{UN}, sampling

a uniform distribution between 30 minutes to 3 hours is used. This is the maximum time length a PEV will be unavailable based on the mobility survey information. In this approach, we assume that the amount of PEV battery energy used during the unavailability interval is the same as the energy amount that would be provided as V2G, if PEV was available in the parking. In the following, the formulation of different steps of the approach is provided along with the modeling framework in Fig. 3.13.

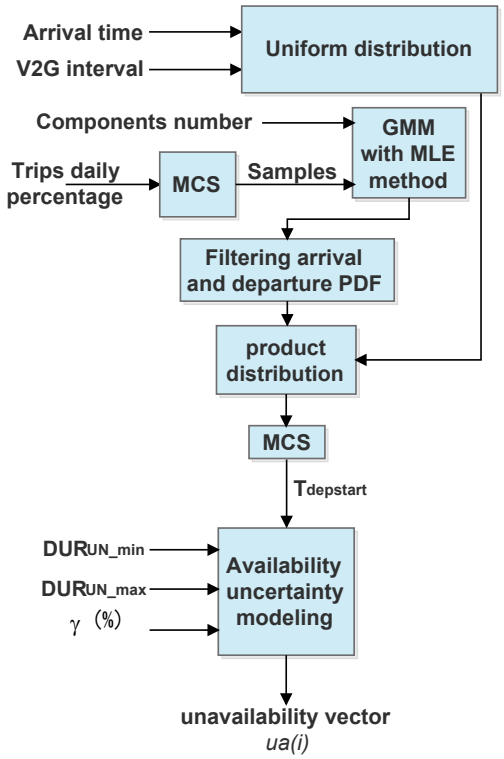

Figure 3.13: The PAUM framework.

3.7.1 Gaussian mixture model

The idea of using the mixture model in this study is to find the sub-populations inside the overall population of daily trips percentage in order to associate an availability uncertainty probability distribution to those sub-populations which are not known. These sub-populations are modeled as Gaussian components in GMM. For this reason, MCS is used to provide samples based on daily trips percentage and their probability distribution is estimated using kernel density estimation. The estimated probability density is used in maximum likelihood estimation (MLE) in order to estimates the parameters of GMM components with maximum likelihood percentage (Fig. 3.14).

One dimensional GMM density function for a set of C components and their parameter sets as $\Theta = (\alpha_1, \alpha_2, ..., \alpha_c, \sigma_1, \sigma_2, ..., \sigma_c, \mu_1, \mu_2, ..., \mu_c)$ is represented as follows [McLachlan 04];

$$f(x_s|\Theta) = \sum_{j=1}^{c} \alpha_j \frac{1}{\sqrt{2\pi\sigma_j^2}} exp(-\frac{(x_s - \mu_j)^2}{2\sigma_j^2}) \tag{3.31}$$

We assume that $\alpha_j \geq 0$, for $j \in [1, ..., c]$ and $\sum_{j=1}^{C} \alpha_j = 1$. x_s represents the samples. The best likelihood is obtained with 6 components with parameters in Table. 3.6.

The last two components can be considered as trips related to departure from home to work in the morning and departure from work to home in the afternoon as their parameters are near

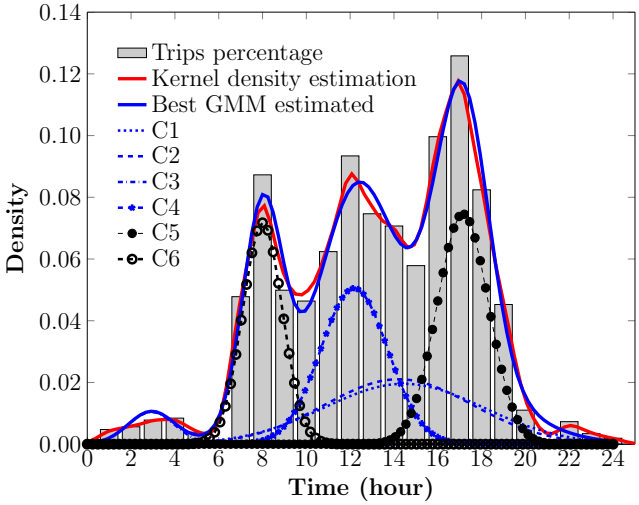

Figure 3.14: Kernel density fitted to trips percentage along with best GMM fit with 6 components.

Table 3.6: parameters of GMM components.

Component j	$\mu_j(hh:mm)$	$\sigma_j(minutes)$
C_1	14:27	217
C_2	14:13	202
C_3	02:55	63
C_4	12:25	92
C_5	17:08	45
C_6	08:00	36

to the ones which have been considered in previous section. Filtering these two components from GMM the density function of other motives trips can be found (Fig. 3.15).

3.7.2 Uniform distribution

Using a uniform distribution the sampling process for parameter $T_{depstart}$ can be bounded on the V2G time interval in order to emphasize uncertainty over AVP. In flexibility study in next section, the interval will be adapted by a flexibility interval. The filled interval in Fig. 3.15 shows the products of uniform distribution and filtered GMM density function, which will be considered as uncertainty density function for uncertainty sampling process. In other words, the sampling process will be done randomly considering the obtained uncertainty density as the probability of selection. This density function can be represented as follows:

$$g_{un}(x_s|\Theta) = \begin{cases} \sum_{j=1}^{4} \alpha_j \frac{1}{\sqrt{2\pi\sigma_j^2}} exp(-\frac{(x_s-\mu_j)^2}{2\sigma_j^2}) & T_{arrival} < x_s < T_{arrival} + T_{v2g} \\ 0 & elsewhere \end{cases} \tag{3.32}$$

Where $T_{arrival}$ will be arrival time of first PEV at work for work V2G scenario and at home for home V2G scenario. For the unavailability period, a uniform distribution is considered with cumulative distribution function as follows:

$$F(DUR_{UN}; a(i), b(i)) = \frac{DUR_{UN}(i) - a(i) + 1}{b(i) - a(i) + 1} \tag{3.33}$$

Where $a(i) = 30min$, $b(i) = 3hours$ and $DUR_{UN}(i) \in [a(i), b(i)]$. The outputs of the model for two scenarios are depicted in Fig. 3.15. This density function will be used as inputs for

uncertainty sampling process, and it will affect the V2G vector as in (3.10). The impact of modeled uncertainty on each bidding capacity during its *pi* is studied using a reliability factor (RF) which is the ratio of available V2G energy with uncertainty divided by V2G energy without uncertainty. The results depicted in Fig. 3.16, show intensive impacts on BC3, particularly for home scenario. The BC1 remains mostly reliable even with highest γ value. This analysis helps to choose the most reliable BCs where the procedure will be completed by assessing the flexibility of each BC in next section.

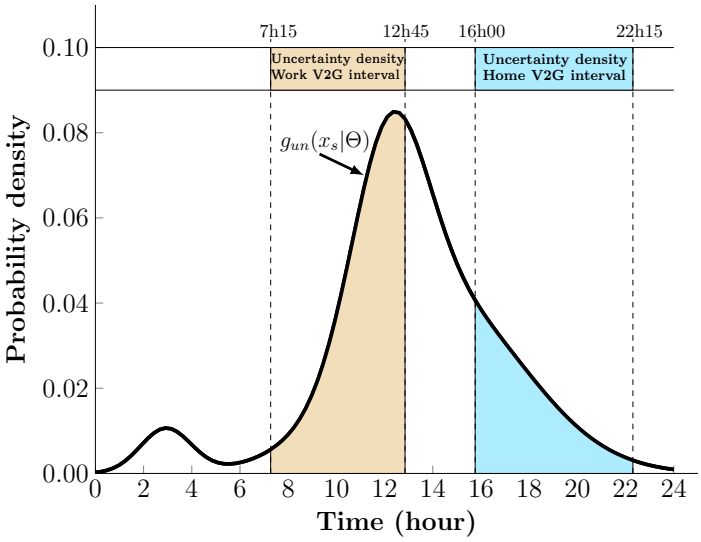

Figure 3.15: Uncertainty probability density function for two V2G scenarios at work starting from 7h15 and at home starting at 16h00.

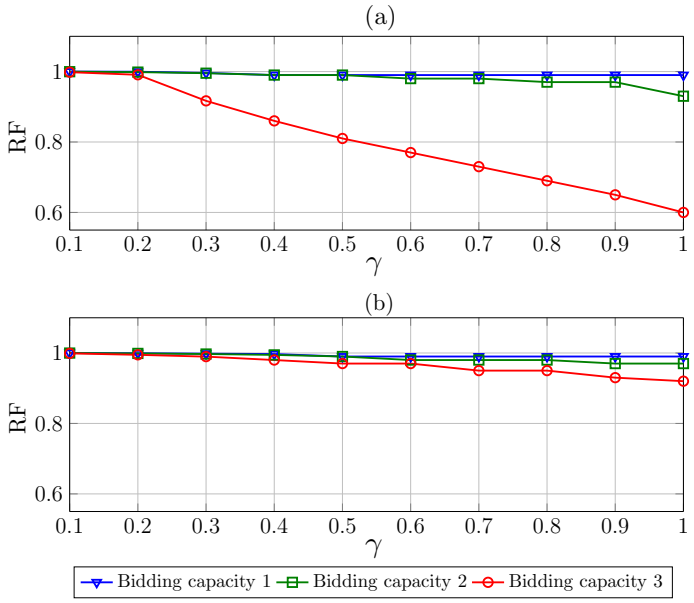

Figure 3.16: Impact of uncertainty on reliability factor for, (a) home scenario, (b) work scenario.

3.8 Bidding flexibility calculation (BFC)

Up to now, the available V2G power for different PEV fleet in two possible time intervals has been modeled. In modeling process the dependency between stochastic variables and availability

uncertainty of PEV have been also considered. In this part, prior to ancillary service assessment, the flexibility of each bidding capacity will be studied. Moreover, the flexibility will be analyzed in terms of different uncertainty penetrations. As we modeled the AVP upon the arrival of the PEVs, it would be also possible to coordinate the discharging time in order to prolong the bidding capacity interval. This so-called "bidding capacity flexibility" is analyzed in this section under a stochastic global optimization problem approach. Considering the BCs defined in previous sections by (3.18) and (3.19), the only way to maximize these capacities is to maximize the potential interval and for this goal, the only degree of freedom is to coordinate the V2G time of PEVs.

3.8.1 Flexibility problem formulation

The purpose of this optimization is to maximize the BC time interval, starting from its availability. For instance, for bidding 1 starting at 16h45, the objective is to maximize the capacity interval using V2G start time coordination of PEVs. This maximization is under constraints of respecting the G2V capacity of the fleet (for home scenario) and possible flexible range of V2G start time. As previously mentioned, mixed planning leads to reduce the V2G capacity of the fleet from aggregator capacity point of view. In addition, however, using a mixed order (*charge*, *discharge* and *not to charge* at the same time horizon) can provide more optimized results, but the increased calculation complexity compared to the better obtained optimum is not worthy of the bidding capacity assessment problem. While, the proposed optimization algorithm in this chapter is efficient and scalable to the dimension increment and can be used for charging/discharging coordination problems. In order to simplify the calculation one parameter per PEV is considered, and it is the V2G start time which varies between arrival time and G2V start time minus V2G time interval. We define the $k(t)$ function as the counter of sample times having a capacity more than each BC.

$$K_z(t) = \begin{cases} 1 & P_{v2g}(t) \geq BC_z(t) \\ 0 & elsewhere \end{cases} \tag{3.34}$$

Objective function:

$$\max_{T_{VS}(i,i+1,\ldots,N)} \sum_{t_1}^{t_2} K_z(t) \tag{3.35}$$

Subject to:

$$\begin{aligned} P_{v2g}(t) &\geq BC_z(t), \forall t \in [t_1, t_2] \\ T_{arrival}(i) \leq T_{VS}(i) &\leq T_{departure}(i) - T_{g2v}(i) - 2 \times T_{v2g}(i) \end{aligned} \tag{3.36}$$

Where $T_{VS}(i)$ is the V2G start time of PEVs arriving after BS_z that should be coordinated in order to maximize the available interval of $BC_z(t)$. Considering the normal distribution empirical rule (three sigma) and number of PEVs per fleet, the number of parameters have to be optimized can be calculated as follows for a fleet with N PEV, $P_1 = 0.6827$ and $P_2 = 0.997$:

$$Param_{num} = \begin{cases} \frac{P_1+P_2}{2} \times N & z = 1 \\ 0.5 \times N & z = 2 \\ \frac{P_2-P_1}{2} \times N & z = 3 \end{cases} \tag{3.37}$$

For instance, for a fleet with 1000 PEV, in order to calculate flexibility of bidding $z = 1$, 838 parameters correspond to the PEVs arriving after BS_1 should be optimized. This expression shows that we face with a relatively large optimization problem which needs a powerful algorithm.

3.8.2 Methodology

The major challenge for this optimization problem is finding the best feasible solutions (global optimum), knowing the potential of high dimension problem and stochastic nature of the problem, which makes difficult to use deterministic and gradient based optimization algorithms. The latter using derivative free algorithms seem effective. In [Wen 13], it is shown that Free Pattern Search (FPS) algorithm is scalable to the dimension increasing and performs better results compared to the other evolutionary algorithms. FPS is a new algorithm inspired by Hooke and Jeeves Pattern Search (HJPS) and Free Search (FS) algorithm. This algorithm employs the HJPS method as a local search algorithm and two operators from FS to guarantee the diversity of search in order to inherit the global search. Long et al. showed that FPS has very fast convergence speed, better solution accuracy, swarm management ability and robustness to the dimension compared to the similar evolutionary algorithms.

In this chapter, a FPS algorithm is implemented on bidding flexibility problem, and its functionality is assessed in both quality of result and dimension increment.

3.8.3 Free Pattern search

FPS is a population-based global optimization algorithm with three main parts; initialization, exploration and termination. In exploration part, there are three operators; search operator for local search based on HJPS, acceleration operator to avoid trapping in local optimums and a throw operator, which ensures the diversity of population. A single individual, $X_j, \{1 \leq j \leq m \in \mathbb{N}\}$, will do the search based on HJPS algorithm in all of its dimensions, $1 \leq i \leq n \in \mathbb{N}$, bounded between lower and upper limits, Low_i and Up_i. The flowchart of the FPS algorithm is illustrated in Fig. 3.17 and the different operators are explained afterwards.

3.8.3.1 Initialization

Random initialization strategy is used in order to initialize the individuals inside their boundaries. The initial search step size is calculated using a size factor α as in equation 3.38.

$$\Delta_{i,init} = (Up_i - Low_i) \times \alpha \tag{3.38}$$

3.8.3.2 Search operator

The search operator uses the HJPS algorithm in order to find local optimum for each individual. HJPS is a single-point search method which uses a pattern to search around the base point. There are three types of points in HJPS; the current point Ψ, the base point ϕ, and previous point θ. Current point is the actual solution of algorithm. Base point is for finding the better solution, and previous point is the last current point. Fig. 3.18 shows a 3D HJPS pattern. The blue points are the trials of base point in black. The best trial will be the result of each iteration. The HJPS contains two parts; exploration move (EMove) and pattern move (PMove). EMove will search in all dimensions of the base point to find the best trial. If the best trial is better than current point, the PMove will be implemented.

3.8.3.3 Acceleration operator

The acceleration operator separates the population in two groups. First group are the individuals trapped in local optimum and need to be accelerated. Using a sensibility factor S, the individuals will be polarized into two groups and the first group individuals X_j^1 will be accelerated thanks to the randomly selected second group individuals X_r^2.

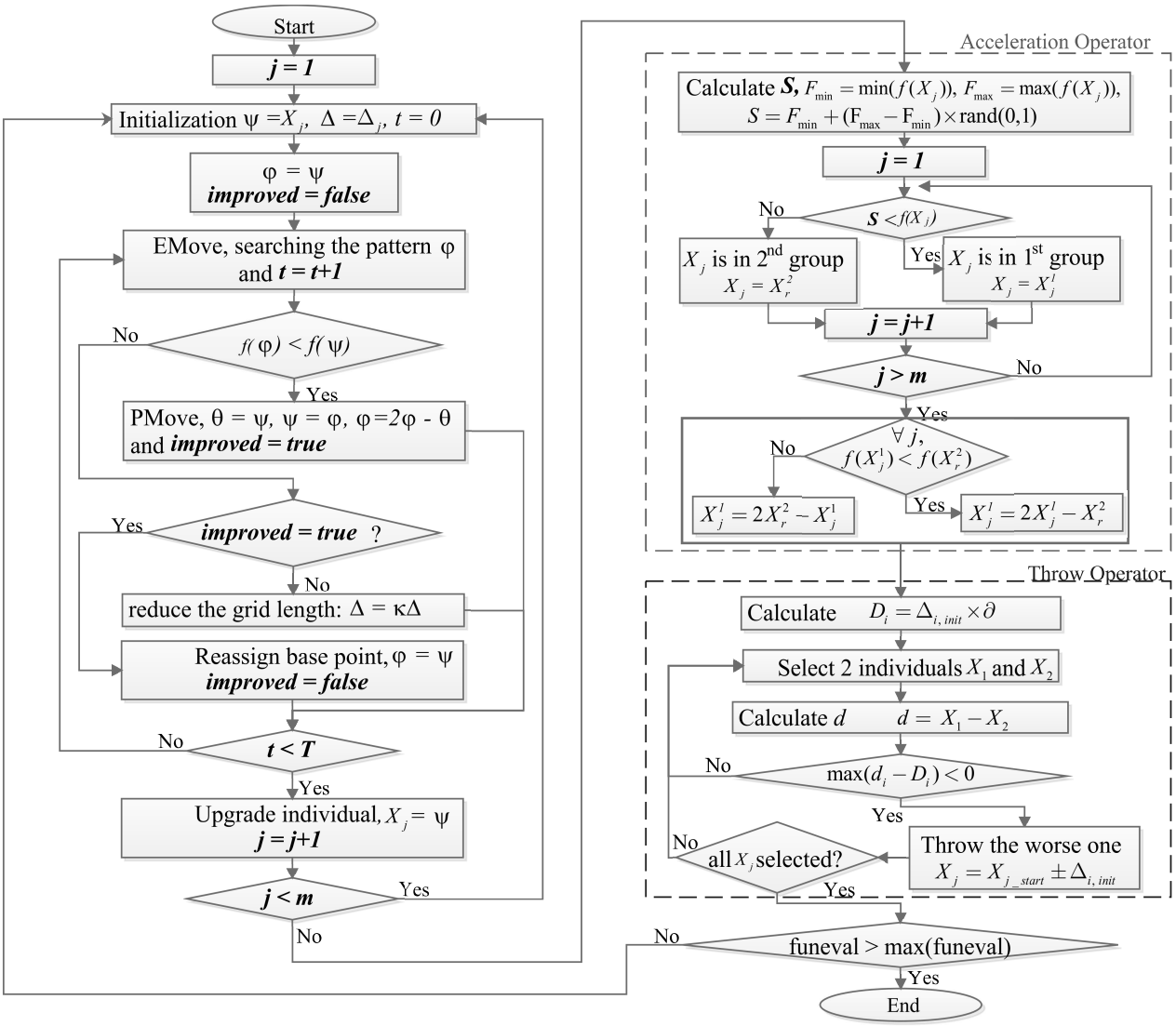

Figure 3.17: FPS algorithm flowchart.

3.8.3.4 Throw operator

Throw operator detects the individuals would gather and search in the same small space. It scatters them by adding or subtracting a $\Delta_{i,init}$ length to every dimension of the start position $X_{i_{start}}$ of gathered individuals. Throw operator keeps the population diversity in the search space. After finishing all operations the algorithm will be terminated facing with maximum step or maximum function call and accuracy of the solution.

3.8.3.5 Results

The method is implemented on the different PEV fleet numbers. Fig. 3.19 shows the function evaluation per all individuals for the fleet of 50, 200 and 500 PEVs. The result shows a complete convergence of all individuals for all cases. This shows the robustness of the algorithm to the dimension increment. The convergence and exploration intervals are indicated on the function evaluation windows. By increasing the dimension the exploration is also prolonged. The optimization is stopped when all the individuals in each evaluation are converged to a single value and there is no further improve in term of optimum result. The best value is obtained as 10.5 hours. In fact as the problem is stochastic, the optimization is repeated to have all cases

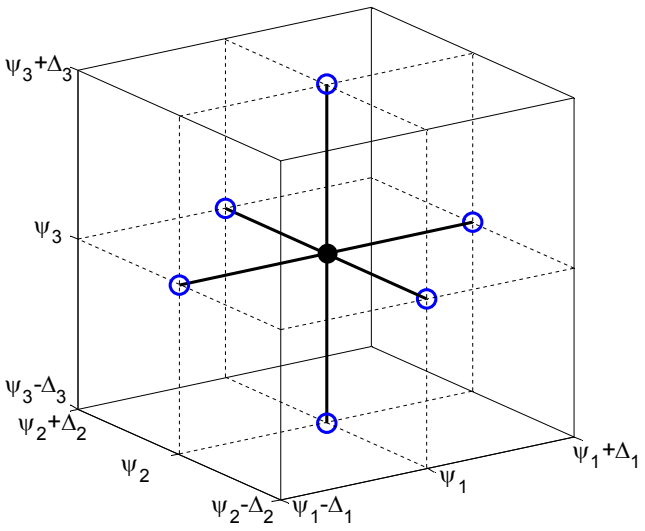

Figure 3.18: Illustration of pattern in 3D.

with the same optimum values while the final results for bidding capacity 1 is almost around 10 hours for all the PEV fleet cases. This optimization is done in presence of different values of uncertainty coefficient, and the results are presented in Fig. 3.20. The impact of uncertainty shows a linearly drop on the flexibility interval and more important on home scenario biddings. The BC3 for both scenarios has flexibility less than 3 hours after 20% uncertainty ($\gamma = 0.2$). It shows that BC3 compared to BC1 and BC2 has less reliability in terms of interval flexibility even by having a power more than them. Since the minimum time requirements for ancillary services discussed in this chapter are 3 hours, the BC3 will not be considered in the further analysis. In order to present an example of flexibility results over the BCs, Fig. 3.21 shows the flexibility of BC1 and BC2 with the uncertainty coefficient of $\gamma = 0$. In BC1, the flexibility algorithm reaches to prolong the potential interval of BC1 from 5 hours up to 10.5 hours. In BC2, the flexibility reaches to 8 hours.

The flexible interval (fi) of each BC will be used for service assessment in next section. The availability uncertainty is considered with $\gamma = 0.1$ in the further analysis. This value is estimated for the PEV fleet in Niort.

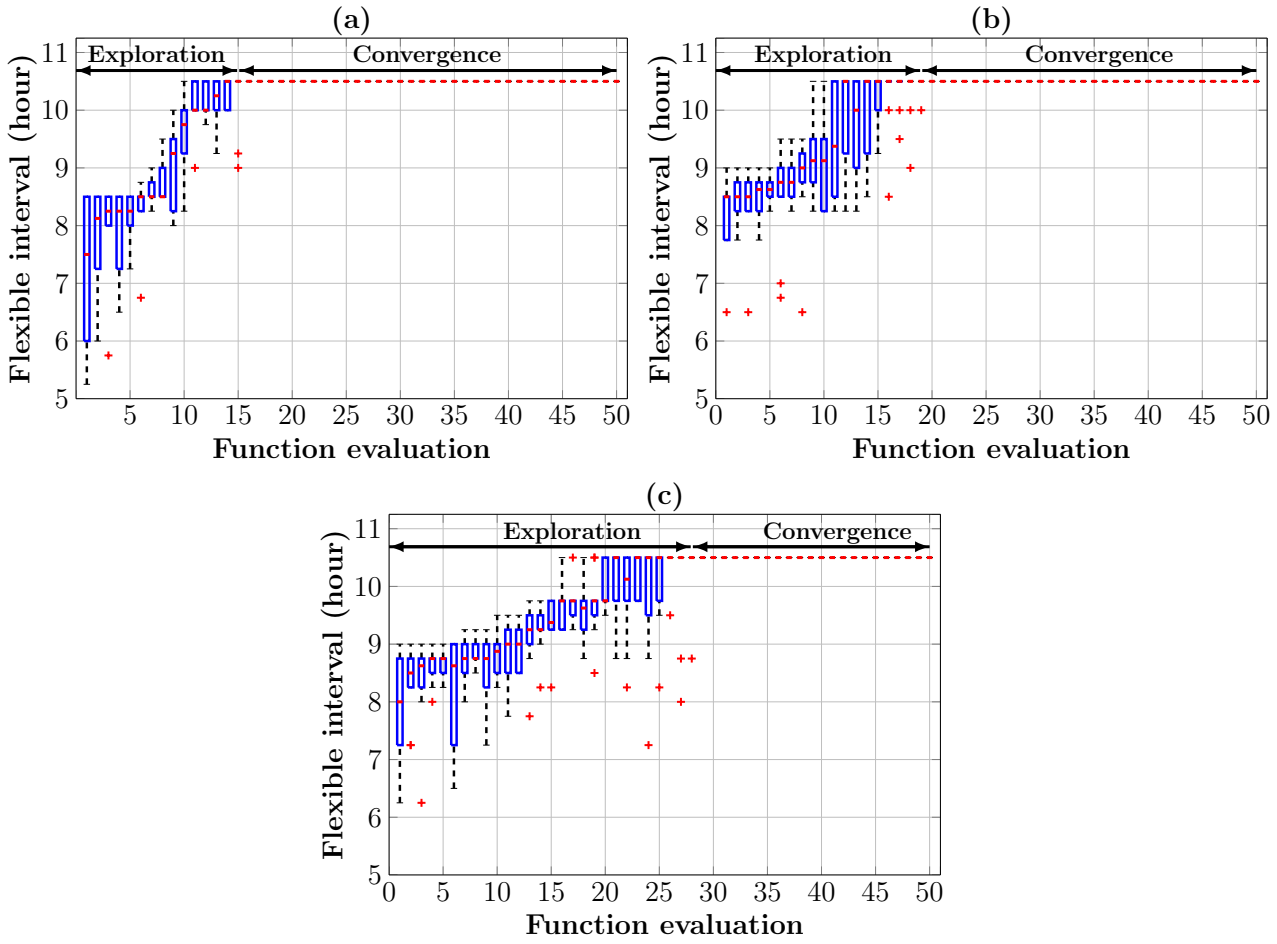

Figure 3.19: Function evaluation (Individuals' boxplot per evaluation) for, (a) 50 PEVs fleet, (b) 200 PEVs fleet and (c) 500 PEVs fleet.

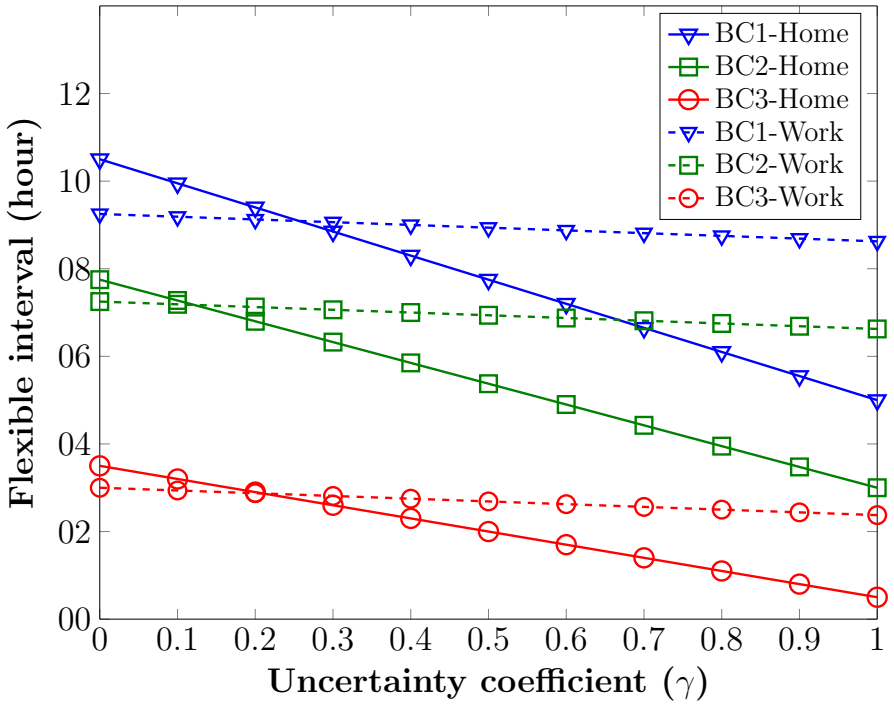

Figure 3.20: Bidding flexibility vs. uncertainty for both scenarios.

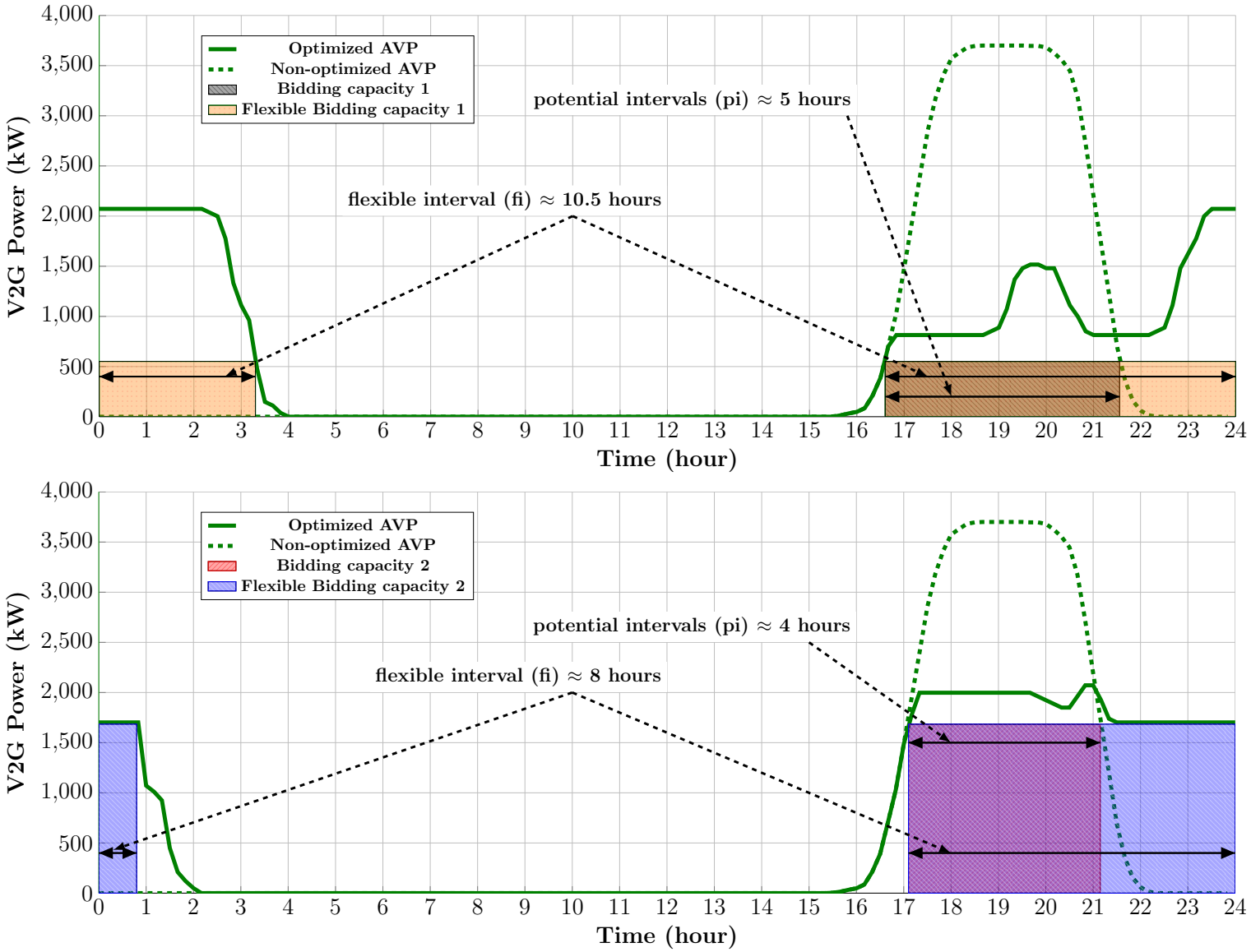

Figure 3.21: Upper plot: BC1 flexible interval, Lower plot: BC2 flexible interval.

3.9 Ancillary service assessment

3.9.1 Ancillary services

In [Delille 09] a possible list of ancillary services for storage systems at the distribution grid level under the confirmation of main French DSOs is proposed. These services' feasibilities are analyzed also for PEVs in previous work of the authors [Sarabi 14]. In this chapter, these services are evaluated for PEVs under an aggregation contract considering each service constraints. The active power based services presented in Table. 3.7 are chosen for this study. The first constraint for each service is the minimum amount of power, and minimum required time interval. These limits are used in order to design the fuzzy inference system for each service. Thanks to a service/localization matrix available in [Delille 09], the localization limitation of each service is also taken into account as another constraint. The utilization frequencies of the services, which depends on the nature of the service and the activation signals, are considered as the last constraint. In this study, three activation signals in form of a probability function are considered (Fig. 3.22). Annual averaged daily load profile (DLP) is considered as probability function for services sensitive to DLP variations. Annual averaged daily frequency *regulation up* signal is used for regulation services and finally, annual averaged daily balancing mechanism (BM) demand is chosen for BM service assessment. In the following, the analyzed services in this study are introduced.

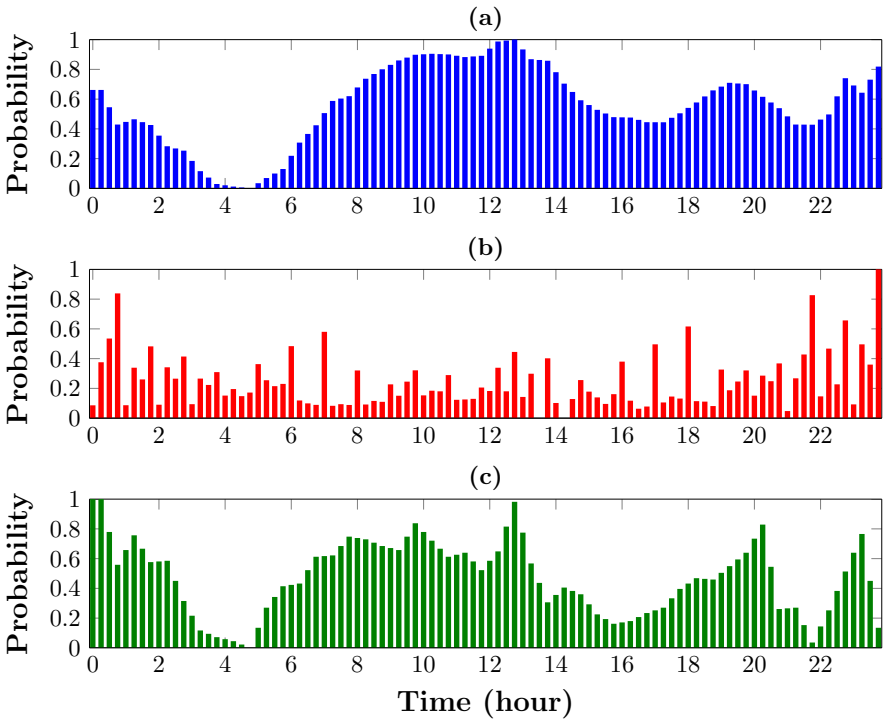

Figure 3.22: Probability of activation signals for, (a) Daily load profile (DLP), (b) Frequency regulation up (RU), (c) Balancing mechanism up (BM).

3.9.1.1 Peak power shaving (PPS)

Peak power shaving (PPS) is evaluated at both MV and LV level of distribution grid (PPSMV and PPSLV). For peak power shaving, the PEVs can be used to be charged during off-peak hours and discharged via V2G services during peak hours. This functionality, provide economic interests for PEV owners and aggregators in a variable price electricity market. In addition, for

Table 3.7: Ancillary services requirements for distribution grid [Delille 09, Robyns 15].

Service	Loc. limit	Min. P (kW)	Max. P (kW)	Min. T (h)	Act. signal
PPSMV	A	500	2000	3	DLP
PPSLV	C	100	500	3	DLP
VRMV	B,D	500	2000	3	DLP
VRLV	C	50	500	3	DLP
LM	A	100	2000	3	DLP
ETCM	A	2000	5000	3	DLP
FR	A	1000	5000	3	RU
BM	A	10000	15000	3	BM

grid operators it provides a reduction in investment for grid infrastructure reinforcement. The rated power of the storage unit must at least match the predictable growth for a given planning time, which is typically between 500 kW to 2 MW for MV grid level and 10 to 500 kW for LV grid level.

3.9.1.2 Voltage regulation (VR)

PEVs can be used to maintain the voltage profile inside acceptable contractual/regulatory boundaries [Azzouz 15]. In distribution grid, voltage regulation can be done by both active and reactive power. At HV/MV substation, Voltage regulation is done using on-load tap changer (OLTC) of the HV/MV transformer, while at MV feeder a few % of regulations needs at least 500 kW to 2 MW [Robyns 15]. This is calculated considering a typical value of MV feeder impedance in the French distribution grid, while at the LV grid level, a minimum of 50 kW is required. This study is focused only on the active power contribution on voltage regulation.

3.9.1.3 Losses minimization (LM)

Losses in the distribution grid are proportional to the square of transited current in the grid. In order to minimize the losses, the peak loads should be avoided and a charging strategy, like the peak power shaving, is necessary. For distribution grid levels, the needed power of the storage units depends on different factors such as the line length and resistance and active/ reactive power of the connected consumers to the feeder. The minimum amount of power for proposing this service is considered as 100 kW to 2MW.

3.9.1.4 Energy transmission cost minimization (ETCM)

The DSO has to pay to TSO an annual bill related to energy transmission from the transmission system to the distribution system. This bill can be minimized by using local renewable energy production and load coordination due to a variable price market. Based on the application of storage units and PEV charging coordination in French distribution grid [Sarabi 15, Bouallaga 13], a minimum of 2 MW to 5 MW is required for this service.

3.9.1.5 Frequency regulation (FR)

In order to provide a stable frequency the production and consumption should be always balanced. There are mainly three control actions for frequency regulation. The primary frequency regulation for French grid is a reserve of 600 MW active power. This value can be considered a minimum of 1 MW for the service providers at the distribution grid level. An example of primary regulation service thanks to PEV fleet for French grid is available in [Codani 15].

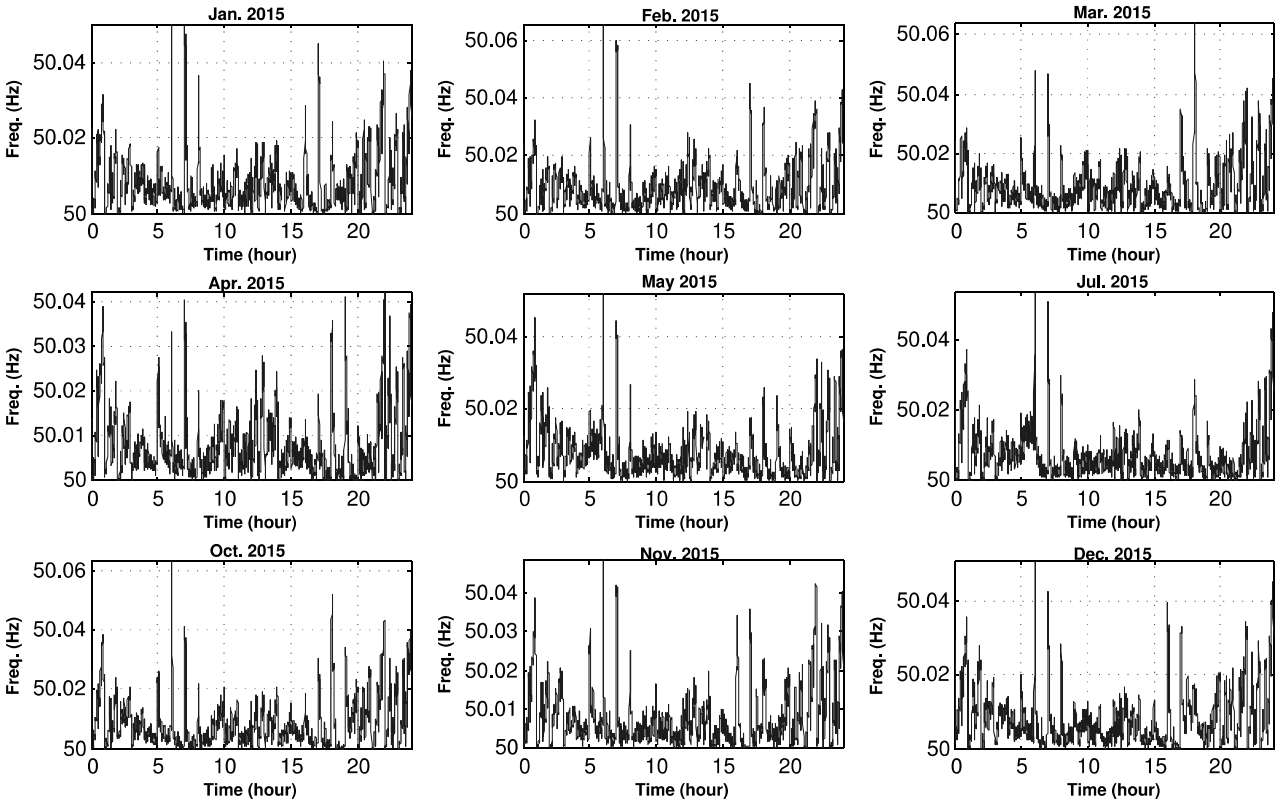

Figure 3.23: Daily averaged absolute frequency variation for 9 months in France.

3.9.1.6 Balancing Mechanism

BM is a part of tertiary control of frequency so-called "the 30 minutes complementary tertiary reserve". The French producers and consumers subject to the availability of 10 MW have the minimum requirement for BM participation [HARMAND 05].

3.9.2 Distribution grid service/localization limitation

At the distribution grid level, effective potential place for each type of ancillary service is different. Reference [Delille 09] under the consultation of major French DSOs, proposes the different candidate locations for installing energy storage systems. These places are considered as the limit for the aggregated number of PEVs in order to assess the service potential. In this study based on the chosen services, 4 candidate points are considered as the limits for each type of service (Fig. 3.24).

- **Point A** is at the topmost level of distribution grid in border of distribution and transmission grid. This point is considered as a HV/MV substation for the range of 63 to 225 kV for HV side and 15 to 20 kV for MV side.
- **Point B** is considered as the MV feeder level for feeders with 15 or 20 kV voltage level.
- **Point C** is considered as the LV bus bar inside the MV/LV substation for the range of 400 V in LV side.
- Finally, for industrial/professional customers possessing a private MV/LV substation, **Point D** is considered, which will be the case for office charging scenarios.

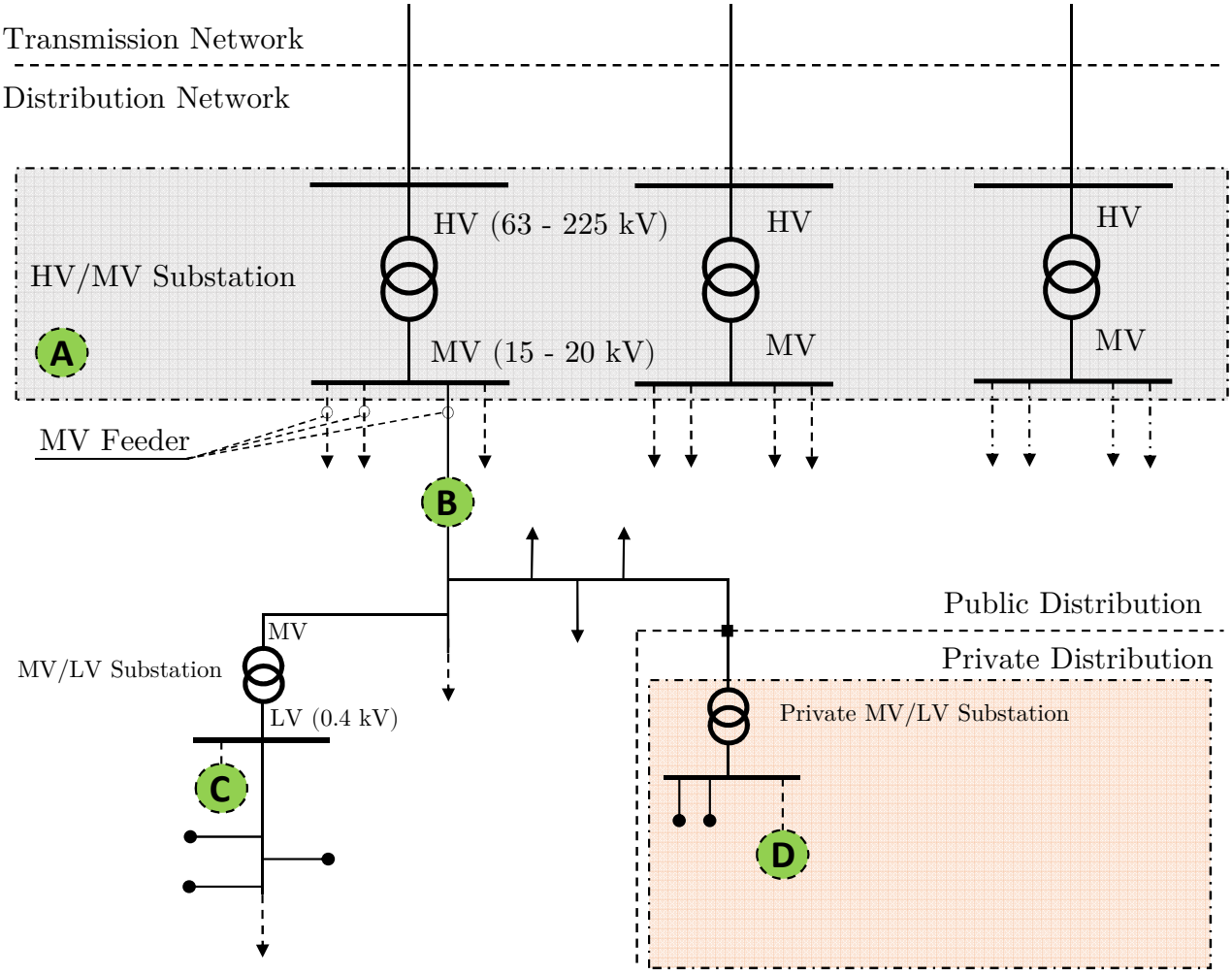

Figure 3.24: Distribution grid schematic with location limitation for ancillary services.

In fact, for each service, based on its localization limitation mentioned in the Table. 3.7 the aggregated number of PEVs fleet will be evaluated at that limit.

For our case study in Niort, a statistical analysis is done in order to discover the distribution of residential customers inside the distribution grid and for the 4 candidate locations. In point A, the possible number of PEVs for home scenarios are brought in Table. 3.8. For office scenario, 2841 PEVs can be aggregated up to the point A. The possible number of PEVs in Niort for each provision scenario are distributed between all MV/LV substations based on the residential consumers' distribution, inside the MV/LV substation (Fig. 3.25a). Distributions of PEVs at the level of MV feeder for home scenario are brought in Fig. 3.25b. The residential consumers are considered as the charging locations at home and for office scenario, the professional consumers are taken into account. For both scenarios, the maximum number of PEVs at each level of the grid are calculated considering the actual subscribed power for each consumer. It means that the capacities of the grid for hosting the PEVs are taken into consideration as constraints. For both evolution scenarios at home scenario, there is no case exceeding the subscription limitation. For office scenario, the maximum possible number of PEV before limitation violation are considered for study, as there is no evidence to justify the exact number of PEVs for office scenarios. It is due to the combination of traffic flow between Niort and its neighbor cities during the day. Their distribution at point B, C and D are brought in Fig. 3.25c along with mean values considered in potential calculation.

Table 3.8: Aggregated number of PEVs up to HV/MV substation (point A) for home scenario.

Evolution horizon	**Low Scenario** (PEV numbers)	**High Scenario** (PEV numbers)
2020	681	1702
2025	1446	4680
2030	2127	7657

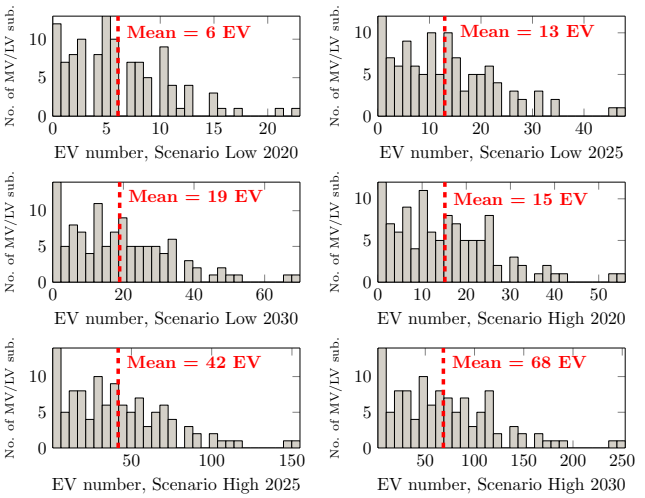

(a) Distribution of PEVs at point C for home scenario.

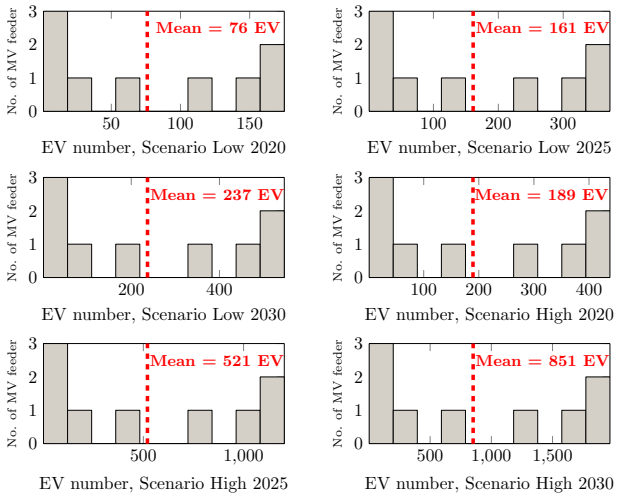

(b) Distribution of PEVs at point B for home scenario.

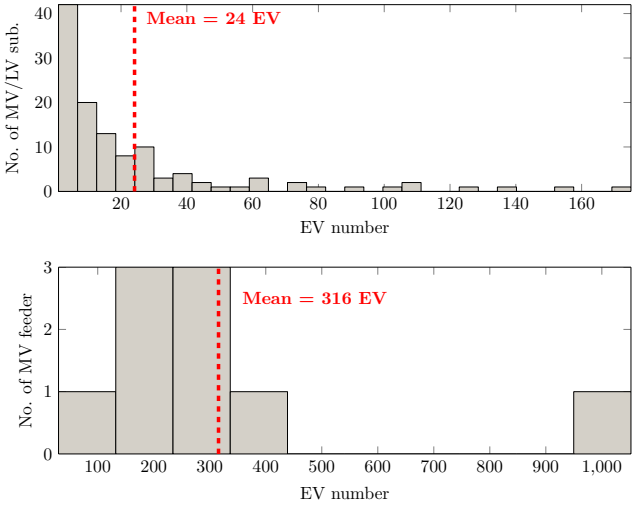

(c) Distribution of PEVs at point B and C/D for office scenario.

3.9.3 Fuzzy inference system service assessment

In order to assess the potential of PEV fleets for V2G ancillary services a methodology is proposed. This method considers the bidding capacities characteristics of each fleet and compares it with potential probability of each service. A fuzzy inference reasoning system is designed to quantify the potential of each fleet and each bidding capacity for each particular ancillary service. As the services' requirements are defined by power and time in form of an interval, the assessment procedure seems to be in a fuzzy form as the exact evaluation needs also accurate requirement. For each service, minimum and maximum power need and time are identified

in Table. 3.7. Two inputs are considered for this system. The first one is dedicated to time interval of each service that can be provided by that particular bidding capacity of the fleet. By considering the probability of the service as $ST(t)$ and probability of bidding capacity as $FT(t)$ the first input is defined as:

$$DUR = \sum_{t=1}^{24} FT(t) \times ST(t) \tag{3.39}$$

Probability of bidding is a vector with value 1 during the flexible interval (fi) of each bidding and 0 for other intervals of the day.

$$FT(t) = \begin{cases} 1, & BS_z \leq t \leq BS_z + fi_z \\ 0, & elswhere \end{cases} \tag{3.40}$$

This input is normalized using g factor as, $g = 1/\sum_{t=1}^{24} ST(t)$. The second input is the power that should be provided for each service. The membership function of this input will be made based on minimum and maximum required power for each service provided in the Table. 3.7. The example of inputs and output for service PPSMV is brought in Fig. 3.26.

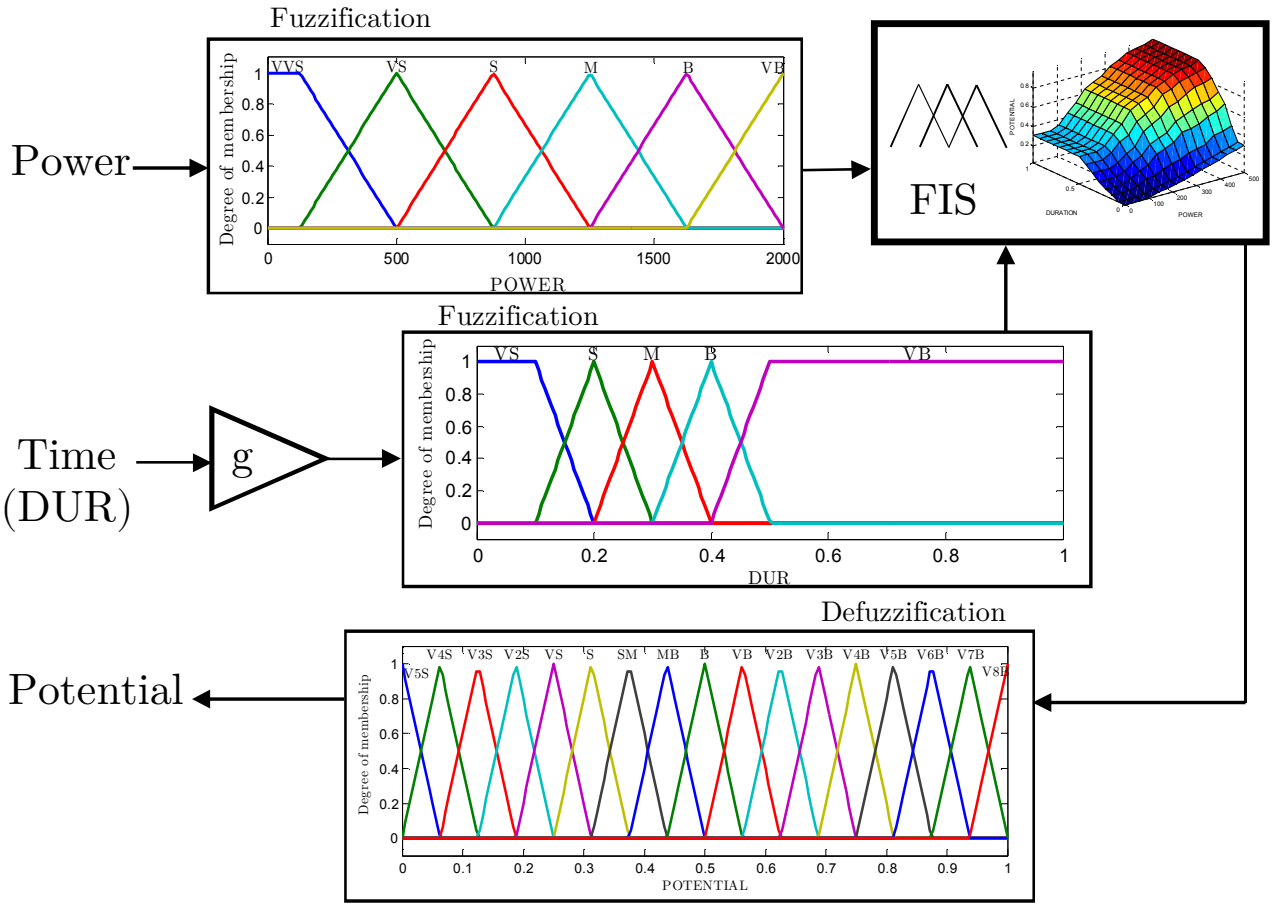

Figure 3.26: FISSA algorithm, inputs and output example for service PPSMV.

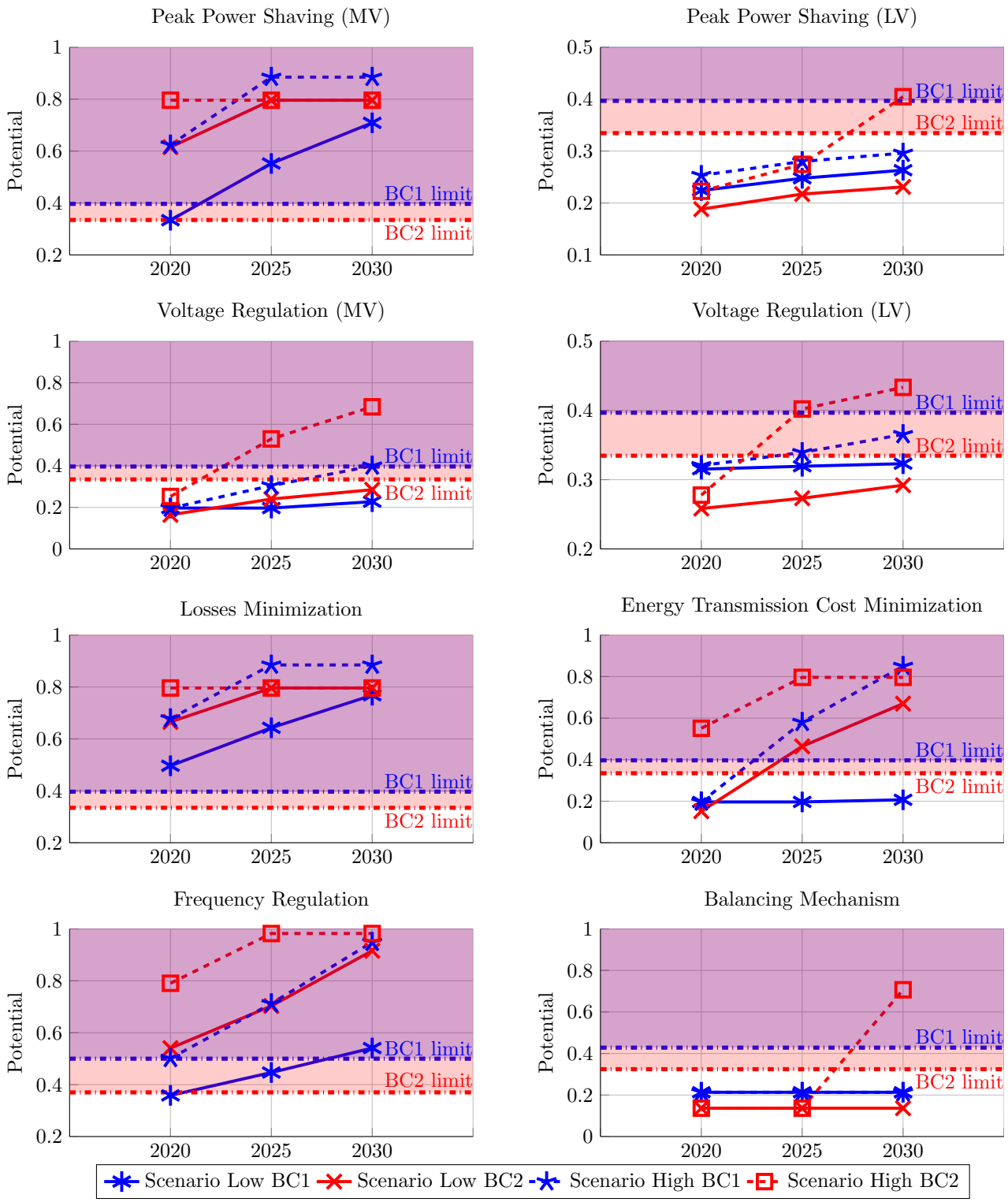

Figure 3.27: Potential evaluation for home scenario under all evolution scenarios.

3.10 Results and discussion

A graphical indicator is designed for potential comparison of different services and bidding capacities represented in Fig. 3.27 for home and Fig. 3.28 for office scenarios. For each BC a minimum potential factor called *BC limit* is calculated using minimum power of the services and flexible interval of the BC. This factor is considered as minimum requirement for each BC of the services and is represented in form of a dotted-dashed line with filled upward area. Based

on this indicator, every fleet evolution scenario should be inside the BC filled area in order to be competitive for that service. Afterwards, the potential of the different fleets' evolution scenarios is assessed using their provided power associated with their aggregated number of PEVs at each service's candidate point.

For home scenario, the services PPSLV and BM are not competitive up to 2030 horizon unless for high scenario of BC2. However, the services PPSMV, LM and FR are mostly well adapted with the provisions. In FR service, the low scenario BC1 can be possible from 2030. For PPSMV, low scenario BC1 is also possible from 2025. In ETCM service, low scenario BC1 is not at all competitive up to 2030. This is the same case for low scenarios BC1 and BC2 in VRLV and VRMV services.

For office scenario in Fig. 3.28, the services PPSLV, VRMV and BM are impossible. The services FR, LM and PPSMV are inside the area, so they can be competitive for the office fleet. The actual study shows that for BC1 the services VRLV and ETCM cannot be competitive. This should be taken into account that in this study, the numbers of PEVs at work are estimated based on actual grid capacity, and the studied volume availability is not at all guarantees.

The results for the both scenarios show that the services in the low voltage grid have not enough potential due to the non-sufficient number of aggregated PEVs at LV grid, i.e. mostly less than 30 PEVs in all provision scenarios. In addition, for service BM due to its huge power capacity requirement, the fleets' provisions are not mostly competitive as the available aggregated number of PEVs at point A cannot cover the BM service power capacity requirement.

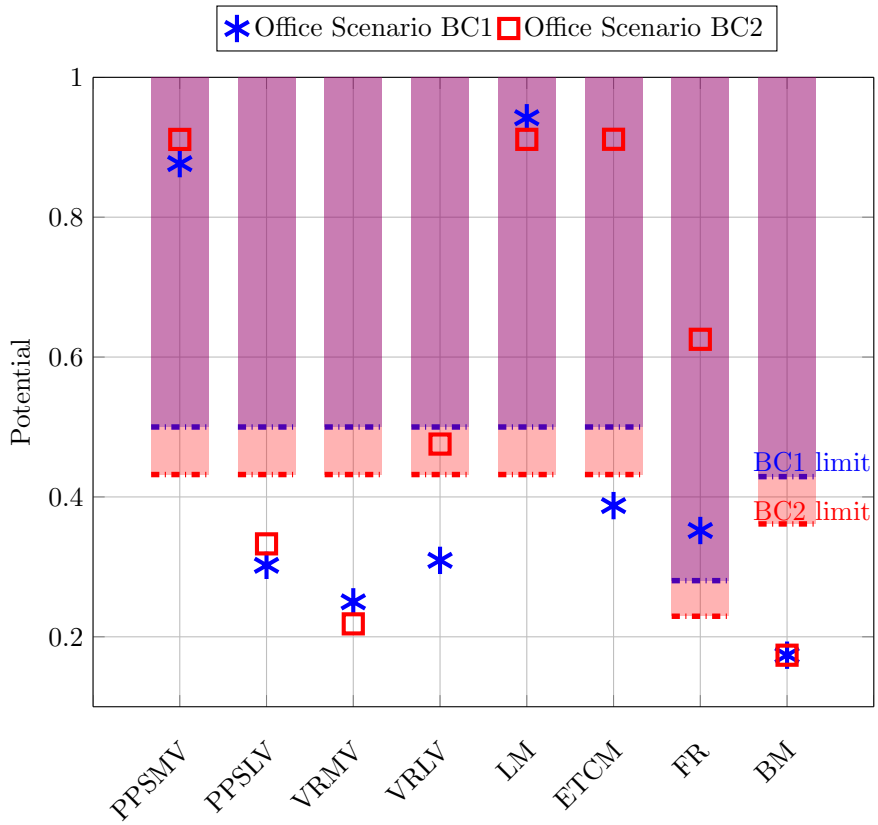

Figure 3.28: Potential evaluation for office scenario with PEV number estimated upto the grid capacity (subscribed power limit).

3.11 Conclusion

V2G ancillary services potential assessment was discussed in this chapter. The available V2G power of the PEV fleets doing daily home-work commuting was modeled. This modeling is based on stochastic data such as arrival/departure time and driving distance and averaged data, containing vehicle's characteristics. The interdependency of stochastic variables was analyzed using copula function. Two rarely discussed important factors affecting the AVP were also modeled and their impacts on AVP were identified. Availability uncertainty of the PEVs during their plug-in interval was modeled using only daily trips percentage and its decomposition thanks to the Gaussian mixture model. Secondly, the service localization limitation was considered in the procedure of V2G service assessment of the PEVs fleet.

The impacts of availability uncertainty were studied on three potential bidding capacities for both home and work scenario. The results indicated that the biddings in work places are more reliable that biddings at home as the probability of uncertainty has less concentration during the work plug-in time compared to the one for home. Flexibility of each bidding capacity was calculated using a robust global optimization technic. The impacts of uncertainty also showed linearly drops on flexibility intervals and generally fewer negative impacts on work biddings' flexibility intervals compared to home scenario. Using the obtained flexible interval for each bidding capacity and V2G power of each PEV fleet, the potential of ancillary service participation of the fleets was studied thanks to a fuzzy inference system. The fuzzy system lets to quantify the potential of each fleet considering the requirement of the services such as minimum power and time and localization limitation of the services inside the different point of distribution grid. This methodology, using the statistical mobility data of Niort, a city in west of France, was applied and possible services for this city were identified.

This study showed that based on the actual provision of PEV evolution in France, the services peak power shaving in MV grid, frequency regulation, losses minimization and energy transmission cost minimization are more competitive compared to balancing mechanism, voltage regulation and peak power shaving in LV grid. It should be taken into account that, the impact of V2G infrastructure development and availability of V2G per each individual vehicle is also another important factor that may affect the presented results. The general approach presented in this chapter is sufficiently discussed, and it has potential to be applied on the other similar case studies.

3.12 Résumé

Dans ce chapitre le potentiel des flottes des véhicules électriques pour participer aux services systèmes sont considérés. Cette étude a considéré les incertitudes concernant la durée de disponibilité des VEs et éventuellement de la flotte, qui garantit la puissance disponible pour chaque service. La Deuxième contrainte considérée est la limite de localisation au niveau des différents nœuds du réseau de distribution pour laquelle la disponibilité des VEs a été évaluée.

D'abord, une étude bibliographique sur les travaux effectués sur ce sujet a été faite au début du chapitre. Ensuite, l'approche générale proposée dans la thèse a été présentée. Après l'introduction du cas d'étude et des entrées attribuées, chaque étape de cette approche est présentée en détail. Finalement, grâce à la méthodologie développée, les différents services systèmes ont été étudiés pour les scenarios bien définis en fonction des années et de l'évolution du nombre de véhicules électriques dans le département des Deux-Sèvres. Enfin, les résultats obtenus ont été évalués pour ce cas d'étude.

3.12.1 Etude bibliographique

Dans une étude bibliographique menée, différentes méthodes ont été proposées pour l'estimation de la capacité de puissance de la flotte de VEs, mais aucun d'entre eux ne considère la limitation de la localisation des services. [Han 11] a calculé la capacité de puissance réalisable par une distribution binomiale des VEs. [Fluhr 10] utilise les données de l'enquête pour identifier l'emplacement des VEs durant la journée. Dans [Soares 11] la méthode de simulation de Monte Carlo est utilisée pour estimer la probabilité de transition entre différents états, comme par exemple, le stationnement ou la circulation. Un processus non-homogène semi-Markov est utilisé dans [Rolink 13] pour identifier la disponibilité des VEs et la charge demandée par la flotte, alors que dans [Gonzalez Vaya 14] une chaîne de Markov non homogène est choisi car les flux de mobilité ne s'acquittent pas de la propriété de Markov.

La référence [Agarwal 14] utilise une modélisation de la mobilité pour les chaînes de déplacement de la flotte des VEs et a conclu que les périodes de stationnements au domicile et au travail sont majoritaires. Aux vues de toutes ces recherches et de notre cas d'étude basé sur l'enquête de mobilité, il est conclu que les VEs sont garés au domicile et au travail la plupart du temps et leur capacité à fournir des services quotidiens est relativement plus élevé que dans d'autres endroits, tels que les parkings des centres commerciaux ou les voiries, qui sont très stochastique et généralement de courte durée.

La deuxième limite concerne les incertitudes associées à la disponibilité des VEs pour fournir les services. Par rapport à la référence [Mathieu 13], les sources d'incertitude sont basées soit sur des modèles ou sur de la prévision. Les incertitudes des modèles proviennent d'une part d'une simplification du modèle des batteries et d'autre part de la prévision de données telles que l'heure de départ et d'arrivée, le comportement de conduite et l'état de charge à l'arrivée des VEs.

Dans [Vayá 14], l'incertitude de comportement de la conduite, est modélisée par le comportement de conduite individuelle avec le processus de chaîne non Markovien ainsi que par les probabilités de transition d'état basées sur les données de l'enquête de mobilité. Dans [Momber 15], une simulation de Monte Carlo est utilisée pour représenter l'incertitude dans le comportement de conduite, en se concentrant sur les variables stochastiques, avec un processus d'échantillonnage indépendant. Alors que dans ce chapitre, l'interdépendance des variables stochastiques est modélisé par une méthode multi variable utilisant la fonction de Copule.

La nouveauté des travaux présents consiste à fournir une méthodologie à plusieurs niveaux afin d'évaluer le potentiel des V2G, qui pourrait être utilisée par les gestionnaires de réseau de

distribution (GRD). Dans cette approche, l'incertitude, la disponibilité des VEs et la limitation de localisation sont considérées comme les principaux facteurs affectant le potentiel de V2G pour la participation aux services systèmes.

Un modèle probabiliste est développé afin d'estimer l'incertitude de la disponibilité en utilisant uniquement des données probabilistes concernant les déplacements quotidiens [ins 03]. L'interdépendance des variables stochastiques est également modélisée à l'aide d'une fonction de Copule. Cette méthode de modélisation, tient compte de l'impact de l'incertitude sur la capacité d'offre et de l'amélioration de la fiabilité de l'offre. En outre, par soucis de réalisme, la distribution de véhicules électriques dans le réseau de distribution.

3.12.2 L'approche générale

L'approche générale est constituée de six parties, chacune faisant référence à une tâche particulière. D'abord la puissance disponible du V2G est calculée dans la première partie (AVPM). Cette puissance est calculée pour la flotte des VEs qui font des déplacements quotidiens du domicile-travail. Dans la deuxième partie (FPE), l'estimation des paramètres fondamentaux, comme le SOC à l'arrivée, l'intervalle de stationnement et l'énergie G2V et V2G, a été effectuée. En troisième partie (MMSV) toutes les variables stochastiques comme le temps d'arrivée et de départ ainsi que les parcours quotidiens de chaque véhicule ont été calculés grâce à une méthodologie probabiliste utilisant la fonction Copule qui prend en compte l'interdépendance des variables stochastiques.

Dans la quatrième partie (PAUM), l'incertitude sur la disponibilité des VEs a été modélisée grâce à une méthode probabiliste. La fonction de probabilité des incertitudes a été identifiée grâce à la méthode de mélange des gaussiennes. Après avoir étudié la capacité et les incertitudes sur chaque flotte de VEs la flexibilité des offres de puissance et/ou d'énergie de chaque flotte a été identifiée dans la cinquième partie (BFC). Finalement, l'évaluation des services système a été étudiée pour chaque flotte en prenant en compte sa capacité, son incertitude et sa flexibilité.

3.12.3 Cas d'étude

Cette étude est proposée afin d'analyser le potentiel d'une flotte de VEs pour fournir des services systèmes, en particulier pour la gestionnaire des réseaux de distribution. Il est supposé pour l'évaluation actuelle, qu'un minimum d'informations statistiques est disponible pour le cas d'étude, afin que l'approche soit applicable à d'autres cas d'études. Ces types de données peuvent être aussi disponibles via les infrastructures de télécommunication des réseaux intelligents (Smart Grid). Cette approche est pratique pour les gestionnaires régionaux de réseau de distribution (GRD). Niort, une ville dans l'ouest de la France, est considérée comme le cas d'étude dans ce chapitre où les données statistiques sont disponibles sur le site INSEE (Institut national de la statistique et des études économiques).

3.12.4 Modélisation de la puissance disponible V2G

Afin de définir un modèle particulaire pour le calcul de la puissance disponible V2G, il est tout d'abord nécessaire d'étudier les entrées du modèle. Le modèle proposé dans cette thèse est basé sur des entrées comme le temps d'arrivée et de départ des VEs, le SOC à l'arrivée et les entrées associées aux caractéristiques des véhicules comme la capacité de la batterie, l'autonomie et le rendement du convertisseur. En prenant en comptes toutes ces entrées le modèle sera ainsi capable de calculer la puissance disponible pour le V2G.

3.12.5 Modélisation des variables stochastiques multi variables

Les variables stochastiques sont le temps d'arrivée, le temps de départ et le distance parcourue. Les fonctions de probabilité de chacune de ces entrées sont définies en fonction de leurs données statistiques. Dans cette étude les fonctions de probabilité pour le temps d'arrivée et de départ sont considérées comme des gaussiennes. Pour la distance parcourue, une fonction particulaire a été créé grâce à la méthode de mélange des gaussiennes.

En outre, l'interdépendance des variables stochastiques est un aspect important qui pourrait imposer des impacts non négligeables sur les résultats finaux dans le processus de calcul de la puissance disponible pour le V2G. Cette interdépendance a été identifiée pour ces variables grâce à la fonction Copule.

3.12.6 Modélisation probabiliste de l'incertitude dans la disponibilité des VEs

Afin de pouvoir étudier l'impact de l'incertitude des disponibilités des VEs, un modèle probabiliste a été développé dans ce chapitre. Grâce à la méthode de mélange des gaussiennes, les composantes inconnues de la densité de probabilité des déplacements quotidien ont été identifiés. Ces composantes sont considérées comme les densités de probabilité des sources de l'incertitude. Différents paramètres de réglage ont été considérés afin de mesurer l'impact de l'incertitude sur la fiabilité des offres fournies pour chaque flotte de VEs.

3.12.7 Calcul de la flexibilité des offres

Après avoir étudié les capacités V2G disponible pour chaque flotte, 3 offres ont été considérées comme les offres principales de chaque flotte pour participer dans les marchés de chaque service systèmes. Ces trois offres ont été considérées comme des offres à haut potentiel par rapport à la disponibilité des véhicules, la puissance fournie et la durée de disponibilité.

Dans cette partie, grâce à la méthode d'optimisation, les flexibilités de ces offres ont été étudiées. Le problème a été d'abord transféré sous forme d'équations puis, une méthode d'optimisation méta-heuristique (Free Pattern Search) a été employée. Ainsi, la flexibilité de chaque offre a été calculée en fonction de la présence d'incertitude sur chaque offre.

3.12.8 Evaluation des services systèmes

Différents services systèmes ont été étudiés dans cette partie du point de vue de la capacité de puissance, de la durée de participation dans chaque service ainsi que de la fréquence d'utilisation des offres. Afin d'évaluer chacun des services, un système d'évaluation basé sur la logique floue a été créé afin de calculer un facteur de potentiel compris entre 0 et 1 pour chaque scenario défini. Les scenarios sont définis par la capacité de puissance, la durée des offres et un coefficient d'incertitude.

3.12.9 Conclusion

L'évaluation du potentiel des services systèmes V2G a été discutée dans ce chapitre. La puissance disponible du V2G des flottes de VEs, qui font un déplacement quotidien domicile-travail, a été modélisée. Cette modélisation est basée sur des données stochastiques telles que les temps d'arrivée/départ et la distance parcourue et des données moyennes, contenant des caractéristiques des véhicules. L'interdépendance des variables stochastiques a été analysée à l'aide de la

fonction de Copule. Deux facteurs importants rarement discutés qui affectent l'AVP ont également été modélisés et leurs impacts sur l'AVP ont été identifiés. L'incertitude de la disponibilité des VEs durant leur durée de plug-in a été modélisée uniquement à l'aide des données reçues à partir des trajets quotidiens et la décomposition de ces trajets grâce au modèle de mélange gaussien. Deuxièmement, la limitation de la localisation du service était considérée dans la procédure d'évaluation des services systèmes du V2G.

Les impacts de l'incertitude de la disponibilité ont été étudiés sur trois capacités d'offres potentielles à domicile et au travail. Les résultats ont indiqué que les offres du scenario au travail sont plus fiables que les offres à domicile car la probabilité de l'incertitude a moins de concentration pendant le moment de stationnement au travail par rapport à celui au domicile. La flexibilité de chaque capacité d'offres a été calculée en utilisant une technique d'optimisation globale et robuste. Les impacts de l'incertitude ont également montré une diminution de façon linéaire de l'intervalle de flexibilité et généralement moins d'impacts négatifs sur la flexibilité des offres au travail par rapport au scénario à domicile.

En utilisant l'intervalle flexible obtenu de chaque capacité et de la puissance V2G de chaque flotte de VEs, le potentiel de services systèmes des flottes a été étudié grâce à un système d'Inférence Floue. Le système flou permet de quantifier le potentiel de chaque flotte, compte tenu des exigences des services, tels que le minimum d'énergie et du temps de connexion ainsi que la limitation de la localisation des services dans les différents points des réseaux de distribution. Cette méthodologie, en utilisant les données statistiques de mobilité de Niort, une ville dans l'ouest de la France, a été appliquée et les services possibles pour cette ville ont été identifiés.

Cette étude a montré qu'en fonction de l'évolution réelle des VEs en France, les services de lissage des pointes en réseau HTA, du réglage de fréquence, la minimisation des pertes et la minimisation de coût d'acheminement d'électricité sont plus compétitifs par rapport aux réglage de tension et de lissage des pointes en réseau BT. Il faut tenir compte du fait que, l'impact de développement de l'infrastructure de V2G et la disponibilité de V2G pour chaque véhicule sont également d'autres facteurs importants qui peuvent avoir un effet non-négligeable sur les résultats présentés. L'approche présentée dans ce chapitre est suffisamment discutée, et a un potentiel d'application sur des cas d'études similaires.

3.13 References

[Agarwal 14] L. Agarwal, Wang Peng & L. Goel. *Probabilistic estimation of aggregated power capacity of EVs for vehicle-to-grid application.* In 2014 International Conference on Probabilistic Methods Applied to Power Systems (PMAPS), pages 1–6, July 2014. 83, 117

[Azzouz 15] M.A. Azzouz, M.F. Shaaban & E.F. El-Saadany. *Real-Time Optimal Voltage Regulation for Distribution Networks Incorporating High Penetration of PEVs.* IEEE Transactions on Power Systems, vol. 30, no. 6, pages 3234–3245, Nov 2015. 109

[Bishop 13] Justin D. K. Bishop, Colin J. Axon, David Bonilla, Martino Tran, David Banister & Malcolm D. McCulloch. *Evaluating the impact of V2G services on the degradation of batteries in PHEV and EV.* Applied Energy, vol. 111, pages 206–218, November 2013. 82

[Bouallaga 13] A. Bouallaga, A. Merdassi, A. Davigny, B. Robyns & V. Courtecuisse. *Minimization of energy transmission cost and CO2 emissions using coordination of electric vehicle and wind power (W2V).* In PowerTech (POWERTECH), 2013 IEEE Grenoble, pages 1–6, June 2013. 109

[Cherubini 04] Umberto Cherubini, Elisa Luciano & Walter Vecchiato. Copula methods in finance. John Wiley & Sons, 2004. 94

[Codani 15] Paul Codani, Marc Petit & Yannick Perez. *Participation of an electric vehicle fleet to primary frequency control in France.* International Journal of Electric and Hybrid Vehicles, vol. 7, no. 3, pages 233–249, 2015. 109

[De Los Rios 12] A. De Los Rios, J. Goentzel, K.E. Nordstrom & C.W. Siegert. *Economic analysis of vehicle-to-grid (V2G)-enabled fleets participating in the regulation service market.* In Innovative Smart Grid Technologies (ISGT), 2012 IEEE PES, pages 1–8, Jan 2012. 82

[Delille 09] Gauthier Delille, Bruno Francois, Gilles Malarange & Jean-Luc Fraisse. *Energy storage systems in distribution grids: new assets to upgrade distribution networks abilities.* In Proc. 20th International Conference and Exhibition on Electricity Distribution (CIRED2009), pages 18–19, 2009. xi, 83, 108, 109, 110

[Demarta 05] Stefano Demarta & Alexander J McNeil. *The t copula and related copulas.* International statistical review, vol. 73, no. 1, pages 111–129, 2005. 94

[Ehsani 12] Mehrdad Ehsani, Milad Falahi & Saeed Lotfifard. *Vehicle to Grid Services: Potential and Applications.* Energies, vol. 5, no. 10, page 4076, 2012. 82

[Falahi 13] M. Falahi, Hung-Ming Chou, M. Ehsani, Le Xie & K.L. Butler-Purry. *Potential Power Quality Benefits of Electric Vehicles.* IEEE Transactions on Sustainable Energy, vol. 4, no. 4, pages 1016–1023, October 2013. 82

[Fluhr 10] J. Fluhr, K.-H. Ahlert & C. Weinhardt. *A Stochastic Model for Simulating the Availability of Electric Vehicles for Services to the Power Grid.* In 2010 43rd Hawaii International Conference on System Sciences (HICSS), pages 1–10, January 2010. 83, 117

[Gao 13] Yang Gao, Yan Chen, Chih-Yu Wang & K.J.R. Liu. *A contract-based approach for ancillary services in V2G networks: Optimality and learning.* In INFOCOM, 2013 Proceedings IEEE, pages 1151–1159, April 2013. 82

[Gill 12] S. Gill, B. Stephen & S. Galloway. *Wind Turbine Condition Assessment Through Power Curve Copula Modeling.* IEEE Transactions on Sustainable Energy, vol. 3, no. 1, pages 94–101, Jan 2012. 93

[Gonzalez Vaya 14] M. Gonzalez Vaya, G. Andersson & S. Boyd. *Decentralized control of plug-in electric vehicles under driving uncertainty.* In Innovative Smart Grid Technologies Conference Europe (ISGT-Europe), 2014 IEEE PES, pages 1–6, October 2014. 83, 117

[Haghi 10] H. Valizadeh Haghi, M. Tavakoli Bina, M.A. Golkar & S.M. Moghaddas-Tafreshi. *Using Copulas for analysis of large datasets in renewable distributed generation: PV and wind power integration in Iran.* Renewable Energy, vol. 35, no. 9, pages 1991 – 2000, 2010. 93

[Han 11] Sekyung Han, Soohee Han & K. Sezaki. *Estimation of Achievable Power Capacity From Plug-in Electric Vehicles for V2G Frequency Regulation: Case Studies for Market Participation.* IEEE Transactions on Smart Grid, vol. 2, no. 4, pages 632–641, December 2011. 82, 83, 117

[Han 12] Sekyung Han, Soohee Han & K. Sezaki. *Economic assessment on V2G frequency regulation regarding the battery degradation.* In Innovative Smart Grid Technologies (ISGT), 2012 IEEE PES, pages 1–6, Jan 2012. 82

[HARMAND 05] Yves HARMAND, Catherine NEBAS-HAMOUDIA, Bernard LARRIPA & Bruno NEUPONT. *Electricity generation and consumption balancing in an open market.* REE. Revue de l'électricité et de l'électronique, no. 6-7, pages 91–102, 2005. 110

[ins 03] *Daily travel survey in Niort.* INSEE Poitou-Charentes, 2003. vii, 88, 118

[ins 10] *Home-work migration statistics in Poitou-Charentes region.* INSEE, 2010. vii, 86, 88

[Jian 15] Linni Jian, Yanchong Zheng, Xinping Xiao & C. C. Chan. *Optimal scheduling for vehicle-to-grid operation with stochastic connection of plug-in electric vehicles to smart grid.* Applied Energy, vol. 146, pages 150–161, May 2015. 82

[Kempton 05] Willett Kempton & Jasna Tomić. *Vehicle-to-grid power implementation: From stabilizing the grid to supporting large-scale renewable energy.* Journal of Power Sources, vol. 144, no. 1, pages 280 – 294, 2005. 82

[Khayyam 12] Hamid Khayyam, Hassan Ranjbarzadeh & Vincenzo Marano. *Intelligent control of vehicle to grid power.* Journal of Power Sources, vol. 201, pages 1 – 9, 2012. 82

[Khayyam 13] Hamid Khayyam, Jemal Abawajy, Bahman Javadi, Andrzej Goscinski, Alex Stojcevski & Alireza Bab-Hadiashar. *Intelligent battery energy management and control for vehicle-to-grid via cloud computing network.* Applied Energy, vol. 111, pages 971 – 981, 2013. 82

[Khayyam 14] Hamid Khayyam & Alireza Bab-Hadiashar. *Adaptive intelligent energy management system of plug-in hybrid electric vehicle.* Energy, vol. 69, pages 319 – 335, 2014. 82

[Lojowska 12] A. Lojowska, D. Kurowicka, G. Papaefthymiou & L. van der Sluis. *Stochastic Modeling of Power Demand Due to EVs Using Copula.* IEEE Transactions on Power Systems, vol. 27, no. 4, pages 1960–1968, Nov 2012. 93, 94

[Luo 12] Zhuowei Luo, Zechun Hu, Yonghua Song, Zhiwei Xu, Hui Liu, Long Jia & Haiyan Lu. *Economic analyses of plug-in electric vehicle battery providing ancillary services.* In Electric Vehicle Conference (IEVC), 2012 IEEE International, pages 1–5, March 2012. 82

[Mathieu 13] J.L. Mathieu, M. Gonzalez Vaya & G. Andersson. *Uncertainty in the flexibility of aggregations of demand response resources.* In IECON 2013 -

39th Annual Conference of the IEEE Industrial Electronics Society, pages 8052–8057, November 2013. 83, 117

[McLachlan 04] Geoffrey McLachlan & David Peel. Finite mixture models. John Wiley & Sons, 2004. 99

[Momber 15] I. Momber, A. Siddiqui, T. Gomez San Roman & L. Soder. *Risk Averse Scheduling by a PEV Aggregator Under Uncertainty*. IEEE Transactions on Power Systems, vol. 30, no. 2, pages 882–891, March 2015. 84, 117

[Papaefthymiou 09] George Papaefthymiou & Dorota Kurowicka. *Using copulas for modeling stochastic dependence in power system uncertainty analysis*. In Power Energy Society General Meeting, 2009. PES '09. IEEE, pages 1–1, July 2009. 93

[Pashajavid 14] E. Pashajavid & M.A. Golkar. *Non-Gaussian multivariate modeling of plug-in electric vehicles load demand*. International Journal of Electrical Power and Energy Systems, vol. 61, pages 197 – 207, 2014. 93, 94

[Pavić 15] Ivan Pavić, Tomislav Capuder & Igor Kuzle. *Value of flexible electric vehicles in providing spinning reserve services*. Applied Energy, vol. 157, pages 60–74, November 2015. 82

[Quinn 10] Casey Quinn, Daniel Zimmerle & Thomas H. Bradley. *The effect of communication architecture on the availability, reliability, and economics of plug-in hybrid electric vehicle-to-grid ancillary services*. Journal of Power Sources, vol. 195, no. 5, pages 1500–1509, March 2010. 82

[Robyns 15] Benoît Robyns, Bruno François, Gauthier Delille & Christophe Saudemont. *Applications and Values of Energy Storage in Power Systems*. In Energy Storage in Electric Power Grids, pages 55–152. Wiley Online Library, 2015. xi, 109

[Rolink 13] J. Rolink & C. Rehtanz. *Large-Scale Modeling of Grid-Connected Electric Vehicles*. IEEE Transactions on Power Delivery, vol. 28, no. 2, pages 894–902, April 2013. 83, 117

[RTEPress 14] RTEPress. *French Transmission System Operator*. https://clients.rte-france.com/lang/fr/visiteurs/services/actualites.jsp?id=9693&mode=detail, 2014. 83

[Salah 15] Florian Salah, Jens P. Ilg, Christoph M. Flath, Hauke Basse & Clemens van Dinther. *Impact of electric vehicles on distribution substations: A Swiss case study*. Applied Energy, vol. 137, pages 88–96, January 2015. 86

[Sarabi 13] Siyamak Sarabi, Laid Kefsi, Asma Merdassi & Benoit Robyns. *Supervision of plug-in electric vehicles connected to the electric distribution grids*. International Journal of Electrical Energy, vol. 1, no. 4, pages 256–263, 2013. 86

[Sarabi 14] Siyamak Sarabi, Anouar Bouallaga, Arnaud Davigny, Benoit Robyns, Vincent Courtecuisse, Yann Riffonneau & Martin Regner. *The feasibility of the ancillary services for Vehicle-to-grid technology*. In European Energy Market (EEM), 2014 11th International Conference on the, pages 1–5, May 2014. 108

[Sarabi 15] S. Sarabi, A. Davigny, Y. Riffonneau, V. Courtecuisse & B. Robyns. *Contribution and Impacts of Grid Integrated Electric Vehicles to the Distribution Networks and Railway Station Parking Lots*. In Electricity Distribution (CIRED 2015), 23rd International Conference and Exhibition on, pages 1–5, June 2015. 86, 109

[Soares 11] F.J. Soares, J.A. Peças Lopes, P.M. Rocha Almeida, C.L. Moreira & Luís Seca. *A stochastic model to simulate electric vehicles motion and quantify the energy required from the grid.* In 17th Power Systems Computation Conference, pages 1–7, Stockholm, 2011. 83, 117

[Tan 14] Jun Tan & Lingfeng Wang. *Integration of Plug-in Hybrid Electric Vehicles into Residential Distribution Grid Based on Two-Layer Intelligent Optimization.* IEEE Transactions on Smart Grid, vol. 5, no. 4, pages 1774–1784, July 2014. 93

[Tomić 07] Jasna Tomić & Willett Kempton. *Using fleets of electric-drive vehicles for grid support.* Journal of Power Sources, vol. 168, no. 2, pages 459 – 468, 2007. 82

[Vayá 14] Marina González Vayá & Göran Andersson. *Smart Charging of Plug-in Electric Vehicles Under Driving Behavior Uncertainty.* In Rajesh Karki, Roy Billinton & Ajit Kumar Verma, editeurs, Reliability Modeling and Analysis of Smart Power Systems, Reliable and Sustainable Electric Power and Energy Systems Management, pages 85–99. Springer India, 2014. 84, 117

[Wang 14] M. Wang, P. Zeng, Y. Mu, H. Jia, W. Liang & Y. Qi. *An efficient power plant model of electric vehicles considering the travel behaviors of EV users.* In Power System Technology (POWERCON), 2014 International Conference on, pages 3322–3327, Oct 2014. 82

[WANG 15] Mingshen WANG, Yunfei MU, Hongjie JIA, Jianzhong WU, Xiuping YAO, Xiaodan YU & Janaka EKANAYAKE. *A preventive control strategy for static voltage stability based on an efficient power plant model of electric vehicles.* Journal of Modern Power Systems and Clean Energy, vol. 3, no. 1, pages 103–113, 2015. 82

[Wen 13] Long Wen, Liang Gao, Xinyu Li & Liping Zhang. *Free Pattern Search for global optimization.* Applied Soft Computing, vol. 13, no. 9, pages 3853 – 3863, 2013. 103

[Zhou 11] Chengke Zhou, Kejun Qian, M. Allan & Wenjun Zhou. *Modeling of the Cost of EV Battery Wear Due to V2G Application in Power Systems.* Energy Conversion, IEEE Transactions on, vol. 26, no. 4, pages 1041–1050, Dec 2011. 89

Chapter 4

Energy management strategies for V2G ancillary services

Contents

4.1 Introduction to Energy management

Energy management includes planning and operations of energy production and consumption units for the aims of resource conservation, climate protection and cost saving. In this thesis, the energy management systems for a fleet of plug-in electric vehicles are studying for the different possible ancillary services. Based on the previous studies in the previous chapter, the main part of the thesis dedicated to a real-time supervision system is presented in this chapter. In this introduction a brief literature review will be presented on the actual energy management for plug-in electric vehicle integration into the distribution grid. After that, the different steps of the designing of real-time supervision will be presented which is applied for two different case studies.

Recently, there are many studies investigating on plug-in electric vehicle (PEV) integration to the electrical grid containing their non controlled charging impacts, coordination charging strategies and vehicle-to-grid (V2G) systems [Clement-Nyns 11a, Green II 11, Chukwu 14a, Putrus 09, Shafiee 13, Clement-Nyns 10b, Yilmaz 13a, Sarabi 15b, Latimier 15]. Among them those who have proposed coordination strategies are mainly devided to two categories: Optimal scheduling and/or coordination and real-time coordination [Deilami 11, Shi 11, Chukwu 14b, Singh 13, Ma 13, Sun 14, Harrabi 14, Tan 14]. We call here the first group as offline or planning studies and second group as on line or real-time supervision.

4.2 Methodologies for energy management of electric vehicle fleet

Plug-in electric vehicles are becoming more and more dominant on the future transportation market. Their contribution to the transportation sector bring challenges of energy need respond which should be taken into account seriously. The charging coordination and V2G technology are introduced as possible solution to cope with energy need increase of the PEV fleet. The methodologies for supervision and coordination of PEV charging demand are analyzed thereafter. The aim of this part is to investigate on current researches on the concept of energy management methodologies for PEVs.

4.2.1 PEV-Grid Energy Management aspects

There are two main aspects of energy management for PEV charging and V2G technology. Both of these aspects are discussed and a predictive real-time supervision is designed in this thesis. Theses aspects are as follows:

- Offline Optimization for planning of the grid operating points based on:

1. Prediction
2. Forecasting
3. Estimation
4. Optimization

- Real-time energy management because of uncertainties in the grid such as

1. Intermittent in renewable generation such as solar and wind
2. randomness of arrival and departure of PEVs
3. unpredictable variation of load profile

4.2.2 List of already implemented EMS for PEV charging problem

A list of already implemented Energy Management System (EMS) for PEV charging/dishcarging problem are brought:

- Linear programming
- Sliding Mode Control
- Model Predictive Control
- Fuzzy Logic Controller
- Multi Agent Systems
- Markov Decision Process (with Q-learning)
- Game Theory

This methodologies are validated for different case studies. Depending on the direction of energy flow, existing work on EV charging scheduling can be classified into two classes: 1) scheduling for charging only, and 2) scheduling for both charging and discharging. In charging-only scheduling, the scheduler tries to optimize the energy flow from the grid to the battery of the EV. [Shafiee 13] optimized the EV battery charging during the low-cost off-peak period to minimize the charging cost in the context of Singapore. The paper in [Deilami 11] examined the problem of optimizing the charge trajectory of a PHEV, defined as the time and the rate with which the PHEV obtains electricity from the power grid. In [Clement-Nyns 11b], a decentralized charging control algorithm was proposed to schedule charging for large populations of EVs.

The paper in [Shi 11] optimized EV battery charging behavior to minimize charging costs, achieving satisfactory state-of-energy levels, and optimal power balancing. [Clement-Nyns 10a] presented smart energy control strategies for charging residential PHEVs, aiming to minimize the peak load and flatten the overall load profile. The impact of different battery charging rates of EVs on the power quality of smart grid distribution systems was studied in [Chukwu 14b]. In [Singh 13] proposed coordinated charging with stochastic programming, which was introduced to represent the error in the load forecasting. In charging and discharging scheduling, the scheduler tries to optimize the bidirectional energy flows: from the grid to the EV battery and from the EV battery to the grid.

Binary particle swarm methods were employed to optimize the V2G scheduling in a parking lot to maximize the profit [Yilmaz 13b, Sarabi 15a, Ma 13]. Sortomme et al. proposed an unidirectional regulation at the aggregator, in which several smart charging algorithms were examined to set the point about which the rate of charge varies while performing regulation [Sun 14]. The paper in [Tan 14] developed an aggregator for V2G frequency regulation with the optimal control strategy, which aims to maximize the revenue. Janget al. proposed a method for an analytic estimation of the probability distribution of the Procured Power Capacity (PPC), based on which the optimal contract size was decided [Song 14]. The paper in [Neffati 13] presented a real-time model of afleet of plug-in vehicles performing V2G power transactions. In [Salmasi 07], Singhet al. demonstrated that the coordinated charging and discharging of EVs can improve the voltage profile and reduce the power transmission loss. The paper in [Harrabi 14] discussed the vehicle to grid integration and described the vehicle-to-grid communication interface [He 12].

4.3 Predictive real-time energy management strategy for "Energy transmission cost minimization": case study of distribution grid

Based on the previous explanation of the selected ancillary services for this thesis, for the case study of regional distribution grid, the service of energy transmission cost minimization has been chosen. The proposition of this thesis for designing a real-time supervision system for a fleet of V2G-enabled PEV are presented in this section. Different steps of the proposition are illustrated in Figure 4.1.

In fact, three main part are controlling the charging/discharging of the vehicles. "Forecasting algorithm" and "Predictive supervision" are working in the level of mid-term supervision. The main advantage of using this level is to have a global estimative vision over the entire time of the real-time supervision. This period is considered as 24 hours in this supervision systems. The mid-term supervision will provide a reference signal for real-time supervision which finally drive it through more optimal solution. In the second level, the real-time supervision will decide the value of reference signal in periods of 10 minutes. Finally, the SOC estimator algorithm will distribute the reference power to all of the vehicles, considering the constraints of each single vehicle connected to the grid.

Each of these levels are explained completely thereafter and their methodological approaches are discussed.

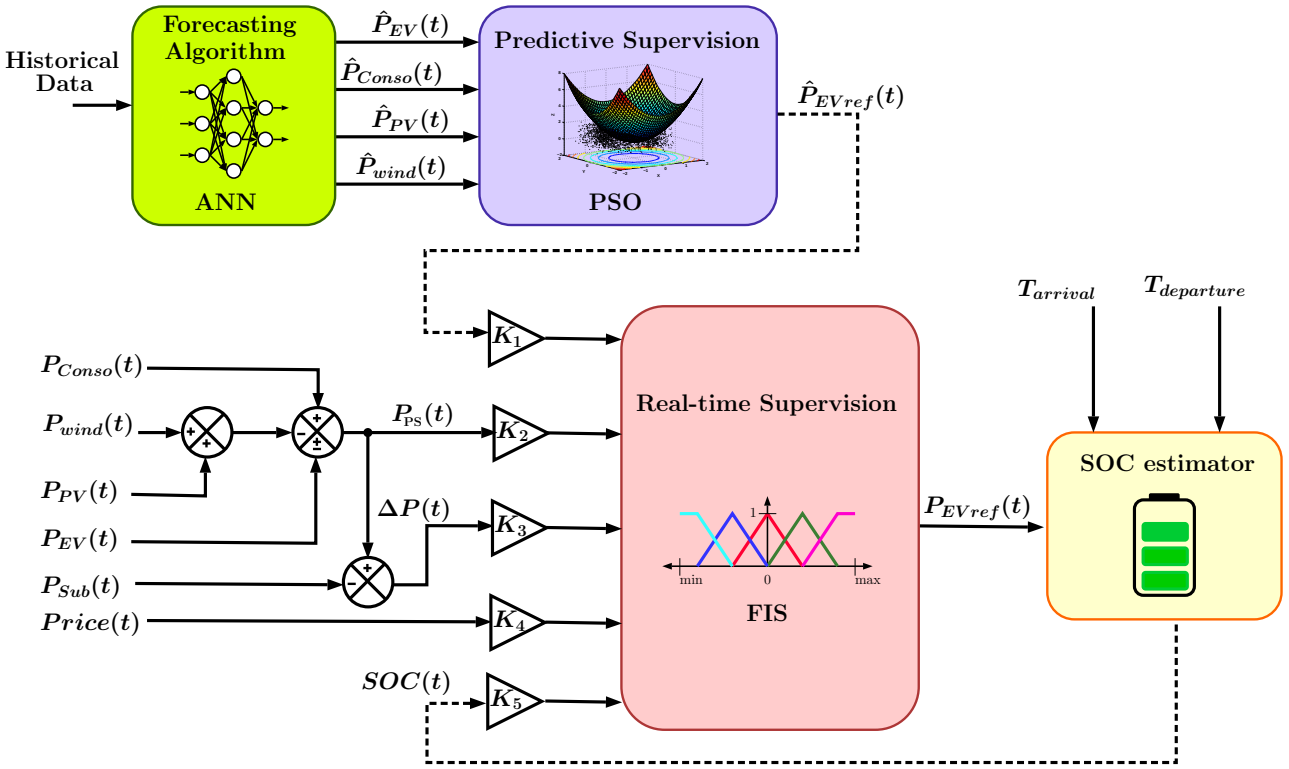

Figure 4.1: Predictive-real-time supervision system for V2G energy management: ETCM service.

4.3.1 Forecasting algorithms

The purpose of using forecasting algorithm in this thesis is to provide a short term vision over the entire period of real-time supervision in order to optimize the decision making strategies

for PEV charging/discharging. In fact, the author believes that with a predictive vision over a short term horizon the quality of the real-time decision making will be increased. This claim has been proved by comparing predictive real-time supervision with only real-time supervision system. The propose of the author is the forecasting algorithms for real-time measurable inputs of the system. These inputs are illustrated in Figure 4.2, contain electric vehicle Power demand $\hat{P}_{EV}(t)$, Consumption $\hat{P}_{conso}(t)$, solar power production, $\hat{P}_{PV}(t)$ and wind power production $\hat{P}_{wind}(t)$, as they are estimated (predicted) values are presented with "ˆ" sign. In fact for each of the mentioned estimated values a forecasting model independent of the other parameters are considered. The development of the forecasting algorithm for $\hat{P}_{conso}(t)$ has been studied in this thesis while the other parameters forecasting are considered as perspective of the thesis. This perspective is on the base of recent researches for solar and wind production and electric vehicle charging load estimation.

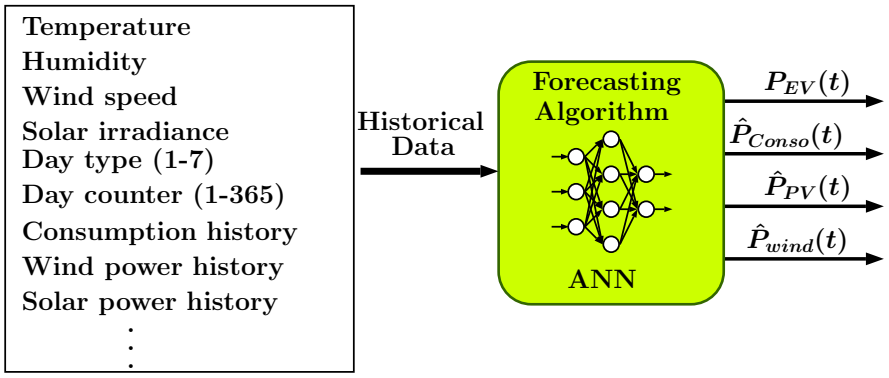

Figure 4.2: Demonstration of forecasting algorithm for consumption, wind and solar production forecasting.

4.3.1.1 Literature review on the forecasting algorithms

Different load forecasting algorithms for different forecasting horizons are discussed in literature [Feinberg 05, Khatoon 14]. Various regression models, time series, neural networks, expert systems, fuzzy logic, and statistical learning algorithms, are used for short-term forecasting. The development, improvements, and investigation of the appropriate mathematical tools will lead to the development of more accurate load forecasting techniques.

Similar day approach, is based on searching the historical data for days within one, two, or three years with similar characteristics to the forecast day. Similar characteristics include weather, day of the week, and the date. The load of a similar day is considered as a forecast. Instead of a single similar day load, the forecast can be a linear combination or regression procedure that can include several similar days.

Regression methods is the one of most widely used statistical techniques. For electric load forecasting regression methods are usually used to model the relationship of load consumption and other factors such as weather, day type, and customer class.

Time series are based on the assumption that the data have an internal structure, such as autocorrelation, trend, or seasonal variation. Time series forecasting methods detect and explore such a structure. Time series have been used for decades in such fields as economics, digital signal processing, as well as electric load forecasting [Paparoditis 13, Barakat 90]. In particular, ARMA (autoregressive moving average), ARIMA (autoregressive integrated moving average), ARMAX (autoregressive moving average with exogenous variables), and ARIMAX (autoregressive integrated moving average with exogenous variables) are the most often used

classical time series methods. ARMA models are usually used for stationary processes while ARIMA is an extension of ARMA to non-stationary processes. ARMA and ARIMA use the time and load as the only input parameters [Cho 95]. Since load generally depends on the weather and time of the day, ARIMAX is the most natural tool for load forecasting among the classical time series models.

Neural network are essentially non-linear circuits that have the demonstrated capability to do non-linear curve fitting. The outputs of an artificial neural network are some linear or nonlinear mathematical function of its inputs. The inputs may be the outputs of other network elements as well as actual network inputs. In practice network elements are arranged in a relatively small number of connected layers of elements between network inputs and outputs. Feedback paths are sometimes used. The most popular artificial neural network architecture for electric load forecasting is back propagation. Back propagation neural networks use continuously valued functions and supervised learning. In this thesis, Artificial Neural Networks are used as short term load forecasting algorithm. The reason is that it has been proved that provided robust and accurate result for load forecasting algorithm [Ding 16].

4.3.1.2 Artificial Neural Networks

Artificial neural Networks (ANN) are one of the main tools for load forecasting purposes [Shahidehpour 02]. In the family of machine learning methods ANN is a method inspired by biological neural networks for the objective of estimation or approximation of the functions when a large number of inputs are provided, in order to estimate the unknown behavior of the system [Wang 03].

Figure 4.3: Central nervous system of human. Flow of axonal signal through the neurons [Emmy 11].

The principle of ANN is based on activation of a neuron under a certain circumstances which would be the inputs that are defined by designer. In fact, Natural neurons receive signals through synapses located on the dendrites or membrane of neurons. When the received signal are strong enough, the neuron is activated and emits a signal though axon. This signal might be sent to another synapses or activate another neuron. The inputs of the artificial neural network can be considered as synapses which are normally multiplied by a weight factor. The activation of signal is computed by a mathematical expression presented in equation 4.1.

$$O_j = f_j \sum_{k=1}^{K} w_{jk} x_k \tag{4.1}$$

Where f_j is the activation function of the neuron in jth layer and x_k is the kth input of the network. O_j represents the output of the jth layer for neuron. The illustrative concept of a neuron is depicted in Figure 4.4. The complete explanation of different steps of the algorithm can be found in [Chen 01, Abraham 05]. The algorithm for learning used in this thesis is based on backpropagation algorithm. Basically, there are three activation functions applied into back propagation, namely, Log-Sigmoid, Tan-Sigmoin and Linear Transfer Function. In this study the back propagation algorithm is used for training part with Tan-sigmoid and Linear function for first and second hidden layer, respectively.

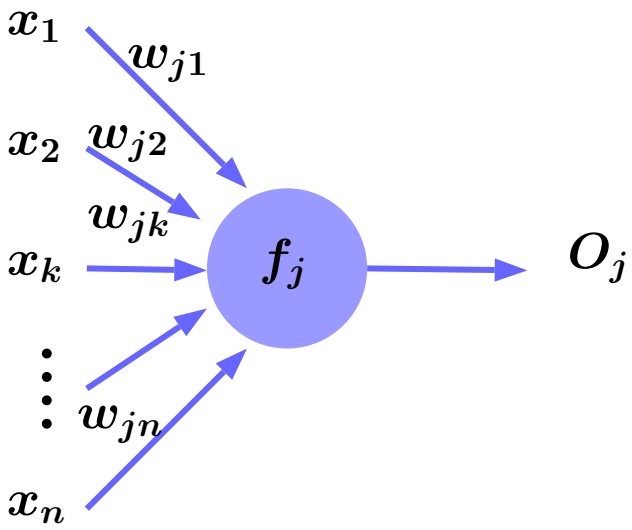

Figure 4.4: Mathematical model of an ANN neuron.

4.3.1.3 Short-term Load forecasting: modeling

In this thesis, for the purpose of short-term load forecasting (STLF) a model is developed which uses the historical data of load consumption and temperature forecast in order to apply a forecasting algorithm for next 24 hours. Different methodologies are applied for STLF in the literature [Lee 92, Gross 87, Huang 03]. In this thesis based on a bibliographical research on the actual models for STLF an algorithm is proposed using Neural network toolbox of MATLAB™. Different steps of the model are presented in the Figure 4.5. At first, the historical data for forecasting purpose are collected. After that a pre-processing level is applied in order to format the data for the training algorithm. In order to avoid saturation problems with activation functions the data will be normalized in normalization level. Then, the training step will be applied by testing level. These two levels will be done iteratively in order to reduce the error of forecasting. Finally, the results will be re-scaled to their original unit at post-processing level. At the end, the performance of the training algorithm will be examined in error analysis step. The overall configuration of ANN using NN toolbox is depicted in Figure 4.6. The general configuration shows the 8 inputs, two hidden layer with Tan-Sigmoid and Linear transfer function, respectively and one single output. The weight and bias factor for each neuron at each hidden layer is also presented. the learning algorithm will search for the best parameters for weight and bias in order to minimize the estimation error.

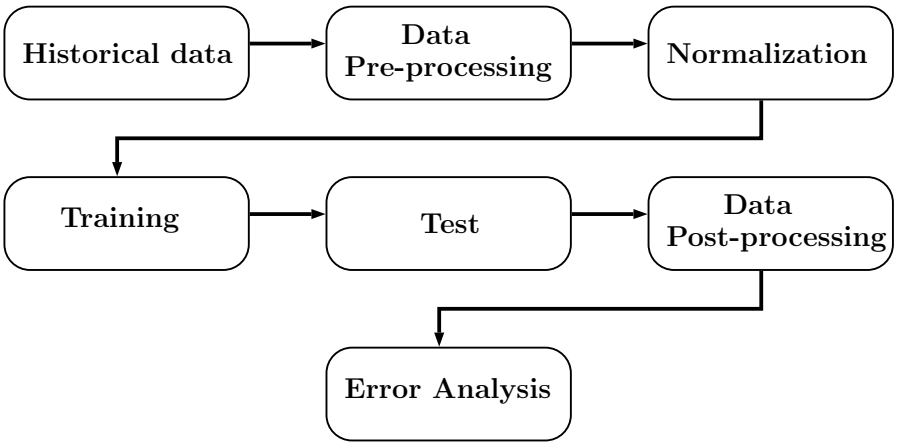

Figure 4.5: ANN-based load forecasting algorithm procedure.

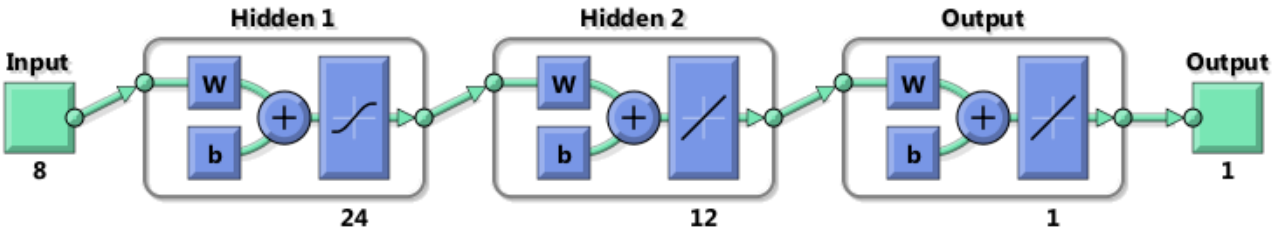

Figure 4.6: ANN model for STLF using MATLAB™ NN toolbox.

4.3.1.3.1 Data collection (historical data)

The required training data can be divided in tow main data; the input variables and output target. The input vectors are normally the data that have influence on the consumption. These inputs normally are the weather information, the type of the day (week-end or week day or holiday) or fault occurring in the grid. The output target is also considered as the objective of forecasting algorithm which is the real load consumption associated to the provided inputs for STLF application. In this thesis, as the forecasting algorithm is applied on the network of GÉRÉDIS Deux-Sèvres, the input variables are chosen based on available data in possession of GÉRÉDIS. These data are as follows:

1. Hour of day (1-24)
2. Day counter (1-365), one year
3. Day type (0-1), weekend, holiday or working day
4. Day type (1-7), 7 days of the week
5. D Temperature (today)
6. D+1 Temperature (tomorrow)
7. D Load profile
8. D-7 Load profile

There are different types of input variables that can be added to the input vectors in order to increase the accuracy of forecasting algorithm such as humidity, visibility(cloud cover %) or even wind speed. An analysis on the data of electricity consumption is done to show the relevance of consumption to temperature variation. This leads to consider the temperature as the main inputs for forecasting purpose in France. Figure 4.7 shows the relationship between temperature and load consumption in one region of Deux-Sèvres. This shows that the temperature and load consumption are varying approximately inverse. Increment of temperature leads to reduction of load consumption and vice versa. However, there are other factors that affect the consumption such as visibility (cloud cover) which leads to using the lighting systems.

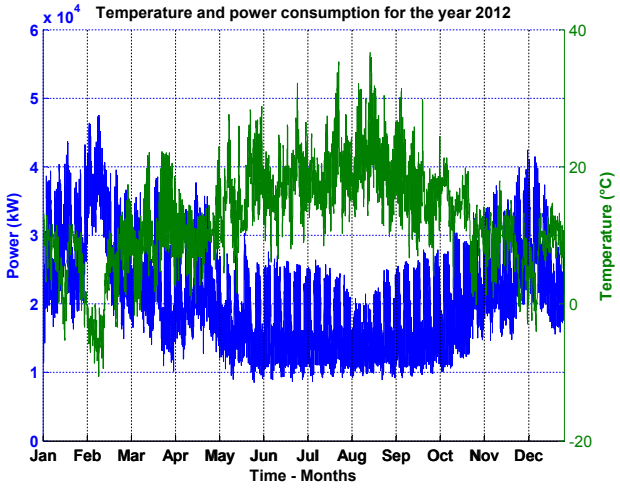

(a) Temperature and load consumption over one year.

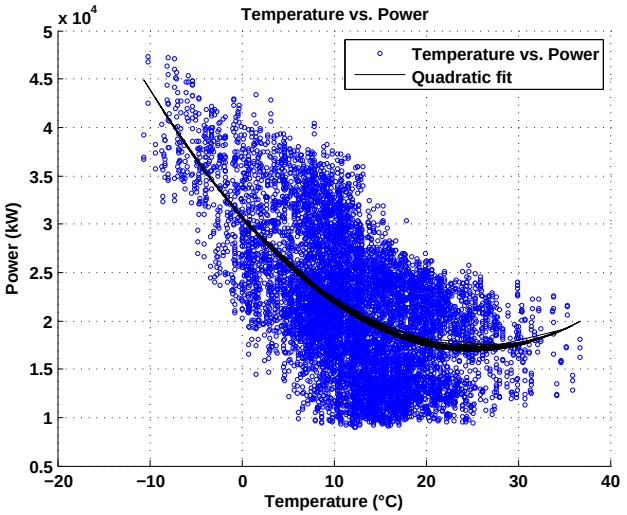

(b) Temperature vs. load consumption.

Figure 4.7: The variation of load consumption vs temperature.This shows the approximately inverse relationship between load and temperature.

A second analysis is done based on conversion of load profile signal to frequency signal, using fast Fourier transform (FFT) algorithm, in order to identify the periodic behavior of the signal. This analysis helps to choose the best length of signal and also identify the period of the signal. Figure 4.8 shows the frequency analysis of the same load consumption signal illustrated in Figure 4.7a. This result shows that there are two main frequency components which indicates the periods of 7 days (1 week) and 3.5 days (half a week). It means that the current load consumption is periodical mainly on the base of a week and half a week.

4.3.1.3.2 Data pre-processing

This step is necessary in order to provide proper set of inputs and output target. Since the set of input and output target will guide the learning algorithm to learn from their relationship. Hence, if there is any error or bad registration of data, the learning will be deviated. Therefore, in this step the data will be analyzed to avoid any mistake on the data. As in this thesis, the load consumption and temperature are the main inputs with shifting in the time, so their modification for preparation of learning set should be done in this step.

Two matrices should be constructed. One for inputs and one for outputs . These matrices have the characteristics as follow:

$$In_{mat} = [X]_{Nb_{in} \times H_l} \tag{4.2}$$

$$Out_{mat} = [Y]_{Nb_{out} \times H_l} \tag{4.3}$$

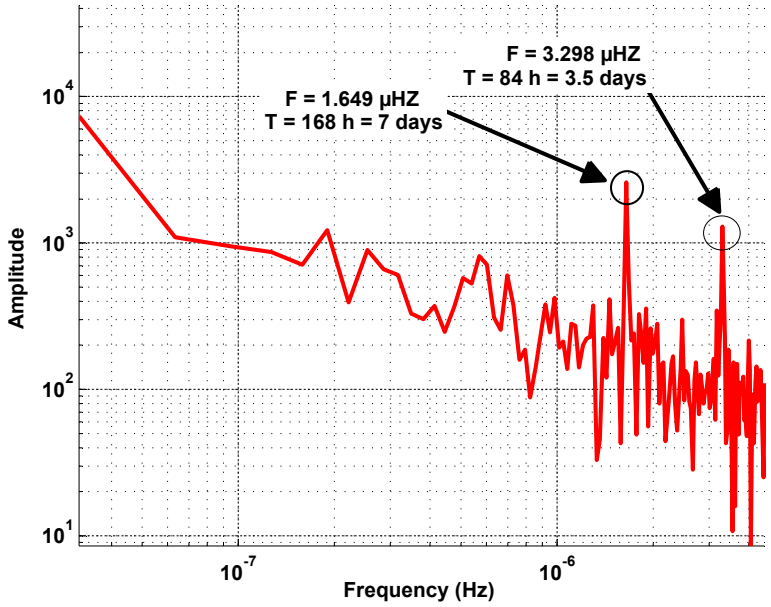

Figure 4.8: Frequency analysis of load consumption signal for 2012.

Where In_{mat} and Out_{mat} are input and output matrices, respectively. Nb_{in} and Nb_{out} are input and output numbers which are 8 and 1 in our case, respectively. H_l is History length or the length of our historical data vector. The input matrix for our case can be rewritten as follow:

$$In_{mat} = [Hour_{day}, Day_{ctr}, Day_{type}^{0,1}, Day_{type}^{1,7}, Temp_D, Temp_{D+1}, Load_D, Load_{D-7}]_{8\times H_l} \quad (4.4)$$

$$Out_{mat} = [Load_{D+1}]_{1\times H_l} \quad (4.5)$$

The inputs are already introduced in previous section. In preparation of data the important point is related to the shift for some inputs. All the inputs with D-1 index should have a 24 hours of shift to be correspond to the output target. For the case of D-7 the data should be shifted by 168 hours in order to present the load profile of the same day as prediction of previous week. H_l in this thesis is considered a historical data of 3 years from 2011 to 2013. The final test in the day of algorithm preparation is done on December 11, 2014. Hence the historical data are approximately 4 years for short term load forecasting of next 24 hours.

4.3.1.3.3 Normalization

This step is applied in order to avoid the saturation problem for activation functions. This is already discussed in some references [Zhang 10, Kiartzis 95]. In fact all collected data will be divided by their absolute maximum value to be in the range of -1 to 1. Besides, $Day_{type}^{0,1}$ is represented as 0 or 1.

4.3.1.3.4 Training and test step

In ANN normally a percentage of historical data are considered for training purpose and the rest of the data will be used for test step. In this thesis training percentage is considered as 70% and test of 30%. Training step is also should have a particular algorithm. There are already defined training algorithms available in MATLAB™ NN toolbox. Generally, Trainbr (bayesian regularization) and Trainlm (Levenberg-Marquardt backpropagation) are the best choices for STLF problem among other available algorithm [Zhang 10]. In this work, Trainbr is chosen as training algorithm as it has faster convergence speed. In Figure 4.9, the generated neural

network for STLF application and used in this thesis is presented. A multi-layer approach is chosen with 2 hidden layer. The first layer has 24 neurons and second layer has 12 neurons. The number of neurons have been chosen based on different tests where the best results in a reasonable time scale was obtained by this configuration. For each neuron the parameter $l_i n_j$ indicates the layer i and neuron j of that layer. w_n depicts the weight value considered for the nth input ($n = 8$). These weights are also exist between each two consecutive layers.

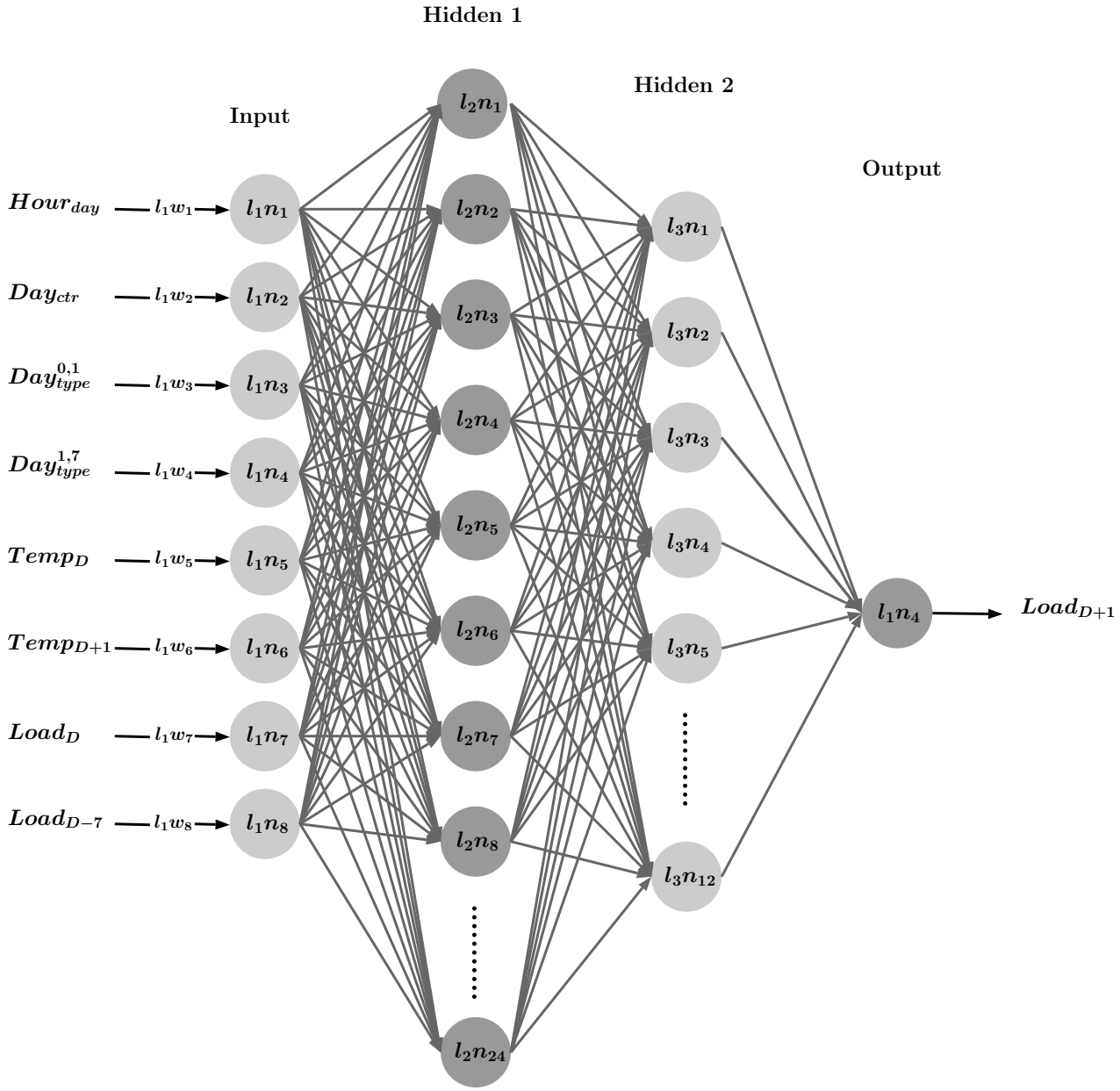

Figure 4.9: Multi-layer feed-forward backpropagation ANN for STLF application.

4.3.1.3.5 Data post-propagation

This level is necessary in order to bring back the output from value of the algorithm range to its original unit. The results should be normally multiplied by the same reference of per unit process in normalization step.

4.3.1.3.6 Error Analysis

In this step the different type of error for forecasting can be applied in order to evaluate the

accuracy of forecasting algorithm, mean absolute percentage error (MAPE) is chosen in order to evaluate the accuracy of forecasting. It usually reresent the accuracy as percentage while there would be some disadvantage using MAPE when there are zero values in the actual values. MAPE is expressed as follow in equation 4.6:

$$MAPE = \frac{1}{n}\sum_{t=1}^{n}\left|\frac{Y_t - \hat{Y}_t}{Y_t}\right| \tag{4.6}$$

Where $\hat{Y}_t$ is the estimated output of the forecasting algorithm and Y_t is the real output value applied to the system for learning purpose.

4.3.1.4 Results and discussion

The results of generated STLF algorithm are presented in this section. In the history of the algorithm all data from 2011 to December 10 2014 have been used for learning purpose. After the learning, the algorithm is used to check its performance by doing load forecasting for December 11 2014. In the following at first, Figure 4.10 shows the training states of the algorithm with a $MAPE = 3.73\%$. It would be possible to enhance the obtained result by increasing the number of neurons, layers or even activation function, but as the calculation time for real-time application is important we suffice this precision which obtained in approximately 15 minutes. Figure 4.11 shows the regression analysis for three sets of data. 70% of the data are used for training which are showing a regression of $R = 0.9888$. 30% of the data are used for testing the trained algorithm with regression of $R = 0.9729$ and the overall set of the data have converged to $R = 0.9861$. This precision for the case of real-time energy management system is acceptable as the algorithm was successful to estimate properly the periodical behavior of the actual signal with approximately the same minimum and maximum values.

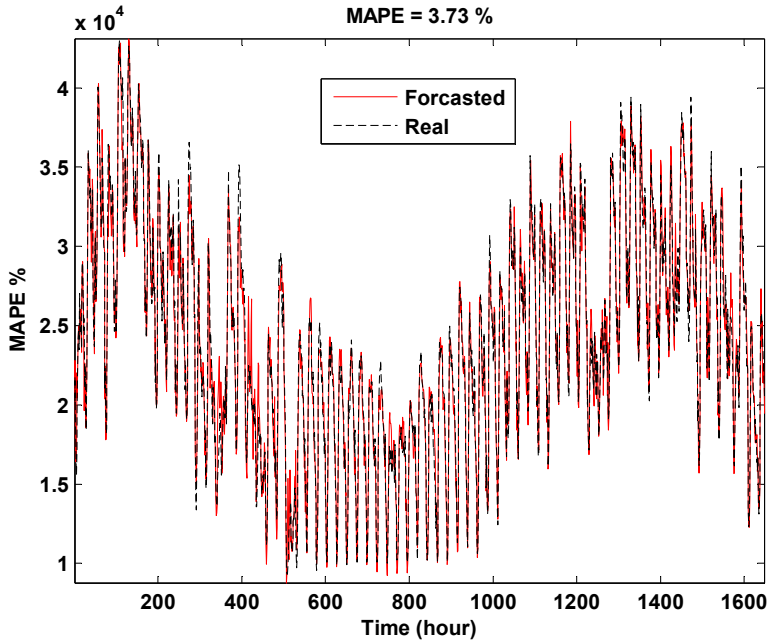

Figure 4.10: Example of training output of ANN algorithm for STLF applied for estimation of 11 December 2014.

The final result of the STLF algorithm for prediction of 11 December 2014 is presented in Figure 4.12. The error of estimation is approximately 3% . The algorithm was successful to predict the peak of consumption but there would be more error in minimum of consumption.

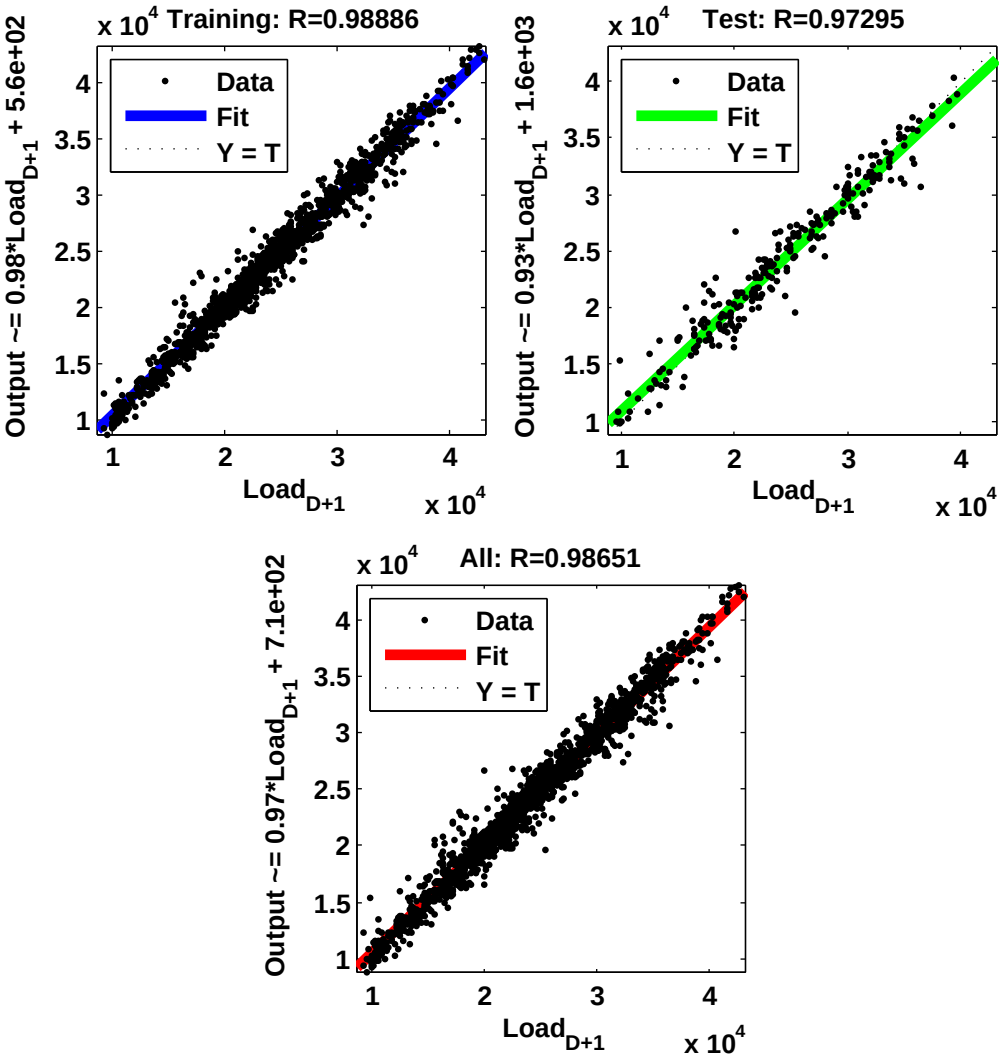

Figure 4.11: Regression analysis of training, test and all of the historical data applied for STLF application.

This algorithm can be used for consumption prediction in order to provide the $\hat{P}_{conso}(t)$. This would be possible to increase the accuracy of the algorithm but the calculation time should be considered. The acceptable marginal variation of forecasted parameters and their impact on the real-time supervision performance is analyzed in the next sections. The compromise of the accuracy, calculation time and their impact on the real-time performance is an important study that would be considered for perspective of this thesis. The proposition of the author is to find the marginal error and use a two level real-time supervision system. This idea will be discussed in next sections.

For the other estimation parameters such as $\hat{P}_{PV}(t)$ and $\hat{P}_{wind}(t)$, the same approach can be applied were these field of study are already developed in literature. In this thesis, their development are considered as perspective of the research as the timing of the project and concentration on main objective of the thesis did not let to spend more time on forecasting algorithm. For $\hat{P}_{EV}$, as the modeling of charging profile is already discussed in chapter 2 and for today application, there is no real available data of EV charging demand, the author suffice to consider the output of the model as the estimated profile. Knowing that, the algorithm is an stochastic based modeling approach there would be always slight variation in the output so it can be considered as difference between real measured values and estimated values for PEV

charging demand.

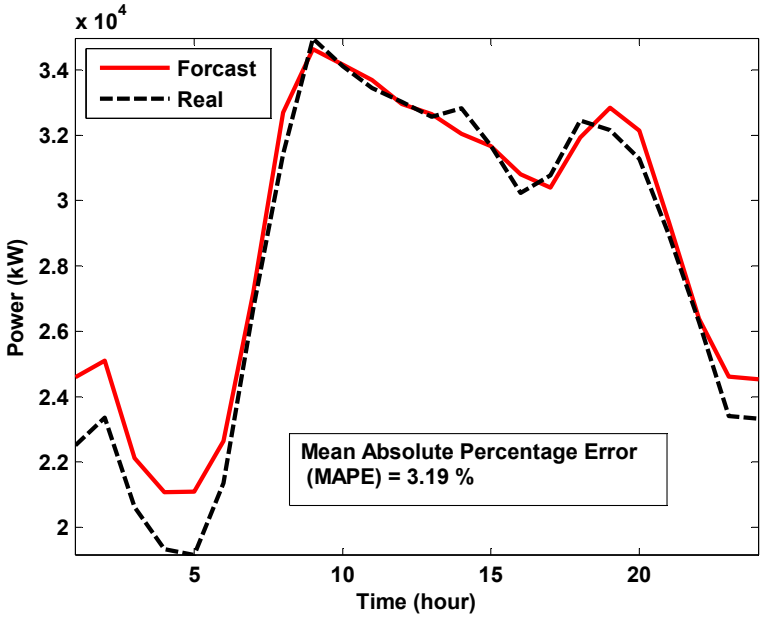

Figure 4.12: Output of the STLF algorithm for prediction of 11 December 2014 consumption(at the level of HV/MV substation).

4.3.2 Predictive supervision (Off-line optimization)

In the second level of the proposed supervision system (cf. Figure 4.1) a predictive supervision or off-line optimization layer is introduced. The aim of this level is to provide *a priori* optimal solution for real-time supervision thanks to an optimization algorithm using the provided inputs from forecasting algorithm. This optimization algorithm should be robust enough in order to handle the stochastic behavior of the problem and also the high dimension nature of the system (number of optimal variables). The output of optimization algorithm would be the reference for real-time supervision which leads the real-time decisions to be nearer to the global optimum. This is certainly depends on the precision and accuracy of at first forecasting algorithm and then optimization algorithm. A literature review on the current available optimization methods and particularly the methods applied on the same problematic are conducted in next section. After that the proposition of the author for the defined problem will be presented.

4.3.2.1 Problem formulation and specification

The optimization problem has the same nature and specification of proposed algorithm in Chapter 2. The problem is the minimization of energy transmission cost (ETC), the bill paid to TSO by DSO corresponds to transmission of energy from power plants to the distribution grid through the transmission grid. In parallel, some other objectives are aimed. For the environmental issues the reduction of produced CO_2 is another objective. This corresponds to the energy transmission inside the power plants leading to CO_2 production. The third objective is to increase the local consumption of renewable energy production in order to avoid active power injection to the transmission grid. This service is applied upto a HV/MV (90/15 kV) substation. This substation is at the border of transmission and distribution grid (Figure 4.13). The under study grid has local wind farm and solar farm.

Table 4.1: Specification of Predictive supervision system for ETCM service for V2G-enabled PEV fleet.

Objective	Sub-objective	Associated inputs	Constraints	Means of actions	Indicators
Energy Tranmission Cost Minimization	Subscribed power exceeding limitation	Delta P	Subscribed power (Optimized)	Charging, Discharging and No charging of PEVs	Transmission cost in euro
	Maximize energy consumption during low cost	Price	Consumption variation		
Environmental and lower CO2 efficiency	Maximize renewable energy consumption	Pps			Auto-consumption of RES (%)
	Maximize PEV owner satisfaction	SOC	PEV energy need (full-battery at departure)		Battery charging rate
	Optimize subscribed power		Battery degradation		CO2 emission rate

The objective function is already defined in equation 2.15. This is to minimize the energy transmission cost. Here the table of specification of the problem are presented in order to provide better understanding of the problem (Table 4.1).

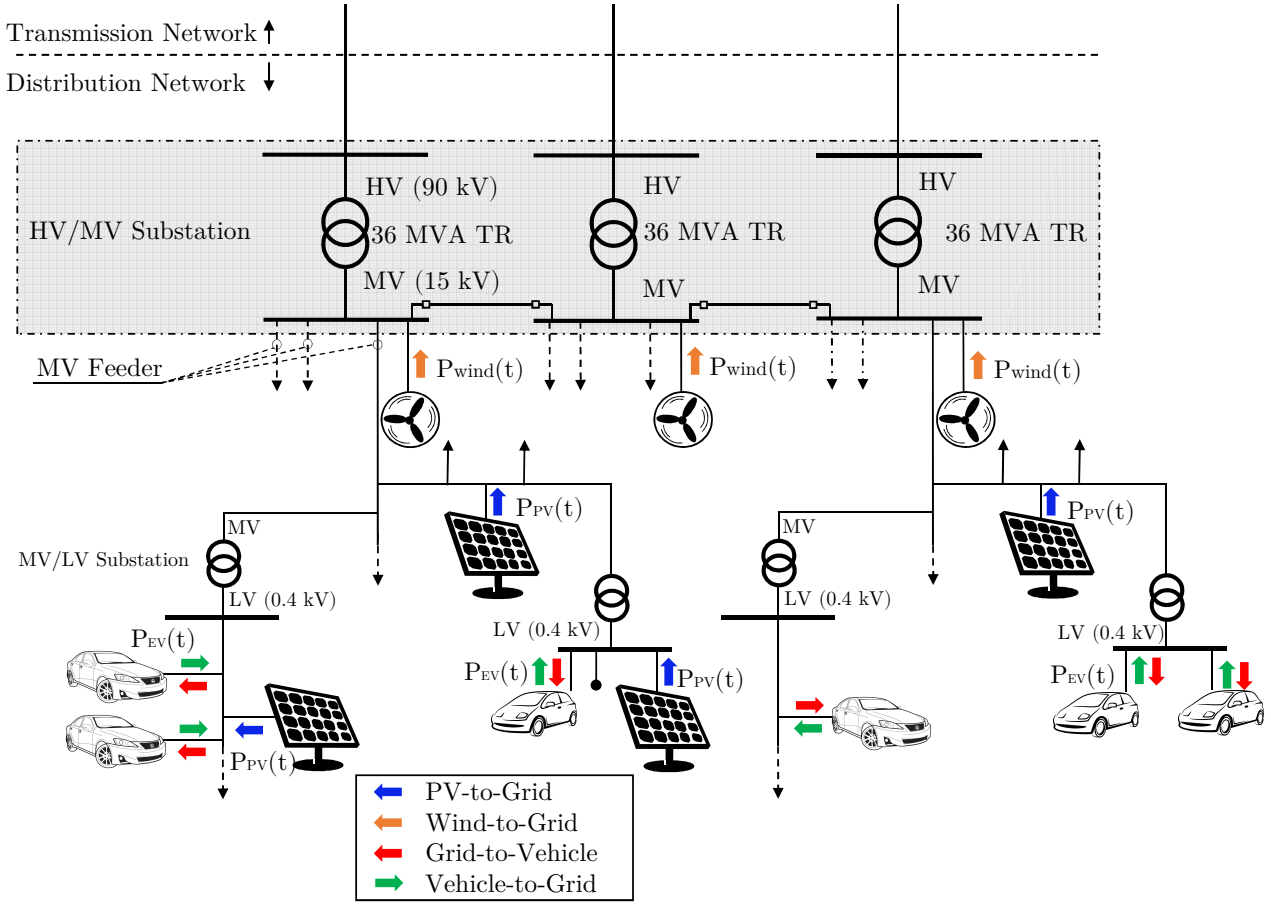

Figure 4.13: Representation of case study, a HV/MV substation at border of transmission and distribution grid containing local wind and solar farms and distributed PEVs.

The dimension of the problem is in range of thousands. As the sampling time of the meters for calculation of energy transmission cost is fixed on 10 minutes, the demand should be controlled every 10 minutes. In other words, for every day 144 variables corresponds to number of 10 minutes in 24 hours should be calculated. In fact, these variables are defining the amount of power that can be delivered/absorbed to/from the PEVs. As the ETC is calculated in a

yearly base the demand control should be applied over the whole year. In fact, for a year of 365 days, 52560 variables should be optimized in order to be able to minimize the ETC using the PEVs battery storage capability. To choose the proper algorithm this feature should be taken into account. The proposition of this project is to try the optimization with hybrid technics. Local search algorithms are able to search in a limited surface based on gradient and providing exact optimum solution. While the global search algorithm and basically stochastic algorithms are able to search a vast search space. While their convergence to the best optimum is not always guaranteed. In this thesis, the author provided a hybrid optimization algorithm which is able to converge to the best optimum. In fact there is two possible aspect of solving the problem.

The first one is to consider the problem day per day. In this case in each optimization problem 144 variables should be optimized. This part is done by local search algorithm.

The second one is to do the optimization for the whole year. In this case there are 52560 variables for optimization. A global search algorithm is introduced for this approach.

The challenge is the value of subscribed power. In fact, since the subscribed power is signed yearly and there is no change during the contract, hence the result of optimization for one day with optimization of whole year would be the same. In other words. if we do the optimization by first approach we will obtain the same result as second approach. The main difference between these to approach is the time of calculation. In next line the problem formulation is presented. After that the hybrid optimization algorithm will be presented. This algorithm is combination of Constrained Particle Swarm optimization (CPSO) and Interior point (IP) method. This hybrid algorithm afterwards is called CPSO-IP.

As presented in Figure 4.13, the power transition of the substation can be expressed as in equation 4.7.

$$P_{PS}(t) = P_{con}(t) \pm P_{EV}(t) - P_{wind}(t) - P_{PV}(t) \tag{4.7}$$

These parameters are already defined in chapter 2. The power of electric vehicles can be either positive (charging case) or negative (discharging case). This is expressed as some of all PEVs power in equation 4.8.

$$P_{EV}(t) = \sum_{i=1}^{NPEV} P_{EV}^{i}(t) \tag{4.8}$$

A single PEV power is expressed as :

$$\begin{cases} P_{EV}^{i}(t) = [a^i(1), a^i(2), ..., a^i(t)] \times CR^i \\ i = [1, NPEV] \in \mathbb{N} \\ a(t) = [-1, 1] \in \mathbb{Z}. \end{cases} \tag{4.9}$$

Where $a(1)$ to $a(t)$ express the parameters of charging/discharging demand correspond to each sample time t (each 10 minutes) and CR^i is a diagonal matrix with diagonal elements equal to charging rate of 3.7 kW. By putting 4.9 to 4.8, the equation 4.8 can be rewritten as:

$$P_{EV}(t) = \sum_{i=1}^{NPEV} [a^i(1), a^i(2), ..., a^i(t)] \times CR^i \tag{4.10}$$

By distributing the sum to the parameters of the vector $P_{EV}(t)$ can be expressed as :

$$P_{EV}(t) = CR^i \times \left[\sum_{i=1}^{NPEV} a^i(1), \sum_{i=1}^{NPEV} a^i(2), ..., \sum_{i=1}^{NPEV} a^i(t) \right] \tag{4.11}$$

Each parameter can be rewritten as follows:

$$A(1) = \sum_{i=1}^{NPEV} a^i(1), \tag{4.12}$$

$$A(2) = \sum_{i=1}^{NPEV} a^i(2), \tag{4.13}$$

$$A(3) = \sum_{i=1}^{NPEV} a^i(3), \tag{4.14}$$

$$\vdots$$

$$A(t) = \sum_{i=1}^{NPEV} a^i(t). \tag{4.15}$$

By putting the new parameters, so-called global parameters, the $P_{EV}(t)$ will be re-expressed as :

$$P_{EV}(t) = [A(1), A(2), ..., A(t)] \times CR^i \tag{4.16}$$

By using the equation 2.15 for ETC, and considering the obtained expression of PEV fleet power,$P_{EV}(t)$, the main objective can be expressed as in follow:

$$\min_{A(1),A(2),...,A(t)} \left(a_2 P_{subscribed} + \sum_{j=1}^{n} \left(d_j \int_{t_j^a}^{t_j^b} (P_{con}(t) \pm P_{EV}(t) - P_{wind}(t) - P_{PV}(t)) \right) + \sum_{m=1}^{12} \sum_{j=1}^{n} \left(\alpha \sqrt{\sum_{t=1}^{52560} (P_{con}(t) \pm P_{EV}(t) - P_{wind}(t) - P_{PV}(t) - P_{subscribed}(t))^2} \right) \right) \tag{4.17}$$

Equation 4.17 shows the ETC function by integration of PEV charging power equation. This equation can be rewritten using the parameters of ETC function. The parameters are defined thereafter.

$$\Delta P(t) = P_{PS}(t) - P_{subscribed}(t) \tag{4.18}$$

Exceeding of subscribed power is represented by ΔP in equation 4.18. Subscribed power exceeding (SPE) parameter of the ETC is expressed by equation 4.19.

$$SPE(t) = \sum_{j=1}^{n} (\alpha . \sqrt{\sum (\Delta P(t)^2)}) \tag{4.19}$$

$$E_j = \int_{t_j^a}^{t_j^b} (P_{con}(t) \pm P_{EV}(t) - P_{wind}(t) - P_{PV}(t)) \tag{4.20}$$

In these equations, j represents the number of periodical tariffs (here $j = 5$). t_a^j and t_a^j represent the start and end time of jth periodical tariff. In equation 4.20, E_j represents the energy consumption during jth periodical tariff. Therefore, putting 4.19 and 4.20 inside 4.17, the ETC objective function for minimization can be rewritten as :

$$\min_{A(1),A(2),...,A(t)} \left(a_2 P_{subscribed} + \sum_{j=1}^{n} (d_j E_j) + \sum_{m=1}^{12} SPE(m) \right) \tag{4.21}$$

Knowing the objective function, now the constraint should be defined. Since the only control-ability of the optimization is on the PEV battery power chargers, the main constraints will be focused on the PEVs available stored energy and their required energy at departure time. In order to formulate the constraints, some new parameters should be defined. The first constraints is the availability of the PEVs which are expressed as the availability of the fleet. A diagonal matrix so-called availability matrix (A_{mat}), is defined to express the availability as in equation 4.22:

$$A_{mat} = \begin{bmatrix} 0 & 0 & 0 & 0 & 0 & 0 & 0 & 0 & 0 \\ 0 & \ddots & 0 & 0 & 0 & 0 & 0 & 0 & 0 \\ 0 & 0 & 0 & 0 & 0 & 0 & 0 & 0 & 0 \\ 0 & 0 & 0 & A'_{ab} & 0 & 0 & 0 & 0 & 0 \\ 0 & 0 & 0 & 0 & \ddots & 0 & 0 & 0 & 0 \\ 0 & 0 & 0 & 0 & 0 & A'_{cd} & 0 & 0 & 0 \\ 0 & 0 & 0 & 0 & 0 & 0 & 0 & 0 & 0 \\ 0 & 0 & 0 & 0 & 0 & 0 & 0 & \ddots & 0 \\ 0 & 0 & 0 & 0 & 0 & 0 & 0 & 0 & 0 \end{bmatrix} \tag{4.22}$$

Where the parameters in this equation are defined as :

$$t_{arrival} = \min_i(T^i_{arrival}) \tag{4.23}$$

$$t_{departure} = \max_i(T^i_{departure}) \tag{4.24}$$

$$a = b = t_{arrival} \tag{4.25}$$

$$c = d = t_{departure} \tag{4.26}$$

$$A'_{ab} = A'_{cd} = 1 \tag{4.27}$$

$$A'_{ef} = 1, \quad \forall\, e = [a, c] \in \mathbb{N}, \quad \forall\, f = [b, d] \in \mathbb{N} \tag{4.28}$$

$t_{arrival}$ is the arrival time of the first PEV in the fleet and $t_{departure}$ is the departure time of the last PEV in the fleet. $T^i_{arrival}$ and $T^i_{departure}$ represent the arrival and departure time of i^{th} PEV in the fleet. In matrix 4.22, all the arrays in red are equal to one as expressed in 4.27 and 4.28. These represent the availability of the fleet for optimization problem.

Now for defining the availability constraint, the parameter vector of $P_{EV}(t)$ defined in 4.16 should be reformulated using A_{mat}.

$$A'' = [A(1), A(2), ..., A(t)]_{[1\times t]} \times A_{mat[t\times t]} \tag{4.29}$$

A'' is a vector of dimension $[1 \times t]$. Now with this formulation, the constraint related to the availability is respected so the $P_{EV}(t)$ can be expressed as :

$$P_{EV}(t) = [A''(1), A''(2), ..., A''(t)] \times CR^i \tag{4.30}$$

The second constraint is related to required energy of the fleet. At the moment of arrival to the parkings the PEVs have an arrival SOC representing the available energy in their batteries. These PEVs have a desired departure SOC which should be declared as the plug-in moment. Hence the energy need of the fleet can be calculated from provided information ($E^i_{arrival}$ and $E^i_{departure}$ provided by the driver of *ith* PEV in form of kWh energy or SOC percentage).

$$E^{fleet}_{need} = \sum_{i=1}^{NPEV} (E^i_{departure} - E^i_{arrival}) \tag{4.31}$$

This energy should be provide to the fleet and is considered as the hard constraint of the problem.

$$\int_{t=1}^{T} P_{EV}(t) = E_{need}^{fleet} \tag{4.32}$$

As the problem is discretized in sample time so the integral can be expressed as summation:

$$\sum_{t=1}^{T} P_{EV}(t) = E_{need}^{fleet} \tag{4.33}$$

Using the new formula of $P_{EV}(t)$ obtained in 4.30 and the discretized constraint in 4.33, the new version of energy need constraint can be reformulated as follows:

$$[A''(1) + A''(2) + \ldots + A''(t)] \times CR_i = E_{need}^{fleet} \tag{4.34}$$

After definition of availability constraint and energy need constraint, the boundary constraints are related to the amount of power that can be delivered or absorbed in each sample time. These constraints are presented in equations 4.37 to 4.40. In these constraints $N_{available}^{PEV}(t)$ represents the number of PEVs available in t^{th} time slot. This should be considered that the actual formulation is concentrated on charging problem at office and the same formulation should be considered for home charging problem. The final application of these formulation on the optimization problem are by summing all formula of office and home in order to apply the formula for one day time slot. This is repeated for each day and the final size of the vector is equal to $T = 52560$ for a year of 365 days. In the current formulation $T = 144$ corresponds to number of 10 minutes sample time for one single day. Now the final set of problem formulated for optimization problem of ETC minimization using V2G-enabled PEV fleet is obtained and presented thereafter:

$$\min_{A''(1),A''(2),\ldots,A''(t)} \left(a_2 P_{subscribed} + \sum_{j=1}^{n} (d_j E_j) + \sum_{m=1}^{12} SPE(m) \right) \tag{4.35}$$

Subject to

$$[A''(1) + A''(2) + \ldots + A''(t)] \times CR_i = E_{need}^{fleet} \tag{4.36}$$

$$-N_{available}^{PEV}(1) \leqslant A''(1) \leqslant N_{available}^{PEV}(1) \tag{4.37}$$

$$-N_{available}^{PEV}(2) \leqslant A''(2) \leqslant N_{available}^{PEV}(2) \tag{4.38}$$

$$-N_{available}^{PEV}(3) \leqslant A''(3) \leqslant N_{available}^{PEV}(3) \tag{4.39}$$

$$\vdots$$

$$-N_{available}^{PEV}(t) \leqslant A''(t) \leqslant N_{available}^{PEV}(t) \tag{4.40}$$

Up to now, the problem formulation and specification is presented. Knowing the nature of the problem (Nan-linear problem), different possible methods are exist. In this thesis based on the literature review presented before, and knowing the features of this problem (high dimension and stochastic behavior), a hybrid optimization technique is applied using Particle Swarm Optimization (PSO) as global stochastic search algorithm and Interior point method as a local search algorithm. These two methods are presented in next sections including the obtained results.

4.3.2.2 Hybrid optimization algorithm: Constrained Particle Swarm Optimization Interior-Point (CPSO-IP)

The idea of hybridization of optimization algorithm has been deeply analyzed in different previous researches. The reasons behind hybridization are different and depend on the application of the optimization problem. In order to guarantee the global optimal solution, a hybrid optimization technique is used to firstly, search the whole possible search space using a global stochastic algorithm and secondly using the optimum parameters of stochastic algorithm as initial point, the second gradient based algorithm ensure the optimality of final solution. For a single gradient based optimization technique, e.g. Interior-point, the optimality of final solution is not guaranteed as the problem has stochastic nature, i.e. stochastic function is used in modeling of PEV charging power. In addition, the gradient based optimization techniques, are sensitive to the initial conditions and their robustness to the variation of initial condition is a major challenge. For this reason, starting the searching process using a global stochastic methods, such as genetic algorithm, particle swarm optimization, simulated annealing or imperialist competitive algorithm, would be a candidate solution to reduce the dependency of gradient based algorithm to the initial condition and avoid local optimum trapping.

An overall view of the hybrid algorithm proposed in this thesis is presented in Figure 4.14. This hybridization starts with PSO algorithm with constrained condition (feasible initial condition), then the final result of PSO algorithm is injected to Interior-Point algorithm as initial condition (initial point) in order to complete the searching process. This completion is necessary since the stochastic based optimization techniques can converge through the global optimum region and their final optimum are stochastic and different in each evolution of algorithm.

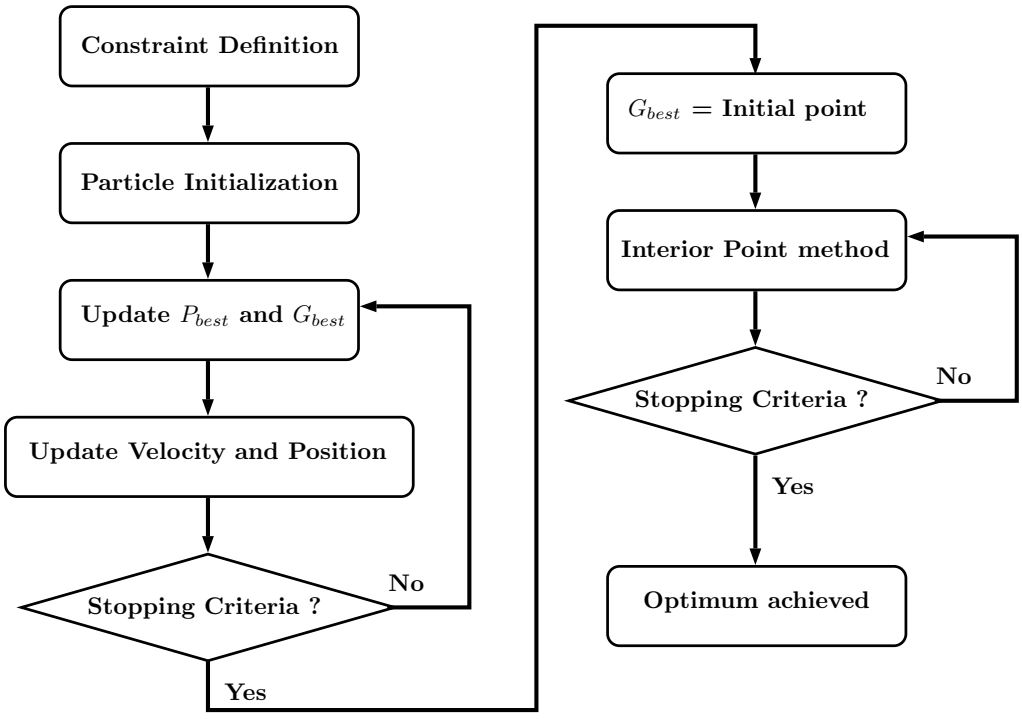

Figure 4.14: Flowchart of hybrid optimization algorithm CPSO-IP.

4.3.2.3 Particle Swarm optimization (PSO)

Particle Swarm Optimization is a population-based meta-heuristic global stochastic optimization algorithm. It is a population based and self-adaptive search optimization technique with

versatility and robustness in seeking the global optimal solution [Cheng 09]. The PSO algorithm includes some tuning parameters that greatly influence the algorithm performance.

This algorithm is developed from swarm intelligent and it is based on the research of birds and fish flock movement behavior. A certain number of particles, e.g., 100, randomly will be generated. After that iteratively, each particle tries to improve its position based on the optimum position. Finally, the particles try to make a swarm around the optimal point or region, where the stopping criteria could be considered as number of iteration or tolerance. Each particle's movement depends on its previous local best solution (P_{best}) and current known positions in the search space by other particles (G_{best}). The mathematical formulation proposed by [Kennedy 11, Poli 07] is presented in 4.41 and 4.42.

$$v_{id}^{k+1} = w.v_{id}^{k} + c_1 r_1^k (pbest_{id}^k - x_{id}^k) + c_2 r_2^k (gbest_{id}^k - x_{id}^k) \tag{4.41}$$

$$x_{id}^{k+1} = x_{id}^{k} + v_{id}^{k+1} \tag{4.42}$$

Where x_{id}^k, is the position of particle i in its d dimension at time k, v_{id}^k is the velocity of the same particle and w is the inertia weight. r_1 and r_2 are random fiction numbers between 0 and 1. c_1 and c_2 are speeding factor for local best solution and global best solution, respectively. The results of optimization is highly depends on speeding factor that should be chosen empirically. If the speeding factors are too small, the results will be far away from the optimum. If they are too big the particles will fly suddenly to the target or beyond the target. The proper choice for c_1 and c_2 leads to good control of flying speed and the final result will not be partial optimism. The parameters of PSO algorithm implemented in this thesis are brought thereafter:

```
c1 = 0.8;    % acceleration coefficients, the cognitive behavior
c2 = 0.1;    % social behavior factor
w  = 0.8;    % inertia weight
Nb_particle = 100;
Nb_dimension = 52560; 10 minutes sample time for 365 days
Nb_iteration = 50;
```

4.3.2.3.1 Constrained Particle Swarm Optimization

A constrained Nan-linear problem can be solved using PSO algorithm if the feasible set of of particles would be defined for the algorithm. The key point in the constrained optimization process is to deal with the constraints [Hu 02]. Some methods are proposed for handling the constraints. Reference [Koziel 99] grouped them into four categories: methods based on preserving feasibility, methods based on penalty functions, methods with clear distinction between feasible and infeasible solutions and other types of hybrid methods. The most straightforward one is the method based on preserving the feasibility of solutions. In order to find the optimum in feasible space, each particle searches the whole space but only keeps tracking feasible solutions. For acceleration of this process, all the particles are initialized as feasible solutions. The flowchart of CPSO is illustrated in Figure 4.15.

The algorithm for Constrained programming is brought thereafter:

```
for kk=1:Nb_particle;
    for jj=1:366;
        for ii = 1:sample_per_day;
            Ct = Constrained_daily_energy - sum(Matrix_base(1,1:ii-1));
            if ii == sample_per_day;
                Matrix_base(1,ii) = Constrained_daily_energy - sum(Matrix_base...
                    (1,1:ii-1));
                if Matrix_base(1,ii) > UB(ii)
```

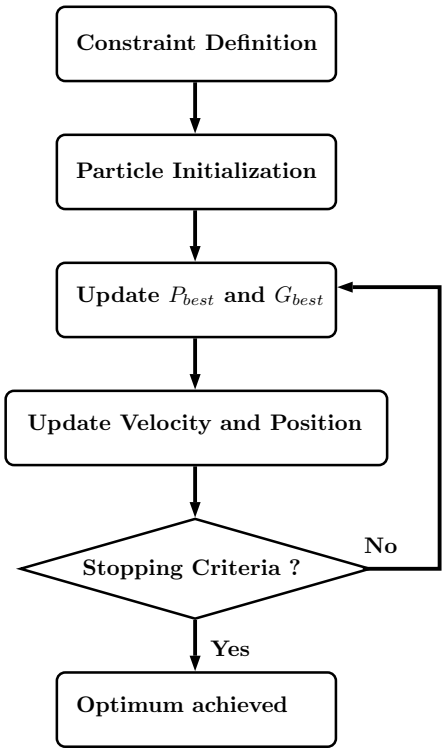

Figure 4.15: Flowchart of CPSO algorithm.

```
                    Matrix_base(1,ii) = (rand(1,1) * (UB(ii) - LB(ii))) + ...
                        LB(ii);

                    extra_energy = Constrained_daily_energy - sum(Matrix_base...
                        (1,1:ii));

                    contributors = Matrix_base > gar_fac ;
                    % -2000 is chosen to gaurantee the search
                    % within big
                    % negative values
                    indice_contributor = find(contributors);
                    contribution_percentage = (UB(indice_contributor) - ...
                        Matrix_base(indice_contributor)...
                        )./ sum(UB(indice_contributor) - Matrix_base...
                        (indice_contributor));

                    Matrix_base(indice_contributor) = Matrix_base...
                        (indice_contributor) + ...
                        (extra_energy.* contribution_percentage);

                end
            elseif UB(ii) <= Ct
                Matrix_base(1,ii) = (rand(1,1) * (UB(ii) - LB(ii))) + LB(ii);
            else
                Matrix_base(1,ii) = (rand(1,1) * (Ct - LB(ii))) + LB(ii);
            end
        end

        Matrix_base_year(1,d(jj):u(jj)) = Matrix_base;
    end
    Particles_mat(kk,:) = Matrix_base_year;
end
```

The output of this algorithm named `Particles_mat` contains all the feasible initial solutions so-called initial particles for PSO algorithm. `Particles_mat` is a matrix of $n \times m$ with n equal

to the number of particles and m equal to the dimension (here $m = 52560$). In this algorithm `Constrained_daily_energy` is the value of energy need of PEV fleet in one day. In fact, using this value the equality constraint of 4.36 will be implemented. `sample_per_day` represents the number of samples per day which is 144 for one day. `Matrix_base` is the temporary memory for particles. In this algorithm, two main constraints are controlled. The first one is the boundary constraints which are checked with `UB` and `LB` as upper bound and lower bound limit. The second constraint is the equality constraint which is checked using `extra_energy`. This parameter handles the difference of the actual energy and the constraint energy. After that, it will distribute this difference between all dimensions. `gar_fac` is introduced in order to guarantee the search through large negative values. Since, if this parameter is not considered, the search space near to big negative will not be explored. This is because of error propagation in form of summation function. This parameter is considered as -2000 MW for the case of year 2030 with 2700 PEVs.This value can be adjusted in function of number of PEVs in the fleet and their maximum available power.

CPSO fitness evaluation for the case study of year 2030 with 2700 PEVs are brought in Figure 4.16. After 50 iterations all the particles are converged through the best solution and there is no further progress. Best fitness is obtained as 1.05 p.u. This is the case that using IP in the next section the final optimum reaches to 1.00 p.u. G_{best} will be provided to IP algorithm as initial condition. In Figure 4.17, a particle in first iteration with randomly generated values and the same particle after 50 iterations is illustrated. This shows the evolution of particle through the optimum region. A similar case but for all the particles containing the boundary condition are presented in Figure 4.18 and 4.19. In Figure 4.18, all 100 particles randomly generated in feasible area are illustrated. As it is shown the whole feasible search space is covered by initial random particles while in Figure 4.19, the same particles converged through the global optimum region and form the final solution. This final solution so-called G_{best} will be provided to IP algorithm for further search. this is explained thoroughly in next section.

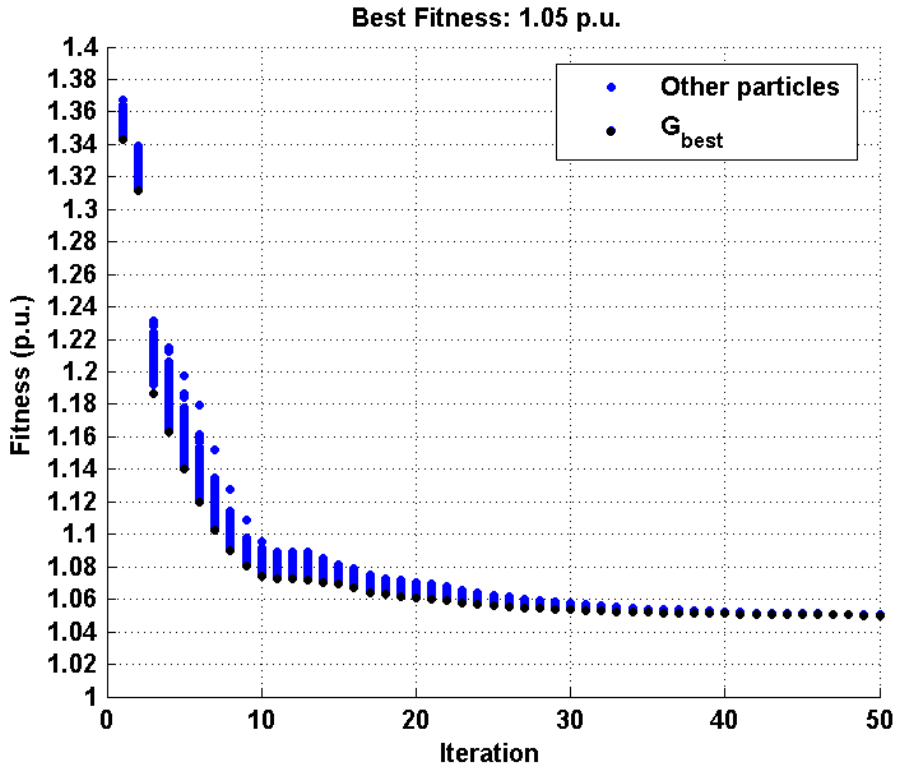

Figure 4.16: Fitness evaluation for CPSO, scenario of 2030 (2700 PEVs).

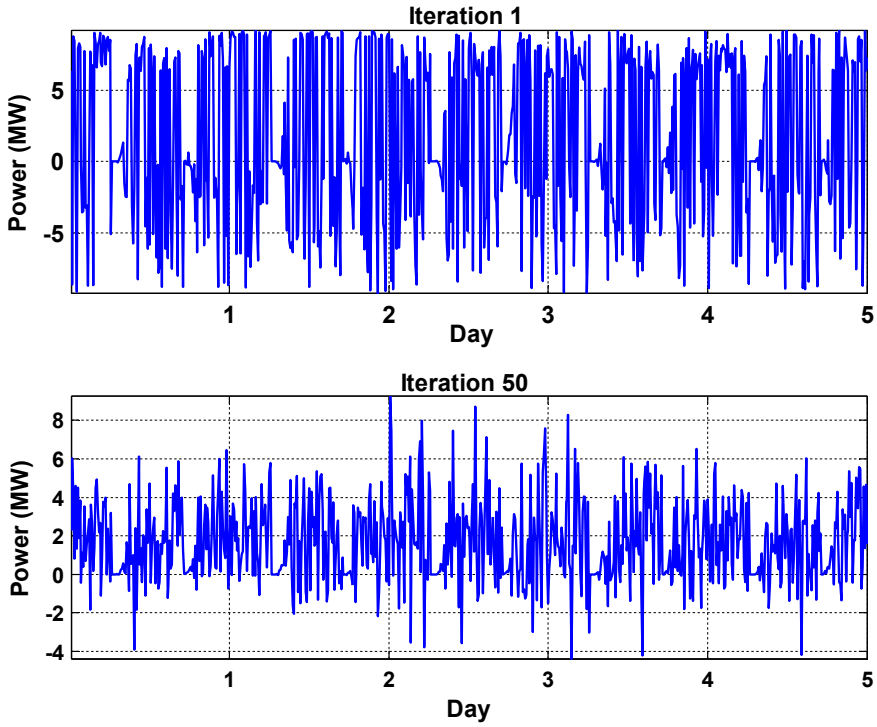

Figure 4.17: Comparison of a particle in first iteration and last iteration for 5 days window.

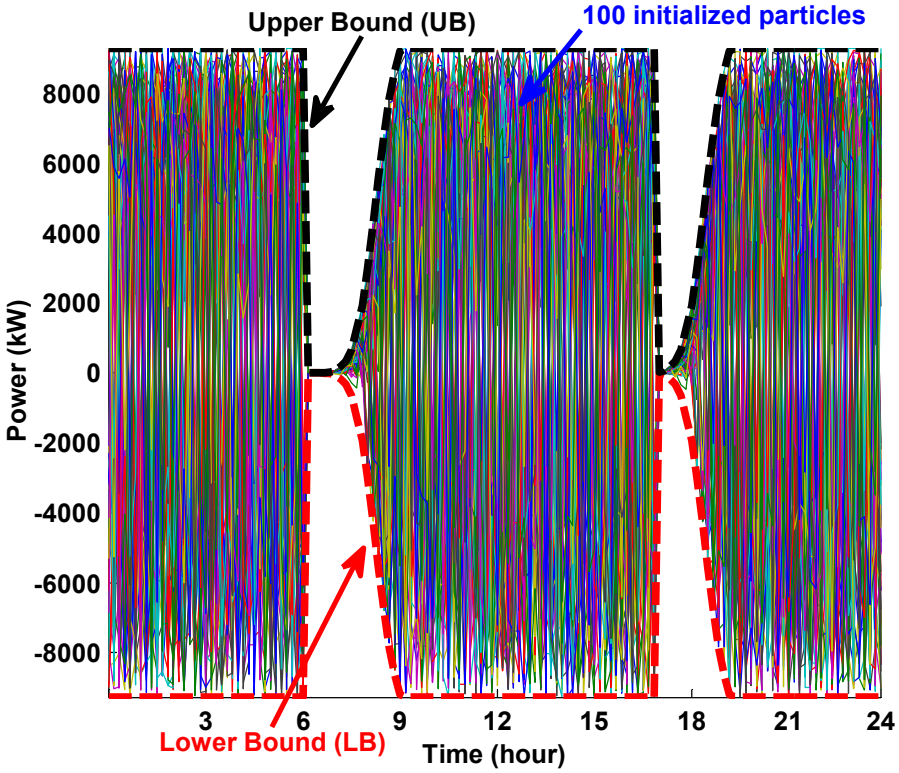

Figure 4.18: Initial random particle generated in feasible search space limited by lower and upper bound limit.

4.3.2.4 Interior-Point (Local search algorithm)

Interior points are a certain class of solvers for linear and non-linear convex optimization problem. As these types of algorithms are based on Hessian calculation and Gradient calculation,

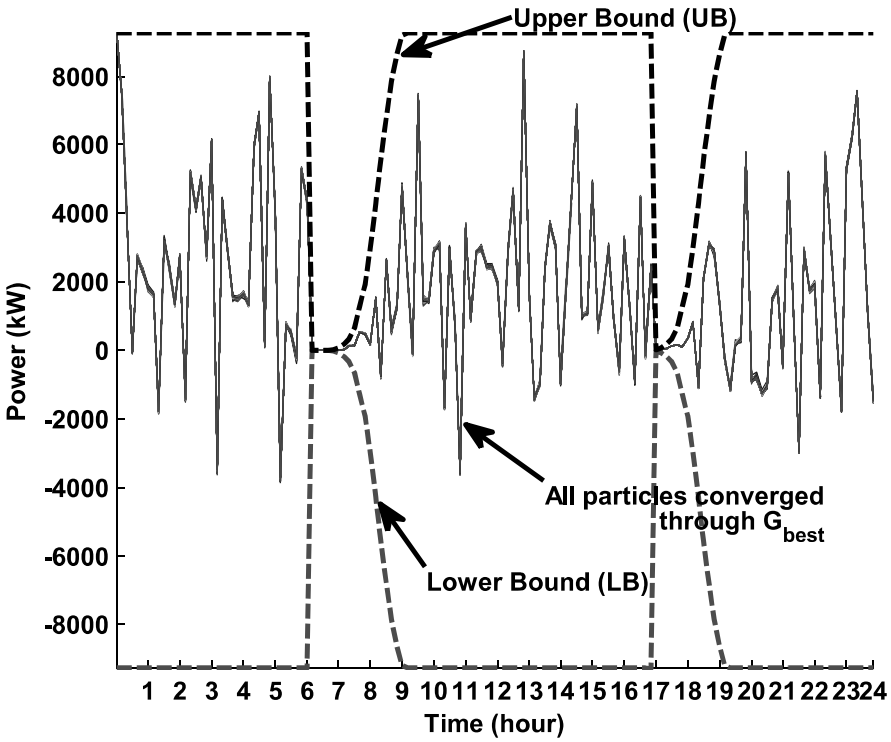

Figure 4.19: Final particles converged through global optimum region in feasible search space limited by lower and upper bound limit.

there would be the drawbacks of local trapping. It is the reason that in this thesis at first the whole search space is searched using a global stochastic algorithm (PSO), then using an Interior point algorithm the optimality of the solution is guaranteed. The flowchart of IP is illustrated in Figure 4.20.

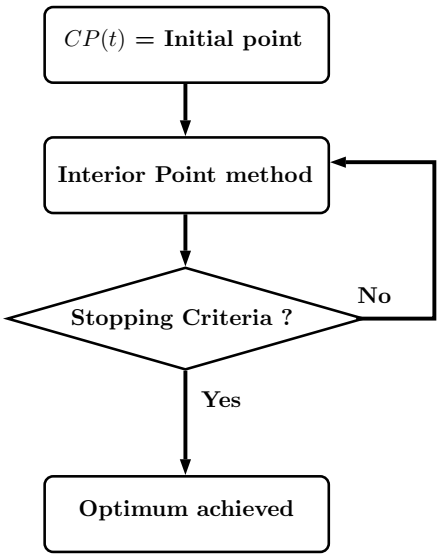

Figure 4.20: Flowchart of Interior point (IP) algorithm.

In the method used in this thesis, Hessian is calculated by a dense quasi-Newton approximation. The original problem is formulated as follow (Barrier function):

$$\min_x f(x) \tag{4.43}$$

subject to:

$$h(x) = 0 \tag{4.44}$$
$$g(x) \leqslant 0 \tag{4.45}$$

The formulation of V2G-enabled PEV charging coordination is replaced by original formulation for IP algorithm. This algorithm is calculated by fmincon function of MATLAB™ with following characteristics.

```
MaxFunEvals: 600000
    MaxIter: 4000
     TolFun: 1.0000e-16
       TolX: 1.0000e-16
ActiveConstrTol: []
  Algorithm: 'interior-point'
```

4.3.2.5 Results and discussion

The results of optimization problem with different forms are presented in this section. Three cases are compared; The CPSO algorithm, the IP algorithm and hybrid CPSO-IP. The main advantages and drawbacks are discussed in term of final function evaluation (optimum), and calculation time. In Figure 4.21, the function evaluations for 3 example days of the year are presented. These plots shows the function evaluation of IP algorithm. In the first example illustrated in Figure 4.21a for IP algorithm with normal charging profile $CP(t)$ as initial point and with the output of CPSO algorithm as initial point, the differences can be interpreted in term of calculation time and final function evaluation. The case with CPSO output as initial particle the convergence is happened with 52 iteration while for the first case it goes until iteration 104. The function evaluation at final step is also slightly better than the case of normal charging as initial point. It shows that using only IP with any arbitrary initial point takes longer time for convergence and it can be trapped in a local optimum. Second case for day 39 in February, shows the same approach. In Figure 4.21b, the convergence takes 98 iteration while with CPSO output as initial parameter it is divided approximately by 2. A better optimal compared to arbitrary initial point is also evident. In third example, the final function evaluation for both cases are the same but the calculation time or convergence speed is much more better with CPSO output compared to arbitrary initial point.

The output of each optimization algorithm are presented in Figures 4.22, 4.23 and 4.24. The first two cases are related to winter period and the third one is the case of summer. Normal charging case in red shows the charging scenario without optimization. It has been considered as reference to compare with other cases. In Figure 4.22, If only the IP algorithm is applied, the proposed power solution consists of coordination of PEVs charging. While using CPSO shows a period of V2G between 12:00 to 14:00. The solution of CPSO-IP is enhanced slightly compared to CPSO only. In Figure 4.23, the three case are approximately proposing the same profile with the advantage of less fluctuation for IP algorithm. In Figure 4.24, using only IP produces a peak power during 9:00 to 10:00 while the CPSO and CPSO-IP smooth the power during PEVs charging period.

4.3.3 Real-time and Predictive Real-time supervisions (On-line optimization)

In this section, real-time supervision algorithm based on Fuzzy logic controller is explained. This supervision system is applied on the same problematic previously explained for predictive

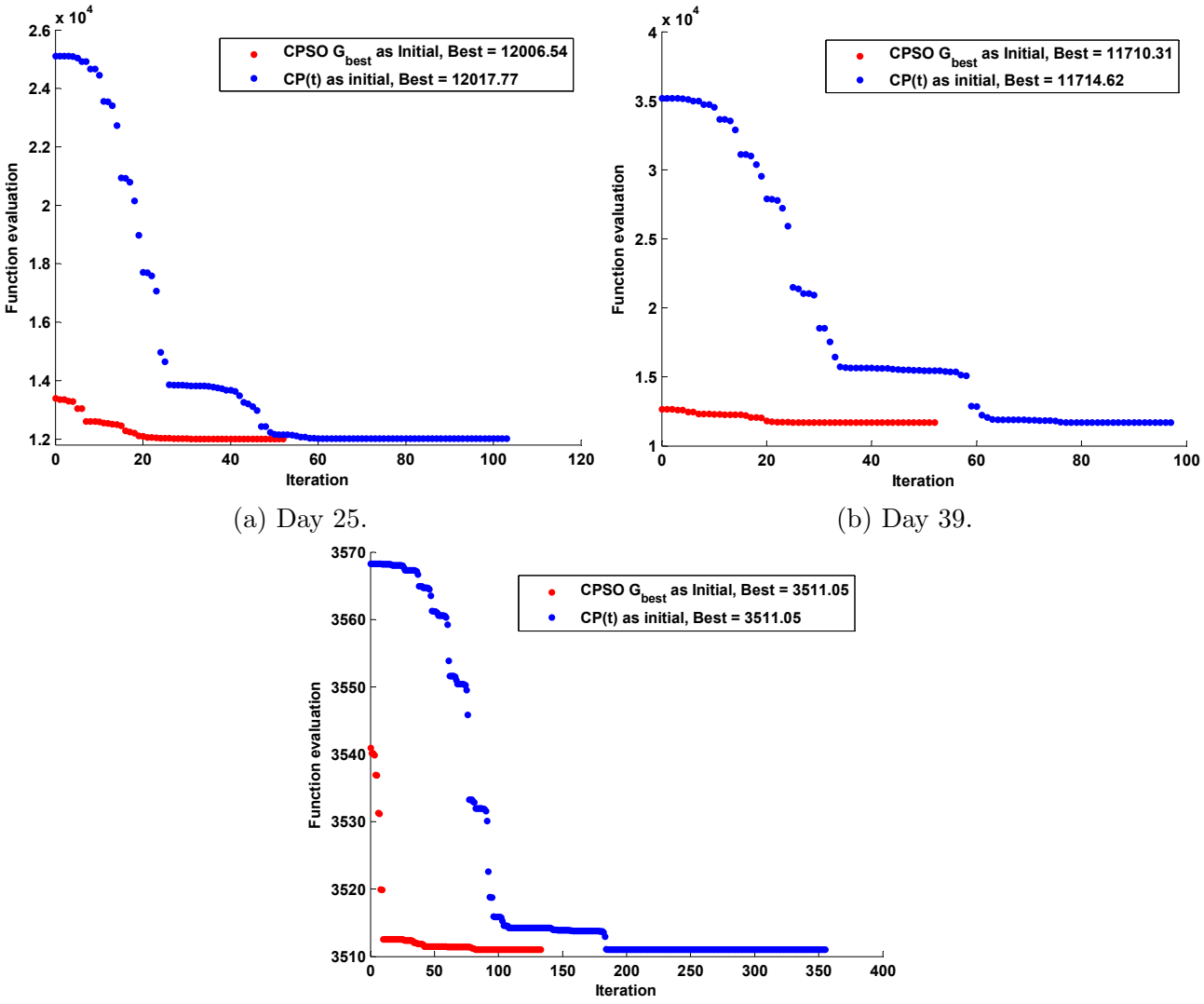

(a) Day 25.

(b) Day 39.

(c) Day 200.

Figure 4.21: Comparison of function evaluation for Interior-Point with different initial point, $CP(t)$ and CPSO G_{best} as Initial.

supervision. This part is the third part of predictive real-time supervision designing presented in Figure 4.1. In Figure 4.25, a real-time supervision system without predictive input is presented. the main focus of this chapter is on the comparison of a real-time supervision with a predictive real-time supervision in order to present the advantages of predictive input for real-time system.

4.3.3.1 Fuzzy logic and its methodological approach

Fuzzy logic an extension of Boolean logic introduced by Lotfi Zadeh in 1965 is based on the theory of fuzzy sets that is a generalization of the classical set theory.

The notion of degree for a condition verification leads to consider a condition in a state other than true or false. In fact, the degree of being true or being false could be other than absolute 1 or 0. Fuzzy logic provides a very valuable flexibility for reasoning, which makes it possible to take into account inaccuracies and uncertainties. The rules in fuzzy logic are classified in natural human language.

Based on the years of research in electrical grid team of L2EP laboratory, an 8 steps of methodological designing procedure for real-time energy management applications are con-

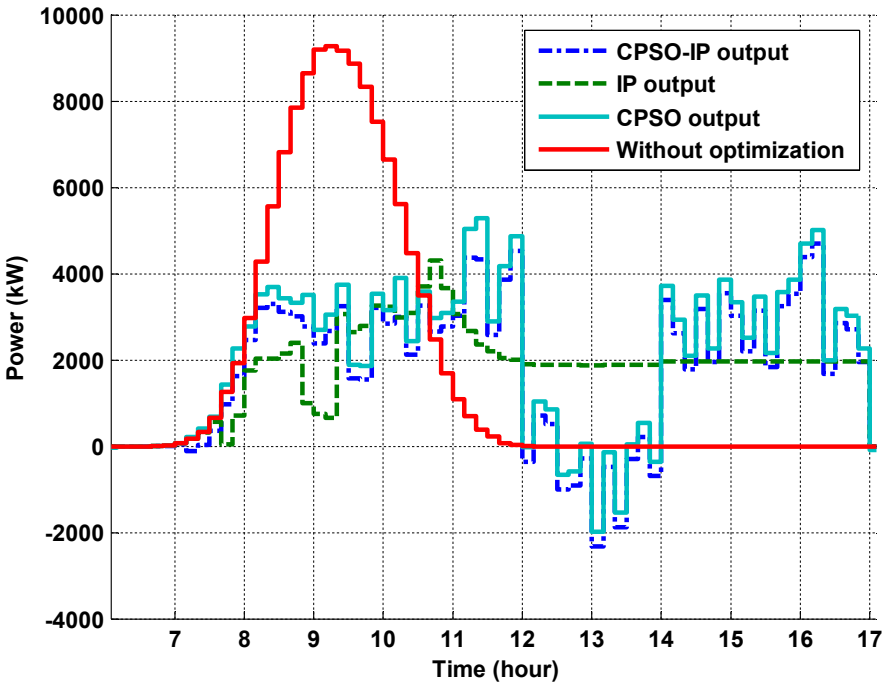

Figure 4.22: Comparison of output power $P_{EVref}(t)$ for office charging scenario for different optimization algorithm , Day 25, January (Winter).

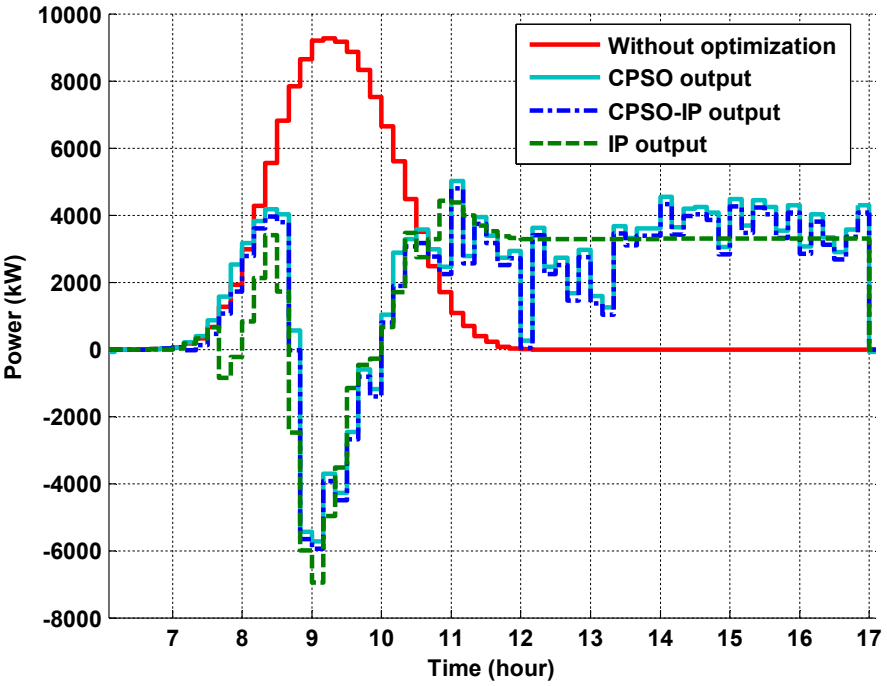

Figure 4.23: Comparison of output power $P_{EVref}(t)$ for office charging scenario for different optimization algorithm , Day 39, February (Winter).

ducted [Robyns 15b, Robyns 13, Courtecuisse 08, Davigny 08]. This methodology is based on the general knowledge of the system and defining the advancement steps for designing procedure of supervision or energy management system. The application of this methodology has been tested and validated for different case studies. For embedded electrical systems this methodology has been validated in [Breban 13]. For hybrid renewable energy systems the methodology test with good performance in [Courtecuisse 10]. This methodology is used also in case of elec-

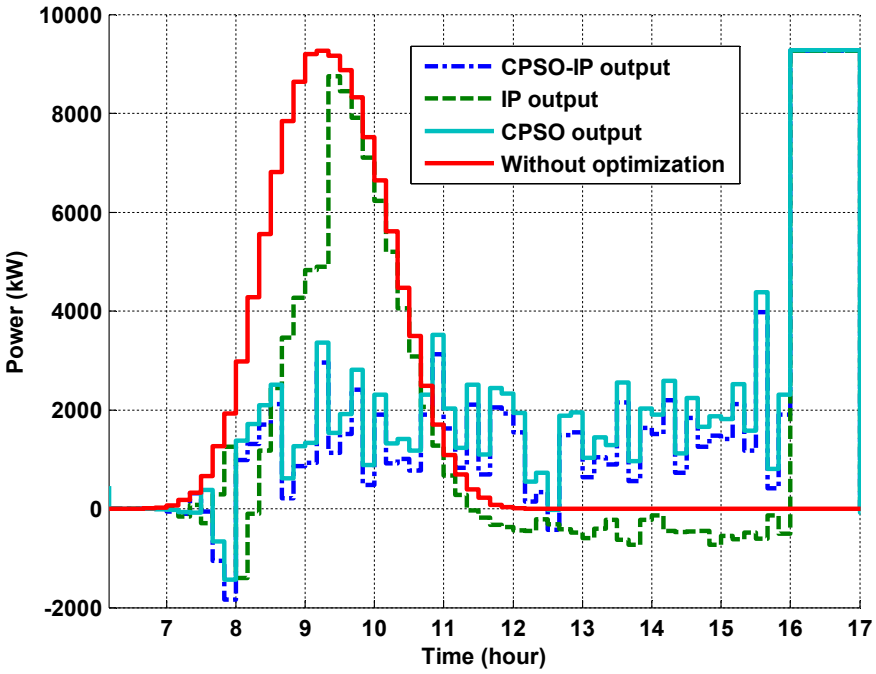

Figure 4.24: Comparison of output power $P_{EVref}(t)$ for office charging scenario for different optimization algorithm , Day 200, July, Summer.

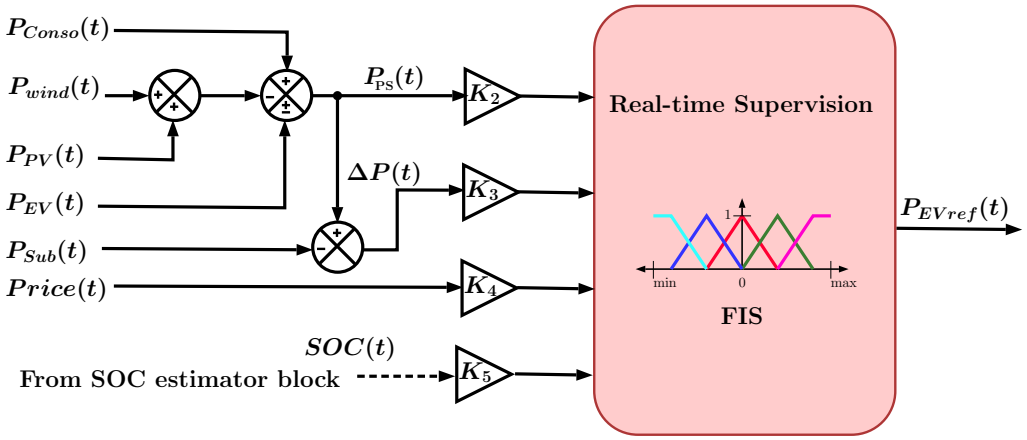

Figure 4.25: A real-time supervision system proposed for ETCM service without predictive input.

tric vehicle charging coordination for the same services of energy transmission cost minimization [Bouallaga 15].

The 8 steps of this methodology is presented in Figure 4.26. The first steps asks for general knowledge of under study systems before starting to designing the supervision. This step has been emphasized by the developers of the methodology as the main and non negligible steps of supervision designing. Work specification contains the main objectives of the supervision system, their constraints and the means of actions or control inputs of the supervision systems. These parameters should be presented in a table format in order to facilitate the understanding of system. The second step which is the main part, is the level of designing the supervision system. In this step all the inputs, outputs and their relationship should be defined. This step should provide the main structure of the supervision system. It contains the feed-backs for closed loop system, filters, gains, extra block of control and main fuzzy logic controller (FLC). Concerning the number of inputs, it is important to take into account the objectives, since for each objective at least one input should be defined [Robyns 15a].

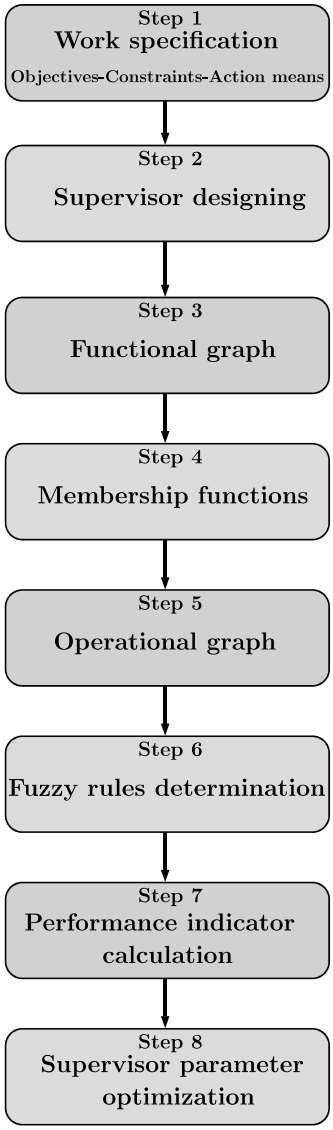

Figure 4.26: Methodology for fuzzy logic supervisor design [Robyns 15a].

4.3.3.2 Problem specification

As discussed previously, ETCM service is considered as the main service for this part. The specification of this problem are mainly discussed in the previous section. The main difference between predictive supervision specification and real-time supervision specification is the inputs. Since, in predictive system the inputs are estimative while in the real-time systems the inputs are measurable and can be communicate to the central supervision system. This study is done for the case study of years 2020 and 2030 over a particular HV/MV substation. The problem details containing the schematic of the grid are presented in section 4.3.2.1. The work specification for this real-time supervision system are presented in Table 4.2. In this table, the first step of Fuzzy logic methodology presented previously is applied for ETCM service for V2G-enabled PEVs. The two main objectives are considered as ETC minimization and environmental efficiency and CO_2 emission reduction. The main difference between this problematic and predictive supervision presented in Table 4.1, is that the subscribed power here is considered as a constraint, while in predictive case the subscribed power is considered as a variable of optimization and a sub-objective. The availability of RES is also a constraint while in predictive supervision, RES is *a priori* available knowledge of the system.

Table 4.2: Specification of real-time supervision system for ETCM service for V2G-enabled PEV fleet.

Objective	Sub-objective	Associated inputs	Constraints	Means of actions	Indicators
Energy Tranmission Cost Minimization	Subscribed power exceeding limitation	ΔP	Subscribed power (technical constraint)	Charging, Discharging and No charging of PEVs	Transmission cost in euro
	Maximize energy consumption during low cost	$Price$	Consumption variation		
Environmental and lower CO_2 efficiency	Maximize renewable energy consumption	P_{PS}	RES availability		Auto-consumption of RES (%)
	Maximize PEV owner satisfaction	SOC	PEV energy need (full-battery at departure)		Battery charging rate
			Battery degradation		CO_2 emission rate

4.3.3.3 Designing of the supervision using fuzzy logic

The first step of introduced methodology for our case study is developed in previous section. The second step is to design the supervision system knowing all the measurable inputs and requested output of real-time supervision system. Defining the inputs is an important task of supervision system. Normally for each objective at least one input should be associated [Robyns 15b]. For the ETCM service as mentioned in Table 4.2, 4 inputs are necessary in order to cover the requirement of the supervision system. In order to check the exceeding of subscribed power ΔP is introduced which is equal to $\Delta P = P_{PS}(t) - P_{sub}(t)$. A price signal is chosen as input in order to check the electricity price for V2G action. P_{PS} is considered as power consumption at HV/MV substation level. Finally SOC is considered in order to supervise the state of charge of PEVs' batteries in order to respect the PEVs' energetic constraints. A general view of designed supervision system is illustrated in Figure 4.25. On the other hand, the predictive real-time supervision system provides an estimated input to the real-time supervision which is based on forecasting and off-line optimization layer. This input enhances the optimality of real-time reference power (P_{EV-ref}). Based on the methodology, the next step of the supervision system designing is concentrated on functional graph for both Predictive real-time and Real-time supervisions.

4.3.3.3.1 Functional graph

Functional graph is a way to represent the different functional mode of supervision system in graphic form. This way of representation was presented for the first time in [Courtecuisse 08]. Using the functional graph, some advantages will be provided to the designer for defining the rules of fuzzy logic control system [Robyns 15b]. The principle theory is presented in [Robyns 15b], while the advantages of using functional graph are summarized thereafter:

- A linguistic expression of objectives and sub-objective, the constraints and the means of actions, will provide:
  - to establish directly the fuzzy rules to each mode of function.
  - to facilitate exchange with others in different disciplines such as economy.
- A better transition between determined modes based on certain state of the system.
- In case of using boolean logic with fuzzy logic, it provides to find the classical approaches such as Petri nets or Grafcet [David 92].

In this section, different functional mode of both Real-time and Predictive real-time supervision are explained along with their functional graph for each mode. The principle functional graph for both supervisions are presented in Figure 4.27. Different functional mode are presented by L as Level. The first Level is L1 is for ensuring the energy need of PEVs.

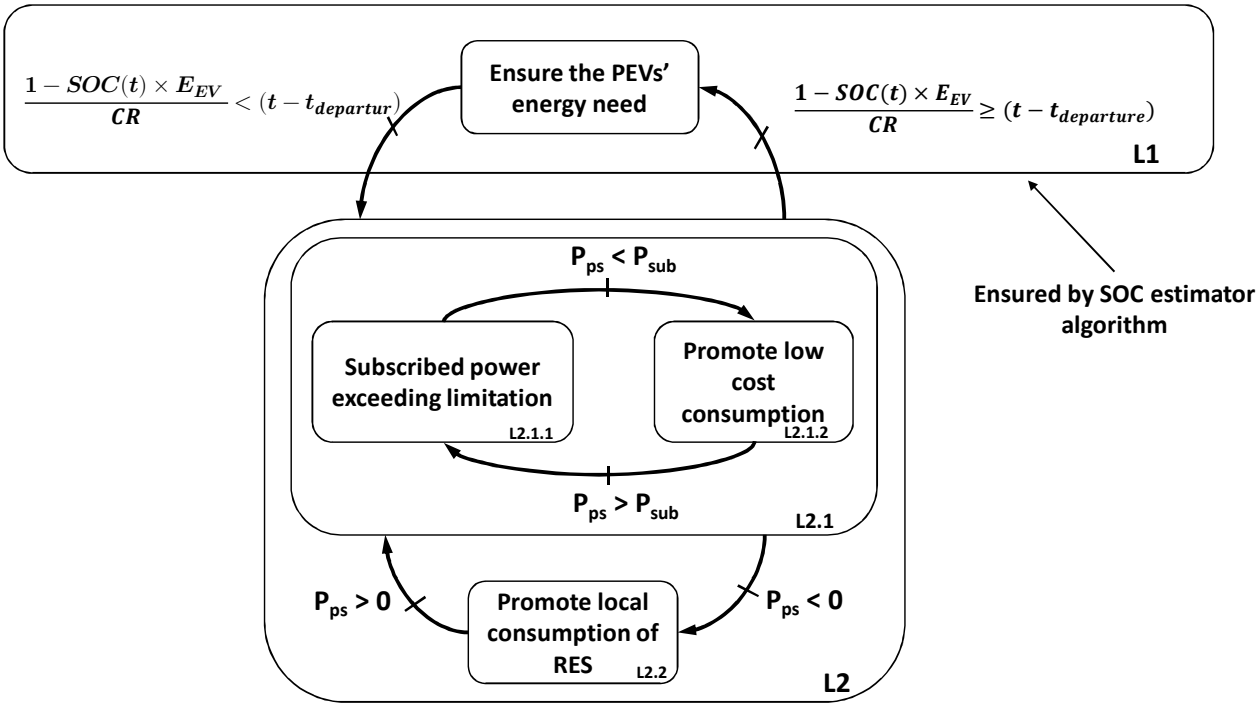

Figure 4.27: Overall Functional graph for both real-time and Predictive real-time supervisions.

If this step is passed the supervision system can be activated for other level of supervision. In L2, the supervision system will be activated. The condition of each level are represented in form of arrow for activation of each mode of function. The sub-functional graph which are the sub-levels of different modes are represeneted in Figure 4.28 for real-time supervision and in Figures 4.29, 4.30 and 4.31 for Predictive real-time. The sub-functional graph for L2.1.2.3 is similar to the L2.1.1 with the input condition of Price is Very High.

The main difference between Predictive Real-time supervision system and Real-time supervision system is that, the final actions for charging/discharging level is controlled by SOC at real-time supervision, while at Predictive one, the estimated reference power, $\hat{P}_{EV-ref}(t)$, will define the membership of reference power, $P_{EV-ref}(t)$. This provides optimality of final proposed reference power, as it has been already controlled based on *a priori* knowledge of the system (i.e. Knowledge coming from predictive inputs). Using Functional graph the representation of the supervision systems are easily understandable and can help the process of rules definition; In next section the membership functions will be introduced for each inputs.

4.3.3.3.2 Membership functions

The membership functions are the functions which are defining the degree of membership to a fuzzy value. For this supervision system the number of membership functions have been chosen based on the characteristics and constraints of each inputs. For each input different number of membership functions are considered. Figure 4.32, shows all membership functions of 4 inputs and one output of Real-time supervision system. For the SOC as first input, 3 membership functions of type trapezoidal are considered. The parameters for each membership

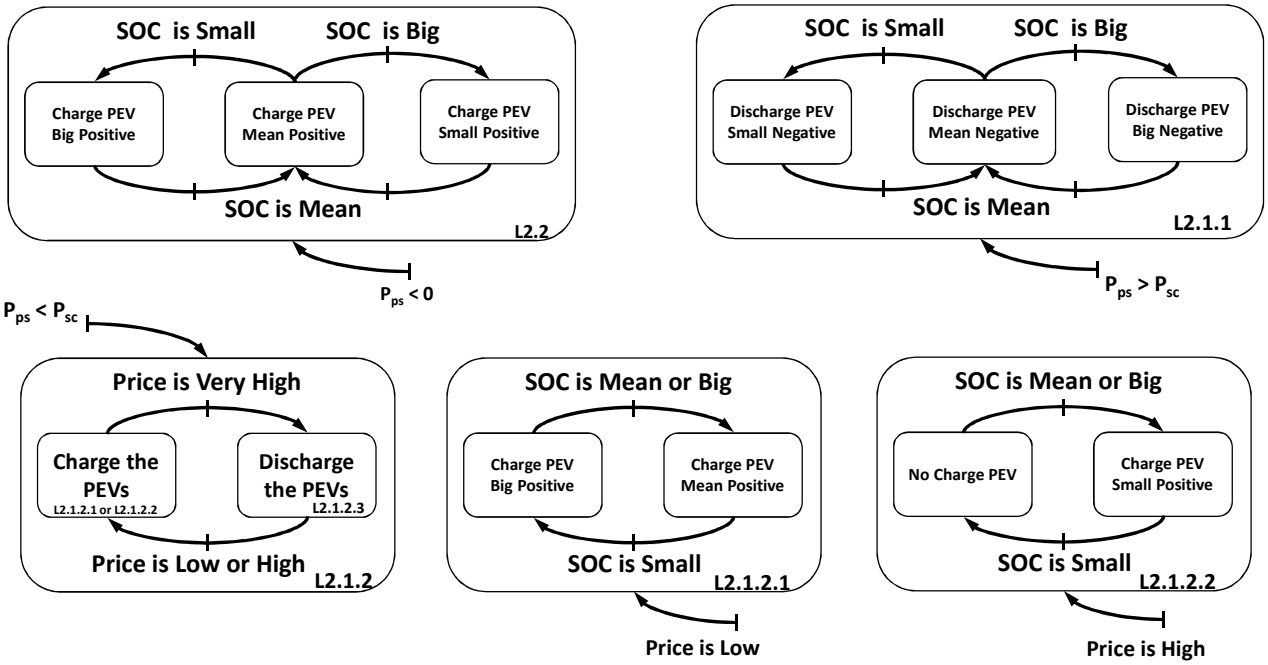

Figure 4.28: Sub-functional graphs for real-time supervision.

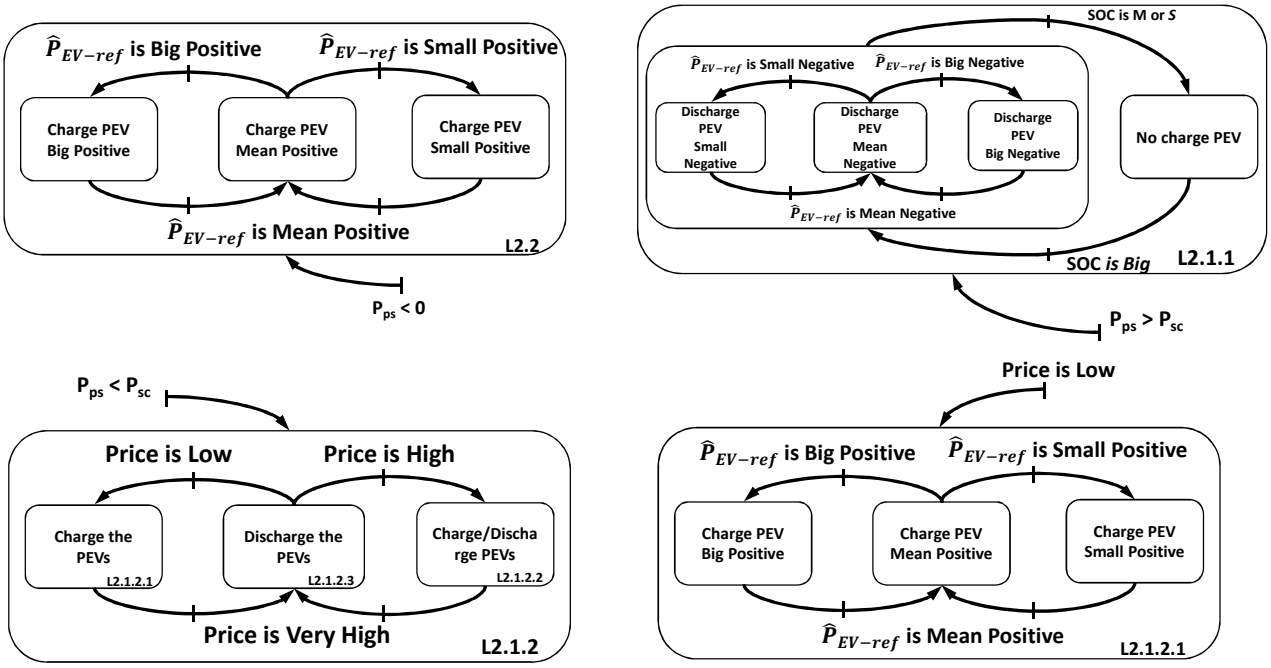

Figure 4.29: Sub-functional graphs for Predictive real-time supervision (Group 1).

function are chosen empirically based on the knowledge on the system. For instance for SOC, three membership functions of **S**mall, **M**ean and **B**ig are considered. For Small it fixes on 20% in order to avoid discharging of PEVs less than 20% of SOC. For P_{PS}, 2 functions for distinguishing of **P**ositive and **N**egative are considered. This is the same case for ΔP. The price signal has been considered in three levels of **L**ow, **H**igh and **V**ery **H**igh Price. The input price signal is normalized in order to be considered at these ranges. Finally, for output P_{EV-ref}, 7 levels are considered in order to make it powerful for control purpose. These levels are **B**ig **N**egative, **M**ean **N**egative, **S**mall **N**egative, **Z**ero, **S**mall **P**ositive, **M**ean **P**ositive and **B**ig **P**ositive. In Figure 4.33, the membership functions of 5 inputs and 1 output of Predictive

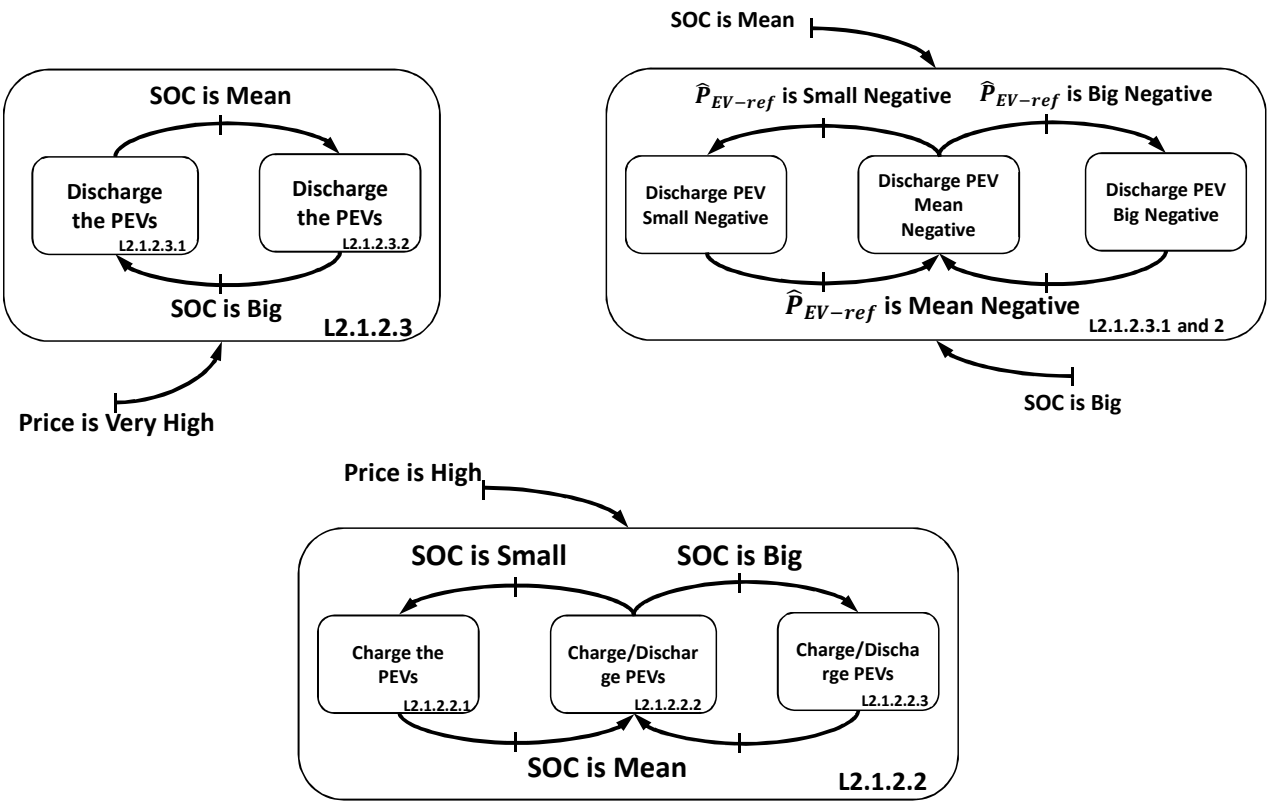

Figure 4.30: Sub-functional graphs for Predictive real-time supervision (Group 2).

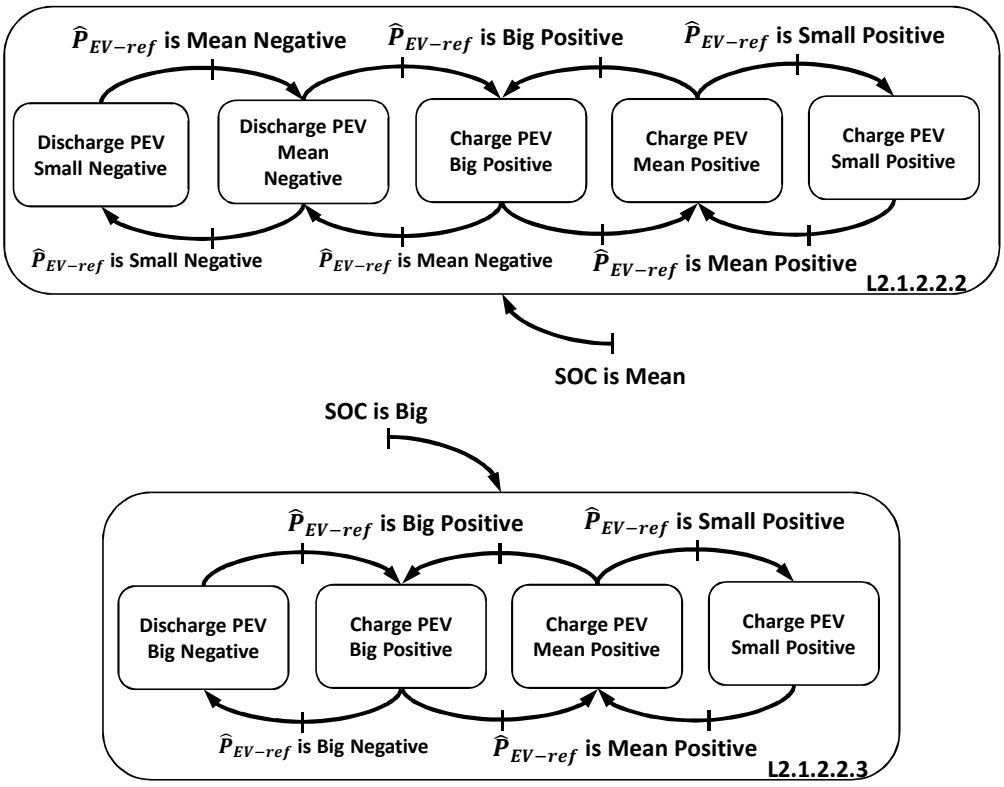

Figure 4.31: Sub-functional graphs for Predictive real-time supervision (Group 3).

real-time supervision system are preseneted. Compared to real-time supervision, it has one more input which is the estimated reference power ($\hat{P}_{EV-ref}$). This input has the same number

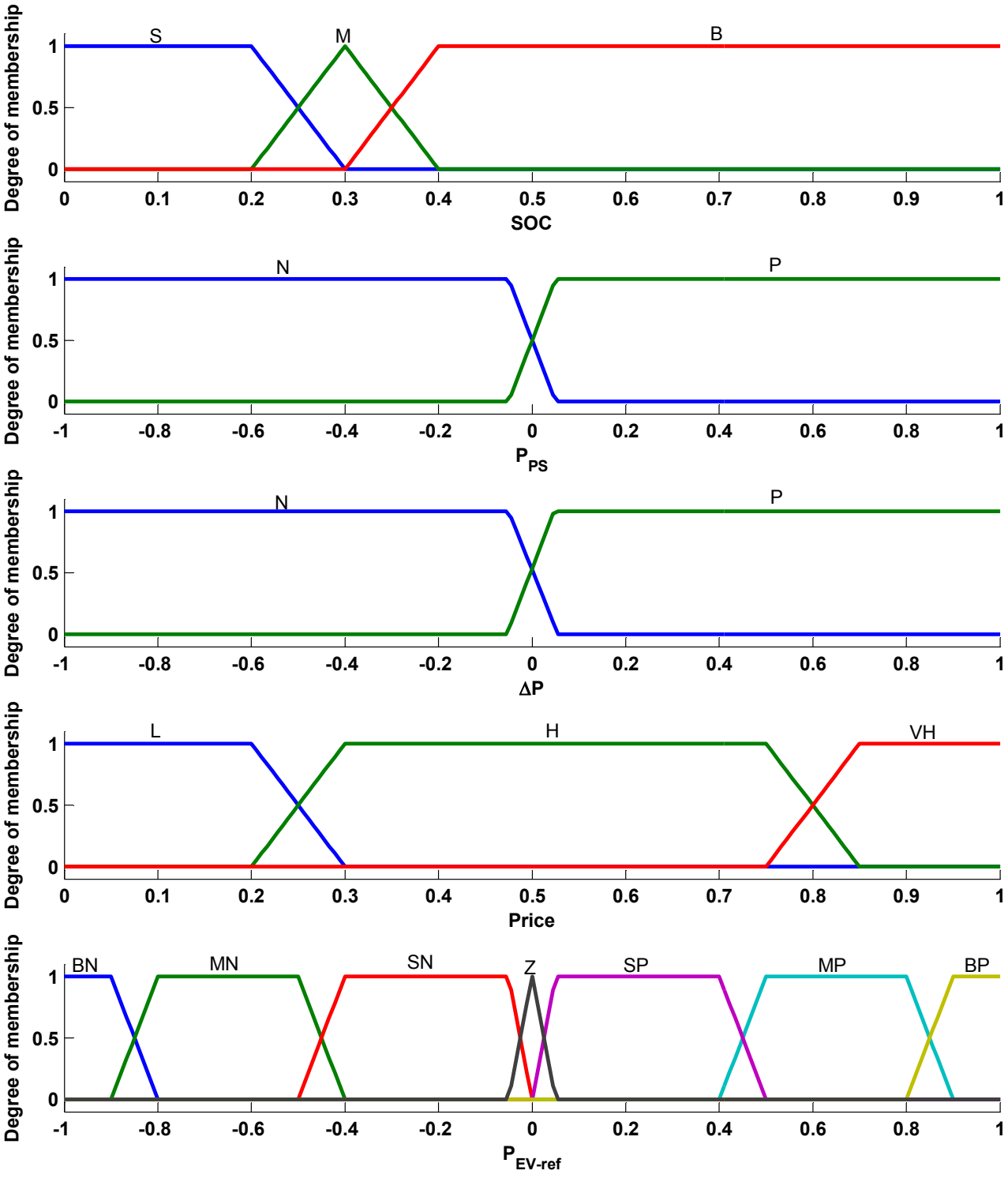

Figure 4.32: Membership functions for 4 inputs and 1 output of Real-time supervision system.

of membership functions as output power explained for real-time supervision system. As explained previously, the choice of membership function parameters are done empirically while the final result are not necessarily optimized based on these choices. Hence an optimization process is done in next sections in order to guarantee the optimality of the choices. In order to be able to write the rules the transformation of functional graph to operational graph are necessary. This transformation is explained in next section which is called operational graph.

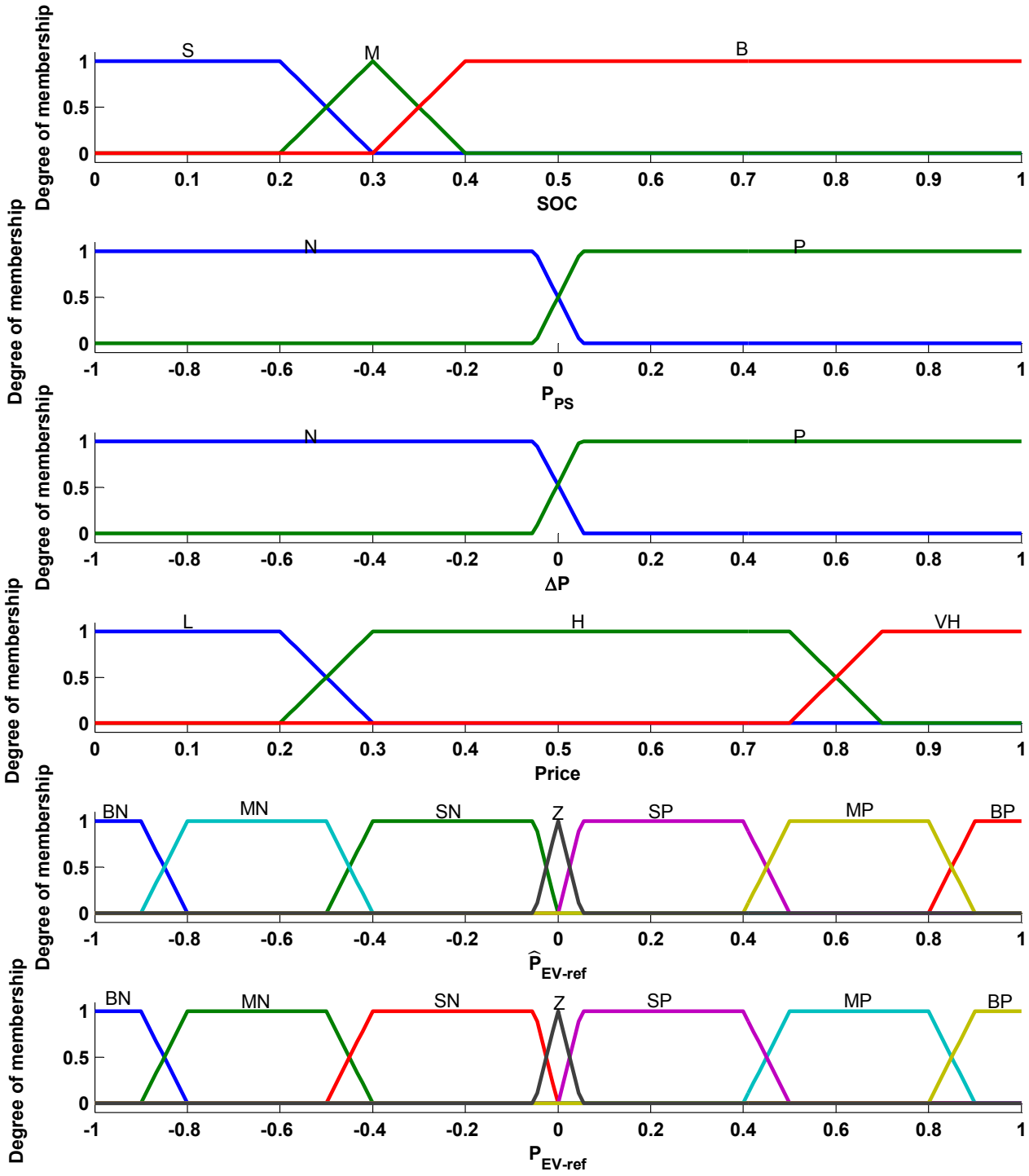

Figure 4.33: Membership functions for 5 inputs and 1 output of Predictive real-time supervision system.

4.3.3.3.3 Operational graph

Operational graphs are the translation of functional graphs using the membership functions which are defined previously. The operational graph is composed of different states presented in rounded rectangles and transitions, represented in form of bent arrows. A general operational graph of Real-time supervision system using the membership functions defined in previous steps are presented in Figure 4.34. For Predictive real-time supervision the same graph is valid. The

only difference would be the activation condition for Predictive real-time which is the $\hat{P}_{EV-ref}$ instead of SOC in Real-time supervision.

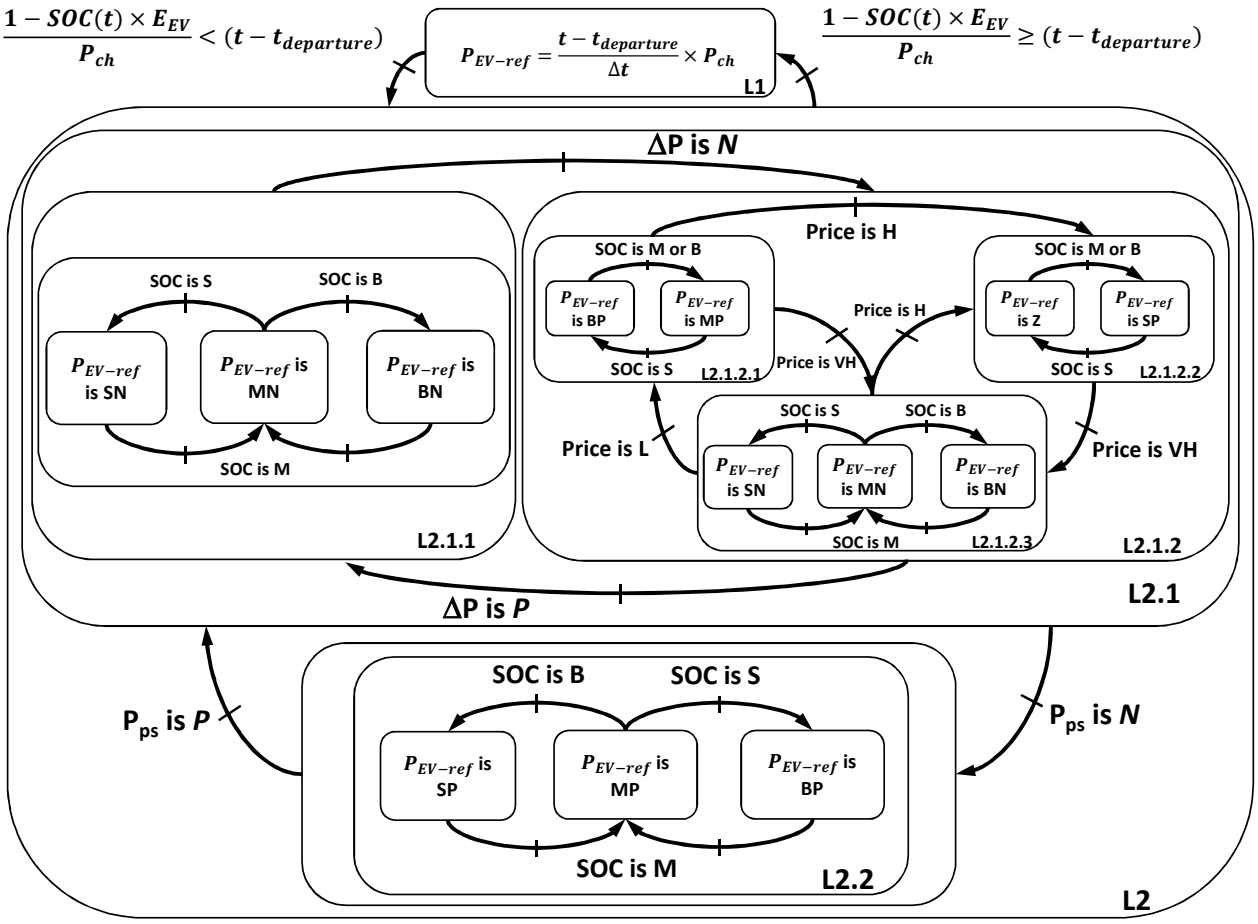

Figure 4.34: Overall Operational graph for real-time supervision.

The advantage of using functional and operational graph will be explained in next section which is minimizing the number of associated rules to the all inputs and membership functions.

4.3.3.3.4 Rules definition

The advantages of using Functional graph is evident in this section where the rules should be defined. In fact, functional and operational graph simplify the steps of rules definition. For a particular case of fuzzy system with n inputs and m membership functions for every input, a total possible number of n^m rules should be associated. For Real-time supervision system this number would be $(3 \times 2 \times 2 \times 3)$ equal to 36 rules. For Predictive real-time it would be $(3 \times 2 \times 2 \times 3 \times 7)$ equal to 252 rules. While, using the tool of functional and operation graph, the number of rules for Real-time supervision system is reduced to 15 rules (Table 4.3) and for Predictive real-time supervision system is reduced to 29 rules (Table 4.4). The rules are defined using **And** operator in form of **If** ... **Then** statements. The association of output membership functions to each rule is done empirically in this study, while the choice can be also optimized using optimization techniques.

4.3.3.3.5 Indicator calculation

Table 4.3: Table of rules associated to functional graphs for real-time supervision (**15 rules**).

L1	Charge PEVs as needed based on their SOC			
L2	L2.1	L2.1.1		**If** P_{PS} is P **and** ΔP is P **and** SOC is B **then** P_{EV-ref} is BN
				If P_{PS} is P **and** ΔP is P **and** SOC is M **then** P_{EV-ref} is MN
				If P_{PS} is P **and** ΔP is P **and** SOC is S **then** P_{EV-ref} is SN
		L2.1.2	L2.1.2.1	**If** P_{PS} is P **and** ΔP is N **and** Price is L **and** SOC is S **then** P_{EV-ref} is BP
				If P_{PS} is P **and** ΔP is N **and** Price is L **and** SOC is M **then** P_{EV-ref} is MP
				If P_{PS} is P **and** ΔP is N **and** Price is L **and** SOC is B **then** P_{EV-ref} is MP
			L2.1.2.2	**If** P_{PS} is P **and** ΔP is N **and** Price is H **and** SOC is S **then** P_{EV-ref} is Z
				If P_{PS} is P **and** ΔP is N **and** Price is H **and** SOC is M **then** P_{EV-ref} is SP
				If P_{PS} is P **and** ΔP is N **and** Price is H **and** SOC is B **then** P_{EV-ref} is SP
			L2.1.2.3	**If** P_{PS} is P **and** ΔP is N **and** Price is VH **and** SOC is S **then** P_{EV-ref} is SN
				If P_{PS} is P **and** ΔP is N **and** Price is VH **and** SOC is M **then** P_{EV-ref} is MN
				If P_{PS} is P **and** ΔP is N **and** Price is VH **and** SOC is B **then** P_{EV-ref} is BN
	L2.2	**If** P_{PS} is N **and** SOC is S **then** P_{EV-ref} is BP		
		If P_{PS} is N **and** SOC is M **then** P_{EV-ref} is MP		
		If P_{PS} is N **and** SOC is B **then** P_{EV-ref} is SP		

The performance indicators are defined in Table 4.2 for ETCM service. These indicators are calculated for each type of supervision system and the results are brought in next sections. Three main indicators for these supervisions are considered.

- Annual energy transmission cost using equation 4.17.
- PEV and renewable energies coordination (in %).
- Generated CO_2.

For Annual energy transmission cost, the value is calculated for each supervision scenario. The profile is in 10 minutes sample time for one year. For calculation of PEV and renewable energy coordination, the negative part of P_{PS} profile are compared for each scenario. The difference between negative part of scenario without PEV and scenario with PEV, either supervised or non-supervized cases, are defining the percentage of coordination. This can be expressed in form of following equation.

$$Coordination(\%) = \frac{\left|\int(P_{PS}^{w/o} < 0)dt\right| - |\int(P_{PS}^{w} < 0)dt|}{\left|\int(P_{PS}^{w/o} < 0)dt\right|} \times 100\% \tag{4.46}$$

Where $P_{PS}^{w/o} < 0$, is the injected power at HV/MV substation to the transmission grid (i.e. surplus of local renewable energy production) for the scenario without PEVs. $P_{PS}^{w} < 0$ is the same power for the scenario with PEVs. The latter is calculated for each scenario with PEVs presence. The *Coordination* parameter shows the percentage of PEV-RES coordination i.e. local consumption of RES using plug-in electric vehicles.

For CO_2 emission calculation, a yearly profile of CO_2 production per kWh of electricity production is used. The data are available on RTE website (The French TSO) [RTE]. Another indicator is considered as battery degradation due to extra charging/discharging cycles of V2G operation. This degradation is modeled using linear and non-linear degradtion function of lithium-ion battery and explained thoroughly in next sections.

Table 4.4: Table of rules associated to functional graphs for Predictive real-time supervision (**29 rules**).

L1	Charge PEVs as needed based on their SOC				
L2	L2.1	L2.1.1	If P_{PS} is P and ΔP is P and SOC is B and $\hat{P}_{EV-ref}$ is SN then P_{EV-ref} is SN		
			If P_{PS} is P and ΔP is P and SOC is B and $\hat{P}_{EV-ref}$ is MN then P_{EV-ref} is MN		
			If P_{PS} is P and ΔP is P and SOC is B and $\hat{P}_{EV-ref}$ is BN then P_{EV-ref} is BN		
			If P_{PS} is P and ΔP is P and SOC is M and $\hat{P}_{EV-ref}$ is Z then P_{EV-ref} is Z		
			If P_{PS} is P and ΔP is P and SOC is S and $\hat{P}_{EV-ref}$ is Z then P_{EV-ref} is Z		
		L2.1.2	L2.1.2.1	If P_{PS} is P and ΔP is N and Price is L and $\hat{P}_{EV-ref}$ is SP then P_{EV-ref} is SP	
				If P_{PS} is P and ΔP is N and Price is L and $\hat{P}_{EV-ref}$ is MP then P_{EV-ref} is MP	
				If P_{PS} is P and ΔP is N and Price is L and $\hat{P}_{EV-ref}$ is BP then P_{EV-ref} is BP	
			L2.1.2.2	L2.1.2.2.1	If P_{PS} is P and ΔP is N and Price is H and SOC is S and $\hat{P}_{EV-ref}$ is SP then P_{EV-ref} is SP
					If P_{PS} is P and ΔP is N and Price is H and SOC is S and $\hat{P}_{EV-ref}$ is MP then P_{EV-ref} is MP
					If P_{PS} is P and ΔP is N and Price is H and SOC is S and $\hat{P}_{EV-ref}$ is BP then P_{EV-ref} is BP
				L2.1.2.2.2	If P_{PS} is P and ΔP is N and Price is H and SOC is M and $\hat{P}_{EV-ref}$ is SN then P_{EV-ref} is SN
					If P_{PS} is P and ΔP is N and Price is H and SOC is M and $\hat{P}_{EV-ref}$ is MN then P_{EV-ref} is MN
					If P_{PS} is P and ΔP is N and Price is H and SOC is M and $\hat{P}_{EV-ref}$ is SP then P_{EV-ref} is SP
					If P_{PS} is P and ΔP is N and Price is H and SOC is M and $\hat{P}_{EV-ref}$ is MP then P_{EV-ref} is MP
					If P_{PS} is P and ΔP is N and Price is H and SOC is M and $\hat{P}_{EV-ref}$ is BP then P_{EV-ref} is BP
				L2.1.2.2.3	If P_{PS} is P and ΔP is N and Price is H and SOC is B and $\hat{P}_{EV-ref}$ is BN then P_{EV-ref} is BN
					If P_{PS} is P and ΔP is N and Price is H and SOC is B and $\hat{P}_{EV-ref}$ is SP then P_{EV-ref} is SP
					If P_{PS} is P and ΔP is N and Price is H and SOC is B and $\hat{P}_{EV-ref}$ is MP then P_{EV-ref} is MP
					If P_{PS} is P and ΔP is N and Price is H and SOC is B and $\hat{P}_{EV-ref}$ is BP then P_{EV-ref} is BP
			L2.1.2.3	L2.1.2.3.1	If P_{PS} is P and ΔP is N and Price is VH and SOC is M and $\hat{P}_{EV-ref}$ is SN then P_{EV-ref} is SN
					If P_{PS} is P and ΔP is N and Price is VH and SOC is M and $\hat{P}_{EV-ref}$ is MN then P_{EV-ref} is MN
					If P_{PS} is P and ΔP is N and Price is VH and SOC is M and $\hat{P}_{EV-ref}$ is BN then P_{EV-ref} is BN
				L2.1.2.3.2	If P_{PS} is P and ΔP is N and Price is VH and SOC is B and $\hat{P}_{EV-ref}$ is SN then P_{EV-ref} is SN
					If P_{PS} is P and ΔP is N and Price is VH and SOC is B and $\hat{P}_{EV-ref}$ is MN then P_{EV-ref} is MN
					If P_{PS} is P and ΔP is N and Price is VH and SOC is B and $\hat{P}_{EV-ref}$ is BN then P_{EV-ref} is BN
	L2.2	If P_{PS} is N and $\hat{P}_{EV-ref}$ is SP then P_{EV-ref} is SP			
		If P_{PS} is N and $\hat{P}_{EV-ref}$ is MP then P_{EV-ref} is MP			
		If P_{PS} is N and $\hat{P}_{EV-ref}$ is BP then P_{EV-ref} is BP			

4.3.3.3.6 Membership function parameter optimization

The choice of membership function parameters and fuzzification gains are mainly based on the designer expertise. While, the optimality of the chosen parameters are not guaranteed. The possibility of using evolutionary optimization algorithms for membership function parameter optimization problem has been studied widely [Breban 13, Cazarez-Castro 10, Evsukoff 02]. This optimization can be applied on the choice of parameters, such as the ones illustrated in Figure 4.35, for two types of membership functions (Trapezoidal and Triangular), or for gain values presented in Figure 4.25 (e.g. K_1, K_2, K_3 and K_4) or even for output membership function association to the rules.

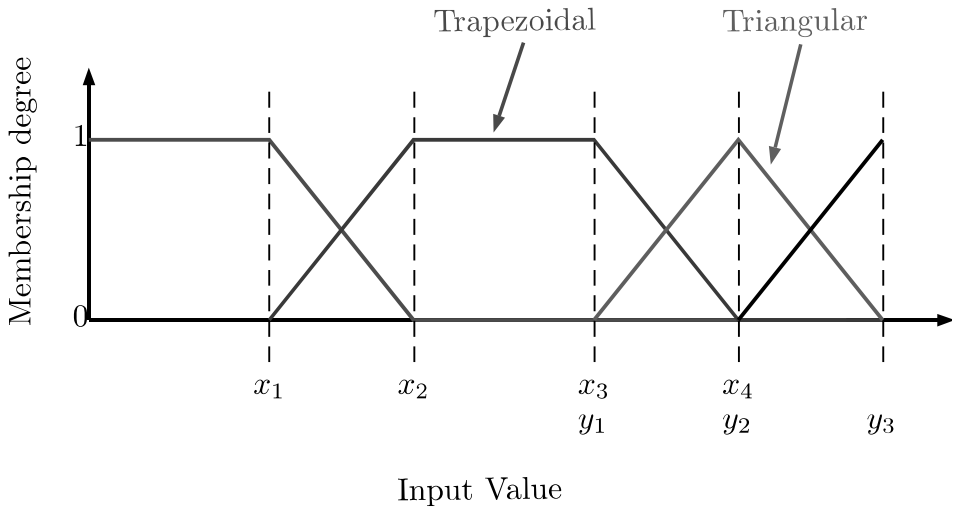

Figure 4.35: Example of two membership function with their parameters for optimization problem.

In this thesis, the optimization is concentrated on membership function parameters while the other elements are considered as perspective work. For this optimization problem, at first, the problem formulation is presented which contains the objective function, the constraints and boundaries for parameters.

The objective function is considered as ETCM function expressed in equation 4.17. The only difference is the optimization variables which are the parameters of membership functions. These parameters for Real-time supervision system are presented in Table 4.5. There are some constraints that should be respected in optimization problem. In order to avoid the overlapping of membership functions, some inequality constraints should be met. The definition of these constraints are brought in form of a first order multi-variable function (equation 4.47).

$$a_1x_1 + a_2x_2 + a_3x_3 + a_4x_4 + a_5x_5 + a_6x_6 + a_7x_7 + a_8x_8 + a_9x_9 + a_{10}x_{10} + a_{11}x_{11} + a_{12}x_{12} + a_{13}x_{13} + a_{14}x_{14} \leqslant 0 \quad (4.47)$$

Where the parameters are embedded in a 14×11 matrix.

The parameters a_1 to a_{14} are either 1 or -1 as are defined in each row of A matrix. In total, there would be 11 inequality constraints that should be considered. In order to simplify the constraints formulation, the same parameters have been considered for the membership functions with common points (e.g. forth parameter of Small membership function of SOC with second parameter of Mean membership function of SOC, which is x_1).

In second step, Genetic Algorithm (GA) is considered as optimization algorithm for this problem as it has robust performance on this problematic [Breban 13, Cazarez-Castro 10].

$$A = \begin{bmatrix} 1 & -1 & 0 & 0 & 0 & 0 & 0 & 0 & 0 & 0 & 0 & 0 & 0 & 0 \\ 0 & 0 & 1 & -1 & 0 & 0 & 0 & 0 & 0 & 0 & 0 & 0 & 0 & 0 \\ 0 & 0 & 0 & 0 & 1 & -1 & 0 & 0 & 0 & 0 & 0 & 0 & 0 & 0 \\ 0 & 0 & 0 & 0 & 0 & 1 & -1 & 0 & 0 & 0 & 0 & 0 & 0 & 0 \\ 0 & 0 & 0 & 0 & 0 & 0 & 1 & -1 & 0 & 0 & 0 & 0 & 0 & 0 \\ 0 & 0 & 0 & 0 & 0 & 0 & 0 & 1 & -1 & 0 & 0 & 0 & 0 & 0 \\ 0 & 0 & 0 & 0 & 0 & 0 & 0 & 0 & 1 & -1 & 0 & 0 & 0 & 0 \\ 0 & 0 & 0 & 0 & 0 & 0 & 0 & 0 & 0 & 1 & -1 & 0 & 0 & 0 \\ 0 & 0 & 0 & 0 & 0 & 0 & 0 & 0 & 0 & 0 & 1 & -1 & 0 & 0 \\ 0 & 0 & 0 & 0 & 0 & 0 & 0 & 0 & 0 & 0 & 0 & 1 & -1 & 0 \\ 0 & 0 & 0 & 0 & 0 & 0 & 0 & 0 & 0 & 0 & 0 & 0 & 1 & -1 \end{bmatrix}$$

Table 4.5: Parameters definition for membership function parameter optimization problem

Variable	Membership Function	Type	Parameter vector
SOC	Small	Trapezoidal	[0 0 0.2 x_1]
	Mean	Triangular	[0.2 x_1 x_2]
	Big	Trapezoidal	[x_1 x_2 1 1]
P_{PS}	Negative	Trapezoidal	[-1 -1 -0.01 0.01]
	Positive	Trapezoidal	[-0.01 0.01 1 1]
ΔP	Negative	Trapezoidal	[-1 -1 -0.01 0.01]
	Positive	Trapezoidal	[-0.01 0.01 1 1]
Price	Low	Trapezoidal	[0 0 0.1 x_3]
	High	Trapezoidal	[0.1 x_3 x_4 0.9]
	Very High	Trapezoidal	[x_4 0.9 1 1]
P_{EV-ref}	Big Negative	Trapezoidal	[-1 -1 x_5 x_6]
	Mean Negative	Trapezoidal	[x_5 x_6 x_7 x_8]
	Small Negative	Trapezoidal	[x_7 x_8 x_9 0]
	Zero	Trapezoidal	[x_{11} x_{12} x_{13} x_{14}]
	Small Positive	Trapezoidal	[0 x_{10} x_{11} x_{12}]
	Mean Positive	Trapezoidal	[x_{13} x_{14} 1 1]
	Big Positive	Triangular	[x_9 0 x_{10}]

- **Genetic Algorithm (GA)**
  Genetic algorithm, invented by John Holland in the 1970s from theory of Darwin. A living organism consists of cells which are composed of identical chromosomes. Chromosomes are strings of DNA and serves as a model for the whole organism. A chromosome consist of genes that are blocks of DNA and encodes a specific protein. Recombination (or crossover) is the first stage of reproduction. Genes from parents generate the whole new chromosome (offspring) that can be mutated. During mutation, one or more elements, also known are individuals of the DNA strand or chromosome is changed. This changes are mainly caused by errors in copying genes from parents. The success of the organism in its life measures its fitness. In computer science, Genetic Algorithms are a way of solving problems by mimicking nature. They use the same combination of selection, recombination and mutation to evolve a set of candidates for resolving a given problem. Each of the genetic operators (selection, cross-over and mutation) relies on a parameter [Nicolas 15, Patrick 13].

  – **Selection rate** is the random threshold value to reduce the current population of chromosomes according to their fitness

  – **Crossover rate** is used to compute the index beyond with the elements or bits of

two parents' chromosomes are exchange.

– **Mutation Rate** is used to compute the index of the element(s) or bit(s) in a chromosome that is/are mutated (or flipped).

The function evaluation for 25 generations of GA algorithm with population size of 20 are presented in Figure 4.36. The fitness function of the objective function value is presented in per unit. The empirical parameter leads to objective function value of 1.0065. It has been shown that already from the first generation, the algorithm has been successful to optimize the objective function. After generation 25 no progress was found. This optimization has been done with the same procedure on predictive real-time supervision. The optimized parameters of membership functions are plotted in Figures 4.37 and 4.38. As it is shown, in most cases, the optimized parameters are obtained in a way to have the most fuzziness interval. This procedure shows also that the empirical parameters in some cases are well-chosen. For instance, for SOC input, the Small membership function is remained unchanged while Mean and Big membership functions are modified. In term of calculation time, as the whole procedure of supervision is considered for 1 year (yearly ETCM function), the calculation time is quite long. For instance, in this thesis a Core i7 CPU at 2.4 GHz, 8 Gb of RAM is used and each iteration of calculation took approximately 3 minutes. It would be consider that each generation of GA algorithm with 20 population size, takes approximately 1 hours. In order to reduce the calculation time, it is possible to reduce the number of parameters by defining the symmetrical membership function. This is consider as one of the possible perspective scheme of the work.

The comparison of supervision systems with optimized membership function parameters and empirical parameters are discussed in next section along with other supervision scenarios.

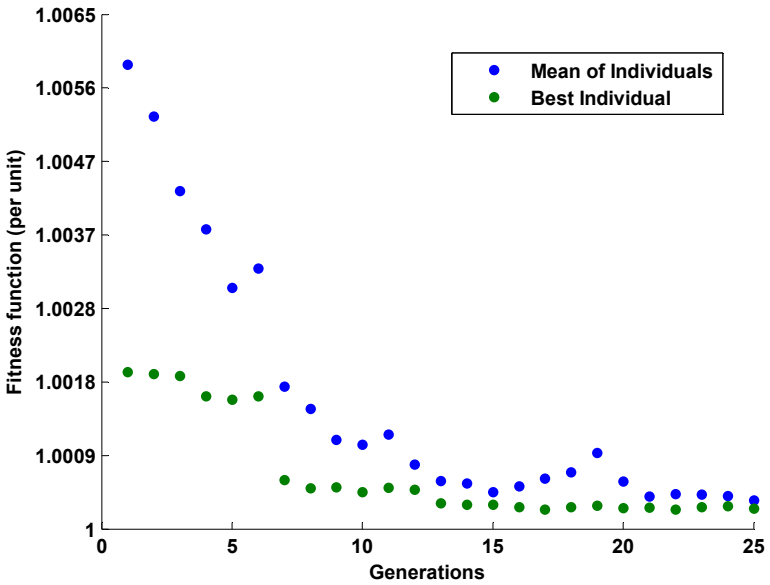

Figure 4.36: Genetic Algorithm function evaluation for membership function optimization problem.

4.3.3.4 Results and discussion

In this section, the results of different supervision scenarios are compared. The comparison purpose is focused on two principles: The methodological comparison and the technological comparison. In methodological comparison the interest of using predictive input for real-time supervision is analyzed. This comparison is done by evaluation of performance indicators of Predictive real-time supervision and Real-time supervision system. In technological comparison

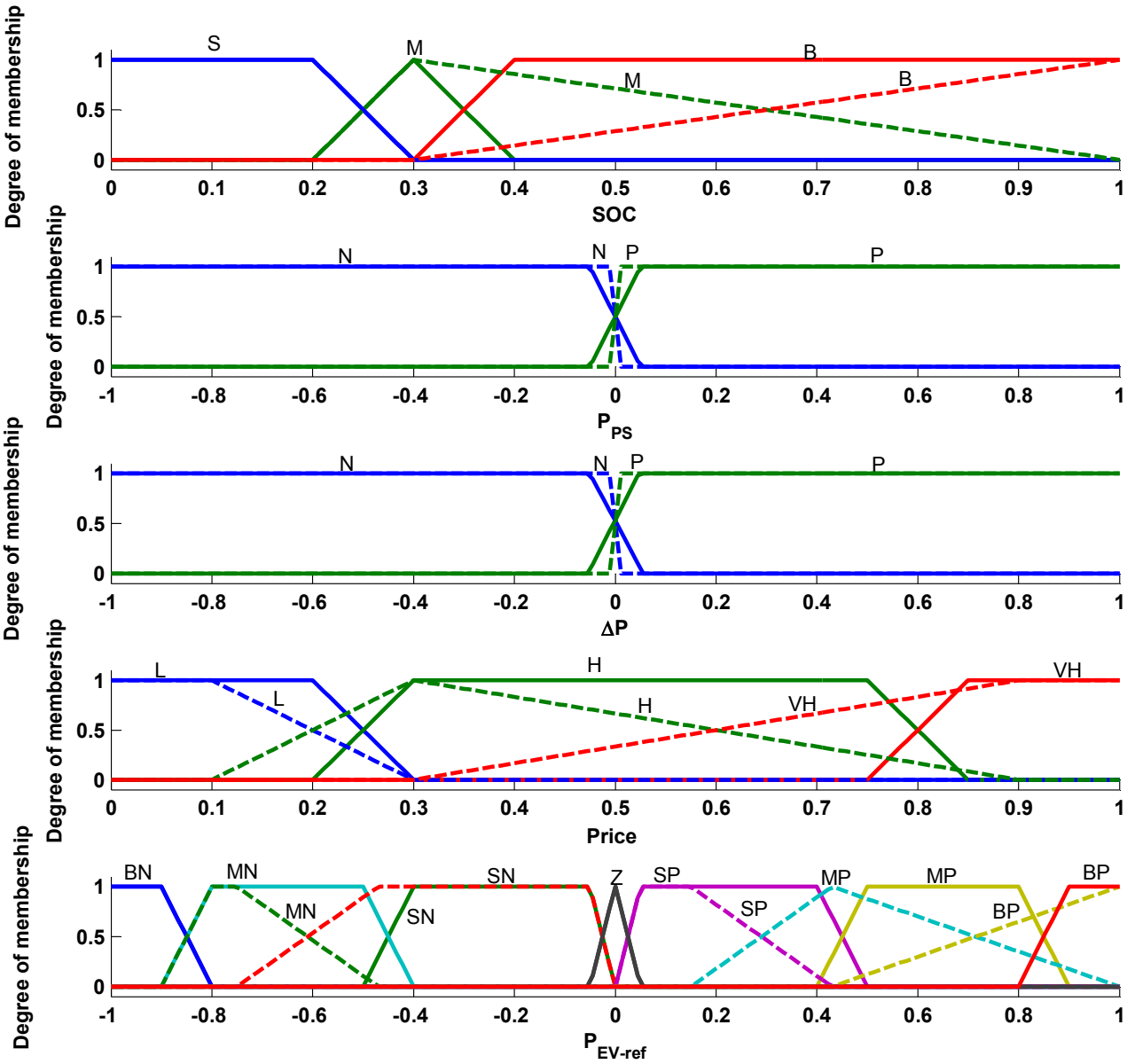

Figure 4.37: Membership functions of Real-time supervision with optimized parameters.

the benefit of using V2G is analyzed using the performance indicator of G2V supervision done in another PhD thesis in L2EP laboratory [Bouallaga 15]. In continue, different scenarios are introduced, then the comparison will be discussed precisely.

Following abbreviations are chosen for different scenarios:

- **W/O-PEV**: Without PEV scenario
- **W-PEV**: With PEV scenario
- **W-PEV-Optim**: With PEV and Off-line optimization (Predictive) scenario
- **W-PEV-RT-Empiric**: With PEV and Empirical Real-Time supervision scenario
- **W-PEV-RT-Optim**: With PEV and Optimized Real-Time supervision scenario (Optimized membership functions)
- **W-PEV-PRT-Empiric**: With PEV and Predictive Real-Time supervision with Empiric membership functions scenario

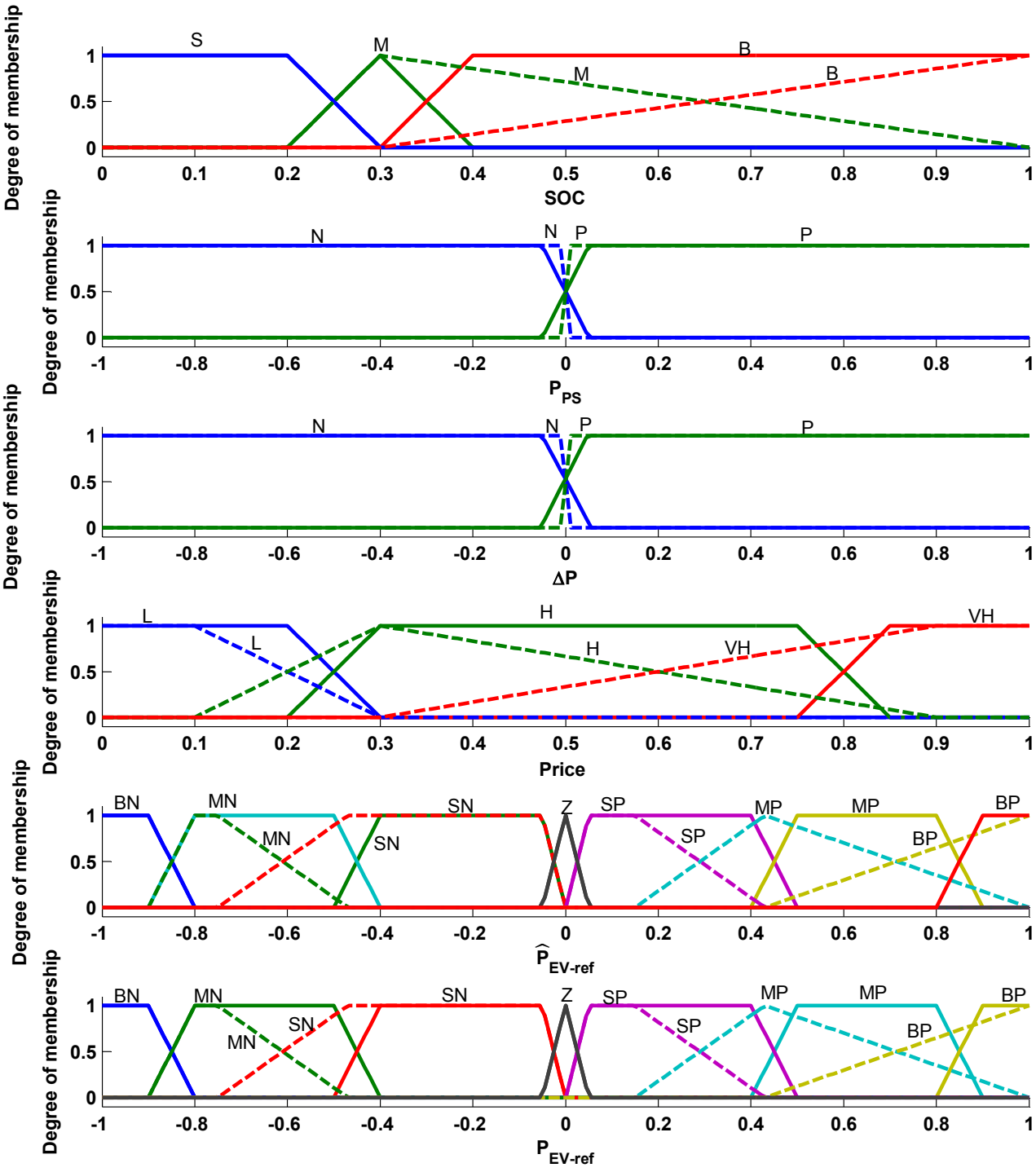

Figure 4.38: Membership functions of Predictive real-time supervision with optimized parameters.

- **W-PEV-PRT-Optim**: With PEV and Predictive Real-Time supervision with Optimized membership functions scenario

Some example of supervision outputs are compared in Figures 4.39 to 4.41. Table 4.6 also shows the results of indicators for different defined scenarios. In Figure 4.39, Real-time supervision with empiric membership function is not able to control the exceeding of subscribed power. In Figure 4.40, optimization of membership function leads to better control of V2G energy in function of price signal. Finally, the predictive real-time supervision is able to minimize the subscribed power exceeding in order to minimize the ETC factor.

Table 4.6: Performance indicators for defined scenarios

Scenarios	ETC (p.u.)	Coordination (%)	CO_2 emission (Tonne)
W/O-PEV	1	-	777
W-PEV	1.10	3.5	851
W-PEV-Optim	1.00038	13.6	830
W-PEV-RT-Empiric	1.038	5.85	846
W-PEV-RT-Optim	1.029	7.71	836
W-PEV-PRT-Empiric	1.007	10.73	835
W-PEV-PRT-Optim	1.005	11.01	834
W-PEV-RT-Empiric-G2V	1.048	6.4	–
W-PEV-RT-Optim-G2V	1.033	9.4	–

The results of indicators for each scenario are brought in Table 4.6. Concerning the energy transmission cost (ETC), it is shown that the presence of 2700 PEVs at distribution grid causes 10% increment in ETC bill (i.e. 237 k€). The interesting point is that the usage of off-line optimization leads to reduction of this increment in such a way that there is no charging demand of 2700 PEV fleet (i.e. maximum power of 10 MW). After that, each level of supervision contributes more efficient to the service. For instance, it starts from 1.038 *p.u.* for **W-PEV-RT-Empiric** to 1.005 *p.u.* for **W-PEV-PRT-Optim**.

The advantage of using predictive layer is proved based on the progress in indicators' optimization. The other indicators such as coordination are also interesting. The Increment of coordination between PEVs and RES are evident in presence of supervision system and it reaches upto 11% for **W-PEV-PRT-Optim** (i.e. 3693 MWh). The results of off-line optimization (**W-PEV-Optim**) shows its perfect coordination upto 13%. In term of CO_2 emission minimization the contribution of predictive real-time supervision is also evident.

The results of this thesis is compared with another PhD project developed in the same laboratory on coordination of PEVs problem (G2V). The indicators calculated in this thesis are also compared with the results of V2G supervision system in this thesis in order to be able to investigate the added values of V2G technology and also technological progress aspects.

The best contribution of coordination scenario has been reached to 1.033 *p.u.* while for V2G supervision in scenario **W-PEV-PRT-Optim** is going to 1.005 *p.u.*. This shows the added contribution of approximately 33% compared to G2V scenario. For coordination between PEVs and RES this indicator shows 2 % extra contribution for **W-PEV-PRT-Optim** scenario compared to **W-PEV-RT-Optim-G2V** which is equivalent to 671 MWh. This extra usage of local RES leads to reduction of CO_2 emission and increase the contribution of V2G technology to environmental protections. In fact, this extra coordination is possible thanks to the V2G technology.

The economic intensives for PEV owners can not be defined in this step since the impact of V2G operation on the battery degradation should be analyzed. Even with the impact, as there is no business model available for V2G contribution in the ancillary services, the pure benefit of PEV from V2G participation can not be defined in this level.

In the continue of this chapter, the impact of V2G operation for ETCM service is analyzed on a single PEV inside the fleet of ETCM service participants. This impact is studied from technical point of view and the economic impact has been considered as perspective of the thesis. The technical indicator is taken into account as the battery degradation due to extra charging/discharging actions in V2G operation. Before that the robustness study has been conducted to ensure the validity bound of predictive input for real-time supervision.

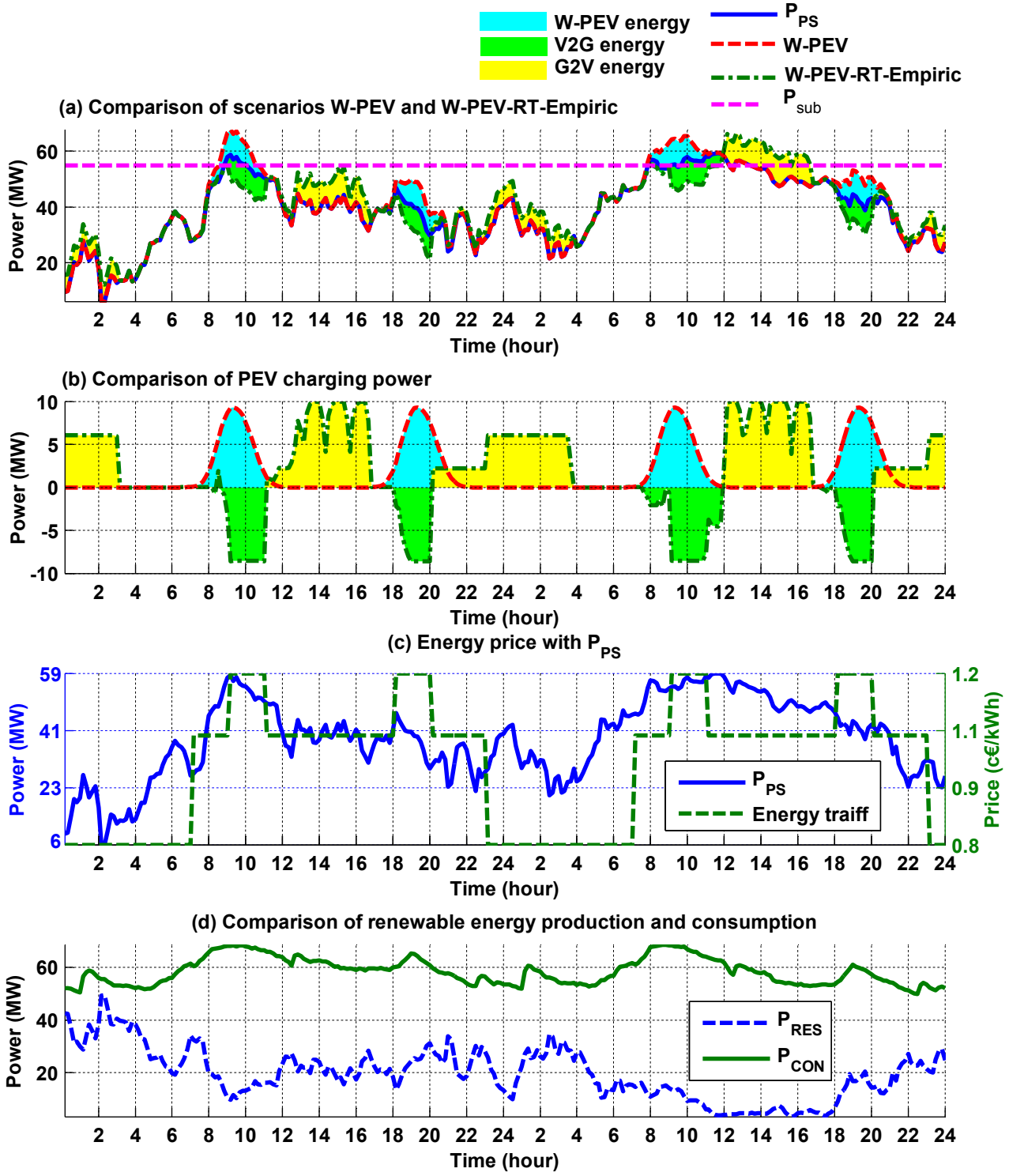

Figure 4.39: 2 days example of supervision for **W-PEV-RT-Empiric** scenario.

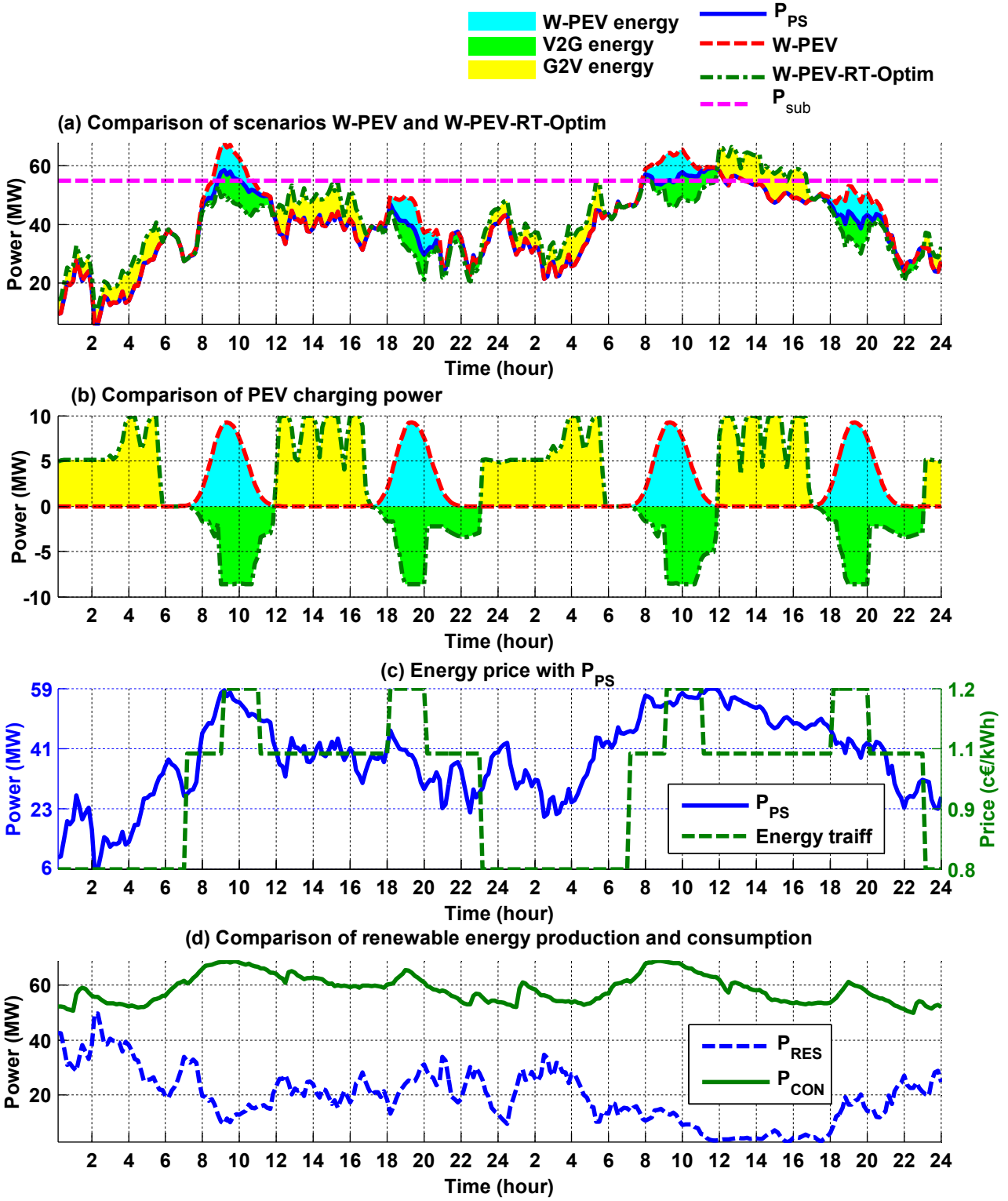

Figure 4.40: 2 days example of supervision for **W-PEV-RT-Optim** scenario.

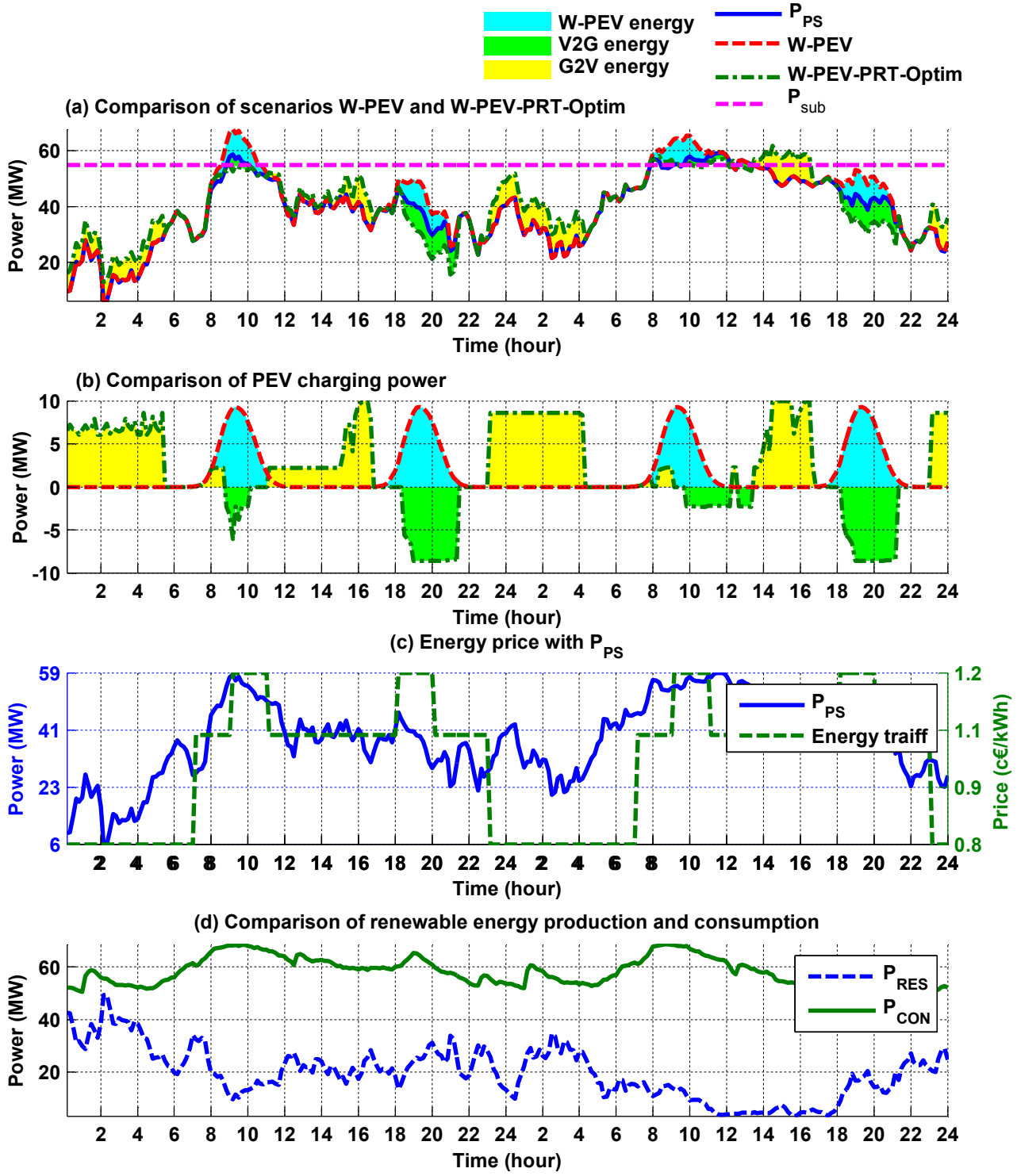

Figure 4.41: 2 days example of supervision for **W-PEV-PRT-Optim** scenario.

4.3.4 Robustness study of predictive real time supervision

In order to analyse the validity of prediction, a robustness study is done to confirm, the acceptable variation bound of predictive supervision system. In fact, in this part, the possible errors in prediction which impose delay or shifting to the reference power are analyzed and their impact on the objective function are studied. In order to show that the predictive input can be useful for the real-time supervision application, the real-time supervision system is considered as reference and the variation of objective function in term of each type of error is compared

with this reference.

The acceptable area of variation is found by focusing on the objective function value for real-time supervision system. In other words, the presence of predictive input is useful while the minimization of objective function is better that the case of only real-time supervision. Therefore, the variation are applied up to the boundary of less objective function value compared to only real-time supervision system. In the following different strategies applied for the error are explained and the results of sensitivity to these variation are brought.

4.3.4.1 Delay in time (shift in x axis)

In order to validate the benefit of predictive input for the real-time supervision, a strategy of applying delay in time axis is proposed. In this strategy, negative and positive time shift are applied and the objective function for each case is compared with real-time optimized supervision (RT-Optim). Figure 4.42a shows the objective function values for different scenarios of delay. The acceptable range of variation based on the value of real-time supervision can be considered as -30 minutes to 20 minutes of delay applied to the reference power. It means that any type of errors in the inputs of predictive part of the supervision which finally imposes a delay of -30 to 20 minutes is acceptable and the supervision can still acquire benefits from the presence of predictive input. This acceptable area of variation is illustrated in Figure 4.43.

4.3.4.2 Delay in Power (shift in y axis)

The second strategy is focused on the amplitude of the reference power from the predictive part. Different variation percentage are applied in the per unit of the reference power and the values of objective function for each case is compared with real-time supervision. Figure 4.42b shows the objective function values for different scenarios of error. The acceptable range of variation based on the value of real-time supervision can be considered as -20 % to 20 % of error applied to the reference power. This acceptable area of variation is illustrated in Figure 4.44.

4.3.5 State of Charge estimator and reference power distribution

The last part of the Predictive real-time is the SOC estimation algorithm. As previously explained the necessity of knowing the SOC evolution for V2G application is evident. Since, the SOC should be controlled to avoid over charging and discharging of the battery. This should be also consider that the SOC estimation is also in closed-loop procedure of supervision system. It means that the real-time supervisor needs the updated information of SOC estimator at the first moment of each sample time.

In this thesis, based on the constraints defined for the project, different limitations and requirements are defined in order to control the charging/discharging procedure of the PEVs. Based on the information provided to the charging station, the estimator algorithm will distribute the charging/discharging commands to the vehicles' batteries. At first the input necessary data are introduced.

The real case of tomorrow, it will be possible to have the precise information about, arrival/departure time of the vehicles, arrival SOC, desired departure time and SOC and etc. In this study, it has been considered that all of these information are accessible and communicable through charging stations at home and office parking. In this thesis, arrival and departure time are considered as input information and the constraints are as follows:

1. Departure SOC = 100 %
2. Minimum SOC limit = 20%

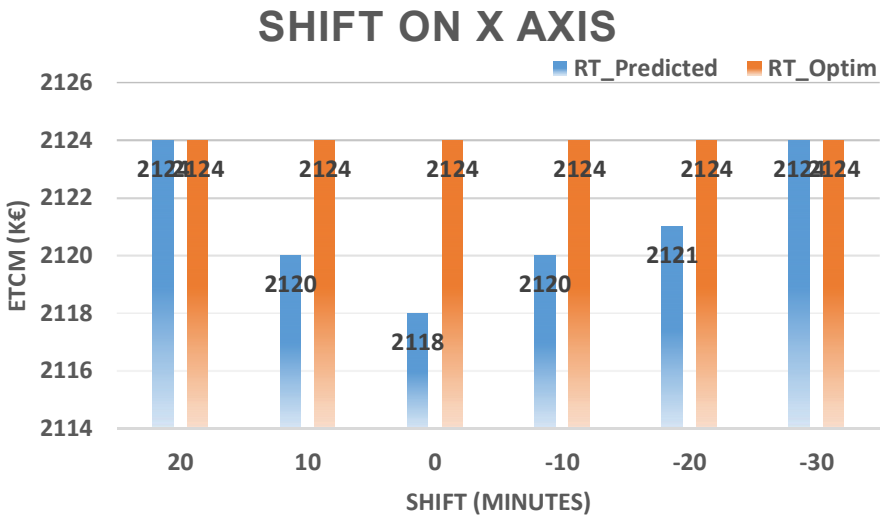

(a) Comparison of objective function for error shift in X axis.

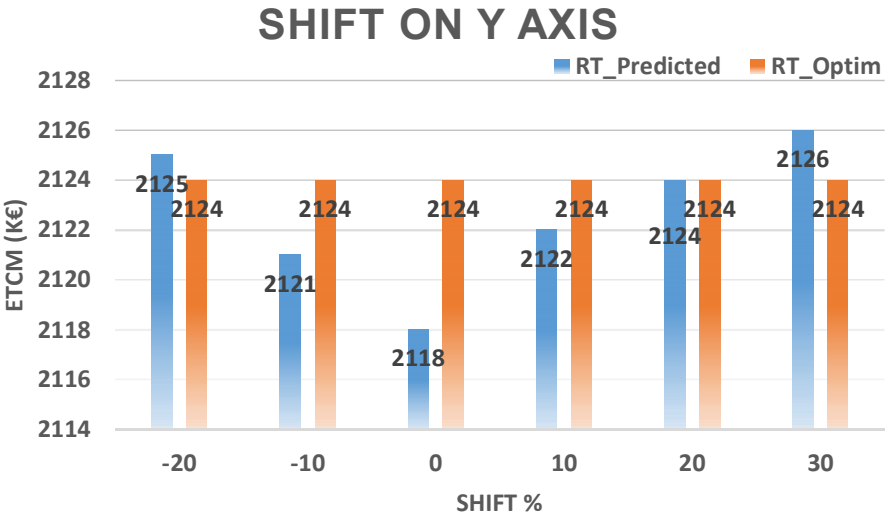

(b) Comparison of objective function for error shift in Y axis.

Figure 4.42: Comparison of objective function for error propagation in reference power.

In addition, in order to avoid extra depth charging/discharging cycles, the following procedures are taken in to account.

1. For charging demand the PEVs are sorted increasing

2. For discharging demand the PEVs are sorted descending

The implemented algorithm for SOC estimator is illustrated in **Algorithm 3**. In this algorithm, $NPEV(t)$ indicates the total number of PEVs available at time slot t, $NPEV^{>20\%}(t)$ memorizes the number of PEVs with SOC more than 20% available at time t, $NPEV^{<20\%}(t)$ the number of PEVs available at time t with SOC less than 20%, $NPEV^{<20\%}(t)$ contains the index of PEVs with SOC more than 20% and finally, SOC_{matrix} is the matrix of SOC with the size of $NPEV \times 144$, 144 indicates number of 10 minutes sample times in one day. The rest time of each PEV is calculated using following equation;

$$RT^i(t) = \frac{(\frac{100-SOC^i(t)}{100}) \times E^i_{EV}}{CR^i} - (T^i_{departure} - T^i(t)) \tag{4.48}$$

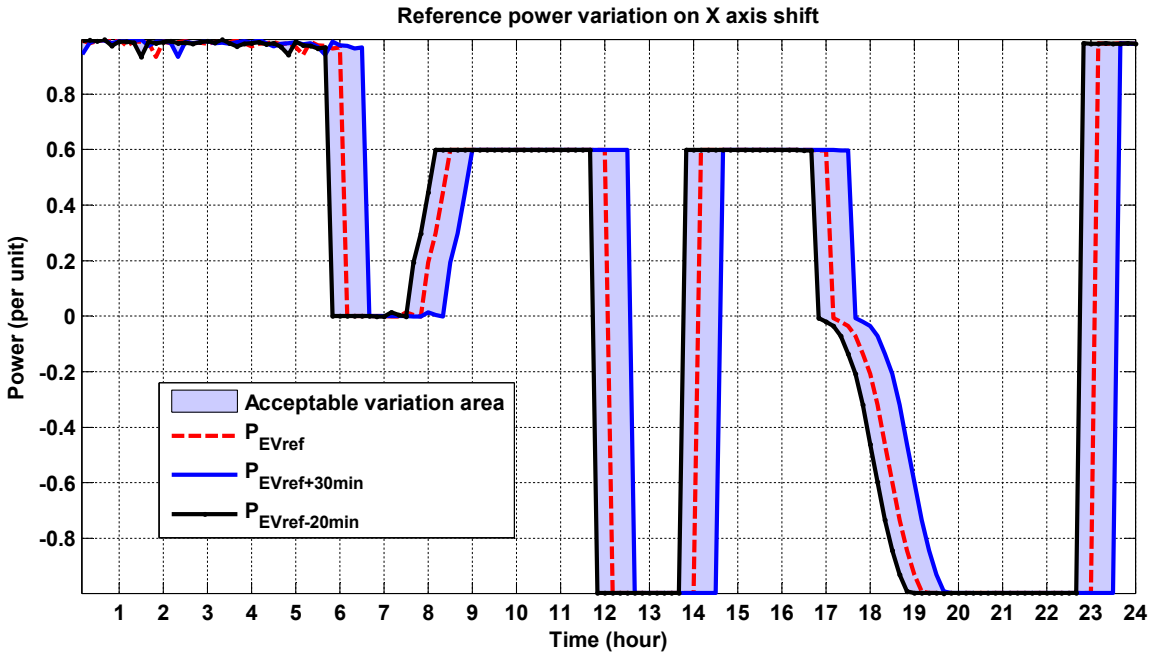

Figure 4.43: Acceptable area of variation for shift in x axis for reference power.

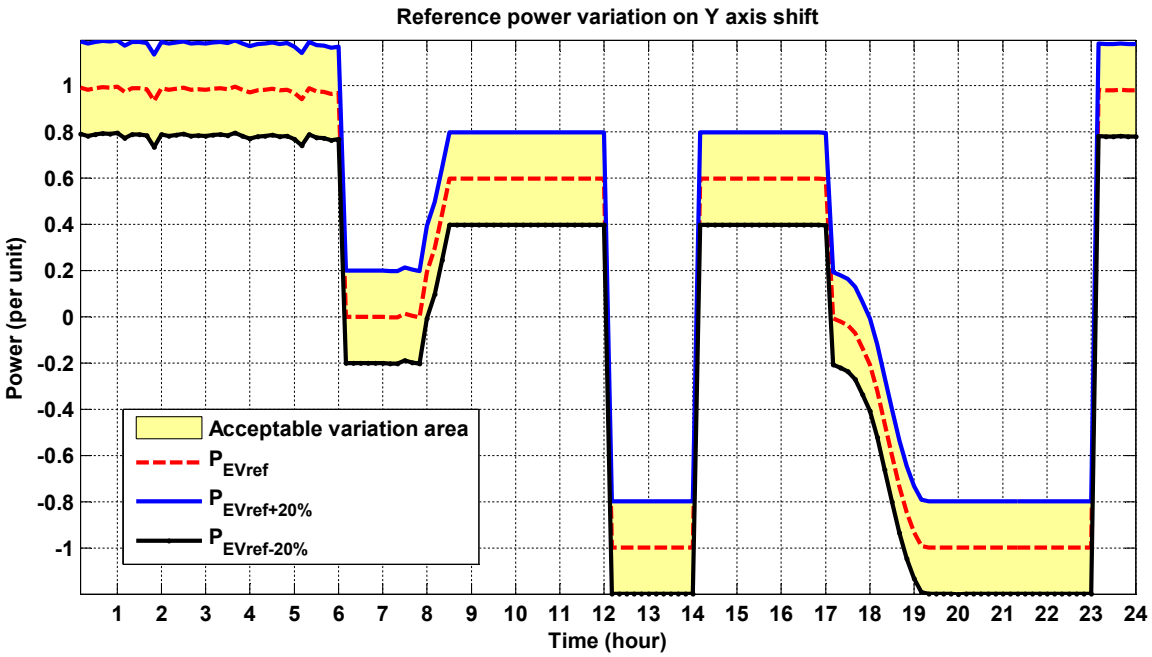

Figure 4.44: Acceptable area of variation for shift in y axis for reference power.

Where, $T^i(t)$ indicates actual sample time of the algorithm. If this RT is zero, it means that the PEV has no time to participate in coordination program and should be necessarily charged.

This algorithm ensures the charging of all PEVs upto their departures and respect the limit of $SOC = 20\%$. A single vehicle SOC profile for one year calculated by this algorithm is depicted in Figure 4.46. It shows that the minimum discharging of the PEV is limited to 20%. Maximum charging state is also limited to 1 *p.u.*. In Figure 4.45, one day SOC of a fleet of 2700 PEVs for scenario 2030 is shown. This indicates that roughly all of the PEVs have been reached to 100% of SOC at departure time. This indicator can be used for each day in order to analyze the performance of the algorithm. As it is shown the algorithm avoids to imply a lot

Algorithm 3 SOC estimator and power distribution algorithm

for $t = 1 : 144$ **do**
    Update $NPEV(t)$
    Update $NPEV^{>20\%}(t)$
    Update $NPEV^{<20\%}(t)$
    Calculate Rest time (RT) for each PEV
    Charge all PEVs with $RT = 0$
    if $P_{EV-ref}(t) < 0$ **then**
        Put PEVs in $Group^{>20\%}$ in descending order
        if $CR \times NPEV^{>20\%}(t) \leqslant |P_{EV-ref}(t)|$ **then**
            Discharge all PEVs of $Group^{>20\%}$
        else
            Discharge from the top of descending list
        end if
    else if $P_{EV-ref}(t) > 0$ **then**
        Put PEVs in $Group^{>20\%}$ in increasing order
        if $CR \times NPEV^{>20\%}(t) \leqslant |P_{EV-ref}(t)|$ **then**
            Charge all PEVs of $Group^{>20\%}$
        else
            Charge from the top of Increasing list
        end if
    else
        Do not charge PEVs
    end if
    Update $SOC_{matrix}(:, t)$
end for

of fluctuation in SOC variation. The charging and discharging commands are well-managed.

A single PEV SOC profile for only 2 days (zoom of previous figure) is provided in Figure 4.47. It shows also the arrival, departure time for home and office. In this model, the SOC variation between each arrival and departure is modeled. While, the SOC variation during driving cycle is not taken into account. Hence a simple constant SOC drop is considered.

This algorithm is used in closed-loop control of supervision system. Moreover, for the degradation study of the batteries used in this service, the algorithm is used to generate the SOC profile for degradation algorithm. This is explained completely in next sections.

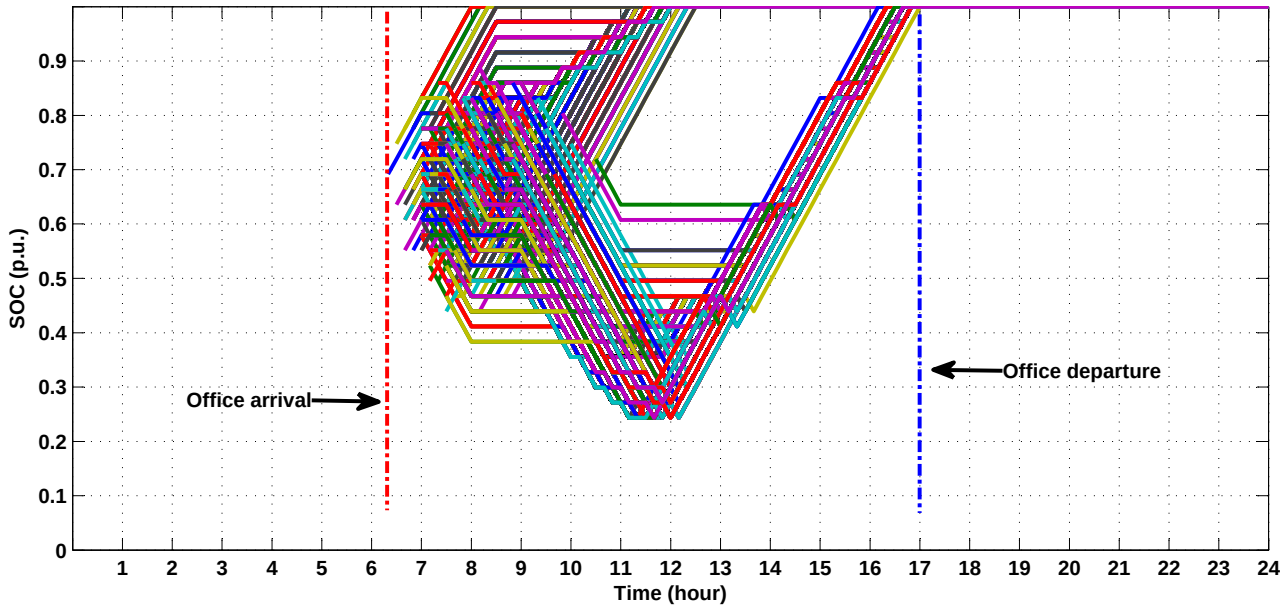

Figure 4.45: Example of SOC variation of 2700 PEVs, Scenario 2030, Service: Energy Transmission Cost Minimization (ETCM).

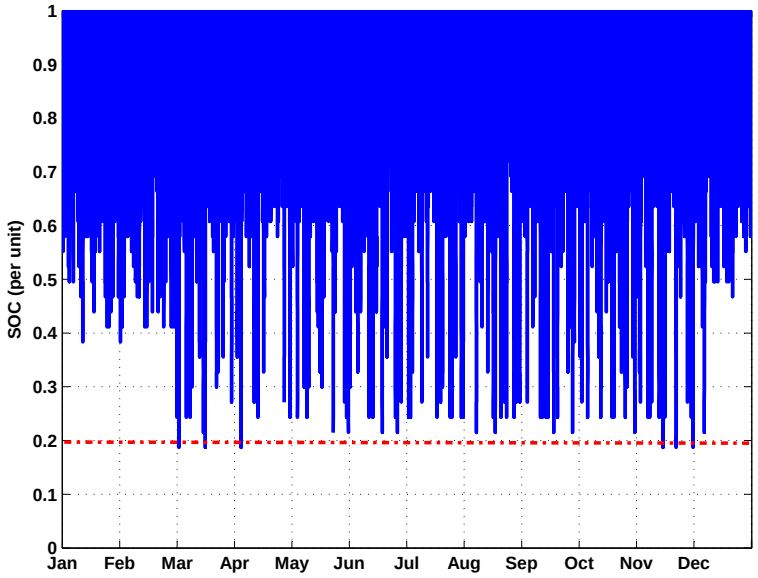

Figure 4.46: One year SOC profile of a PEV from SOC estimator algorithm.

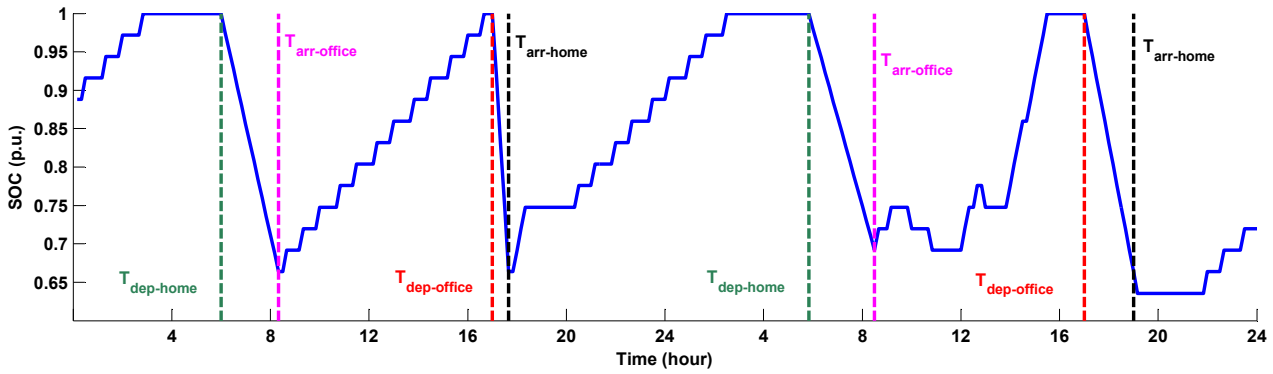

Figure 4.47: Two days example of SOC profile for a single PEV with arrival and departure times to the office and home.

4.4 Battery degradation modeling and analysis of V2G services

Consideration of PEV's battery as a storage unit for grid services, leads to extra degradation of the battery's lifespan. This is one of the challenges of V2G technology. In parallel of this thesis, a master of science project (Internship) has been defined by author, concerning the impact of different charging/discharging actions of V2G technology on the battery degradation. In this project a degradation model for lithium-ion battery has been developed, which is able to calculate the battery lifespan degradation using Rainflow cycle counting algorithm [Downing 82]. In the continue a summary of developed model is presented. After that, different scenarios of Normal and V2G charging have been tested using degradation model in order to identify the impact of each scenario on the battery degradation. An example of two days SOC variation for two scenarios, one for Normal charging and the other one for V2G charging, are depicted in Figure 4.49. The following flowchart summarizes the methodology for the interdisciplinary work, where three developmental stages are clearly mentioned (Figure 4.48).

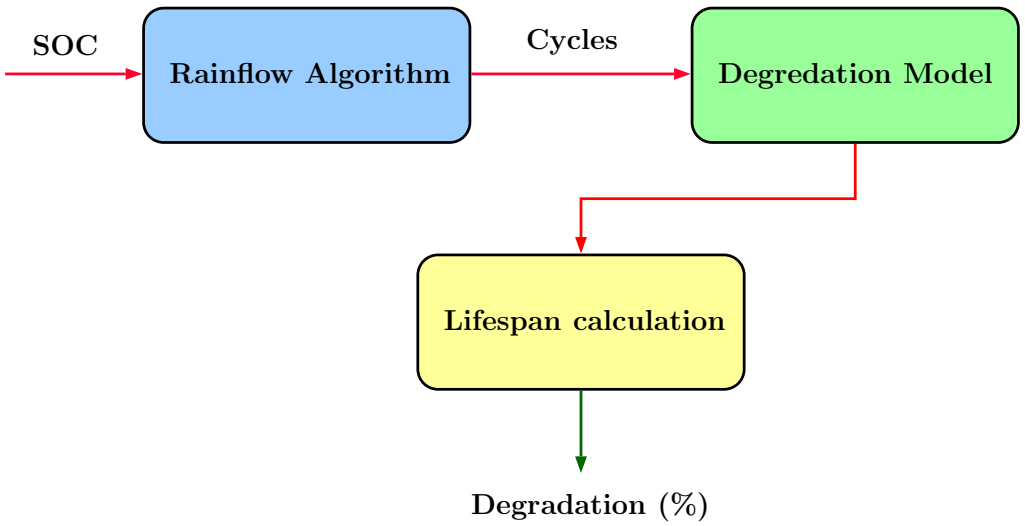

Figure 4.48: Procedure of degradation calculation.

4.4.1 Rainflow algorithm

One of the efficient cycle counting algorithms is rain flow algorithm [Amzallag 94]. This algorithm is able to count the cycles with their magnitude. This algorithm is widely used for fatigue analysis and fulfill task whether its regular cycle profile or irregular cycle profile. The algorithm used in this thesis is available in Mathwork[1] website. This algorithm provides following outputs from a given state of charge.

1. Cycle amplitude
2. Cycle mean value
3. Cycle type (0.5 or 1)
4. Cycle start time
5. Cycle duration

These data are used in battery degradation model for different stress models of the degradation. The summary of model is presented in next section.

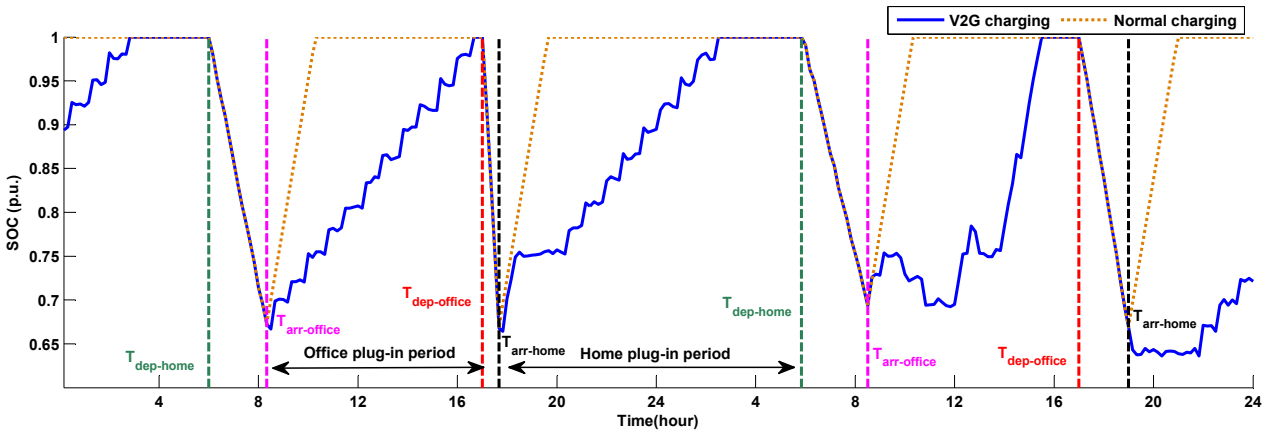

Figure 4.49: Two days example of SOC profile for a single PEV with arrival and departure times to the office and home, comparison of V2G charging and Normal charging scenarios.

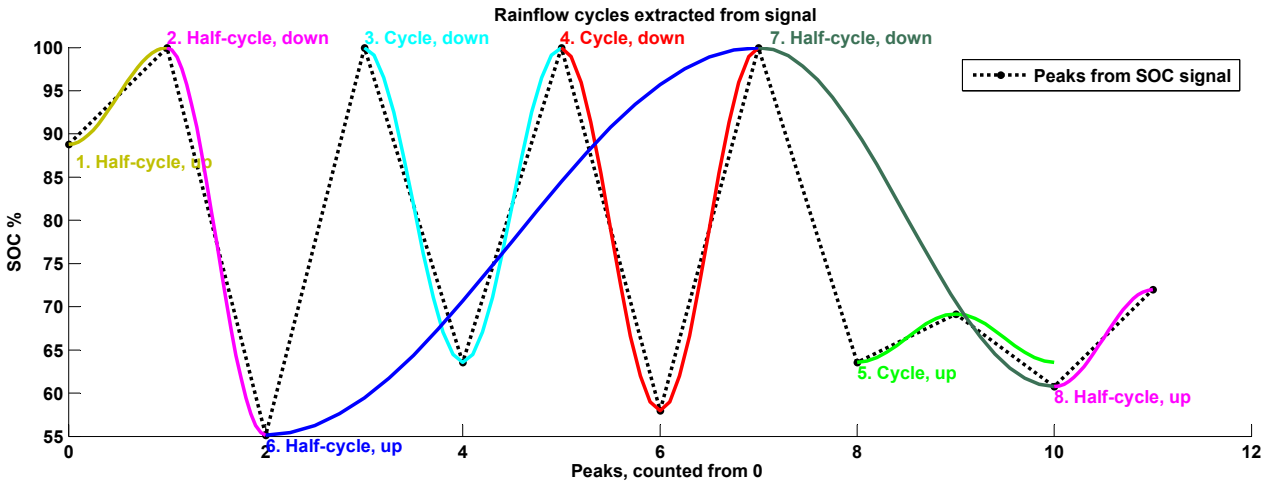

Figure 4.50: Rainflow algorithm cycles extracted from SOC signal.

[1]Rainflow counting algorithm http://www.mathworks.com/matlabcentral/fileexchange/3026-rainflow-counting-algorithm

4.4.2 Battery degradation model

Battery degradation includes decrease in maximum charge capacity, power and voltage fade. There are many internal and external factors that affect the performance and lifespan of a lithium-ion battery. Several studies have been conducted on the influence of ambient temperature, breakdown of the electrolyte's organic solvents and active material in the electrodes. Such factors are the reason of degradation. The process of capacity decrease is usually affected not by one, but several factors and occurs at similar time scales. These factors can be independent of each other, such as SOC, Depth Of Discharge (DOD), Number of cycles and charging rate. This makes battery degradation highly complicated and multi-dimension problem, and it is impossible to describe it by a single theory. Hence, there are plenty of modeling approaches including chemistry theory, empirical model and semi-empirical model. The main focus of the model presented in this thesis is on the development of Semi-empirical model [Xu 13, Millner 10].

Degradation model starts with two exponential functions (two term exponential), describing capacity loss due to Solid Electrolyte Interphase (SEI) film formation and normal operation, respectively [Zhurkov 84]. Degradation model consists of non-linear degradation function and linearized degradation function. Non-linear part is shown as in equation 4.49

$$L = 1 - (p_{SEI}.e^{-r_{SEI}.f_d} + (1 - p_{SEI}).e^{-f_d}) \tag{4.49}$$

Where L is battery aging life indicator with 0 value (0%) corresponds to a new battery and 1 (100%) corresponds to end of life of the battery. p_{SEI} is SEI formation portion coefficient, r_{SEI} is SEI formation rate ratio coefficient and f_d is linearized degradation function.

The linearized degradation function is developed as the summation of cycling aging and calendar aging factors as represented in equation 4.50:

$$\begin{aligned}
&f_d(DOD, SOC, C, T, n, N, t) = \\
&f_{cyc}(DOD, SOC, C, T, n, N) + f_{cal}(t, SOC_{avg}, T_{avg}),
\end{aligned}$$

$$\begin{aligned}
&DOD = (DOD_1, DOD_2, \ldots, DOD_N), \\
&SOC = (SOC_1, SOC_2, \ldots, SOC_N), \\
&C = (C_1, C_2, \ldots, C_N), \\
&T = (T_1, T_2, \ldots, T_N), \\
&n = (n_1, n_2, \ldots, n_N), \\
&SOC_{avg} = \frac{\sum_{i=1}^{N} SOC_i}{N}, \\
&T_{avg} = \frac{\sum_{i=1}^{N} T_i}{N}
\end{aligned} \tag{4.50}$$

Where cycling aging is calculated from stress factors, containing DOD, SOC, C-rate (charging rate) and temperature of each cycle (equation 4.51).

$$\begin{aligned}
&f_{cyc}(DOD, SOC, C, T, n, N) = \\
&\sum_{i=1}^{N} f_{DOD}(DOD_i).f_{SOC}(SOC_i).f_C(C_i).f_T(T_i).n_i
\end{aligned} \tag{4.51}$$

Calendar aging is calculated from time duration of the operation (simulation), and the profile-average of SOC and temperature (equation 4.52).

$$f_{cal}(t, SOC_{avg}, T_{avg}) = k_t.t.f_{SOC}(SOC_{avg}).f_T(T_{avg}) \tag{4.52}$$

Where k_t is the time stress coefficient and the stress model of each factor is represented as in equations 4.53 to 4.56.

$$f_{DOD}(DOD) = (k_{DOD1} DOD^{k_{DOD_2}} + k_{DOD3})^{-1} \tag{4.53}$$

$$f_{SOC}(SOC) = e^{k_{SOC}(SOC - SOC_{ref})^2} \tag{4.54}$$

$$f_C(C) = e^{k_C(C - C_{ref})} \tag{4.55}$$

$$f_T(T) = e^{k_T(T - T_{ref}).\frac{T_{ref}}{T}} \tag{4.56}$$

According to the capacity fading test of Lithium Manganese Oxide (LMO) battery the model coefficients are calculated (see Appendix) [Xu 13].

This model is used for battery degradation calculation, using the cycle statistics provided by rainflow algorithm. In order to be able to study the impact of V2G on the battery degradation different scenarios have been defined and tested. These scenarios and the results are brought in next section in detail.

4.4.3 Scenario definition and degradation results

In order to compare to extra impact of V2G functionality on the battery degradation with normal functionality of the PEVs, three different scenarios are defined.

1. **V2G charging**, where the PEV is used for both driving purpose and V2G service (e.g. ETCM service)

2. **Normal charging at home and office**, where the PEV is used only for driving purpose and is charged two times per day, once at office and once at home.

3. **Normal charging at home**, where PEV is used just for driving purpose and is charged once a day and only at home.

The charging power at home is considered as Normal charging standard (see Table 1.1). Figure 4.51, shows a two days example of SOC variation for these three scenarios. In first subplot, the SOC decrease due to driving cycles are indicated by the arrival and departure times to home and office. Between each arrival and departure, the PEV is used to provide V2G service to the grid.

In second subplot, the normal charging at home and office is applied. The PEV is charged right after its arrival to office or home. In third subplot, the PEV is just charged once a day and only after arrival at home.

Figure 4.52, shows one year SOC variation for the three scenarios. It is visible that the DOD is bigger in case of Normal charging at home. While, in normal charging at home and office the DOD is limited. The DOD due to V2G scenario is fixed to 80% as the constraint of supervision system.

The rainflow algorithm is implemented on the three scenarios and the results are depicted in Figure 4.53.

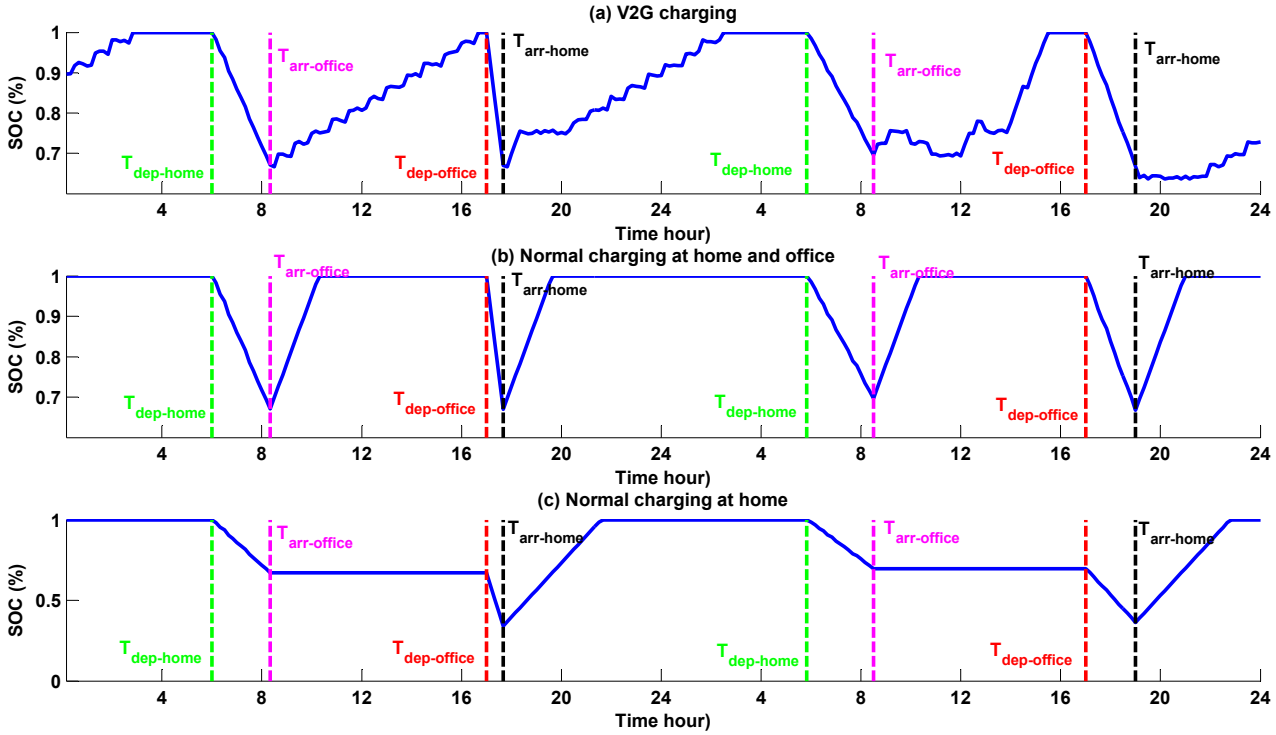

Figure 4.51: Comparison of different scenarios of PEV charging for degradation study.

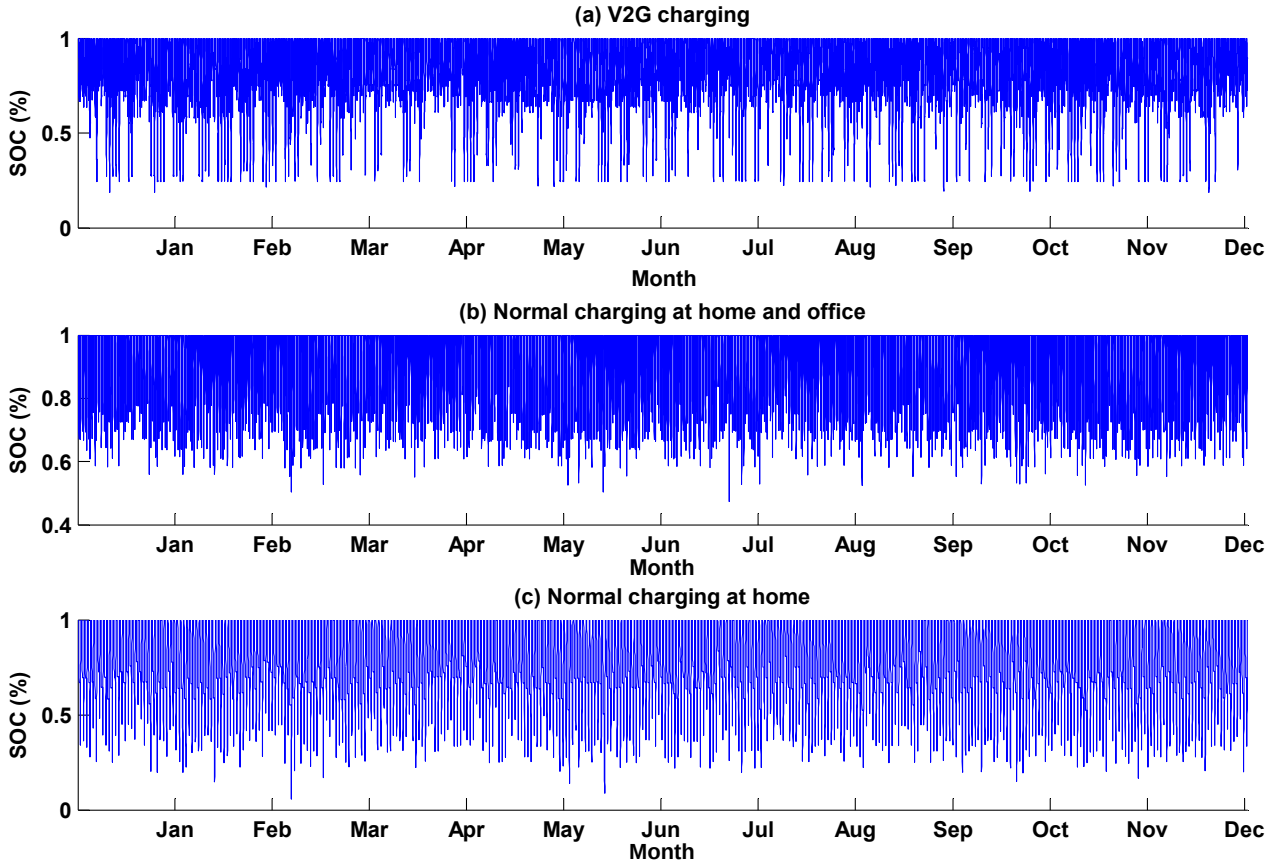

Figure 4.52: one year Comparison of different scenarios of a single PEV charging for degradation study.

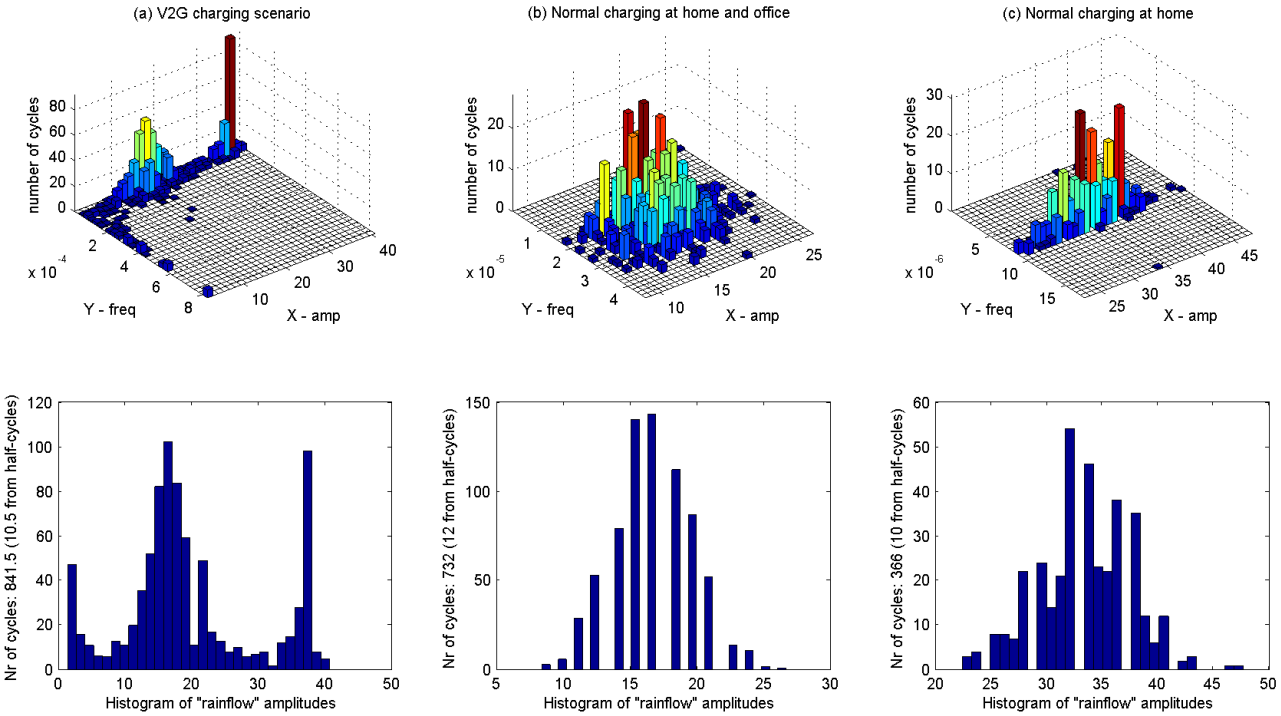

Figure 4.53: Comparison of rainflow results for three scenarios.

Table 4.7: The results of degradation study for three scenarios

Scenarios	Nb. cycles	Mean of amplitude (DOD %)	Degradation per year	Lifespan
V2G charging	841	20.31 %	8.85 %	9 years
Normal charging at home/office	732	16.8 %	8.04 %	10 years
Normal charging at home	366	33.6 %	7.66 %	10.5 years

In three upper subplots, the frequency of the cycles and their amplitude are presented in function of number of cycles. It is visible that the number of cycles are generally bigger for V2G charging scenario. The frequency of the cycles is much more bigger than two other scenarios. It is due to the fact that the mini charging/discharging cycles are available in V2G scenario which causes extra degradation. The histograms of cycles versus amplitude (DOD) are presented in lower subplots.

In Table 4.7, number of cycles and mean amplitude for each scenario are given. Using the degradation model, the degradation factor and lifespan can be calculated. Lifespan is calculated based on the fact that battery end of life is considered at 80% of degradation and the simulation period of one year. These results indicate that using a PEV for ETCM service can decrease the lifespan of the battery for approximately 1.5 year. This result is quite interesting in term of the magnitude of impact. It should be also considered that the degradation can be affected in other type of services. These results show that the number of cycles are more important than depth of discharge of the cycles (amplitude). Normal charging at home scenario shows less degradation even with bigger amplitude compared to normal charging at home and office.

4.5 Predictive Real-time energy management strategy for "Energy bill minimization": case study of railway station

The second case study in this thesis, as presented in chapter 2, is the energy hub concept of railway stations. These stations contain limited number of PEVs charging stations with possible scenarios of Normal, Accelerated and Rapid charging.

SNCF has provided measured data of 3 typical railway stations in France containing the real power consumption of station in 10 minutes sample time. These data are used for testing the supervision system of V2G-enabled PEVs inside the railway stations. Based on the scenarios defined in chapter 2, arrival of PEVs to the stations has been considered around 8 AM and their departure around 6 PM. During this period, the batteries of PEVs are used for load balancing of the railway station. The objective of the energy management system is considered as Annual Energy Bill Minimization (AEBM).

There are two scenarios of energy bill contract which are considered in this study.

- Regulatory Tariff Sales (RTS)
- Spot Market Tariff (SMT)

The first type of contract was the previous version of contract for industrial consumers in France (Tarif Vert), which is not applicable after January 1^{st} 2016 [CRE 16]. The second type of contract is applicable after this date. The advantages of participation in each type of market using V2G technology are analyzed in this section.

In this section, three categories of railway stations are considered as case study with assumption provided in the Table 4.8.

Table 4.8: Scenarios of energy hub for V2G supervision system

Categories	A	B	C
PEV number	30	20	10
Optimum subscribed power for RTS	270 kW	220 kW	69 kW

Two Predictive real-time supervisions are designed for each scenarios of energy bill contract. The results of energy bill minimization are presented for each category and each scenario. Finally, the benefits of using V2G supervision system are concluded.

4.5.1 Predictive real-time supervision for Regulatory Tariff Sales

Based on the RTS market, there are different types of contracts for consumers in function of the level of their consumption. The railway stations are the case of consumers with more than 36 kVA consumption. Category C is the case of consumption between 36 kVA to 250 kVA which is called yellow tariff (Tarif jaune). Categories A and B are the stations with consumption more than 250 kVA. This type of tariff is called Green tariff (Tarif vert). The annual energy bill is calculated using the equation 2.20 presented in chapter 2, which is also recalled thereafter:

$$Cost = \sum_{j=1}^{5}(d_j E_j) + \sum_{j=1}^{5}(K.T_j\sqrt{\sum(\Delta P_j)^2}) + \alpha.P_{sub} \tag{4.57}$$

Three components exist in this function; Exceeding component,Energy component and Subscription component. A the subscribed power is signed one time per year, the subscription component can not be affected in optimization problem. Hence, the optimization of energy bill is done by minimizing exceeding and energy components. The effect of V2G can be interesting to discover on both components. Different inputs are considered for the supervision system. In this study for energy hub concept, because of lack of data, the only energy provider is the PEV fleet. The perspective is to consider solar panels as another source of energy in railway station microgrid. The model of case study is depicted in Figure 4.54. This energy hub contains the PEVs connected to the microgrid of the station and classical loads of the railway stations.

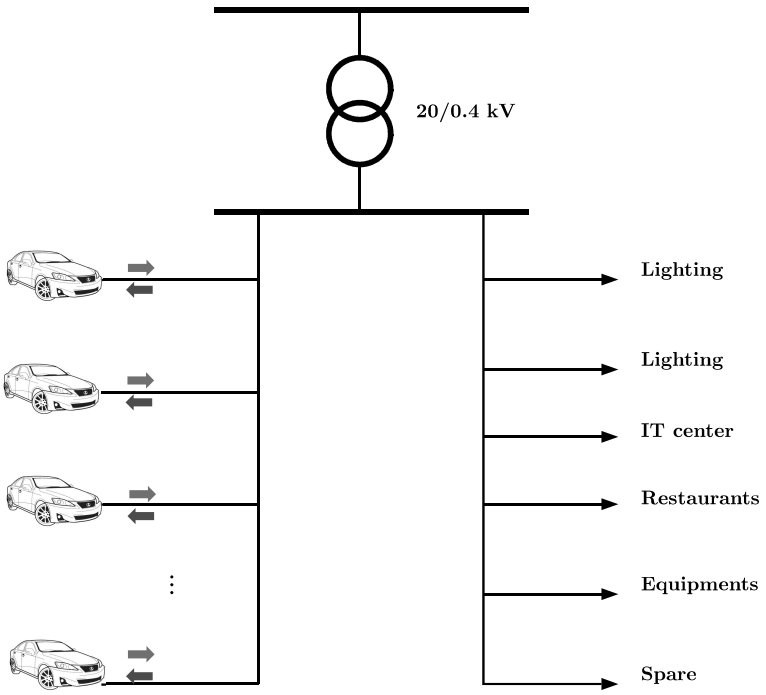

Figure 4.54: Representation of case study, MV/LV substation inside the railway station, containing PEVs in station parking and classical loads.

For real-time control of load consumption using storage ability of PEVs, the following inputs have been considered:

- SOC (State of charge of ensemble of PEVs)
- ΔP (Difference between consumption and subscribed power)
- Price
- $\hat{P}_{EV-ref}$ The reference power from predictive input

The only output of supervision system will be the real-time reference power. This supervision is designed using fuzzy logic with 32 rules, 3 membership function for SOC, 4 for ΔP, 3 for Price and 7 for $\hat{P}_{EV-ref}$. The same SOC estimation algorithm presented in section 4.3.5 is used for reference power distribution and closed-loop SOC estimation. The Predictive part is handled by Binary linear programming algorithm presented in chapter 2 section 2.6.2. The subscribed power is also optimized for each category based on their real consumption without PEVs using the optimization procedure explained in section 2.6.2.1.

4.5.1.1 Results and discussion

The Predictive real-time supervision is applied on three railway station categories. The results for RTS market are brought thereafter. Figure 4.55 shows the annual load profile of the station for different scenarios. The green curve shows the case of PEV charging without supervision. The increment of peak is evident and wide range of subscribed power exceeding is happened. While, the curve in red, representing the supervised consumption, is controlled majorly against the subscribed power exceeding. These exceeding are due to the coincidence of PEV charge demand at arrival and railway station consumption.

In Figure 4.56, the same result for category B is presented. The exceeding is controlled using predictive supervision system. However, the captured data during summer are not reliable, Hence the real interest of supervision can not be analyzed.

In Figure 4.57, annual load profile for different scenarios are depicted for category C. In this case study, the exceeding of subscribed power limitation using the supervision system is evident.

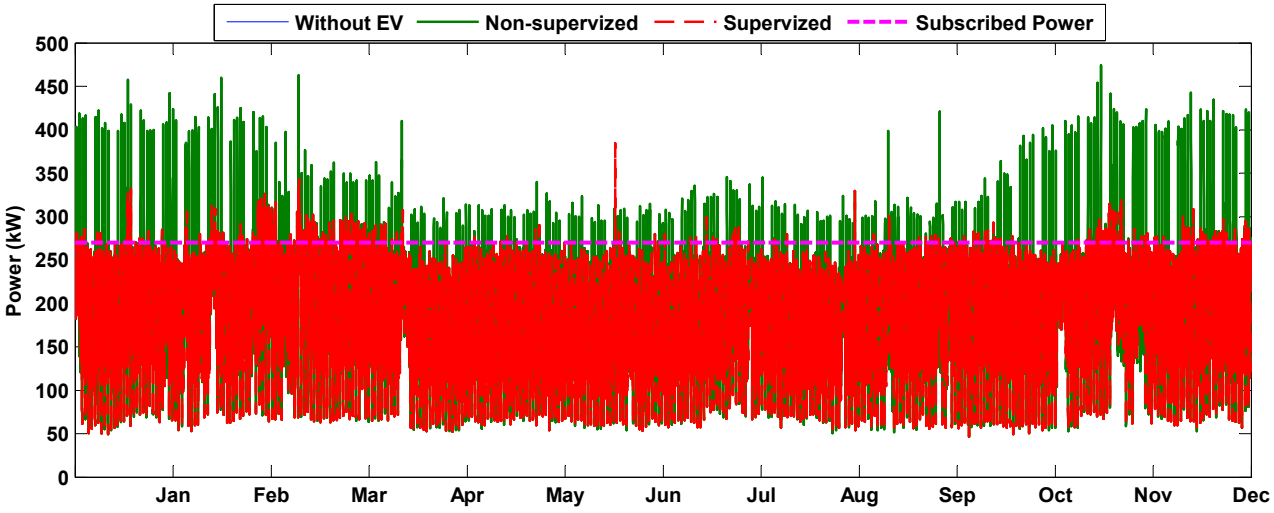

Figure 4.55: Annual load profile comparison for supervised scenario, non-supervized and without PEV scenarios (**Category A**).

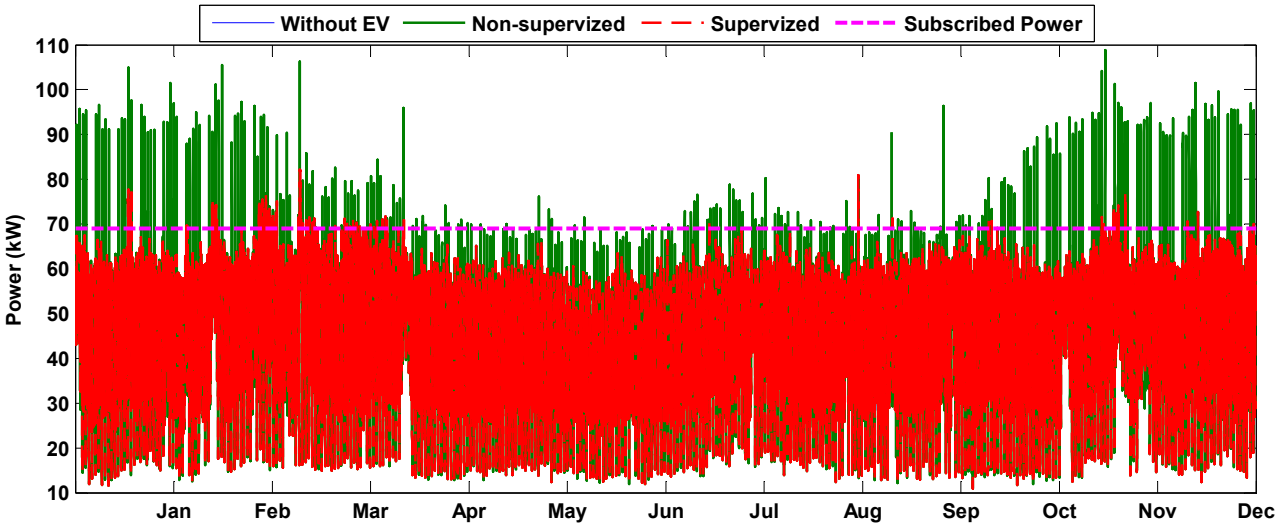

Figure 4.57: Annual load profile comparison for supervised scenario, non-supervized and without PEV scenarios (**Category C**).

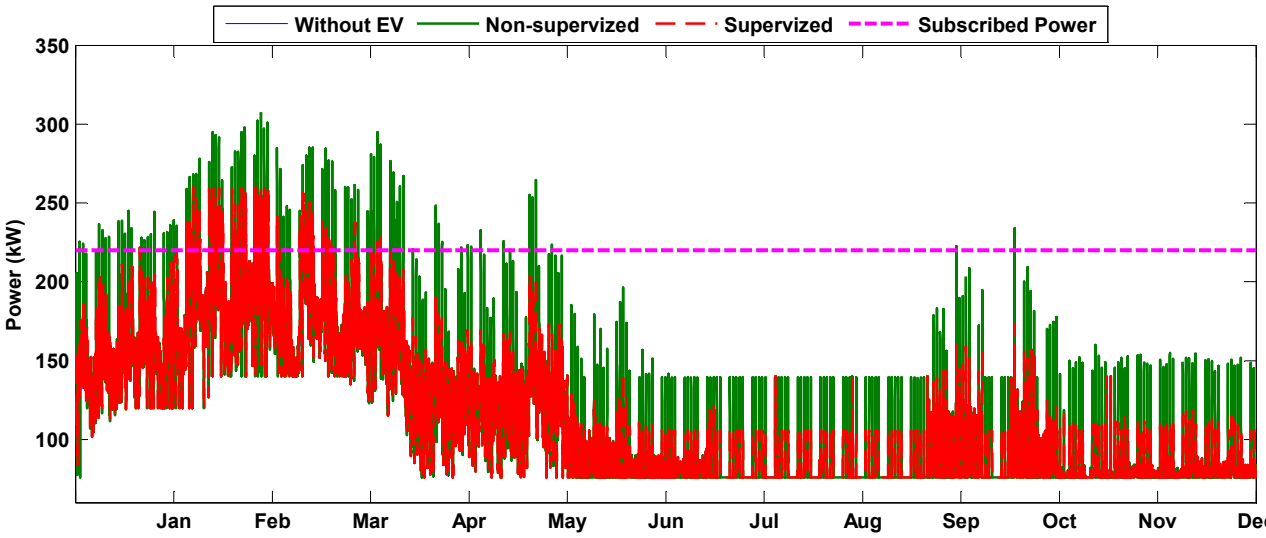

Figure 4.56: Annual load profile comparison for supervised scenario, non-supervized and without PEV scenarios (**Category B**).

In fact, as the predictive input has already provided a vision over next 24 hours, the real-time supervision is able to minimize the subscribed power exceeding. However, in RTS market, as the energy price during the availability of PEVs in the station is constant there would not be a major interest for consumed energy component of annual bill.

The performance indicators for these three cases are calculated and presented in Figures 4.58 to 4.60. The abbreviations are chosen to facilitate illustration [2].

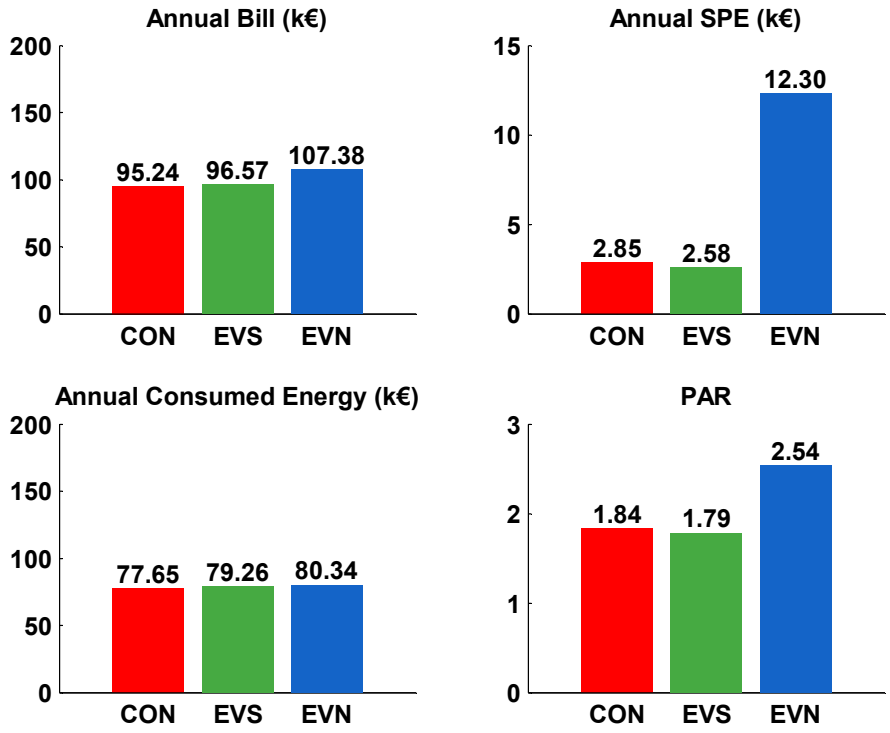

Figure 4.58: Predictive real-time supervision indicator result (**Category A**).

[2] Peak-to-Average Ratio (PAR), Electric Vehicle Supervised (EVS), Electric Vehicle Non-supervised (EVN), Consumption without Plug-in Electric Vehicle (CON)

4 parameters are analyzed for each case study. In category A, it is shown that the presence of predictive real-time supervision leads to minimization of Annual bill upto 10 % (10.81 k€). The major contribution is related to SPE limitation upto 80 % (9.72 k€). The contribution to the consumed energy component is not so much (1.3 %).

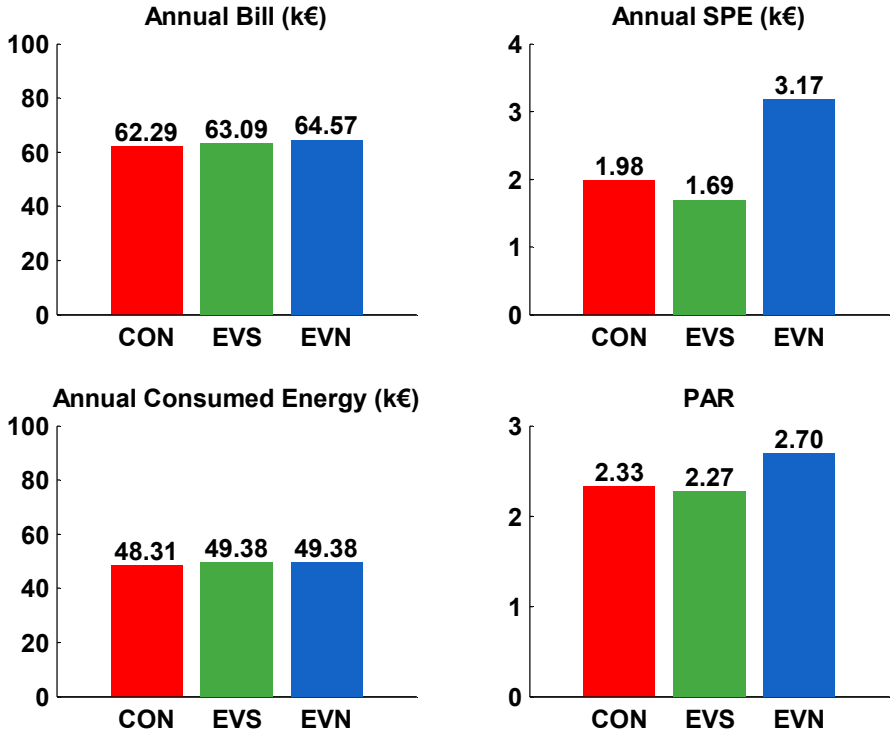

Figure 4.59: Predictive real-time supervision indicator result (**Category B**).

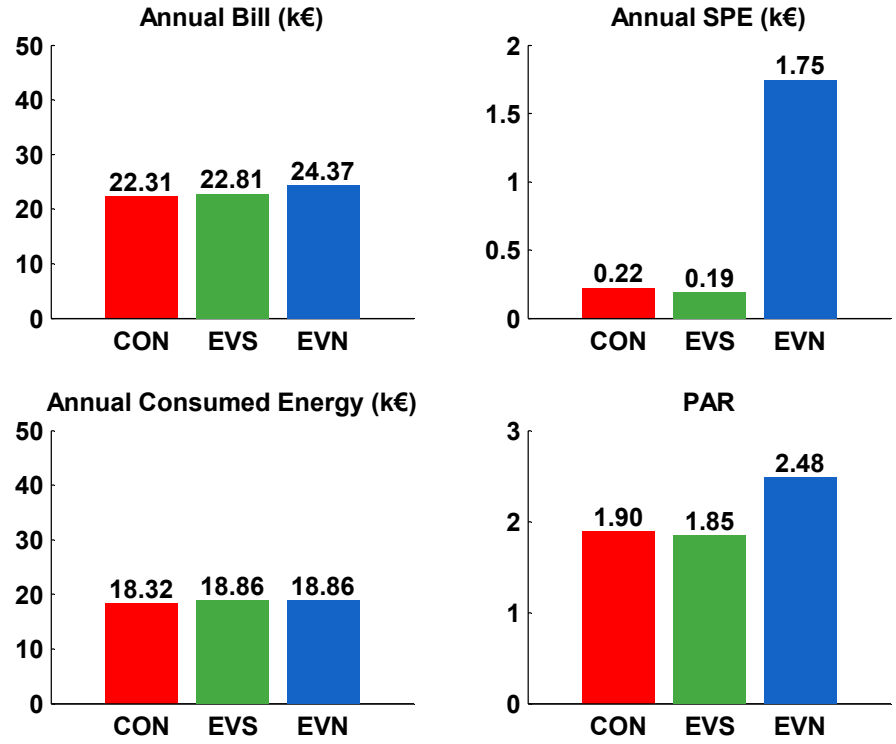

Figure 4.60: Predictive real-time supervision indicator result (**Category C**).

The forth indicator is considered as Peak-to-Average Ratio (PAR) of each profile. The reason to choose this indicator is to show the advantage of using V2G for peak shaving of railway station load profile. In fact, the more PAR is nearer to 1, the less losses and voltage drop may be occurred. In category A, the PAR value for supervised scenario is even less that the case of only consumption profile. The PAR value in Category A is reduced upto 30%. A slight reduction of PAR after supervision compared to consumption profile without PEV is also evident.

The same results for category B is depicted in Figure 4.59. It is shown that the contribution of supervision for this category is less than the category A. Only 2.2% reduction of annual bill is obtained. However, the major contribution is again focused on SPE component. For Par value, a minimization of 16% is founded. However, as previously mentioned. The results for this category are not reliable as the captured data from the measurement devices are not reliable.

For Category C, a minimization of 6.4% (1.56 k€) is obtained. These benefits considering the number of PEVs inside the vehicle are not really interesting. Considering the infrastructure and capital costs for smart charging equipment, and availability of vehicles, the feasibility of supervision implementation should be analyzed seriously.

4.5.2 Predictive real-time supervision for Spot Market Tariff

In this part, the provision of railway stations in electricity market using V2G technology is analyzed. This is based on the spot market[3] data in France. The economic interest is analyzed if the V2G-enabled PEVs participate in the service considering market spot price as reference.

The associated input for this supervision will be less than previous case, as there is no exceeding component. In this market, the consumers have freedom to choose their own energy provider. They would also pay based on spot market price. The inputs for supervision system are as follow:

- SOC (State of charge of ensemble of PEVs)
- Price
- $\hat{P}_{EV-ref}$ The reference power from predictive input

In this case, the supervision will try to provide charging reference when the spot price is low, and discharging reference when the spot price is high. The supervision has been tested on three categories and the results are brought thereafter. The general conclusion is that there is not an interesting economical benefit for spot market participation due to the price of electricity during the PEVs availability. Figure 4.61 is illustrating the performance indicators , which are PAR and annual bill in this market (i.e. there is no exceeding and subscription component) for three categories. The results shows a little minimization of annual bill due to the fact that the difference of electricity price during availability of PEVs is not so important. It is important to take into account, that in SMT scenario, the annual bill should be compared with consumed energy component in RTS scenario. This comparison shows the interest over consumed energy component minimization in SMT compared to RTS, however the minimization is negligible.

[3]The spot is a market for financial instruments such as commodities and securities which are traded immediately or on the spot. In spot markets, spot trades are made with spot prices. Unlike the futures market, orders made in the spot market are settled instantly. Spot markets can be organized markets or exchanges or over-the-counter (OTC) markets.

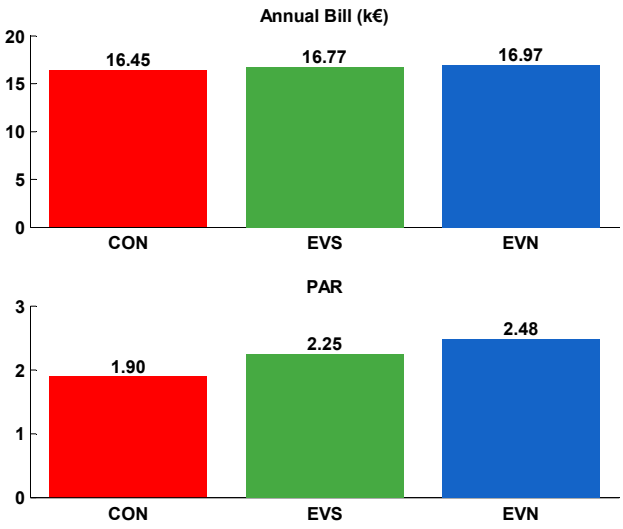

(a) **Category C**.

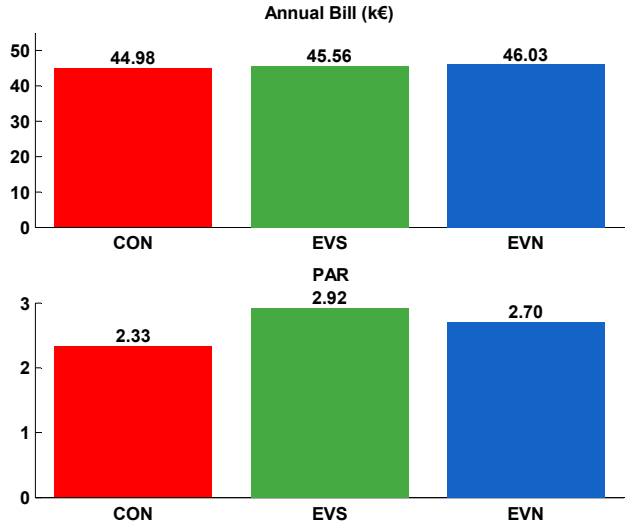

(b) **Category B**.

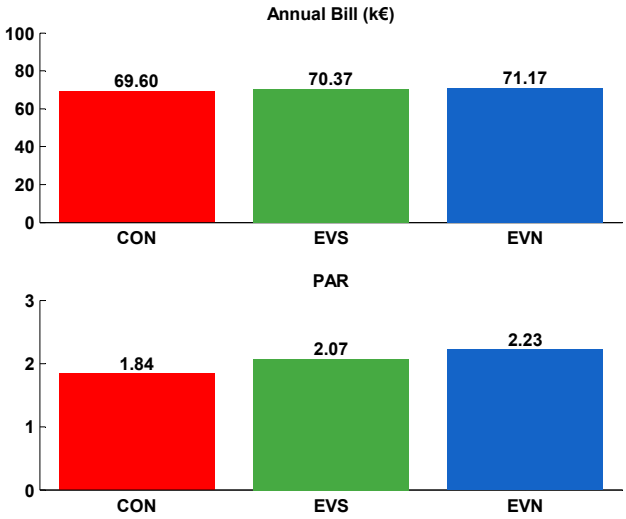

(c) **Category A**.

Figure 4.61: Predictive real-time supervision indicator for SMT contract.

The second indicator calculated for each category is PAR value. For categories A and C, the PAR is reduced while in category B the PAR value is increased after supervision. This is normal from the fact that the main order of the supervision is price input which causes the peak increment in some particular cases.

Some examples of load profiles after and before supervision are brought for three categories in Figures 4.62 to 4.64. In Figure 4.62 the result of supervised and non-supervized scenarios are brought for category C. As the availability of PEVs is between 8 AM upto 6 PM, the supervision is concentrated in this period. In red dashed-line, the case of non-supervized is depicted where a peak of consumption at the moment of arrival of PEVs is happened. While in green dashed-line, the supervised scenario using predictive real-time supervision shows the smart charging and discharging of PEVs in function of spot market reference. In first and third day the PEVs upon their arrivals are asked to be discharged since the price is higher than afternoon. Instead, the vehicles are charged during afternoon as the price is lower.

In Figure 4.63, the same result is presented for category B. In this type of market, as there is no subscribed power, the peak of consumption can be regenerated even after supervision. This is evident for the first day case in category B. A new peak is generated during 16:00 with approximately the same value of non-supervized case at 8:00. The discharging period are

normally between 8 AM to 12 AM when the electricity price is high. The PEVs are again charged near to the departure time.

In Figure 4.62, the same result is depicted for category A. Another three days example are depicted and it is shown that the discharging command is not so visible in these three days.

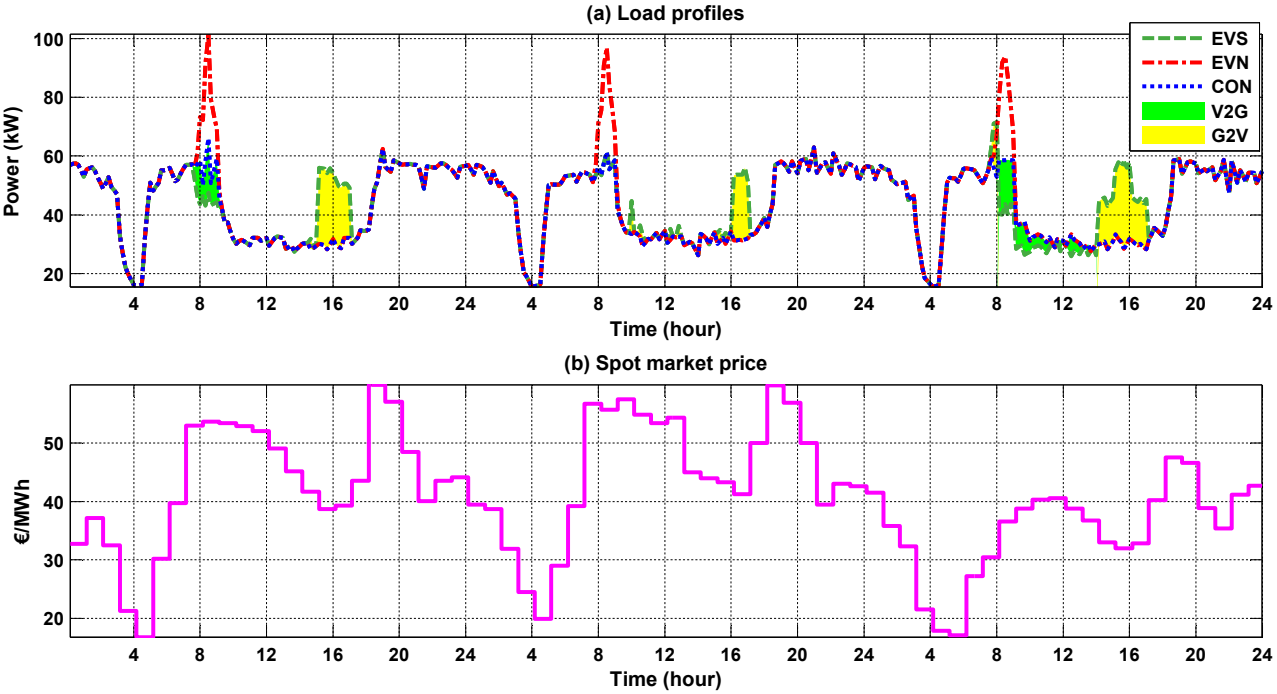

Figure 4.62: Comparison of supervised (EVS), and unsupervised (EVN) scenarios in spot market (**Category C**).

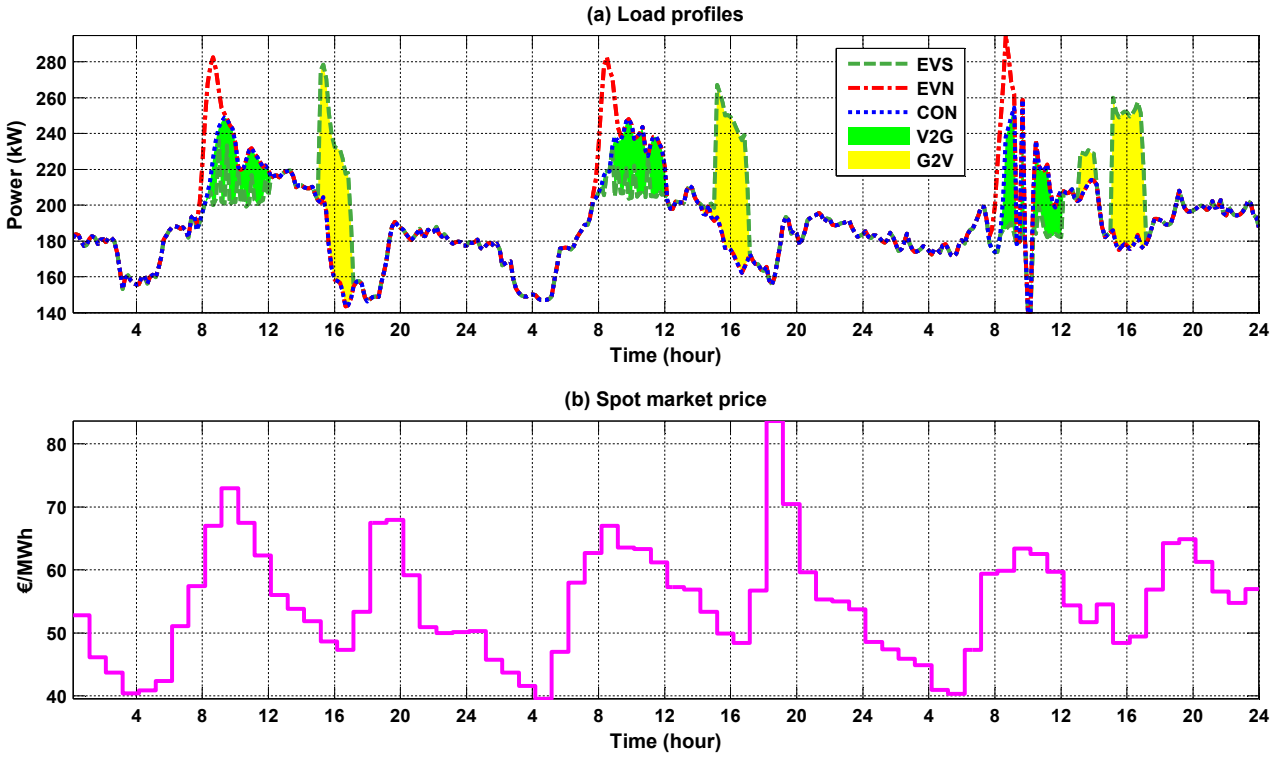

Figure 4.63: Comparison of supervised (EVS), and unsupervised (EVN) scenarios in spot market (**Category B**).

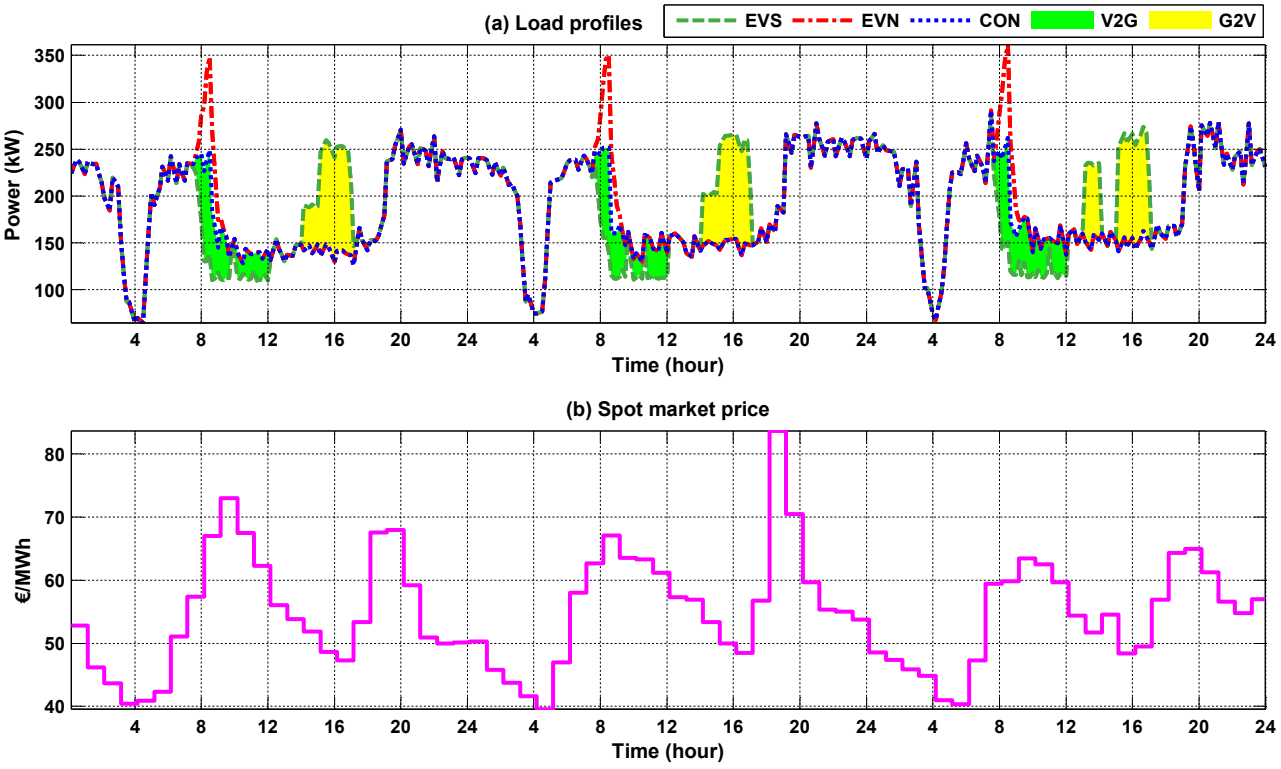

Figure 4.64: Comparison of supervised (EVS), and unsupervised (EVN) scenarios in spot market (**Category A**).

This is due to the fact that the spot price is not so interesting in term of V2G point of view. As mentioned previously, the interest of V2G participation in annual bill minimization for SMT is less competitive compared to RTS scenario. This is due to the slight price difference during PEVs availability and also the fact that in SMT there is no subscription limitation. Hence, the major advantage of exceeding component in RTS is not achievable in SMT scenario.

The possible suggestion for further studies is that, the increment of benefit in spot market participation depends highly on the spot market and energy provider. Hence, other type of markets can be analyzed in order to be able to find the best market among available provider markets. The second aspect is related to the availability of the vehicles considering the spot market price. The possibility of providing services during nights can be analyzed in order to consider the advantages related to the spot market participation.

4.6 Conclusion

In this chapter the main contribution of the thesis has been developed. A predictive real-time supervision system for a V2G-enabled fleet of PEVs has been developed. This supervision system has been applied on two different case studies where different economic ancillary services were tested as scenarios. The results indicated that the presence of a real-time energy management system is necessary in order to reduce the negative impact of charging demand of PEVs on the distribution grid. The main development of the thesis is concentrated on a predictive input generation, using artificial neural network as learning algorithm and a hybrid optimization technic using particle swarm optimization and interior point algorithm as an off-line optimizer.

In addition, a real-time supervision system based on fuzzy logic, using the methodology developed in L2EP laboratory, is designed, where the two layers are connected. Finally a repartition algorithm which is able to estimate the state of charge of the PEVs is developed in

order to provide closed-loop control for real-time supervision system. A battery degradation modeling is also developed in order to estimate the impact of V2G technology on the electric vehicle battery's lifespan. All of these development are applicable on the other case studies and have ability to be considered as a methodological approach for future studies on the smart grid technologies.

The obtained results indicated that the participation of PEVs to the ancillary services in two different level of distribution system operator and industrial consumers could be efficient in term of economic interests. However further studies are needed to guarantee the pure benefit of each part near of the V2G contract which is subject to availability of a proposer business model between different actors of the contract.

4.7 Résumé

Dans ce chapitre le principal développement de la thèse a été expliqué. La gestion énergétique pour les véhicules électriques avec la technologie V2G pour les différents services systèmes et cas d'études a été évaluée. D'abord, une étude bibliographique sur les méthodologies déjà appliquées sur la problématique de la gestion énergétique des flottes des VEs a été faite.

Ensuite, la proposition de la gestion énergétique pour les deux cas d'études définies auparavant a été introduite. Le service minimisation de coût d'acheminement d'électricité pour une flotte de VEs raccordée aux réseaux de distribution du département de Deux-Sèvres, et le service minimisation du facteur énergétique de la gare pour les véhicules électriques connectés aux bornes de recharges qui sont installées dans le parking de la gare ont été considérés comme cas d'études principales de la thèse, où les différentes méthodologies de la gestion ont été mises en examen.

En outre, pour la simple raison qu'un surplus de dégradation de la batterie des véhicules électriques a été introduit dans la procédure de gestion des services du réseau, un modèle de calcul de la dégradation des batteries , grâce à l'algorithme Rainflow, a été établi dans la dernière partie de ce chapitre.

4.7.1 La stratégie de la gestion énergétique temps réel prédictive, cas d'étude: Le réseau de distribution des Deux-Sèvres

Afin de contrôler la demande de charge des VEs, il faudrait mettre en place un système de gestion énergétique qui sera capable de minimiser les impacts négatifs de coïncidence des demandes de rechargement des VEs sur le réseau électrique. Les incertitudes en termes des disponibilités des VEs et de production d'énergie de source renouvelables type PV et éolien apportent des difficultés dans la gestion en temps réel. Pour cette raison, l'idée d'ajouter une étape de prévision qui sera capable de fournir une vision à court terme (j+1) sur la consommation, production et disponibilité des véhicules électriques a été proposée pour la première fois dans cette thèse.

Dans le cadre du développement de superviseur, deux systèmes de supervision différents ont été comparés : le superviseur temps réel et le superviseur temps réel prédictif. La possibilité de construire d'un système de prévision de la consommation a été étudiée. Celle-ci pourrait être basée sur les méthodes d'intelligence artificielle comme les réseaux des neurones artificielles. Dans ce chapitre, le système de prévision de la consommation a été présenté et le résultat sur un cas d'étude réel a été évalué. Ce système pourrait être intégré pour la prévision des productions des énergies renouvelables ainsi que la prévision de la disponibilité des véhicules électriques. La performance de l'algorithme de prévision développé a été évaluée sur un réseau de distribution, au niveau d'un poste source (90/15kV). La performance de cet algorithme a été évaluée avec 3.19% de moyenne de pourcentage d'erreur absolue.

4.7.2 Le superviseur prédictif (optimisation hors-ligne)

Après avoir réalisé la prévision j+1 qui sert de référence pour le superviseur temps réel, l'établissement d'une étape d'optimisation sera indispensable. L'algorithme d'optimisation sera capable de fournir une référence assez précise (sachant que la prévision a été faite avec une grande précision) grâce à la sortie de l'algorithme de prévision. Cette référence va être utilisée pour le pilotage du système en temps réel.

Avant d'aller en détail dans la méthodologie des algorithmes de supervision, la formulation du problème a été faite en considérant toutes les conditions et les contraintes du système. La fonction d'objectif du problème d'optimisation a été considérée en fonction du service choisi. Par

exemple, pour le cas d'étude de minimisation de coût d'acheminement, la fonction d'objectif a été définie comme la somme des composants de la facture d'acheminement qui sont bien détaillés dans le TURPE 4 établi par ENEDIS.

La proposition de l'algorithme d'optimisation a été faite après une étude bibliographique sur les méthodes d'optimisation actuelles en prenant en compte les caractéristiques du problème d'optimisation. L'une de ces caractéristiques est de hautes dimensions du variable d'optimisation. Cette fonctionnalité nous obligera de travailler plutôt avec les méthodes d'optimisation évolutionnaires et méta-heuristiques comme elles disposent d'une capacité de recherche en surfaces à hautes dimensions dans un temps raisonnable. En revanche, le problème commun entre la majorité des méthodes évolutionnaires, qui est l'imprécision du résultat final obtenu due aux départs stochastiques des paramètres initiaux, nous obligera à évaluer la possibilité d'hybridation de ces types d'algorithmes avec des méthodes déterministes afin d'augmenter la précision du résultat d'optimum final.

Pour ces raisons, la méthode d'optimisation par essaims particulaires (PSO en anglais) a été développée pour la recherche globale de la surface de recherche et en fin, le résultat d'obtenu a été injecté dans un deuxième d'algorithme d'optimisation déterministe afin de garantir l'optimalité du résultat final. Cet algorithme hybride, qui est nommé CPSO-IP, a été expliqué en détail dans ce chapitre. Ainsi, les résultats finaux de chacun des algorithmes ont été comparés afin de valider la performance de l'algorithme développé.

4.7.3 Le superviseur temps réel et le superviseur temps réel prédictif (optimisation en ligne)

Dans cette partie, l'algorithme de supervision temps réel basé sur la logique floue a été développé. Ce superviseur a été appliqué sur la même problématique définie dans l'étape précédente. L'approche méthodologique développée par les experts de l'équipe réseaux du laboratoire L2EP a été utilisée pour la construction du système de supervision temps réel. Grâce à cette méthodologie, le nombre de combinaisons utiles des règles floues a été limité sous forme d'une approche basée sur le graphe fonctionnel et le graphe opérationnel. Les différentes étapes de cette approche ont été définies en détail dans cette partie.

Les fonctions d'appartenances et leurs paramètres sont choisis selon l'expertise concernant l'opération du système. De ce fait, les choix ne sont pas forcément optimisés par rapport à la performance réelle du système. Pour cette raison, la mise en place d'une étude d'optimisation est indispensable. En fonction des nombres des paramètres à optimiser et du temps de calcul de chaque itération, l'algorithme génétique a été choisi comme méthode d'optimisation des paramètres des fonctions d'appartenances. Les performances des systèmes de superviseur pour les deux cas, superviseur temps réel empirique et le superviseur temps réel optimisé, ont été comparées et le résultat montre un progrès sur la valeur de la fonction d'objectif.

A la fin de cette partie, les indicateurs de performance des systèmes de superviseurs ont été comparés afin de valoriser l'exigence de chaque opérateur du système de supervision temps réel prédictif. L'existence d'une étape de prévision apporte un bénéfice de 2.33% sur le coût d'acheminement d'électricité.

4.7.4 L'estimateur d'état de charge (SOC) et l'algorithme de répartition des consignes de charge/décharge

Après avoir construit le superviseur temps réel, il est important de savoir que la sortie du superviseur reste globale et que le système de supervision exigera de répartir cette sortie (nous l'appelons consigne) entre tous les véhicules électriques raccordés au réseau électrique. La

deuxième difficulté dans cette étape est le pilotage en temps réel de l'état de charge de tous les véhicules raccordés au réseau. Un algorithme a été développé dans cette partie afin de répondre à ces deux problématiques précédemment définies. Les contraintes de tous les véhicules ont été considérées dans chaque étape de l'algorithme afin de pouvoir répondre au besoin énergétique de tous les véhicules et les contraintes déjà définies par les conducteurs. La performance de cet algorithme a été évaluée sous forme de nombre des véhicules rechargés au moment de départ. Cette indication a été présentée sous forme graphique qui garantit le déchargement des batteries jusqu'à 80% de profondeur de décharge et le respect du besoin énergétique de tous les véhicules raccordés au réseau.

4.7.5 Modélisation de la dégradation des batteries des véhicules électriques

Afin de pouvoir quantifier les impacts négatifs des V2G sur le vieillissement des batteries des véhicules électriques, un modèle de dégradation des batteries basé sur les comportements électrochimiques des batteries et sur l'algorithme de rainflow a été développé dans cette partie. Le comptage rainflow est un algorithme développé par les mécaniciens, dans le domaine des fatigues des matériaux, qui permet de compter le nombre de cycles de recharge/décharge de la batterie à partir du profil de SOC de la batterie.

Dans l'algorithme développé, tout d'abord, le nombre de cycles et de demi-cycles sur un temps donné sont comptés par rainflow. Ensuite, grâce au modèle mathématique de dégradation, la valeur de perte de vie de la batterie est calculée. Après, la durée de vie de la batterie sera calculée en fonction des caractéristiques de la batterie fournies dans les catalogues par les constructeurs de la batterie. Finalement, pour évaluer l'impact de V2G sur la dégradation de la batterie, plusieurs scenarios ont été établis pour pouvoir distinguer le cas avec V2G et le cas sans V2G. Le résultat montre un impact non-négligeable sur la vie de la batterie en présence du V2G pour le service de minimisation de coût d'acheminement d'électricité. Un véhicule utilisé pour fournir ce service pendant un an perdra un an et demi de la vie de sa batterie par rapport au cas sans V2G.

Ce modèle est bien développé et pourra être utilisé pour les autres services systèmes. Dans la perspective de travail ce modèle sera appliqué sur les autres services.

4.7.6 La stratégie de la gestion énergétique temps réel prédictive, cas d'étude: parking d'une gare

Le superviseur développé dans les parties précédentes a été appliqué sur le deuxième cas d'étude de la thèse. Le cahier des charges du superviseur a été défini et les entrées et leurs fonctions d'appartenances ont été déterminées par rapport aux caractéristiques des services. La minimisation du facteur énergétique de la gare en utilisant la technologie V2G a été considérée comme service offert pour ce cas d'étude. Ce service a été étudié en deux formes selon le tarif : tarif réglementaire de vente (TRV) et tarif sur le marché spot. La minimisation du facteur énergétique a été identifiée pour les deux cas et leurs influences sur les composants de ce facteur ont été étudiées. Les trois catégories type des gares en France sont considérées et l'impact du V2G sur les facteurs énergétiques de toutes les catégories a été identifié. Les résultats sont expliqués en détail dans cette partie. Dans le TRV, le composant le plus influencé est le dépassement de puissance souscrite alors que sur le marché spot cette influence n'existe pas car il n'y a aucun composant de dépassement.

4.8 References

[Abraham 05] Ajith Abraham. *Artificial neural networks*. handbook of measuring system design, 2005. 132

[Amzallag 94] C Amzallag, JP Gerey, JL Robert & J Bahuaud. *Standardization of the rainflow counting method for fatigue analysis*. International journal of fatigue, vol. 16, no. 4, pages 287–293, 1994. 180

[Barakat 90] EH Barakat, MA Qayyum, MN Hamed & SA Al Rashed. *Short-term peak demand forecasting in fast developing utility with inherit dynamic load characteristics. I. Application of classical time-series methods. II. Improved modelling of system dynamic load characteristics*. Power Systems, IEEE Transactions on, vol. 5, no. 3, pages 813–824, 1990. 130

[Bouallaga 15] Anouar Bouallaga. *Gestion énergétique d'une infrastructure de charge intelligente de véhicules électriques dans un réseau de distribution intégrant des énergies renouvelables.* PhD thesis, Université Lille 1 Sciences et Technologies, 2015. 154, 168

[Breban 13] Stefan Breban, Christophe Saudemont, Sébastien Vieillard & Benoît Robyns. *Experimental design and genetic algorithm optimization of a fuzzy-logic supervisor for embedded electrical power systems*. Mathematics and Computers in Simulation, vol. 91, pages 91 – 107, 2013. {ELECTRIMACS} 2011 - {PART} {II}. 153, 165

[Cazarez-Castro 10] Nohe R Cazarez-Castro, Luis T Aguilar & Oscar Castillo. *Fuzzy logic control with genetic membership function parameters optimization for the output regulation of a servomechanism with nonlinear backlash*. Expert Systems with Applications, vol. 37, no. 6, pages 4368–4378, 2010. 165

[Chen 01] Hong Chen, Claudio A Canizares & Ajit Singh. *ANN-based short-term load forecasting in electricity markets*. In Power Engineering Society Winter Meeting, 2001. IEEE, volume 2, pages 411–415. IEEE, 2001. 132

[Cheng 09] Chun-tian Cheng, Sheng-li Liao, Zi-Tian Tang & Ming-yan Zhao. *Comparison of particle swarm optimization and dynamic programming for large scale hydro unit load dispatch*. Energy Conversion and Management, vol. 50, no. 12, pages 3007–3014, 2009. 146

[Cho 95] MY Cho, JC Hwang & CS Chen. *Customer short term load forecasting by using ARIMA transfer function model*. In Energy Management and Power Delivery, 1995. Proceedings of EMPD'95., 1995 International Conference on, volume 1, pages 317–322. IEEE, 1995. 131

[Chukwu 14a] Uwakwe C Chukwu & Satish M Mahajan. *Impact of V2G on Distribution Feeder: An Energy Loss Reduction Approach*. International Transaction of Electrical and Computer Engineers System, vol. 2, no. 1, pages 19–27, 2014. 127

[Chukwu 14b] Uwakwe Christian Chukwu & Satish M Mahajan. *Real-time management of power systems with V2G facility for smart-grid applications*. Sustainable Energy, IEEE Transactions on, vol. 5, no. 2, pages 558–566, 2014. 127, 128

[Clement-Nyns 10a] K. Clement-Nyns, E. Haesen & J. Driesen. *The Impact of Charging Plug-In Hybrid Electric Vehicles on a Residential Distribution Grid*. IEEE Transactions on Power Systems, vol. 25, no. 1, pages 371–380, February 2010. 128

[Clement-Nyns 10b] Kristien Clement-Nyns, Edwin Haesen & Johan Driesen. *The impact of*

charging plug-in hybrid electric vehicles on a residential distribution grid. Power Systems, IEEE Transactions on, vol. 25, no. 1, pages 371–380, 2010. 127

[Clement-Nyns 11a] Kristien Clement-Nyns, Edwin Haesen & Johan Driesen. *The impact of vehicle-to-grid on the distribution grid.* Electric Power Systems Research, vol. 81, no. 1, pages 185–192, 2011. 127

[Clement-Nyns 11b] Kristien Clement-Nyns, Edwin Haesen & Johan Driesen. *The impact of vehicle-to-grid on the distribution grid.* Electric Power Systems Research, vol. 81, no. 1, pages 185 – 192, 2011. 128

[Courtecuisse 08] Vincent Courtecuisse. *Supervision d'une centrale multisources à base d'éoliennes et de stockage d'énergie connectée au réseau électrique.* PhD thesis, Arts et Métiers ParisTech, 2008. 153, 156

[Courtecuisse 10] Vincent Courtecuisse, Jonathan Sprooten, Benoît Robyns, Marc Petit, Bruno Francois & Jacques Deuse. *A methodology to design a fuzzy logic based supervision of Hybrid Renewable Energy Systems.* Mathematics and computers in simulation, vol. 81, no. 2, pages 208–224, 2010. 153

[CRE 16] CRE. *La fin des tarifs réglementés de vente pour les consommateurs professionnels : s'informer et anticiper.* http://www.cre.fr/infos-consommateurs/s-informer-sur-la-fin-des-tarifs-reglementes-pour-les-conso.-pro, 2016. 185

[David 92] Rene David & Hassane Alla. *Petri nets and Grafcet: tools for modelling discrete event systems.* 1992. 156

[Davigny 08] Arnaud Davigny. *Participation aux services système de fermes d'éoliennes à vitesse variable intégrant du stockage inertiel d'énergie.* PhD thesis, Hautes Etudes d'Ingénieur, 2008. 153

[Deilami 11] Sara Deilami, Amir S Masoum, Paul S Moses & Mohammad AS Masoum. *Real-time coordination of plug-in electric vehicle charging in smart grids to minimize power losses and improve voltage profile.* Smart Grid, IEEE Transactions on, vol. 2, no. 3, pages 456–467, 2011. 127, 128

[Ding 16] Ni Ding, Clementine Benoit, Guillaume Foggia, Yvon Besanger & Frederic Wurtz. *Neural Network-Based Model Design for Short-Term Load Forecast in Distribution Systems.* Power Systems, IEEE Transactions on, vol. 31, no. 1, pages 72–81, 2016. 131

[Downing 82] Stephen D Downing & DF Socie. *Simple rainflow counting algorithms.* International journal of fatigue, vol. 4, no. 1, pages 31–40, 1982. 179

[Emmy 11] Koeleman Emmy. *Artificial neural networks: A new tool in poultry research.* 2011. viii, 131

[Evsukoff 02] Alexandre Evsukoff, Antonio CS Branco & Sylvie Galichet. *Structure identification and parameter optimization for non-linear fuzzy modeling.* Fuzzy Sets and Systems, vol. 132, no. 2, pages 173–188, 2002. 165

[Feinberg 05] Eugene A Feinberg & Dora Genethliou. *Load forecasting.* In Applied mathematics for restructured electric power systems, pages 269–285. Springer, 2005. 130

[Green II 11] Robert C Green II, Lingfeng Wang & Mansoor Alam. *The impact of plug-in hybrid electric vehicles on distribution networks: A review and outlook.* Renewable and Sustainable Energy Reviews, vol. 15, no. 1, pages 544–553, 2011. 127

[Gross 87] George Gross & Francisco D Galiana. *Short-term load forecasting.* Proceedings of the IEEE, vol. 75, no. 12, pages 1558–1573, 1987. 132

[Harrabi 14] I. Harrabi & M. Maier. *Performance analysis of a real-time decentralized algorithm for coordinated PEV charging at home and workplace with PV solar panel integration.* In PES General Meeting | Conference Exposition, 2014 IEEE, pages 1–5, July 2014. 127, 128

[He 12] Yifeng He, B. Venkatesh & Ling Guan. *Optimal Scheduling for Charging and Discharging of Electric Vehicles.* Smart Grid, IEEE Transactions on, vol. 3, no. 3, pages 1095–1105, Sept 2012. 128

[Hu 02] Xiaohui Hu & Russell Eberhart. *Solving constrained nonlinear optimization problems with particle swarm optimization.* In Proceedings of the sixth world multiconference on systemics, cybernetics and informatics, volume 5, pages 203–206. Citeseer, 2002. 146

[Huang 03] Shyh-Jier Huang & Kuang-Rong Shih. *Short-term load forecasting via ARMA model identification including non-Gaussian process considerations.* Power Systems, IEEE Transactions on, vol. 18, no. 2, pages 673–679, 2003. 132

[Kennedy 11] James Kennedy. *Particle swarm optimization.* In Encyclopedia of machine learning, pages 760–766. Springer, 2011. 146

[Khatoon 14] Shahida Khatoon, AK Singh*et al.* *Analysis and comparison of various methods available for load forecasting: An overview.* In Computational Intelligence on Power, Energy and Controls with their impact on Humanity (CIPECH), 2014 Innovative Applications of, pages 243–247. IEEE, 2014. 130

[Kiartzis 95] SJ Kiartzis, AG Bakirtzis & V Petridis. *Short-term load forecasting using neural networks.* Electric Power Systems Research, vol. 33, no. 1, pages 1–6, 1995. 135

[Koziel 99] Slawomir Koziel & Zbigniew Michalewicz. *Evolutionary algorithms, homomorphous mappings, and constrained parameter optimization.* Evolutionary computation, vol. 7, no. 1, pages 19–44, 1999. 146

[Latimier 15] R Le Goff Latimier, B Multon, H Ben Ahmed, Franck Baraer & Mickael Acquitter. *Stochastic optimization of an Electric Vehicle Fleet Charging with Uncertain Photovoltaic Production.* In 2015 International Conference on Renewable Energy Research and Applications (ICRERA), pages 721–726. IEEE, 2015. 127

[Lee 92] KY Lee, YT Cha & JH Park. *Short-term load forecasting using an artificial neural network.* Power Systems, IEEE Transactions on, vol. 7, no. 1, pages 124–132, 1992. 132

[Ma 13] Tan Ma & O. Mohammed. *Real-time plug-in electric vehicles charging control for V2G frequency regulation.* In Industrial Electronics Society, IECON 2013 - 39th Annual Conference of the IEEE, pages 1197–1202, Nov 2013. 127, 128

[Millner 10] Alan Millner. *Modeling lithium ion battery degradation in electric vehicles.* In Innovative Technologies for an Efficient and Reliable Electricity Supply (CITRES), 2010 IEEE Conference on, pages 349–356. IEEE, 2010. 181

[Neffati 13] Ahmed Neffati, Mouloud Guemri, Stéphane Caux & Maurice Fadel. *Energy management strategies for multi source systems.* Electric Power Systems Research, vol. 102, pages 42–49, 2013. 128

[Nicolas 15] Patrick R Nicolas. Scala for machine learning. Packt Publishing Ltd, 2015. 166

[Paparoditis 13] Efstathios Paparoditis & Theofanis Sapatinas. *Short-term load forecasting: the similar shape functional time-series predictor*. Power Systems, IEEE Transactions on, vol. 28, no. 4, pages 3818–3825, 2013. 130

[Patrick 13] R. Nicolas Patrick. *Scala for machine learning*. http://www.scalaformachinelearning.com/2013/05/genetic-algorithm-in-scala.html, 2013. 166

[Poli 07] Riccardo Poli, James Kennedy & Tim Blackwell. *Particle swarm optimization*. Swarm intelligence, vol. 1, no. 1, pages 33–57, 2007. 146

[Putrus 09] GA Putrus, Pasist Suwanapingkarl, David Johnston, EC Bentley & Mahinsasa Narayana. *Impact of electric vehicles on power distribution networks*. In Vehicle Power and Propulsion Conference, 2009. VPPC'09. IEEE, pages 827–831. IEEE, 2009. 127

[Robyns 13] Benoît Robyns, Arnaud Davigny & Christophe Saudemont. *Methodologies for supervision of hybrid energy sources based on storage systems–A survey*. Mathematics and Computers in Simulation, vol. 91, pages 52–71, 2013. 153

[Robyns 15a] Benoît Robyns, Bruno François, Gauthier Delille & Christophe Saudemont. *Applications and Values of Energy Storage in Power Systems*. In Energy Storage in Electric Power Grids, pages 55–152. Wiley Online Library, 2015. ix, 154, 155

[Robyns 15b] Benoît Robyns, Bruno François, Gauthier Delille & Christophe Saudemont. Recent developments in energy storage, pages 17–53. John Wiley & Sons, Inc., 2015. 153, 156

[RTE] RTE. *Réseau de transport d'électricité, CO2 emission profile*. http://www.rte-france.com/fr/eco2mix/eco2mix-co2. 163

[Salmasi 07] Farzad Rajaei Salmasi. *Control strategies for hybrid electric vehicles: Evolution, classification, comparison, and future trends*. Vehicular Technology, IEEE Transactions on, vol. 56, no. 5, pages 2393–2404, 2007. 128

[Sarabi 15a] S. Sarabi, A. Davigny, Y. Riffonneau, V. Courtecuisse & B. Robyns. *Contribution and Impacts of Grid Integrated Electric Vehicles to the Distribution Networks and Railway Station Parking Lots*. In Electricity Distribution (CIRED 2015), 23rd International Conference and Exhibition on, pages 1–5, June 2015. 128

[Sarabi 15b] Siyamak Sarabi, Arnaud Davigny, Yann Riffonneau, Vincent Courtecuisse & Benoit Robyns. *Contribution and impacts of grid integrated electric vehicles to the distribution networks and railway station parking lots*. pages 1–5. cired proceeding, 2015. 127

[Shafiee 13] Soroush Shafiee, Mahmud Fotuhi-Firuzabad & Mohammad Rastegar. *Investigating the impacts of plug-in hybrid electric vehicles on power distribution systems*. Smart Grid, IEEE Transactions on, vol. 4, no. 3, pages 1351–1360, 2013. 127, 128

[Shahidehpour 02] Mohammad Shahidehpour, Hatim Yamin & Zuyi Li. Market operations in electric power systems. John Wiley & Sons, Inc., 2002. 131

[Shi 11] Wenbo Shi & Vincent WS Wong. *Real-time vehicle-to-grid control algorithm under price uncertainty*. In Smart Grid Communications (SmartGridComm), 2011 IEEE International Conference on, pages 261–266. IEEE, 2011. 127, 128

[Singh 13] M. Singh, K. Thirugnanam, P. Kumar & I. Kar. *Real-Time Coordination of Electric Vehicles to Support the Grid at the Distribution Substation Level*. Systems Journal, IEEE, vol. PP, no. 99, pages 1–11, 2013. 127, 128

[Song 14] Ziyou Song, Heath Hofmann, Jianqiu Li, Jun Hou, Xuebing Han & Minggao Ouyang. *Energy management strategies comparison for electric vehicles with hybrid energy storage system*. Applied Energy, vol. 134, pages 321–331, 2014. 128

[Sun 14] Sun Sun, Min Dong & Ben Liang. *Real-Time Welfare-Maximizing Regulation Allocation in Dynamic Aggregator-EVs System*. Smart Grid, IEEE Transactions on, vol. 5, no. 3, pages 1397–1409, May 2014. 127, 128

[Tan 14] Jun Tan & Lingfeng Wang. *Real-time coordinated management of PHEVs at residential level via MDPs and game theory*. In PES General Meeting | Conference Exposition, 2014 IEEE, pages 1–5, July 2014. 127, 128

[Wang 03] Sun-Chong Wang. *Artificial neural network*. In Interdisciplinary Computing in Java Programming, pages 81–100. Springer, 2003. 131

[Xu 13] Bolun Xu & Dipl. ing Andreas Ulbig. Degradation-limiting optimization of battery energy storage systems operation. Master's thesis, ETH Zurich, 2013. 181, 182

[Yilmaz 13a] M. Yilmaz & P.T. Krein. *Review of the Impact of Vehicle-to-Grid Technologies on Distribution Systems and Utility Interfaces*. Power Electronics, IEEE Transactions on, vol. 28, no. 12, pages 5673–5689, Dec 2013. 127

[Yilmaz 13b] Murat Yilmaz & Philip T. Krein. *Review of the Impact of Vehicle-to-Grid Technologies on Distribution Systems and Utility Interfaces*. IEEE Transactions on Power Electronics, vol. 28, no. 12, pages 5673–5689, December 2013. 128

[Zhang 10] Hao-Tian Zhang, Fang-Yuan Xu & Long Zhou. *Artificial neural network for load forecasting in smart grid*. In Machine Learning and Cybernetics (ICMLC), 2010 International Conference on, volume 6, pages 3200–3205. IEEE, 2010. 135

[Zhurkov 84] SN Zhurkov. *Kinetic concept of the strength of solids*. International Journal of Fracture, vol. 26, no. 4, pages 295–307, 1984. 181

Chapter 5

Application of V2G ancillary services on distribution grid: A Co-simulation approach

Contents

5.1 Introduction

This chapter is concentrated on a quasi-experimental validation of developed energy management strategies for V2G-enabled PEV fleet. A co-simulation platform using PowerFactory/DIgSILENT software and MATLAB™/Simulink is used in order to test the impact of developed supervision systems on the technical characteristics of a distribution grid. Previous researchers of L2EP laboratory have developed this platform using the guidance of a research in [Andrén 11]. This platform has been tested for only PEV charging coordination previously [Bouallaga 15]. In this thesis the V2G-enabled PEVs are tested for ETCM service and applied on a real MV feeder (15 kV) connected to the same HV/MV (90/15 kV) substation presented in chapter 4. In this chapter at first, the co-simulation platform is introduced. After that, the previously developed supervision system are tested on the co-simulation platform and their impacts on, voltage drop, Losses, grid load rate and maximum active power are evaluated. The service is energy transmission cost minimization and is applied at the level of HV/MV substation. However, the impacts have been analyzed at both HV/MV substation level and MV feeder level. The impacts analysis are proposing new horizons of research for V2G supervision system and will study the impact o technical aspects rather than economic aspects.

5.2 Co-simulation platform

DIgSILENT PowerFactory is a power system analysis software for applications in generation, transmission, distribution and industrial systems. This software nowadays is used frequently by grid operators and particularly the DSOs. In this thesis a model of distribution grid in Deux-Sèvres departement of France is used at case study which is modeled in DIgSILENT. Using Newton-Raphson method the load flow calculation is done in this software. On the other hand, the supervision system is implemented in MATLAB™/Simulink environment. Using an interface so-called OPC[1] server, the communication between MATLAB™/Simulink and DIgSILENT software is handled. In Figure 5.1 the procedure of data flow is explained illustratively and the inputs and outputs of each block are defined. The reference power of global fleet $P_{EV-ref}(t)$, and the reference power for each single vehicle which is calculated by supervision algorithm are transferred through OPC server to DIgSILENT for power flow calculation on the MV feeder. The calculation time depends on the size of the grid and number of necessary iteration of Newton-Raphson for convergence. For this case study, each sample time takes approximately 1 second for load flow calculation. The sample time in this study is considered as 5 minutes. Hence, for one day simulation 288 samples are needed. Therefore, the total calculation time for one day will be approximately 5 minutes. It should be added that the simulation in DIgSILENT takes in to account the phasor value hence the simulation is validate at steady state of the system and the transient effects are not considered in this study.

The data transfer between MATLAB™ and OPC contains the reference power and also the single refrence power for each PEVs. These values are either 0, 1 or -1 for *No charging*, *Charging* and *Discharging* commands, respectively. These data will be received by DIgSILENT for load flow calculation and grid real-time state estimation. These states are voltage magnitude and angle, current magnitude and angle, active and reactive powers. The powers are measured at each MV/LV substation point. The calculated states will be finally transferred using OPC server to the MATLAB™ for supervision system step based on the measured states of the grid.

[1]OPC is the interoperability standard for the secure and reliable exchange of data in the industrial automation space and in other industries. It is platform independent and ensures the seamless flow of information among devices from multiple vendors. The OPC Foundation is responsible for the development and maintenance of this standard [1].

This should be considered that, the real-time concept in this simulation is with t+1 delay. It means that they delay of measured data are one t sample time equivalent to 5 minutes in this simulation.

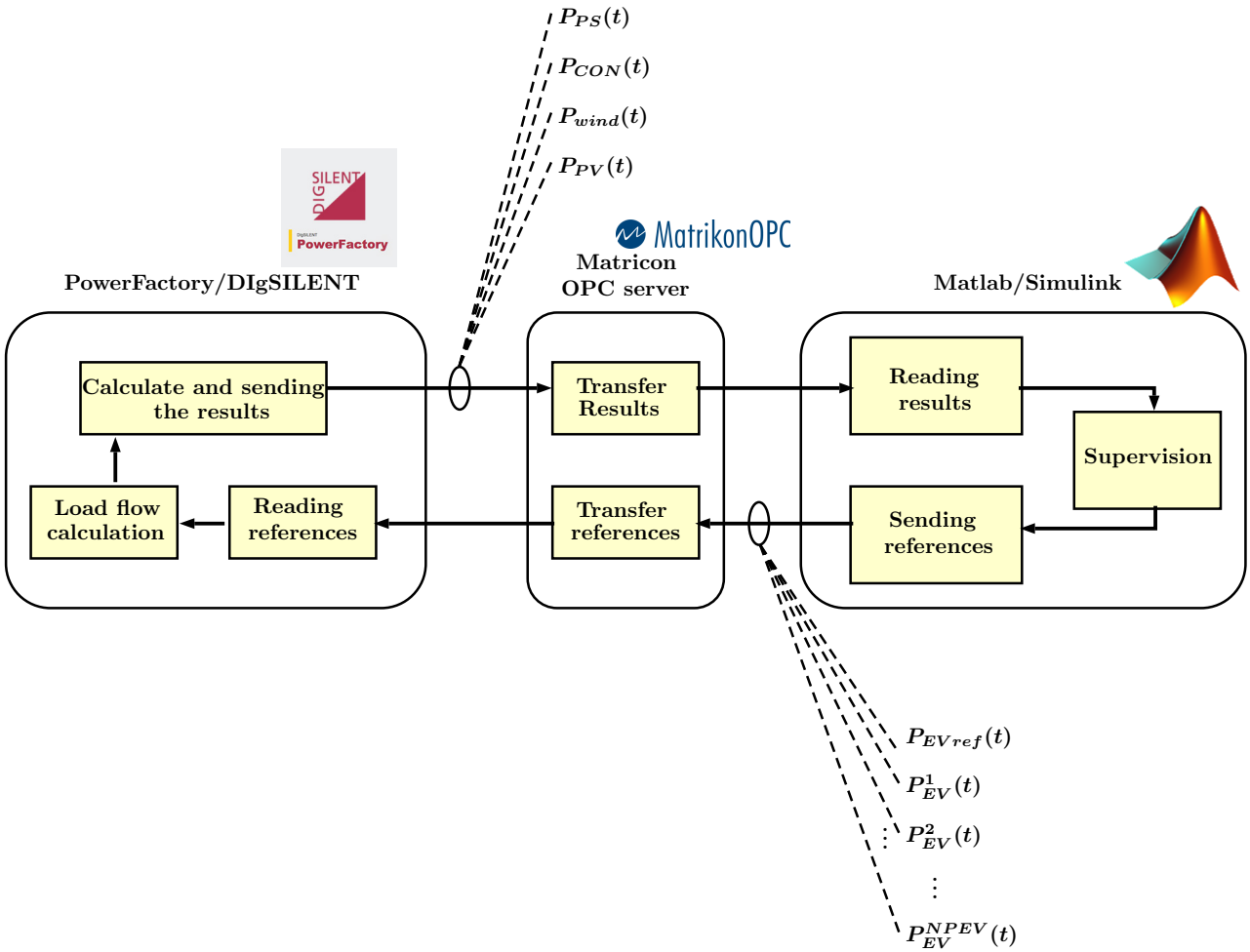

Figure 5.1: Co-simulation flowchart between MATLAB™, OPC server and DIgSILENT for V2G supervision system.

5.3 Distribution grid characteristics

In this thesis, the same case study presented in the work of [Bouallaga 15] is used in order to be able to compare the results of supervision for V2G-enabled PEV fleet with charging coordination supervision. The distribution grid characteristics are brought thereafter. The same substation presented in previous chapter is considered as case study where its position and all supplied MV feeders are illustrated in green color in Figure 5.2. In Figure 5.3 a more detailed image shows under study MV feeder in magenta color. This is a 15 kV Medium Voltage feeder of the same HV/MV substation modeled in DIgSILENT. This grid contains three wind farms connected to dedicated MV feeders (Figre 5.4) with global installed power of 62 MW. For Solar farm based on 2020 scenario total installed power of 8 MW is predicted in this substation where, 1365 kWc is connected to under study MV feeder E88640 (Figure 5.5). The number of PEVs are estimated to be 1200 at this substation where 150 PEVs are considered for MV feeder E88640. As the ETCM service is applied at the level of HV/MV substation, this service is considered at MV feeder as well. This MV feeder contains 447 nodes, 336 lines, 81 MV/LV

substation (15/0.4 kV magenta circles in Figure 5.3), 1100 customers and 385 kWp installed PV distributed in the feeder. Different measurement point of the feeder are also shown in Figure 5.6. The voltage drop is analyzed in two points, one in beginning of the feeder and the other one at furthest point. The regular voltage of the feeder is 15 kV. This feeder is connected to a 36 MVA transformer with OLTC (Over Load Tap Changer) at 23 steps. Each step has a regulation capacity of 1%. Therefore, the nominal variation range of the feeder voltage is between 15.6 and 15.75 kV. The acceptable marginal drop voltage is also considered as ±5%.

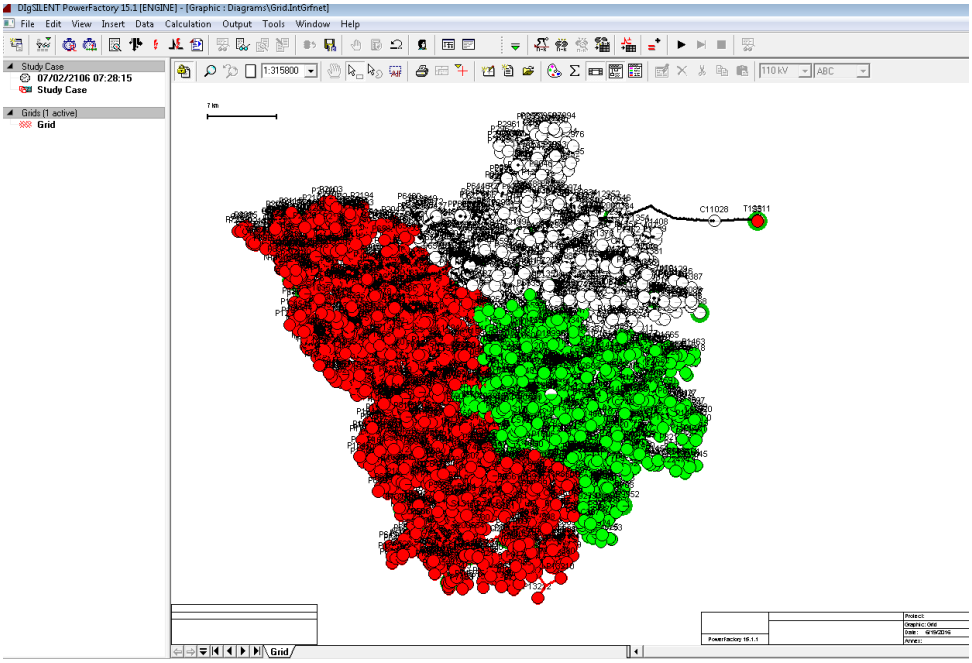

Figure 5.2: HV/MV (90/15 kV) substation (S2) modeled as case study and illustrated with all its supplied MV feeder in green color.

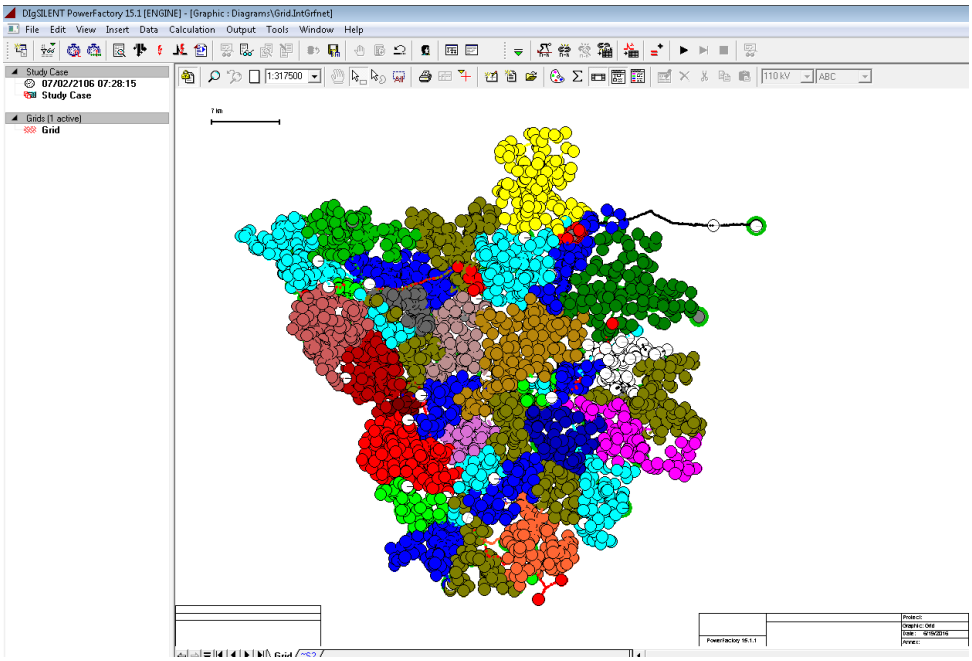

Figure 5.3: Differentiated MV feeders and under study MV feeder(E88640) in magenta color.

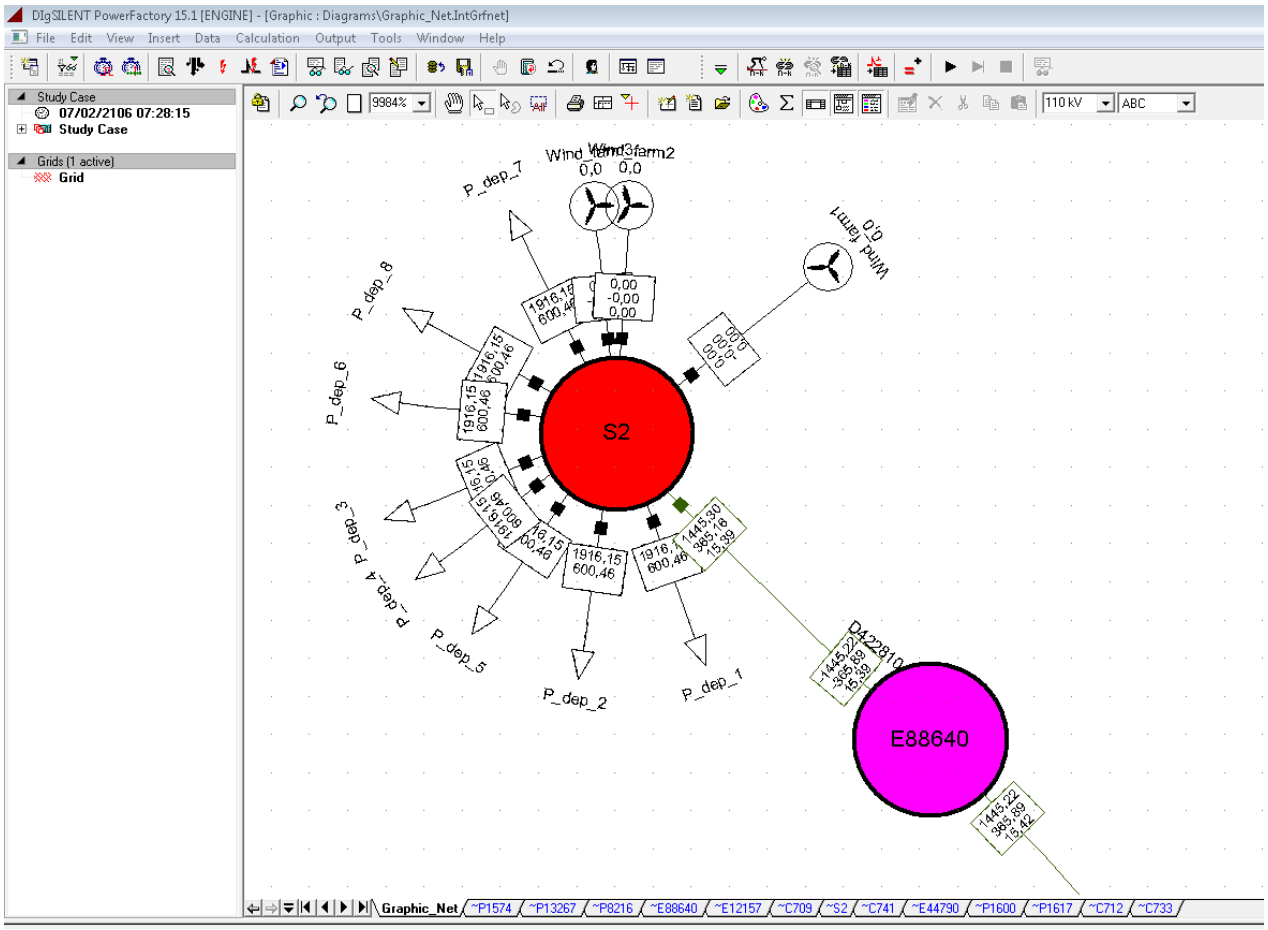

Figure 5.4: HV/MV substation model in DIgSILENT containing three dedicated wind farms MV feeders and 9 consumption feeders. E88640 denotes the modeled MV feeder (15 kV) . S2 indicates the HV/MV substation (90/15 kV).

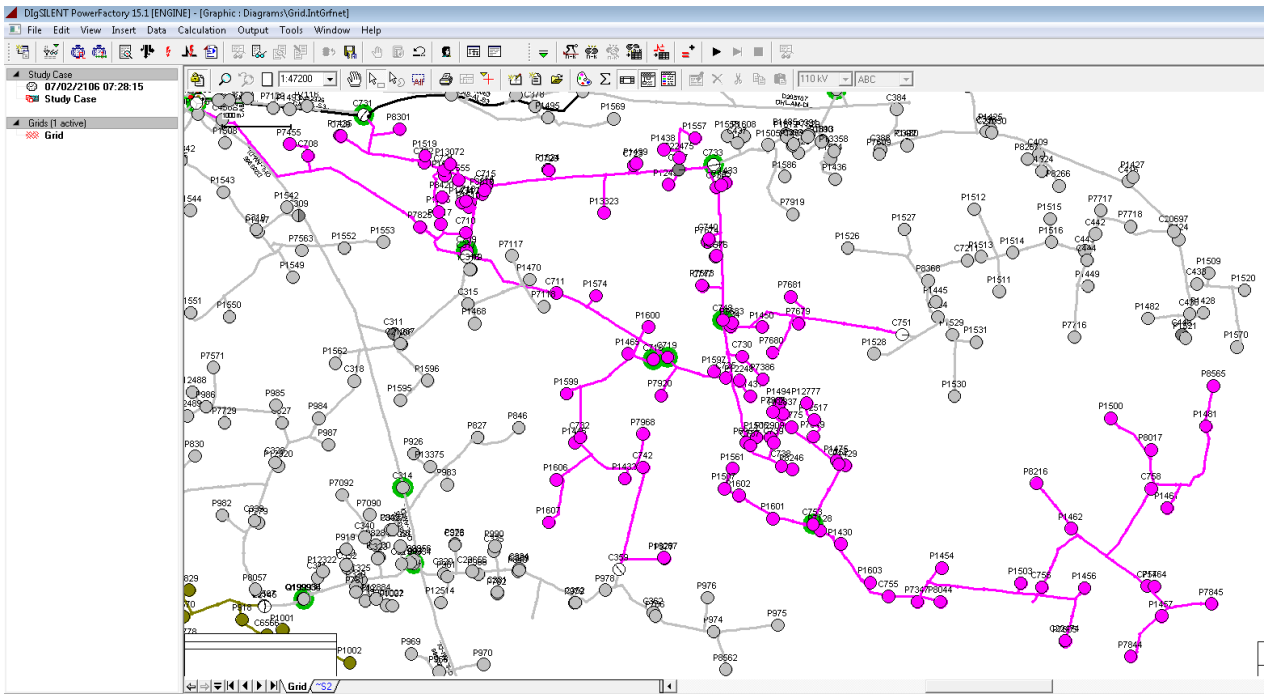

Figure 5.5: MV feeder (E88640) modeled in DIgSILENT illustrated in magenta color. The circles shows MV/LV substations (15/0.4 kV).

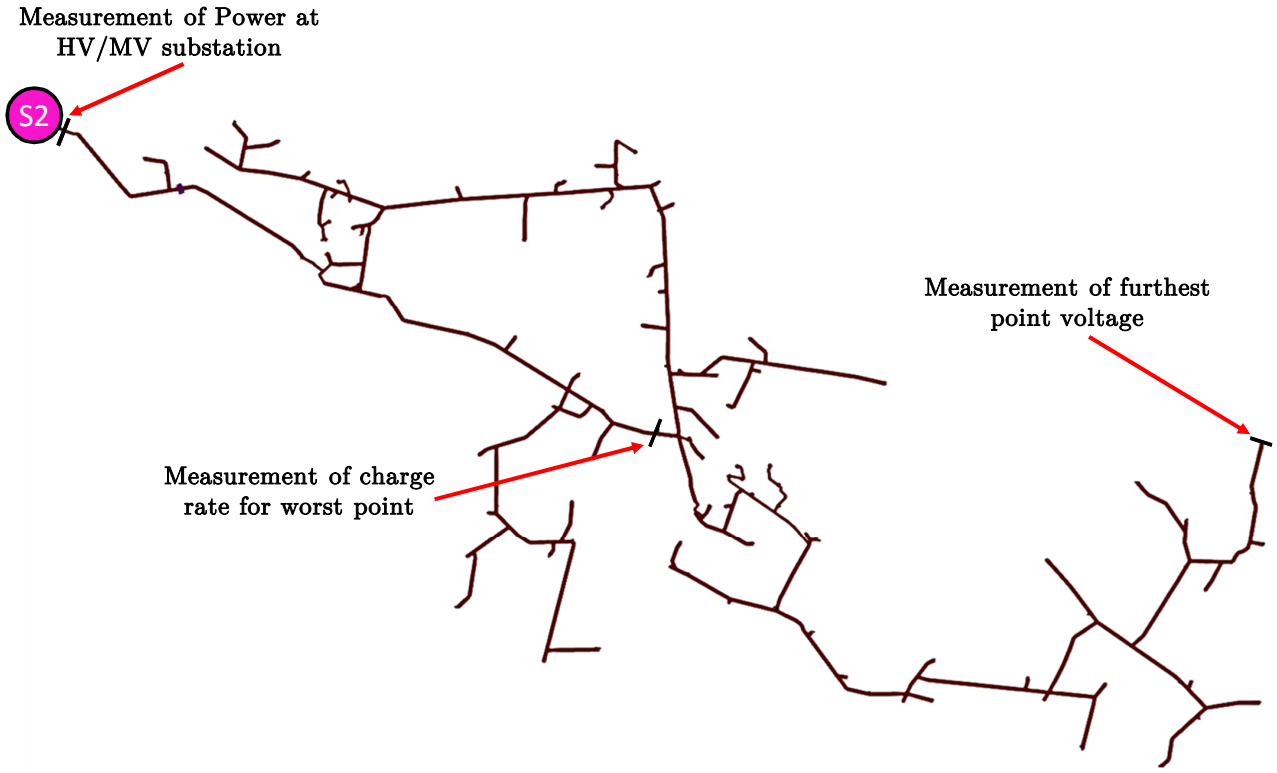

Figure 5.6: MV feeder with measurement point for voltage drop and load rate.

5.4 Scenarios and results

In this study, three example day of the year are considered to shows the impact of different supervision strategy on the technical limitation of the grid. Two winter days from the periods of February and December which are the 38^{th} and 345^{th} days of the year and one summer day at low consumption rate which is the 178^{th} days of the year. The results of voltage drop at furthest point, voltage profile at HV/MV substation, Power at HV/MV substation, Losses profile and load rate of worst point of the grid are investigated for each three example days. For each example, 5 possible supervision cases are considered. **Without PEV** denotes the case of load profile without any Plug-in Electric vehicle. **With PEV no supervision** is for the case of PEV presence where there is no supervision or energy management strategy on the charging process of the vehicles. The charging profile is considered as plug and charge scenario when the vehicles are connected and be charged after their arrival. This leads to charging profile of uncontrolled case. **RT-Empirical** denotes the scenario of Real-time supervision with Empirical membership function parameters. **RT-Optimized** is for the case of Real-time with Optimized membership functions. Finally, *RT-Predictive* indicates the scenario of Predictive real-time supervision with optimized membership function parameters. In fact, these scenarios are chosen for comparison in co-simulation to investigate the impact of different supervision strategies on the technical parameters of the grid such as voltage drop and losses in the distribution grid.

5.4.1 Scenario of 38^{th} day (Winter)

Co-simulation over a complete day of 38 has been applied. The simulation took 5 minutes, approximately. Comparison of supervision cases are considered in 5 possible cases. Figures 5.7 to 5.12 show theresults of simulation for different measurements for day 38.

In Figure 5.7, MV feeder voltage profile at HV/MV substation is shown for all 5 scenarios.

This measurement point is visible in Figure 5.6 near to S2. As it is shown, the voltage drop is important for the scenario Without Supervision at two time of 9 AM and 7 PM. These are the periods of PEVs peak demand at work and home, respectively. This voltage drop is controlled in different supervision system. It is shown that the Predictive real-time supervision has the best reaction concerning the voltage drop at this level.

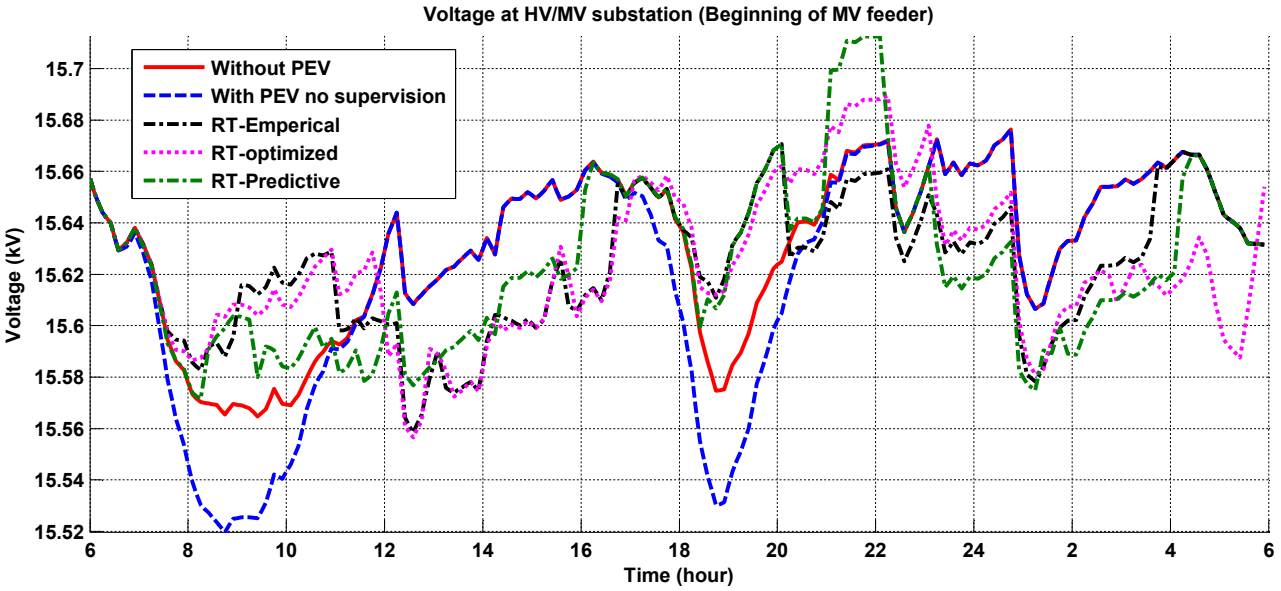

Figure 5.7: MV feeder voltage profile at HV/MV substation, day 38.

Figure 5.8, shows the total measured power at S2 (HV/MV substation). The peak of consumption is reduced in all of the supervision system with a slight better charging management of Predictive real-time supervision.

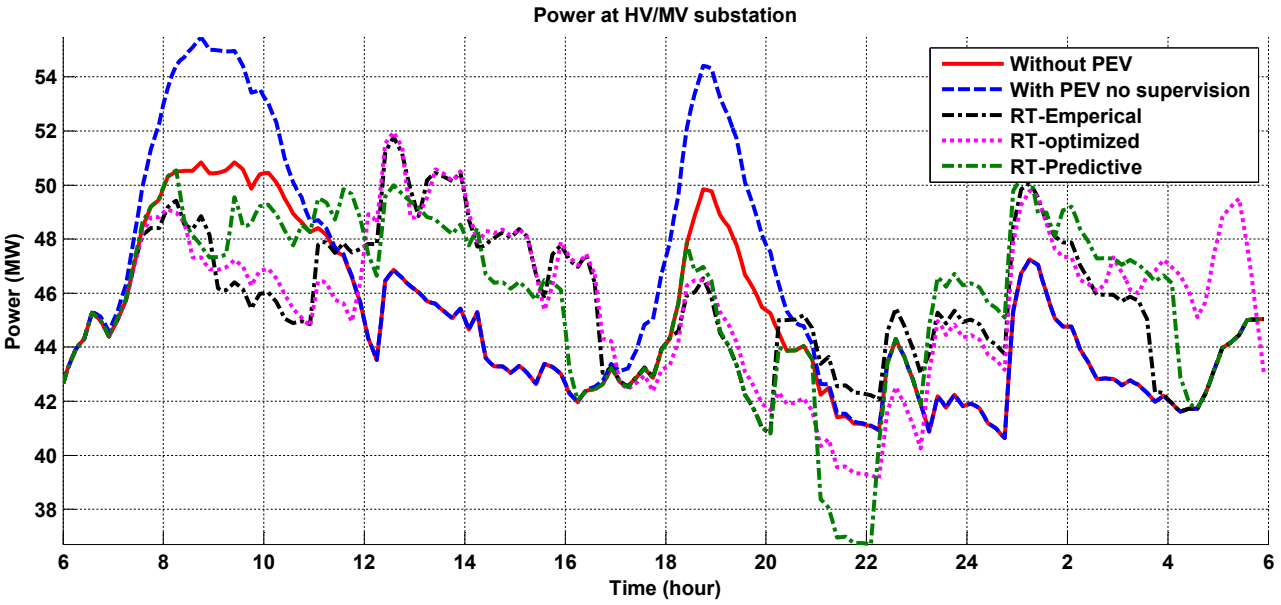

Figure 5.8: Load profile at HV/MV substation, day 38.

In Figure 5.9, the furthest point voltage at MV feeder shows some different results. For two cases of RT-Empiric and RT-Optimized there are exceeding the voltage drop at 14.25 kV. While the Predictive supervision keeps the voltage drop in the margin. Figure 5.12, shows the

power at beginning of MV feeder. The same phenomenon as the voltage drop at furthest point is evident. As the supervision system is applied at the HV/MV substation level, the power inside the MV feeder is not taken into account and it causes the peak generation even by using supervision system. However, Predictive supervision has minimized this impact compared to the Real-time supervisions.

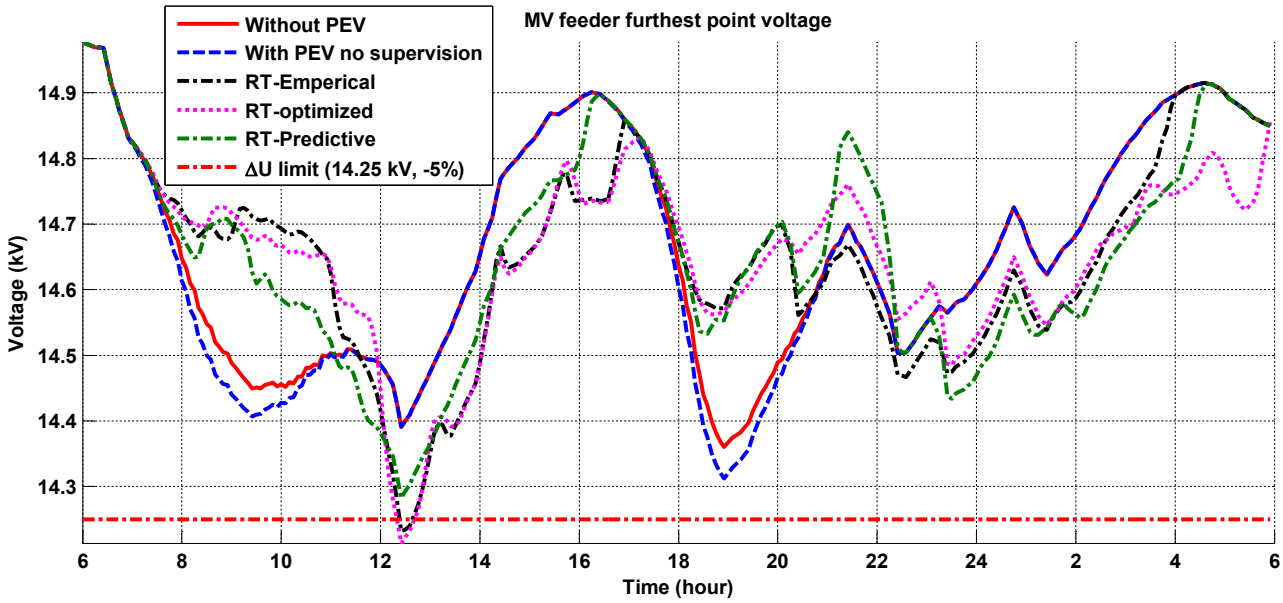

Figure 5.9: MV feeder furthest point voltage profile, day 38.

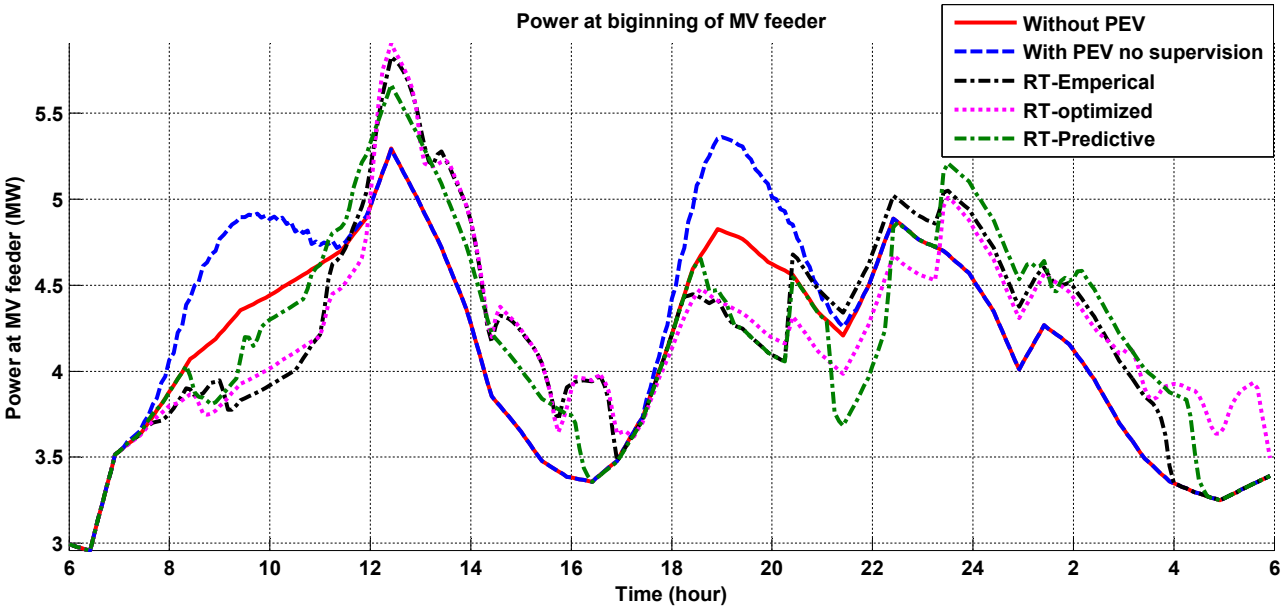

Figure 5.10: Power at beginning of MV feeder, day 38.

The losses in MV feeder are depicted in Figure 5.11. It shows correlation to the Power and voltage curve in previous figures. Losses at 11 AM is minimized with Predictive real-time supervision.

Finally, the load rate of worst point of the grid shows a correlation with voltage drop at farthest point in Figure 5.12.

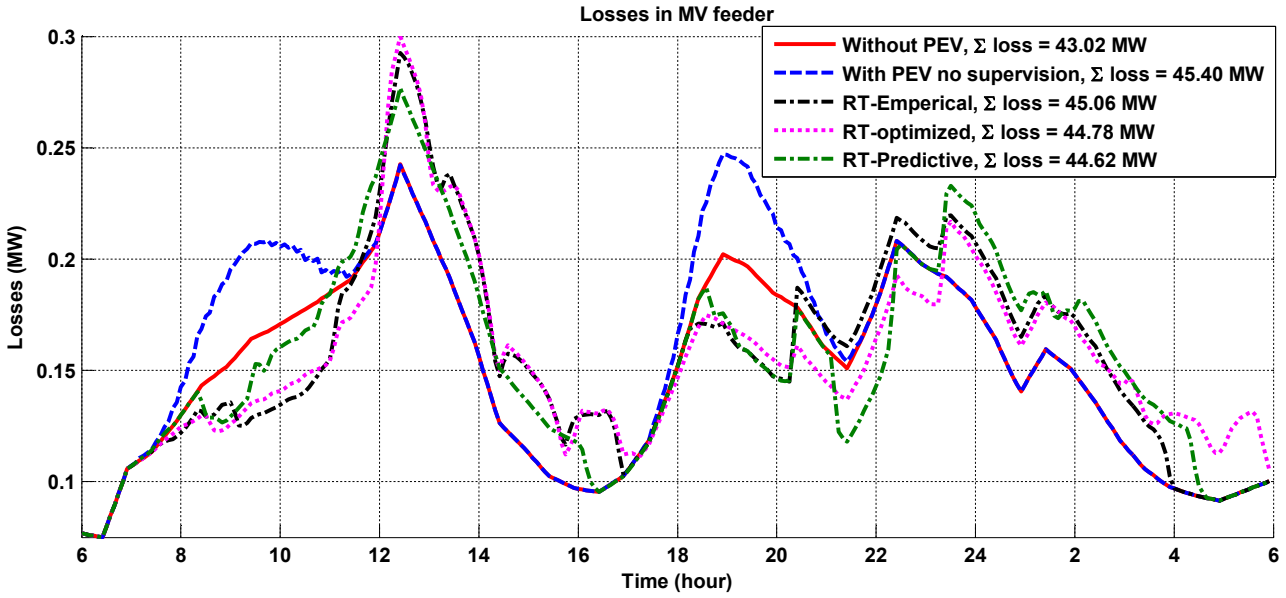

Figure 5.11: Losses in MV feeder, day 38.

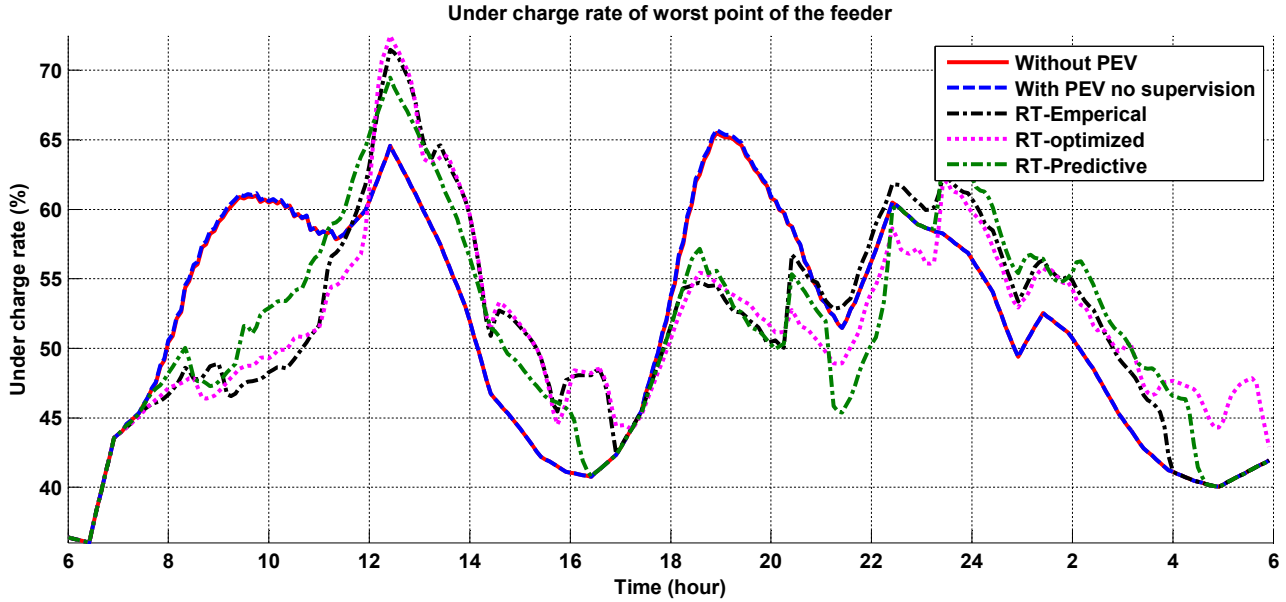

Figure 5.12: Worst point of feeder load rate, day 38.

The general results tables is presented in Table 5.1. Voltage drop, Losses, Load rate and Maximum Power are represented. The comparison shows that using the supervision at MV feeder causes extra voltage drop, losses and load rate. This is due to the fact that the supervision is applied at HV/MV substation level and there is no vision on the power variation at MV feeder. However, the Predictive real-time thanks to its predictive input, is able to reduce these negative impacts compared to the real-time supervision. Voltage drop is out of its acceptable limit (e.g. $\pm 5\%$) for Scenarios RT-Empirical and RT-Optimized, while Predictive Real-time supervision limits this exceeding.

Table 5.1: Comparison of different supervision from technical characteristics, winter day (day 38).

Supervision cases	Voltage drop (%)	Losses (MW)	Load rate (%)	Maximum Power (MW)
Without PEV	-4.26	43.02	65.49	5.29
With PEV no supervision	-4.59	45.40	65.70	5.36
RT-Empirical	-5.11	45.06	71.46	5.82
RT-Optimized	-5.24	44.78	72.46	5.90
RT-Predictive	-4.78	44.62	69.47	5.66

5.4.2 Scenario of 345^{th} day (Winter)

In this scenario, the same simulation is applied and results are brought in Figures 5.13 to 5.14. Figure 5.13 shows the MV feeder voltage profile at HV/MV substation. The regulation bound for OLTC is 15.6 to 15.75 kV. During 12 AM to 2 PM the Predictive real-time supervision leads to increase of the voltage therefore the OLTC was activated and it regulated the voltage to 15.6 kV. This happened during 8 PM to 10 PM and 11 PM to 1 AM, for three cases of supervision. These are mostly the impact of V2G on the voltage profile that should be taken into account for supervision system designing.

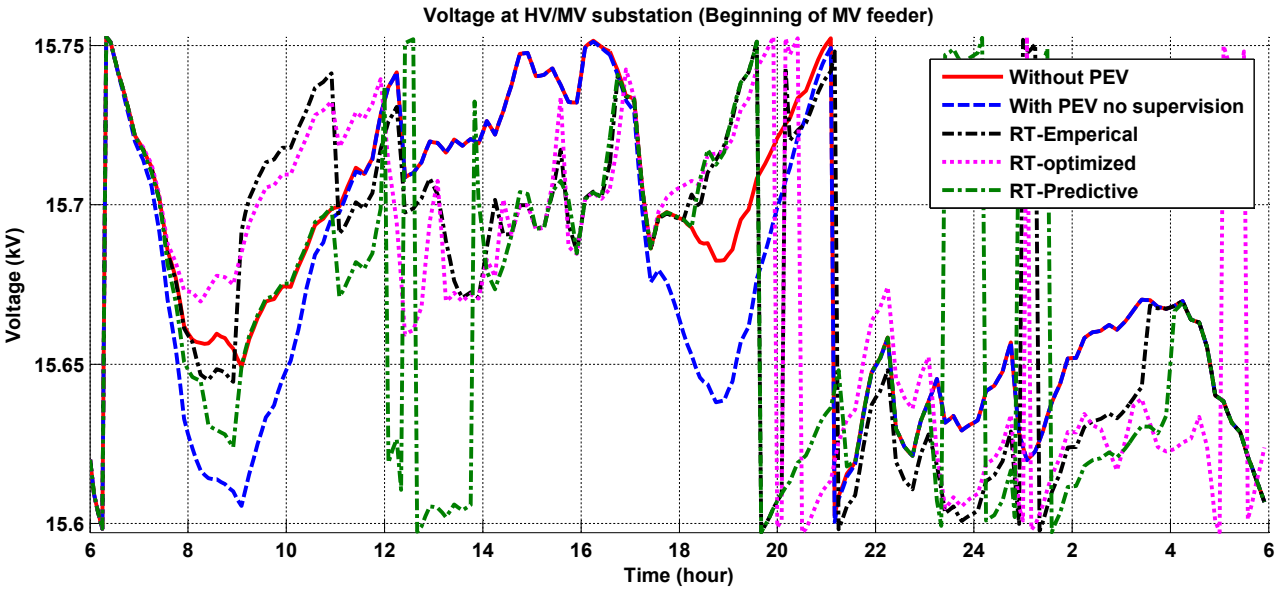

Figure 5.13: MV feeder voltage profile at HV/MV substation, day 345.

Figure 5.14 is showing the voltage profile at furthest point. In this case again the advantage of Predictive real-time supervision is visible during 12 AM to 2 PM. However in all cases the voltage profile is within the acceptable variation bound.

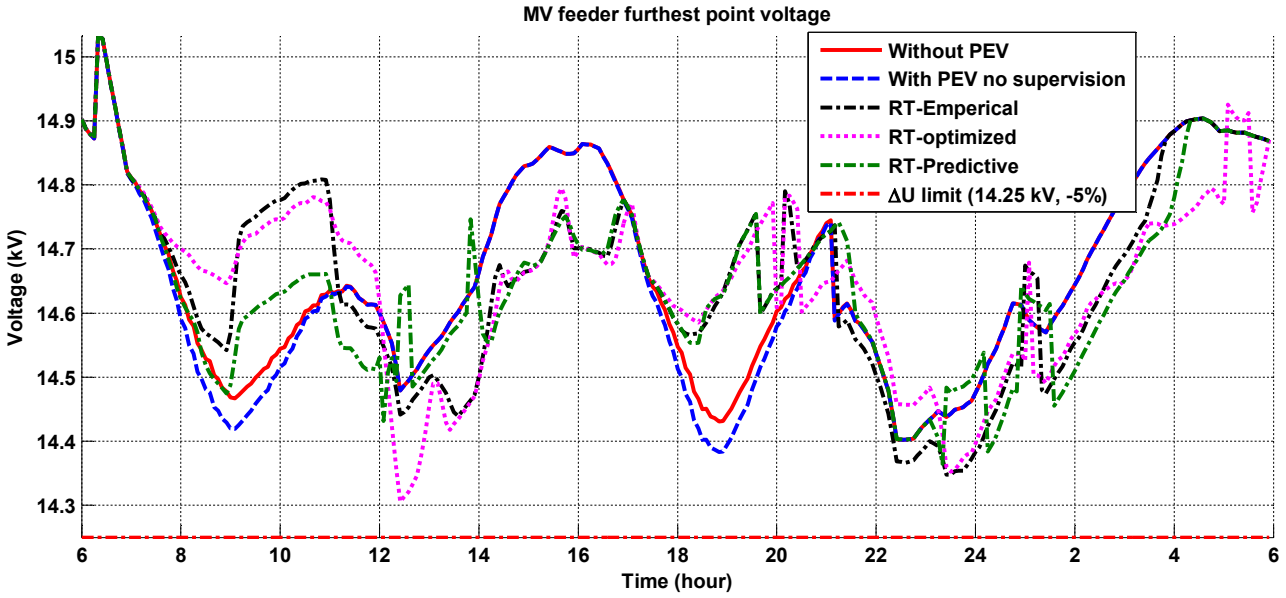

Figure 5.14: MV feeder furthest point voltage profile, day 345.

Finally, the results of simulation for all the indicators are brought in Table 5.2. The voltage drop is kept in limit for three supervision scenarios. Moreover, for RT-Predictive, the voltage drop is improved compared to RT-Empirical and RT-Optimized. This is the same case for Losses, load rate and Maximum power.

Table 5.2: Comparison of different supervision from technical characteristics, winter day (day 345).

Supervision cases	Voltage drop (%)	Losses (MW)	Load rate (%)	Maximum Power (MW)
Without PEV	-4.11	48.09	68.09	5.34
With PEV no supervision	-4.45	50.55	68.89	5.51
RT-Empirical	-4.34	50.25	67.36	5.47
RT-Optimized	-4.63	50.01	73.31	5.95
RT-Predictive	-4.23	49.80	68.51	5.61

5.4.3 Scenario of 178^{th} day (Summer)

The simulation is applied on a summer day with low rate consumption. As it is shown in Figure 5.15, the voltage drop with RT-Optimized scenario is critical during 2 PM. Hence the OLTC is activated to regulate the voltage in its normal variation rate. It shows the optimization of membership function can be also negative for technical point of the grid, If the voltage drop is not considered in real-time simulation. From the farthest point of the grid the voltage drop is not important and even the Predictive real-time supervision regulates the voltage better than other scenarios.

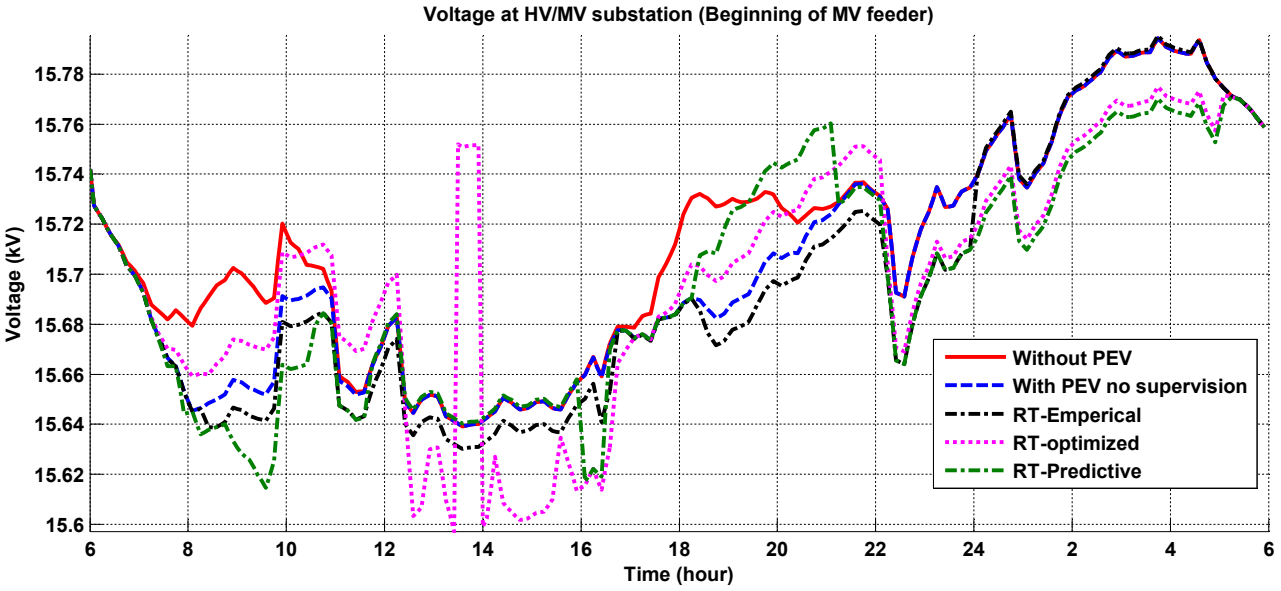

Figure 5.15: MV feeder voltage profile at HV/MV substation, day 178.

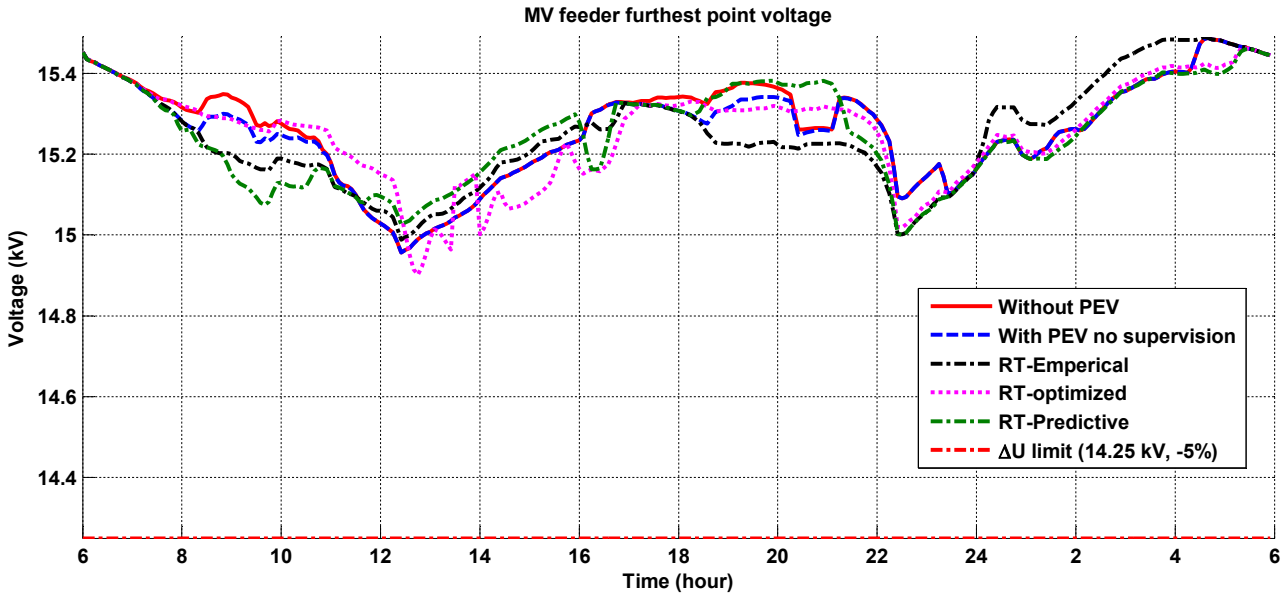

Figure 5.16: MV feeder furthest point voltage profile, day 178.

The results of simulation for day 178 are brought in Table 5.3. Concerning the voltage drop, the predictive real-time supervision acts better than other scenarios and keeps voltage in a good range compared to the other scenarios. Losses is controlled compared to RT-Empirical and RT-Optimized. These results also show that the performance of RT-Predictive is better than RT-Optimized and Empirical.

Table 5.3: Comparison of different supervision from technical characteristics, summer day (day 178)

Supervision cases	Voltage drop (%)	Losses (MW)	Load rate (%)	Maximum Power (MW)
Without PEV	-0.28	10.77	37.69	3.08
With PEV no supervision	-0.35	11.1	37.98	3.014
RT-Empirical	-0.07	10.56	36.09	3.03
RT-Optimized	-0.6	10.85	38.67	3.22
RT-Predictive	+0.007	10.21	36.10	3.03

5.5 Conclusion

In this chapter, a co-simulation platform was used for technical assessment of V2G-enabled supervision systems presented in previous chapter. The co-simulation platform was a simulation between MATLAB™ and DIgSILENT software. DIgSILENT does the load flow calculation and MATLAB™ involves with supervision system.

The simulation is done for three sample days, two from winter and one from summer day with low rate consumption. The results indicate that the supervision system can have negative impacts in terms of voltage drop and losses increment, if a reference for voltage is not considered in the supervision. However, using a predictive input showed that can help to reducing the negative impact. For instance the voltage drop, having a predictive input over a horizon of 24 hours (1 day), can be minimized compared to real-time supervision without predictive input.

As a perspective, it is recommended to consider voltage profile as one of the inputs of supervision system. This should be taken into account that, if the objective is at level of HV/MV substation, the variation profile at MV feeder should be also taken into account in order to avoid local negative impacts on the voltage profile. As the objective function in this study was an economic function, the impact of voltage drop and losses can be expressed as economical function in order to be able to measure the real economic benefits of using V2G for ancillary services.

5.6 Résumé

Dans ce chapitre, en utilisant le superviseur temps réel développé dans le chapitre précèdent, grâce à l'une plateforme d'essais développée dans le laboratoire L2EP, la performance du superviseur a été évalué. Cette plateforme permet de lancer une Co-simulation entre les logiciels PowerFactory, qui est un logiciel expert en modélisation et simulation des réseaux de distribution, et Matlab, qui est utilisé pour le développement de superviseur temps réel prédictif.

Dans ce chapitre, dans un premier temps, la plateforme de Co-simulation est introduite. Après cela, les systèmes de supervision mis au point antérieurement sont testés sur la plateforme de Co-simulation, et leurs impacts sur la chute de tension, les pertes en ligne, le taux de charge de réseau et la puissance active maximale sont évalués. Le service evalué est la minimisation des coûts d'acheminement de l'électricité et est appliqué au niveau des postes source HTB/HTA. Cependant, les impacts ont été analysés tant au niveau des postes source et les départs HTA. L'analyse des impacts permet de proposer de nouveaux horizons de recherche pour le V2G et des systèmes de supervision et montre l'importance de l'étude des impacts sur des aspects techniques plutôt que les aspects économiques.

La Co-simulation est effectuée pour trois jours, deux jours d'hiver et une journée d'été avec des faibles taux de consommation. Les résultats indiquent que le système de supervision peut avoir des effets négatifs en termes de chute de tension et les pertes, si une tension de référence n'est pas prise en compte dans la supervision. Toutefois, l'utilisation d'une entrée prédictive a montré la possibilité de réduire l'impact négatif. Par exemple, la chute de tension, lorsqu'on dispose d'une entrée prédictive sur un horizon de 24 heures (1 jour), peut être minimisée par rapport à la supervision en temps réel sans entrée prédictive.

En perspective, il est recommandé d'examiner le profil de tension comme une des entrées du système de supervision. Celui-ci doit être pris en compte si l'objectif est au niveau des postes sources HTB/HTA. La variation du profil au départ HTA doit être également considéré afin d'éviter les impacts négatifs sur le plan de tension. Comme la fonction d'objectif dans cette étude était une fonction économique, l'impact de la chute de tension et les pertes peuvent être exprimées comme une fonction économique afin de pouvoir mesurer les avantages économiques réels de l'utilisation de V2G pour les différents services systèmes.

5.7 References

[1] *Foundation of Interoperability Standard for Industrial Automation.* https://opcfoundation.org/about/what-is-opc/. 204

[Andrén 11] F. Andrén, M. Stifter, T. Strasser & D. Burnier de Castro. *Framework for coordinated simulation of power networks and components in Smart Grids using common communication protocols.* In IECON 2011 - 37th Annual Conference on IEEE Industrial Electronics Society, pages 2700–2705, Nov 2011. 204

[Bouallaga 15] Anouar Bouallaga. *Gestion énergétique d'une infrastructure de charge intelligente de véhicules électriques dans un réseau de distribution intégrant des énergies renouvelables.* PhD thesis, Université Lille 1 Sciences et Technologies, 2015. 204, 205

General Conclusion and Perspective

General Conclusion

In this thesis, the results of 3 years research on one of the challenging technologies of future transportation and smart grids has been presented. Vehicle-to-Grid has been analyzed from both technical and economic aspects and its possible ancillary services were analyzed. As the main development of the thesis, a real-time centralized supervision system at the level of HV/MV substation of distribution grid has been developed in order to manage the charging demand of the electric vehicle fleet. In addition, the ability of delivering the power from EV batteries to the grid has been embedded in this real-time supervision (so-called V2G). The main conclusion of the work can be expressed in different parts, each dedicated to the thesis developments.

Possible ancillary services: By analyzing the features of distributed energy storage systems (DESS) and their similarities with electric vehicles' batteries, the ancillary services of DESS have been analyzed for V2G technology. The main criteria is about the quantity of the power available for grid and the availability of the vehicles in order to provide the power. If a considerable number of vehicles would be available in the particular time, interesting services can be offered by the energy stored in their batteries. The question of availability and uncertainty in the availability has been also discussed and analyzed. This should be taken into account that when we talk about the ancillary services and vehicle-to-grid, different factors should be considered before providing a feasibility. These factors are mainly the type of service and its requirements in term of time and amount of power and vehicles availability taking into account the transportation nature of vehicles' fleet. For instance, for the vehicles doing daily home-work trips, the potential of ancillary service providing at working hours is higher than at home. This is due to the fact that the concentration of uncertainty probability at working hours is lower than at home.

In general, the ancillary services such as regulation market and peak power market are among the most competitive services based on the investigation done in this thesis. The economic interests of regulation market are also one of the intensive aspects of this service for V2G technology. This should be considered that a real cost/revenue analysis in order to clarify efficiency of V2G ancillary services is still needed as it is highly depend on the business model that would be proposed for V2G technology in future.

Real-time energy management: The task of developing a real-time energy management algorithm has been done properly in this thesis. The concept of energy management for V2G-enabled electric vehicles for two possible economic services has been developed. In order to provide better result in term of optimality, a predictive layer has been added to the real-time supervision system. This real-time predictive supervision system is able to predict the consumption of the grid, provide a reference power for PEV fleet in real-time and finally distribute

the charging/discharging command between the PEVs inside the fleet. Based on the objective function, the supervision system will provide the reference power leading to the optimization of that specific function. For instance, in this thesis, energy transmission cost minimization for distribution system operators and annual energy bill for railway station parking facilities have been considered as objective function. Minimization of yearly transmission cost up to 230 k€ has been validated in this research. This amount by considering the impact of degradation of the battery should be restudied in order to provide real benefit for grid operator. However, this task is limited to knowing a proper economic model between smart grid and V2G aggregators.

Real-time supervision has been compared with predictive real-time supervision. The results indicated that the presence of predictive input for real-time supervision could be useful if the uncertainty is low and prediction error is negligible. As the prediction layer has the ability to provide a perspective on the behavior of the system, let us say 24 hours a head prediction, the real-time action and decision making would be more optimal compared to the case without prediction.

The same supervision system has been applied on the case study of railway stations, where they have considered as future energy hub inside the stations. Different numbers of PEVs connected to the micro grid of the station have been tested to analyze the impact of V2G services can be provided. The results indicated that in both regulated and spot markets, the highly attractive benefit of V2G could be achieved only by combining of different services, in order to increase the benefits versus the costs of services, infrastructures and battery degradation.

PEV Battery degradation: In order to analyze the impact of V2G technology on the PEV's battery, the development of a degradation model is necessary. Thanks to the literature review a degradation model for lithium-ion battery has been developed. The model was used to analyze the impact of V2G participation of PEVs on the battery lifespan. The degradation modeling is done using rainflow counting algorithm by counting the number of cycles, depth of discharges, state of charges and type of each cycle. Hence the model measures the sensitivity of degradation to the different factors. This investigation showed that for the services which are discharging the battery deeply, such as peak power shaving, the impacts of V2G on battery degradation is considerable. However for the services with smaller depth of discharge the condition would be different.

Technical constraints of V2G: In this thesis, the main objectives have been considered as economic functions. However for real implementation of such technology, the infrastructure for V2G technology, both inside the vehicles and in the charging stations are needed. In addition, concerning the distribution grid, new grid code has to be established in order to accept the presence of such programmable loads inside the LV distribution grid. For instance for participation of PEVs to the frequency regulation market, the grid code should be updated in a way to keep security of the grid in presence of bidirectional load and also provide opportunity of participation for downstream customers in distribution grid (PEVs).

A co-simulation process on a distribution grid has been developed in this thesis, where the participation of V2G-enabled PEVs was investigated. The impacts of charging/discharging coordination on the voltage drop, losses in the grid, and maximum power of the grid have been analyzed. The results indicated that considering only an economic objective function without taking into account the technical states of the grid as an input can causes some negative effects on the voltage profile of the grid. Following that the losses can be increased. This is due to the fact that when the supervision is applied at the top level of distribution grid (HV/MV substations) the variation of voltage profile at MV feeder is not monitored. Hence, it can provide voltage drop or even increment in case V2G power injection, at the level of MV feeder.

These aspects should be taken in to account for future development of real-time supervision system at distribution grid level.

Perspectives

Based on the development done in this thesis, different axis and horizons of researches have been opened for V2G technology. Each development introduces different perspective for future of the work. As in this thesis the idea of predictive real-time supervision has been introduced, this is considerably important to develop prediction algorithm for renewable energy production and plug-in electric vehicles availability. For renewable energy prediction, there are already large amount of researches done in the world and it would be not a complicated cases. This is also due to the fact that the historical data for renewable energies production are available. While, the prediction of PEV availability is a major challenge as today there would not be such enough historical data which can provide the learning procedure.

The other possible perspective of the work is related to development of a proper economic model, describing the economic flow between the grid operators and PEV aggregators. This will help to identify the pure benefits of both grid operators and PEV owners. A business model should be designed in a way that can consider all aspects of the complex system of smart grid. In this system the connection between renewable energy producers, PEV aggregators and automobile makers, industrial aggregators, energy production operators and grid operators at both transmission and distribution level should be defined and the benefit/cost for each participant should be modeled. This horizon of research is so vast and needs deep analysis at energy market domain.

In the development of supervision system, a predictive layer was proposed to be added in order to enhance the performance of the supervision system in real-time. One of the major perspectives of the work in this level is the increment of robustness of predictive layer versus the real-time layer. In fact the possibility of a marginal control area designing should be studied in order to guarantee the optimality of taken decision in real-time. In fact, by defining a marginal area the acceptability of prediction should be tested in real-time. Another possible perspective for real-time supervision is the possibility of on-line optimization implementation in order to update the predictive inputs in function of any variation in real-time state of the system. Theses axis of research are mainly interesting to be considered in future works on V2G technology and particularly for energy management designing of PEV fleet.

As explained in conclusion, the degradation model for PEV battery lifespan has been developed in this thesis. In this axis of research the application of developed model on the other economic and technical services could be important to taken into account. A comparison of degradation impact between different services could be another interesting horizon of research where the results would be valuable for both grid operator in order to choose the best services in term of least impact on the batteries, and for PEV owner in order to choose the services that have lower impact on the battery lifespan of the vehicle. Another horizon of research could be the development of a business model for degradation in order to identify the economic impact of battery degradation. This study should be considered in a way that is able to provide a benefit/cost analysis for PEV owners. It could be attractive in terms of motivation of PEV owners' participation in the V2G services.

The perspective of the research for railway station case study is about two different axis. First is about the economic intensive offers for the PEV owners in order to motivate them for participation to the V2G services. This analysis should be done in a way that make an equilibrium between the provided services and benefits for V2G participation. These are connected to large investigation on economic aspects of V2G service in railway station parking facilities.

The second is related to possibility of participation in more attractive services such as capacity market, where in such services the capacity payment provides high motivation for PEV owners to let their vehicle in the hands of grid operators. In fact, only the availability of vehicles can bring economic benefit for the owners and service providers or even the aggregator, which is responsible of aggregated power.

The final word, the V2G technology is a new and vast domain of research which needs collaboration of the scientists, engineers, economists and social science experts in order to make applicable this new type of technology which is one of the main part of future smart grid.

Contribution du Vehicle-to-Grid (V2G) à la gestion énergétique d'un parc de Véhicules Électriques sur le réseau de distribution

RESUME :

L'augmentation des densités de puissance et d'énergie des SSE (système de stockage électrique) des véhicules électriques/véhicules hybrides rechargeable (VEs/VHRs), tout en conservant des coûts raisonnables pour l'utilisateur, et le développement de convertisseurs d'énergie électrique à haute densité de puissance volumique, et de plus en plus performant vont favoriser la production en masse de véhicules électrifiés. Une partie de ces véhicules électriques (VEs/VHRs) nécessitent une connexion au réseau pour la recharge des batteries. L'insertion de ces nouvelles charges dans le réseau présentera alors plusieurs enjeux et impacts significatifs pour les réseaux électriques puisqu'ils doivent répondre localement à des demandes de puissance non négligeables. Ce projet de thèse vise à étudier et réduire les impacts des VEs/VHRs sur les réseaux de distribution grâce à la technologie Vehicle-to-Grid (V2G). Le véhicule électrique alimente le réseau en fonction des besoins du système électrique (modèle bidirectionnel) et lui offre un service de flexibilité. Ces travaux de recherche ont pour but d'approfondir les concepts dans lequel l'alimentation des véhicules électriques (VE) et/ou hybrides de type P-VEH est intégrée à la gestion du réseau de distribution et des « hubs énergétiques » du futur. L'objectif de la thèse est d'abord étudier les services systèmes possibles à fournir grâce au V2G, ensuite de concevoir un système de supervision qui assurera une gestion énergétique de ces nouvelles charges en choisissant le mode de recharge et/ou décharge adéquat et en prenant également en considération la demande de consommation locale et la présence de production de type renouvelable (photovoltaïque, éolien) dans le réseau de distribution. Cette supervision se fera dans un premier temps « en hors ligne » et par la suite « en ligne ». On aura recours à l'utilisation de méthodes d'intelligence artificielle comme l'apprentissage automatique (Machine Learning) et la logique floue, la commande prédictive ainsi que des méthodes d'optimisation hybrides (stochastiques et déterministes).

Mots clés : Véhicule électrique rechargeable, Réseaux de distribution, Gestion énergétique

Contribution of Vehicle-to-Grid (V2G) to the energy management of Plug-in Electric Vehicles' fleet on the distribution network

ABSTRACT:

The power and energy density increment of the electrical storage system (ESS) of electric vehicles/Plug-in hybrid electric vehicles (EVs/PHEVs), while maintaining reasonable costs for the user, and the development of converters of electrical energy to high power density and more and more powerful, will encourage the mass production of electrified vehicles. Beyond, electric vehicles (EVs/PHEVs) require a connection to the grid for the charging of the batteries. The insertion of these new loads in the grid will then present several issues and significant impacts for electrical networks since they must respond locally to non-negligible power requests. This PhD thesis aims to study and reduce the impacts of the EVs/PHEVs on the distribution grid thanks to the vehicle-to-Grid (V2G) technology. The electric vehicle supplies the grid depending on the needs of the electrical system (bi-directional model) and offers a flexible service. These works of research have aimed to deepen the concepts in which the supply of electric vehicles (EV) and/or hybrids of type PHEV is integrated with the management of the distribution network and the future "energy hubs". The objective of the thesis is at first to examine the possible ancillary services provided by V2G, then to design a system of supervision which will ensure an energy management of these new loads by choosing the adequate mode of charge/discharge and also taking into consideration the request of local consumption and the presence of renewable production of type photovoltaic and wind in the distribution grid. This supervision will be in a first step "offline" and subsequently "online". The methods which are used in this thesis are as follows; artificial intelligence such as machine learning and fuzzy logic, the predictive control as well as the methods of hybrids optimization (stochastic and deterministic).

Keywords: Vehicle-to-Grid, Plug-in Electric Vehicle, Distribution grid, Energy management

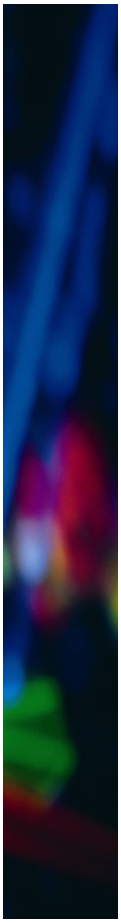

ARTS ET MÉTIERS ParisTech

ParisTech
INSTITUT DES SCIENCES ET TECHNOLOGIES
PARIS INSTITUTE OF TECHNOLOGY